

Organized by:
Faculty of Industrial Technology, Institut Teknologi Nasional (Itenas) Bandung, West Java Indonesia.

Supported by:
Institut Teknologi Nasional (Itenas) Bandung, West Java Indonesia.

Conference Proceedings

Vol 3, October 2021

The 3rd FoITIC 2021

Enriching Engineering Science Through Collaboration of Multidisciplinary Fields

International Conference

October 28 - 29, 2021
Faculty Building, 3rd floor
Campus of Itenas Bandung – Indonesia



**FACULTY OF INDUSTRIAL TECHNOLOGY INTERNATIONAL CONGRESS
(FoITIC)**

CONFERENCE PROCEEDINGS

Vol 3, October 2021

The 3rd FoITIC 2021

***“Enriching Engineering Science Through Collaboration
of Multidisciplinary Fields”***

ISSN 2962 - 1798



**Campus of Institut Teknologi Nasional Bandung West Java – Indonesia
October 28-29, 2021**

**FACULTY OF INDUSTRIAL TECHNOLOGY INSTITUT TEKNOLOGI
NASIONAL BANDUNG**

Proceedings of FoITIC 2021 – International Conference

Editorial Board:

Prof. Istvan Farkas	Hungarian University of Agriculture and Life Sciences – Hungary
Prof. István Seres	Hungarian University of Agriculture and Life Sciences – Hungary
Prof. József Horabik	Polish of Academy of Sciences – Poland
Prof. Zuzana Hlaváčová	Slovak University of Agriculture in Nitra – Slovak Republic
Prof. Dr. Rizalman Mamat	University Malaysia Pahang - Malaysia
Dr. Husnul Azan Bin Tajarudin	Universiti Sains - Malaysia
Dr. Hasan Al Abdulgader	Saudi Aramco – Saudi Arabia
Dr. Agus Saptoro	Curtin University – Malaysia
Dr. Waluyo	Institut Teknologi Nasional Bandung– Indonesia
Dr. Niken Syafitri	Institut Teknologi Nasional Bandung– Indonesia
Dr. Tarsisius Kristyadi	Institut Teknologi Nasional Bandung– Indonesia
Dr. Dani Rusirawan	Institut Teknologi Nasional Bandung– Indonesia
Dr. Ing. M. Alexin Putra	Institut Teknologi Nasional Bandung– Indonesia
Dr. Dwi Kurniawan	Institut Teknologi Nasional Bandung– Indonesia
Dr. Arif Imran	Institut Teknologi Nasional Bandung– Indonesia
Dr. Caecilia S. Wahyuning	Institut Teknologi Nasional Bandung– Indonesia
Dr. Jono Suhartono	Institut Teknologi Nasional Bandung– Indonesia
Dr. Winarno ugeng	Institut Teknologi Nasional Bandung– Indonesia
Dr. Lisa Kristiana	Institut Teknologi Nasional Bandung– Indonesia
Dr. Fahmi Arif	Institut Teknologi Nasional Bandung– Indonesia
Ms. Arie Desrianty	Institut Teknologi Nasional Bandung– Indonesia
Ms. Lauditta Irianti	Institut Teknologi Nasional Bandung– Indonesia
Prof. Dr. Soegijardjo Soegijoko	Institut Teknologi Nasional Bandung– Indonesia
	IEEE SSIT
Dr. Ahmad Taufik Joenoes	Indonesian Society for Reliability

Cover Design and Layout of Proceedings:

Mr. Aldrian Agusta(Cover Design)

Ms. Dina Budhi Utami

Copyright @ 2022 by the FTI – Itenas and the authors

Conference Organizer:

Faculty of Industrial Technology, Institut Teknologi Nasional Bandung - IndonesiaJl.

PKHH. Mustapa No. 23 Bandung 40124, West Java - INDONESIA

Email: foitic@itenas.ac.id, Website: <http://foitic.itenas.ac.id>, www.itenas.ac.id

ISSN 2692 - 1798

All rights reserved. No part of the publication may be produced, transmitted, in any form or by means of electronic, mechanical, photocopying, recording or otherwise, without the permission of the publisher, except the case in critical articles and reviewor where prior rights are preserved.

Produced by:

Faculty of Industrial Technology Institut
Teknologi Nasional Bandung

5 4 3 2

COMMITTEE

Organizing Committee:

Chairman	: Dr. Jono Suhartono	Institut Teknologi Indonesia	Nasional	Bandung–
Co-chairman	: Dr. Ing. Mohammad Alexin Putra	Institut Teknologi Indonesia	Nasional	Bandung–
	Dr. Fahmi Arif	Institut Teknologi Indonesia	Nasional	Bandung–
	Dr. Jasman Pardede	Institut Teknologi Indonesia	Nasional	Bandung–
Members	: Ms. Nuha Desi Anggraeni	Institut Teknologi Indonesia	Nasional	Bandung–
	Mr. Liman Hartawan	Institut Teknologi Indonesia	Nasional	Bandung–
	Ms. Youllia Indrawati	Institut Teknologi Indonesia	Nasional	Bandung–
	Mr. Febrian Hadiatna	Institut Teknologi Indonesia	Nasional	Bandung–
	Ms. Noviyanti Nugraha	Institut Teknologi Indonesia	Nasional	Bandung–
	Ms. Lita Lidyawati	Institut Teknologi Indonesia	Nasional	Bandung–
	Ms. Arie Desrianty	Institut Teknologi Indonesia	Nasional	Bandung–
	Mr. Iwan Agustiawan	Institut Teknologi Indonesia	Nasional	Bandung–
	Mr. Rispianda	Institut Teknologi Indonesia	Nasional	Bandung–
	Ms. Lauditta Irianti	Institut Teknologi Indonesia	Nasional	Bandung–
	Ms. Vibianti Dwi Pratiwi	Institut Teknologi Indonesia	Nasional	Bandung–
	Ms. Irma Amelia	Institut Teknologi Indonesia	Nasional	Bandung–
	Ms. Sofia Umaroh	Institut Teknologi Indonesia	Nasional	Bandung–

Advisory Board:

Prof. Dr. Meilinda Nurbanasari	Institut Teknologi Nasional Bandung– Indonesia
Dr. Tarsisius Kristiyadi	Institut Teknologi Nasional Bandung– Indonesia
Mr. Abinhot Sihotang	Institut Teknologi Nasional Bandung– Indonesia
Dr. Dani Rusirawan	Institut Teknologi Nasional Bandung– Indonesia
Prof. Dr. Soegijardjo Soegijoko	Institut Teknologi Nasional Bandung– Indonesia IEEE SSIT
Prof. Dr. Isa Setiasah Toha	ITB – Indonesia
Dr. Kusmaningrum Soemadi	Institut Teknologi Nasional Bandung– Indonesia
Dr. Iwan Inrawan Wiratmadja	ITB – Indonesia
Dr. Ahmad Taufik Joenoes	Indonesian Society for Reliability

National Scientific Committee:

Dr. Waluyo	Electrical Engineering	Institut Teknologi Nasional Bandung– Indonesia
Dr. Niken Syafitri	Electrical Engineering	Institut Teknologi Nasional Bandung– Indonesia
Dr. Tarsisius Kristiyadi	Mechanical Engineering	Institut Teknologi Nasional Bandung– Indonesia
Dr. Dani Rusirawan	Mechanical Engineering	Institut Teknologi Nasional Bandung– Indonesia
Dr. Ing. M. Alexin Putra	Mechanical Engineering	Institut Teknologi Nasional Bandung– Indonesia
Dr. Dwi Kurniawan	Industrial Engineering	Institut Teknologi Nasional Bandung– Indonesia
Dr. Arif Imran	Industrial Engineering	Institut Teknologi Nasional Bandung– Indonesia
Dr. Caecilia S. Wahyuning	Industrial Engineering	Institut Teknologi Nasional Bandung– Indonesia
Dr. Jono Suhartono	Chemical Engineering	Institut Teknologi Nasional Bandung– Indonesia
Dr. Winarno ugeng	Informatics Engineering	Institut Teknologi Nasional Bandung– Indonesia
Dr. Lisa Kristiana	Informatics Engineering	Institut Teknologi Nasional Bandung– Indonesia
Dr. Fahmi Arif	Industrial Engineering	Institut Teknologi Nasional Bandung– Indonesia
Ms. Arie Desrianty	Industrial Engineering	Institut Teknologi Nasional Bandung– Indonesia
Ms. Lauditta Irianti	Industrial Engineering	Institut Teknologi Nasional Bandung– Indonesia
Prof. Dr. Soegijardjo Soegijoko		Institut Teknologi Nasional Bandung– Indonesia IEEESSIT
Dr. Ahmad Taufik Joenoes		Indonesian Society for Reliability

International Scientific Committee:

Prof. Istvan Farkas	Hungarian University of Agriculture and Life Sciences – Hungary
Prof. István Seres	Hungarian University of Agriculture and Life Sciences – Hungary
Prof. József Horabik	Polish of Academy of Sciences – Poland
Prof. Zuzana Hlaváčová	Slovak University of Agriculture in Nitra – Slovak Republic
Prof. Dr. Rizalman Mamat	Universiti Malaysia Pahang – Malaysia
Dr. Husnul Azan Bin Tajarudin	Universiti Sains Malaysia – Malaysia
Dr. Hasan Al Abdulgader	Saudi Aramco – Saudi Arabia
Dr. Agus Saptoro	Curtin University – Malaysia

PREFACE

WELCOME SPEECH FROM THE RECTOR

INSTITUT TEKNOLOGI NASIONAL BANDUNG

Dear speakers and participants,

I am pleased to welcome you to the webinar on 3rd Faculty of Industrial Technology International Congress (FoITIC) 2021.

The theme for the 3rd FoITIC (FoITIC 2021) is: “Enriching Engineering Science through Collaboration of Multidisciplinary Fields”. A glance through the list of presentations planned for the next few days reveals the amazing diversity of these collaborations.

We all understand the importance of science, technology, and innovation in our day-to-day lives and the ways in which they are transforming the world. We believe that scientists and researchers will hand in hand with industrial experts, to create and develop new concepts/systems related to technologies that enable humans to make products and services more efficient in various sectors.

I am deeply grateful appreciative to the Faculty of Industrial Technology Itenas, the Hungarian University of Agriculture and Life Science in Godollo-Hungary, Institute of Agrophysics PAS in Lublin-Poland, the Slovak University of Agriculture in Nitra-Slovakia, Indonesian Society Reliability, Universiti Sains Malaysia, delegates, organizing committee and many others who have contributed to the success of this conference.

I am confident that this event will serve to promote much valuable communication and information exchange among scientists – researchers and industrial experts.

I wish you all a very successful webinar. Again, thank you for joining this virtual conference organized by our campus, and let us together accelerate the collaboration for Enriching Engineering Science.

Prof. Meilinda Nurbanasari, Ph.D.

Rector

Institut Teknologi Nasional Bandung

PREFACE

WELCOME SPEECH FROM THE DEAN OF FACULTY OF INDUSTRIAL TECHNOLOGY, INSTITUT TEKNOLOGI NASIONAL BANDUNG

Dear

Distinguished Guest, Excellencies,

Ladies and Gentlemen,

Welcome to the 3rd Faculty of Industrial Technology International Congress (FoITIC) at October 28-29 2021, which is organized by Faculty of Industrial Technology, Institut Teknologi Nasional (Itenas), Bandung – Indonesia, with supported by Hungarian University of Agriculture and Life Science, Slovak University of Agriculture in Nitra, Institute of Agrophysics Polish Academy of Sciences, Universiti Sains Malaysia, Saudi Aramco, Indonesian Society for Reliability (ISR) and American Institute of Physics (AIP).

The main theme for the 3rd congress is “Enriching Engineering Science through Collaboration of Multidisciplinary Fields”. Different from the previous FOITIC events, the 3rd congress is gathering virtually due to the current pandemic situation.

The aim of the Congress is inviting academics, researchers, engineers, government officers, company delegates and students from the field of industrial technology and other disciplines (such as electrical, mechanical, industrial, chemical, informatics, civil, architect, physics, environment, social, economic, design and etc.), to gather, present and share the results of their research and/or work and discuss the future and impact of industry 4.0.

Taking this opportunity, I would like to convey my sincere thanks and appreciation to our keynote speakers, invited speakers, and national and international scientific committee for their support of this important event.

I would also like to invite all participants in expressing our appreciation to all members of the FoITIC 2021 organizing committee for their hard work in making this conference successful.

Finally, we wish you all fruitful networking during the conference, and we do hope that you will reap the most benefit of it.

Thank you!

Dr. Jono Suhartono

Dean Faculty of Industrial Technology – Institut Teknologi Nasional Bandung

ACKNOWLEDGEMENT

The completion of this undertaking could not have been possible without the participation and assistance of so many people whose names may not all be enumerated. The contributions are sincerely appreciated and gratefully acknowledged. However, we would like to express our especial deep appreciation and gratitude to the following:

1. Institut Teknologi Nasional Bandung (Itenas) – Indonesia
2. Hungarian University of Agriculture and Life Science - Hungary
3. Slovak University of Agriculture in Nitra – Slovak Republic
4. Institute of Agrophysics Polish Academy of Sciences - Poland
5. Universiti Sains Malaysia - Malaysia
6. Saudi Aramco – Saudi Arabia
7. Indonesian Society for Reliability (ISR) – Indonesia
8. IEEE Society on Social Implications of Technology (SSIT)

KEYNOTE AND INVITED SPEAKERS INTERNATIONAL CONFERENCE

Prof. Istvan Seres (Hungarian University of Agriculture and Life Sciences)

Prof. Dr. Istvan Farkas is a university professor and researcher at Hungarian University of Agriculture and Life Sciences, Gödöllő – Hungary. He also a core member and administration coordinator of MATE Doctoral School of Mechanical Engineering. He got his Ph.D in Agricultural Engineering from Szent Istvan University. He published 227 scientific publications, 1 monograph and professional books, 4 monograph/books in which chapters/sections were contributed, and 189 independent citations to his publications and creative works. His research area focused on physics education, solar energy utilization, sensor and measurement.

Prof. Istvan Farkas (Hungarian University of Agriculture and Life Sciences)

Prof. Istvan Farkas is professor emeritus at Hungarian University of Agriculture and Life Sciences, Gödöllő. He is a core member of MATE Doctoral School of Mechanical Engineering, academic staff member of BME Géza Pattantyús-Ábrahám, Doctoral School of Mechanical Engineering and Academic staff member of MATE Festetics Doctoral School. He got Doctor of Science Degree in 1993 from HAS University. He has published 1082 scientific publications, 4 monograph and professional books, and contributed in 22 monograph/books. His research area is in modelling & computer simulation, process control identification and optimization, heat and mass transfer processes (drying, greenhouse processes), and solar energy applications. Presently, a lot of his activities devotes on International professional societies such as: International Solar Energy Societies (ISES), International Federation of Automatic Control (IFAC), European Federation of Chemical Engineering (EFChE), European Thematic Network on Education and Research in Biosystems Engineering, European Network on Photovoltaic Technologies, FAO Regional Working Group on Greenhouse Crops in the SEE Countries, Solar Energy Journal Associate Editor, Drying Technology Journal Editorial Board, etc. He was a visiting Professor in several universities: Solar Energy Applications Laboratory, Colorado University State University, Fort Collins - USA; Department of Energy, Helsinki University of Technology, Espoo - Finland; Institut for Meteorology and Physics, University of Agriculture Sciences, Vienna - Austria; Laboratory of Bioprocess Engineering, The University of Tokyo - Japan.

Prof. Jozef Horabik (Institute of Agrophysics of the Polish Academy of Sciences)

Prof. Jozef Horabik is a professor at Bohdan Dobrzański Institute of Agrophysics, Polish Academy of Sciences, Lublin, Poland. In 1986, he got his PhD in Technical Science from Faculty of Agriculture Engineering, University of Agriculture in, Lublin, Poland. In 2003, he is appointed as Professor in Agricultural Science in Institute of Agrophysics PAS, Lublin, Poland. He is a membership of American Society of Agricultural and Biological Engineers, Polish Society of Agrophysics, Polish Society of Agricultural Engineering and

Committee of Agrophysics of PAS. He has 94 publications and 1237 citations to his publications. His expertise are mechanical properties, material characteristics, mechanical behavior of materials and mechanical testing. Currently, he is is a Director of the Institute of Agrophysics, Polish Academy of Sciences Lublin, Poland. He also works as an Editor in Chief of Acta Agrophysica, Associated Editor of International Agrophysics, Member of Editorial Board of Polish Journal of Soil Science. He actively cooperates with over 20 scientific institutions in Poland and abroad. Over 260 scientific publications. His research interests are in applied physics, agrophysics, physical properties of agro-materials, modeling of mechanics of granular solids and food powders.

Prof. Zuzana Hlavacova (Slovak University of Agriculture)

Prof. Zuzana Hlavacova is a professor at Slovak University of Agriculture, Slovakia. She's also managing director at Department of Physics. She obtained her Ph.D. in Moisture content metrology from the Slovak University of Agriculture in Nitra, Slovakia, RNDr.. Her area of interest related to electrical properties of biological materials, electrical properties utilization in agriculture and food processing, physical properties of food, and biophysics. She has published 58 publications and got 156 citations to her publications. She gain award from Ministry of Education, Science, Research and Sport of the Slovak Republic on March, 2019.

Dr. Husnul Azan Bin Tajarudin (Universiti Sains Malaysia)

Dr. Husnul Azan Bin Tajarudin is a Associate Professor and Deputi Dean (Academic, Career & International) at School of Industrial Techonology, Universiti Sains Malaysia. He obtained his Ph.D form Swansea University, UK. His area expertise are fermentation technology, waste treatment through bioprocess technology and bioprocess technology. He has published 121 scientific publications with 704 citations to his publications.

Dr. Hasan Al Abdulgader (Saudi Aramco)

Dr. Hasan Al Abdulgader is a Head of Produced Treatment R&D Program at Saudi Aramco. He is an adjunct professor in Chemical Engineering at King Fahd University of Petroleum and Minerals. He is also Member of The Board of Advisors at KFU College of Engineering. He got his Ph.D in water processing engineering from Swansea University in 2014 where he did his research project at the Centre for Water Advanced Technologies and Environmental Research (CWATER). He has established a proven track record of industrial, research and academic experience in water treatment and desalination.

Dr. Dwi Kurniawan (Institut Teknologi Nasional Bandung)

Dr. Dwi Kurniawan is an Associate Professor and the Head of Industrial Engineering Master Program, Institut Teknologi Nasional, Bandung, Indonesia. He received his BS, MSc and Doctor from Industrial Engineering Department, Bandung Institute of Technology (ITB), Indonesia. He teaches and conducts research in production planning and

controlling, operations research and research methodology. He currently published his research in JIEM, IJMR, and in Asia Pacific Industrial Engineering and Management Society (APIEMS) conference proceedings.

LIST OF CONTENTS

Preface: The Rector of Itenas Bandung	vii
Preface: The Dean of Faculty of Industrial Technology / Chairman of FoITIC 2021	viii
Acknowledgement	ix
Keynote and invited speaker International Conference	x
Hanifah Apriliani, Fadillah Ramadhan, Sugih Arijanto	The Influence of TOE Framework on Social Media Adoption to Improve MSME Performance During the Covid-19 Pandemic 1
Yudistira Ridla Ichfany , Yanti Helianty	Minimization of Return Product by Implementing Deming Cycle and Quality Loss Function 6
Hadida Dellasaviaputra, Fadillah Ramadhan	Design of Profile Matching Decision Support System Software Against E-Commerce Selection for Sellers 15
Ghifari Hamzah, Fadillah Ramadhan	Production Scheduling Software Design Using First In First Out and Earliest Due Date Methods at PT. Synergy Gem Creations 27
Doddy Mudhoffar, Lauditta Irianti	Proposed Improvement Of The Quality Of Screen T-Shirt Products At Pt. Indo Anugerah Semesta 38
Muhammad Farhan Mustaqim, Eka Taufiq Firmansjah P.A	Control Making for Elevator Simulation of Three Floor Building Based on Arduino Uno 49
Hendriksen Samuel K , Marsono	Manufacturing and Testing Static of Rear Suspension System KMLI Car 54
Dony Perdana	The Role Of Nitrogen Gas And Variations Of The Magnetic Field On The Characteristics Of Flame On Combustion Of Premixed Vegetable Oil Blends (B50) 61
Asaad Yasseen Al-Rabeeah, Istvan Seres, Istvan Farkas,	Performance Enhancement Of Ptsc By Using Mono And Hybrid Nanofluids 67
Moch Rizal Priatna , Wima Haikal Palit, Ronny Kurniawan	Effect of Hydrolysis Temperature and Acid Solution Concentration on Hydrolysis of Hyacinth 74
Apriliana Dwijayanti , Safril Kartika	Isolation Of Linalool From Coriander Seeds By Soxhlet Extraction Method 83
Ichsan Nurmansyah , Waluyo, Dini Fauziah	Illumination and Power Monitoring on Internet of Things-Based Solar Panels 88
Matúš Bilčík, Monika Božiková, Ľubomír Kubík, Ján Csillag, Patrik Kósa, Tímea Szabóová, Ján Čimo, Ľuboš Moravčík, Stanislav Paulovič	The Power Comparison Of Photovoltaic Modules Different Types 97
Muhammad Arif Ramdani	Data Communication On Motorcycle Rental Based On Internet Of Things 101
Fadli Padriyana	Lora Data Communication For Fishing Boat Monitoring 106

Ceppy Ari Sugiharto, Decy Nataliana, Niken Syafitri	Implementation of Human Detection on Robot Prototype Using Admp401 Sensor	115
Silviana Dwi Cahyani, Hendi Handian Rachmat	Web Camera-Based Spectrometer System Precision Testing in Wavelength Measurement	125
Tubagus Nur Muhammad Rizqi Zakaria, Fahmi Arif	Automatic Fish Feeder Design Based on IoT	129
Ahssan Alshibil, Piroška Vig, Istvan Farkas	Seasonal Performance Evaluation of Hybrid Solar Collectors in a Hot Climate Area	136

The Influence of TOE FRAMEWORK on Social Media Adoption to Improve MSME Performance during the COVID-19 Pandemic

Hanifah Apriliani^{1,a)}, Fadillah Ramadhan¹, Sugih Arijanto¹

¹Department of Industrial Engineering, Institut Teknologi Nasional Bandung

^{a)}Email : hanifah2526@mhs.itenas.ac.id

Abstract. Micro, Small and Medium Enterprises (MSME) play an important role in the Indonesian economy. The large number of MSME causes MSME to support the Indonesian economy. The Covid-19 pandemic that occurred in Indonesia had an impact on the Indonesian economy. The Covid-19 outbreak has resulted in several businesses experiencing a decline due to the declining Indonesian economy. The use of social media can help businesses in terms of marketing. Factors that can influence the adoption of social media by SME are technological, organizational and environmental factors. Factors that influence the adoption of social media can be seen by conducting a survey on MSME and using the PLS-SEM method. The results of the research conducted, technological factors are the most influential factors in the adoption of social media. The recommendations given are recommendations to increase social media adoption and strategies to improve MSME performance.

INTRODUCTION

Micro, small and medium enterprises are the main actors of the Indonesian economy. The contribution of micro, small and medium enterprises to Gross Domestic Product in Indonesia is about 60%. Micro, Small and Medium Enterprises (MSME) play an important role in anticipating the future economy. According to data from the Central Statistics Agency, the number of MSME spread across Indonesia reached 64 million and 99.9% of its efforts supported the Indonesian economy[1]. Indonesia's economy is currently looking at the results of the Central Statistics Agency, Tauhid Ahmad as Executive Director of the Institute for Development of Economics and Finance said it can be expected that the Indonesian economy will fall into the category of recession due to the COVID-19 pandemic period.

The economic impact of the COVID-19 pandemic is also experienced by MSME in Indonesia. This was revealed based on the results of research conducted by the Indonesian Institute of Sciences (LIPI) which showed a decrease in MSME performance due to Covid-19. This shows that there needs to be a way for MSME to stay afloat in Indonesia even in the midst of pandemic conditions. One way that can be used is the use of social media as a source of marketing for MSME products. The application of digitalization will facilitate in facing the current conditions, and also facilitate the exchange of technology to MSME so that they can survive in business competition Social media that can be used for marketing products such as social media Instagram, Facebook, Twitter and others. Currently MSME have not fully implemented the use of social media to help market their products. This prompted some researchers to conduct research on the influence of technological, organizational and environmental factors on social media adoption to improve MSME performance. Research has been conducted in the United Arab Emirates [2] that examined the influence of TOE on social media adoption and its effect on MSME performance. Another study was conducted in jogja [3] to examine the technological, organizational and environmental aspects of social media adoption and the influence of adoption on social media awareness. Another study [4] examined instagram's social media use and its effect on MSME performance.

From the results of previous research, there are several different opinions. The bandwagon effect is the variable that most influences social media adoption in previous research[2]. Environmental uncertainty became one of the factors of social media adoption in the city of Jogja during the Covid-19 pandemic. In the instagram social media

adoption study [4] interactivity has a fairly strong influence on the adoption of Instagram social media. The objectives of this study are: (1) identify the influence of technology, organization, and environment on social media adoption (2) identify the influence of social media adoption on the performance of MSME (3) provide recommendations for Increase the adoption of social media.

RESEARCH METHODOLOGY

Research Methods

Partial Least Square – Structural Equation Modeling (PLS-SEM) is a method that can be used to test and analyze hypotheses in research models. Model evaluation can be done by evaluating the outer model to measure the validity and reliability of the model and evaluating the inner model to predict the causal relationship between latent variables [5].

Research Model

This study consists of 4 research hypotheses that will be tested. The research model consists of technological, organizational and environmental factors that influence social media adoption and the influence of social media adoption through MSME performance. Figure 1 shows the new research model used in the study.

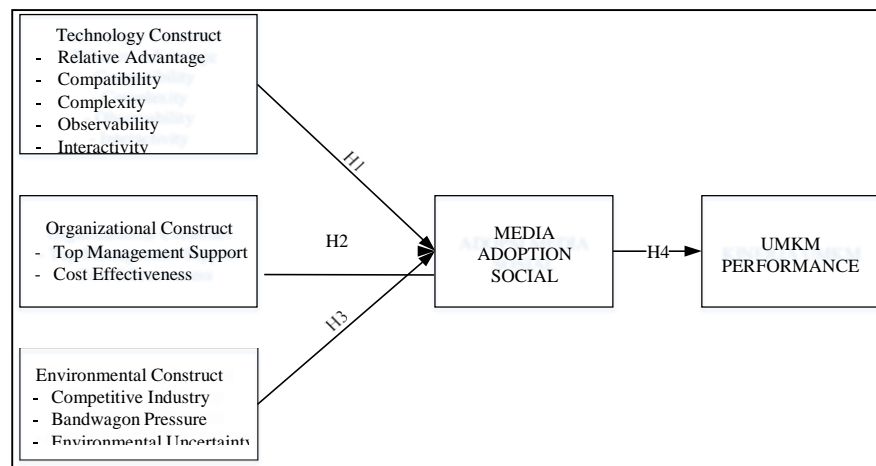


Figure 1. Research Model

The technological context is the technical knowledge necessary for the use of social media. The technological context refers to internal and external technologies that have benefits to the company. Relative excellence means the extent to which an idea or innovation is considered better than a pre-existing idea. Compatibility means whether an innovation is consistent with other technologies already used in the organization. Complexity means the extent to which innovation is perceived as difficult to use, the adoption of innovation will increase if innovation is perceived as easy to use. Observability is the extent to which the results of the application of an innovation can be seen. Interactivity is communication that occurs to elicit consumer responses.

H₁. Technology has a significant and positive influence on the adoption of social media by MSME.

Organizational context is a variety of internal organizational factors that have the potential to influence the adoption and implementation of innovation. Top management support is essential to building a supportive environment and also providing sufficient resources for innovation implementation. Cost effectiveness is the financial advantage for a company that can be gained from the adoption of an innovation.

H₂. Organizations have a significant and positive influence on the adoption of social media by MSME.

The environmental context relates to the social and business context of companies such as infrastructure, industrial

competition and customer sentiment. Competitive industry is a pressure that arises as a result of the threat of losing competitive advantage. Bandwagon effect is the phenomenon of decision making by a person or organization that is influenced by decisions taken by the majority. Environmental uncertainty consists of conditions that change very complex and rapidly.

H3. The environment has a significant and positive influence on the adoption of social media by MSME.

Various studies have found that social media adoption is identified as a positive influence on business performance. Instagram adoption has a positive effect on business performance. In the United Arab Emirates, the adoption of social media has a positive effect on the performance of SME. Relationship adoption social media and business performance occurs because social media provides benefits, influences purchasing decisions and positively impacts financial and non-financial performance.

H4. The adoption of social media has a significant and positive influence on business performance.

Data Collection

The survey was conducted by distributing questionnaires. Questionnaires are distributed online using google form to MSME in Bandung. Purposive sampling was used in this study. This sampling technique requires respondents who will fill out a questionnaire according to predetermined criteria. Of the total data, 90 data can be processed for this study.

Data Processing

The research instrument consists of 22 items adopted from the literature and adapted to the item, so that the item can be used for research. The test that can be done is testing the outer model and the inner model. Based on the results of these responses, research instruments can be tested for validity and reliability as well as outer model testing. Validity testing is divided into convergent validity and discriminant validity. Internal model testing is done to test hypotheses from between variables.

FILL

Measurement Model Assessment (Outer Model)

In the convergent validity test there are 4 invalid items, so they are omitted. Once the item is omitted, the results of the measurement of validity and reliability can be seen in Table 1 and Table 2. Based on these results, valid and reliable measurement models mean outer loading > 0.7 ; AVE > 0.5 ; the root of AVE $>$ correlation between constructs; alpha cronbach > 0.6 ; and composite reliability > 0.7 [6]. The results of the validity and reliability test can be seen in Table 1 and Table 2.

Table 1. Outer Model Calculation Results

Construct	AVE	(Root) AVE	CR	CA
Technology	0.596	0.772	0.880	0.830
Organization	0.610	0.781	0.825	0.700
Environment	0.623	0.789	0.868	0.798
Social Media Adoption	0.619	0.787	0.829	0.693
Business Performance	0.572	0.756	0.800	0.628

Table 2. Correlation Matrix Between Variables

Variable	Technology	Organization	Environment	Social Media Adoption	Business Performance
Technology	1.000				
Organization	0.526	1.000			
Environment	0.563	0.430	1.000		
Social Media Adoption	0.588	0.475	0.541	1.000	
Business Performance	0.665	0.415	0.604	0.505	1.000

Structural Model Assessment (Inner Model)

Hypothesis testing is done by calculating the values t and p-value. All hypothetical relationships are supported except H3 (t = 1.346; p-value = 0.179). H1 (t = 3.138; value p = 0.002), H2 (t = 2,899; p = 0.004) and H4 (t = 6.885; p value = 0.000). The results of the model's inner testing can be seen in Table 3, Table 4 and Table 5.

Table 3. Inner Model Test Results Based on Calculated T

Variable	T _{count}	Reference T _{count}
Technology - > The Adoption of Social Media	3.138	1.96
Organizations - > Social Media Adoption	2.899	1.96
Environment - > Social Media Adoption	1.346	1.96
Social Media Adoption -> Performance	6.885	1.96

Table 4. Inner Model Test Results Based on P-Values

Variable	P- values	Reference p-values
Technology - > The Adoption of Social Media	0.002	0.05
Organizations - > Adoption of Social Media	0.004	0.05
Environment - > Social Media Adoption	0.179	0.05
Social Media Adoption -> Performance	0.000	0.05

Table 5. Inner Model Test Results Based on Original Sample

Variable	Original Sample	Direction Relationship
Technology -> Social Media Adoption	0.43	Positive
Organizations -> Adoption of Environmental	0.292	Positive
Social Media -> Social Media Adoption	0.145	Positive
Social Media Adoption -> Performance	0.562	Positive

ANALYSIS

Based on the results of structural model measurements, technological constructs have a significant influence on social media adoption. [3]explained that MSME began using internet technology for adoption because during COVID-19 MSME could not do offline marketing due to rules of working from home and advice to stay at home. These findings are incompatible with previous research [2] which noted that the link between technology and social media adoption is irrelevant in United Arab Emirates MSME. These results show that social media is an easy to use technology, in accordance with the company's strategy and profitable for the company.

Based on the results of structural model measurements, organizations have a significant influence with the adoption of social media. [3]explained that during the COVID-19 pandemic, MSME managers work with their companies to prepare their online marketing infrastructure. Top management at their companies is looking for more knowledge about social media. Ahmad's findings [2] show that social media adoption in MSME is directed by top management. Top management support seems to have an important role in helping facilitate employees to implement social media. The cost effectiveness gained from using social media also provides an advantage for companies, as social media can

help for online marketing that has lower costs than offline marketing. Another factor that can be observed from organizational factors is the availability of good human resources to support the adoption of social media in the company.

Based on the measurement results of structural models, the environment is irrelevant to the adoption of social media. [3] found that environmental context has a significant influence on social media. The condition of sales uncertainty makes MSME managers increasingly aware of the existence of social media. [2] found that the main environmental factors that affect MSME using social media are simply the bandwagon effect. Based on the results obtained, respondents using social media were not influenced by industry competition factors, participating effects and environmental uncertainties. MSME use social media due to considerations regarding suitability with the company or because of the benefits for the company. This is supported by the significant technological factors that see the suitability of the technology adopted with the company's strategy and also the benefits that can be obtained for the company such as cost effectiveness. This can be seen as an organizational factor. Another factor that can be observed from the environment is government support, because there is currently a government movement such as MSME Go-Online which could be the influence of MSME adopting social media.

Based on the results of structural model measurements, social media adoption is relevant to business performance. Previous research explained that the adoption of social media has an impact on the performance of MSME such as increasing sales volume, number of customers, quality of service, company image which will have an impact on increasing MSME profits. Another factor that can be observed from performance is the expansion of the market that occurs.

CONCLUSION

This research discusses the influence of technology, organization and the environment on social media adoption and the influence of social media adoption on business performance. Technology and organizations are related to the adoption of social media and the adoption of social media related to business performance. The environment is not related to the adoption of social media, this may be because many companies have adopted social media related to the benefits of using technology for companies and organizational strategies or goals. Adoption of social media is done by companies not because the environment also adopts, or because of industry competition and environmental uncertainties that occur complexly and quickly. The influence of SME social media adoption on business performance can help SME cope with the impact of the COVID-19 pandemic and SME can help the country's economy.

BIBLIOGRAPHY

1. S., Sugianti, "Peran Usaha Mikro Kecil dan Menengah (UMKM) dalam Mensejahterakan Karyawan di Pusat Oleh-Oleh Mak Denok Desa Serdang Jaya Kabupaten Tanjung Jabung Barat", *Repository UIN Sulthan Thaha Saifuddin*, (2019).
2. S.Z., Ahmad, A.R.A., Bakar, and N., Ahmad, "Social Media Adoption and Its Impact On Firm Performance: The Case Of The UAE", *International Journal of Entrepreneurial Behavior & Research* (2018).
3. M.I., Effendi, D., Sugandini, and Y., Istanto, Y., "Social Media Adoption in SME Impacted by COVID-19: The TOE Model", *Journal of Asian Finance, Economics and Business*, 7 (11), pp.915-925 (2020).
4. L., Soelaiman, and A.R., Utami, "Faktor-faktor yang Mempengaruhi Adopsi Media Sosial Instagram dan Dampaknya Terhadap Kinerja UMKM", *Jurnal Muara Ilmu Ekonomi dan Bisnis*, 5 (1), pp. 124-133 (2021).
5. J.F., Hair, W.C., Black, B., Black, B.J., Babin and R.E., Anderson, *Multivariate Data Analysis (7th Edition)*
6. I., Ghazali, *Structural Equation Modeling, Metode Alternatif dengan Partial Least Square (PLS)* (Semarang : Badan Penerbit Universitas Diponegoro, 2014).

Minimization of Return Product by Implementing Deming Cycle and Quality Loss Function

Yudistira Ridla Ichfany^{1,a)}, Yanti Helianty¹

¹Department of Industrial Engineering, Institut Teknologi Nasional Bandung

^{a)}Email: yudistiraridlaichfany@gmail.com

Abstract. The rapid development of the industry requires every company to make efforts to control and reduce the number of product returns, so that the company does not suffer losses continuously. In this study, problems were identified according to the company's business process flow, calculating losses using the Quality Loss Function (QLF) approach, implementing the deming cycle as an effort to reduce product returns by providing SOPs, work instructions, and checking forms in the section associated with the source. the occurrence of product returns, as well as calculating losses after implementation using Quality Loss Function (QLF). From the results of monitoring after implementation, there is a decrease in the number of return products. Before the implementation of the average product return of 4.19% per month, the lowest rate of return occurred in December 2020, which was 1.96% with a loss of Rp. 383.543.63. After the implementation, there was a decrease in the percentage of the number of return products to 1.63% with a loss of Rp. 195.685.50.

INTRODUCTION

Background

Currently the development of the industry in Indonesia is growing so rapidly along with the company's competition to be able to meet consumer demand. The company must be competitive in thinking creatively and able to innovate in carrying out strategies that can compete against its competitors by producing good quality products, low prices, and fast service. Product quality has an important role in the reputation of manufacturing companies to create consumer confidence, in addition, aspects of product quality produced can also be used as a standard for the company's readiness to compete with similar competitors[1].

The company studied is one of the manufacturing industries in Bandung Regency engaged in textile with products produced in the form of fabric dye powder. The company manufactures dyes according to demand from fixed consumers and other consumers according to demand. To maintain the quality of its products, the company has established a product inspection system in the production section by conducting two inspection stages, namely, the first stage of conducting color concentration checks using rapid machines during the production process. The examination technique at this stage is carried out with technical sampling techniques. The second stage is inspection of the packaging process, at this stage is done only with visual techniques seen from the feasibility of the case.

Consumer demand for fabric dye powder products fluctuated each period, recorded an average demand in February 2020 to January 2021 as much as 9,308.75 kg or 372.35 box per month. During this period there has been an average monthly product development of 389.58 kg. It can be calculated that the percentage of return of defective products that occur is 4.19% per month or equivalent to 15.58 box. Based on the report recorded, the return of the product caused by a torn packaging seal, products contaminated with metal or foreign objects, clumping products, and the exchange of color concentration labels on the packaging. While the company's management has set a product return limit of 5 box per month. The high return of the product has an impact on the company's losses, because the company

has to reimburse the cost of the failed product. For that, efforts need to be made that can reduce the number of return products.

Problems

One of the manufacturing industry companies engaged in textiles in Bandung Regency has problems regarding the high number of return products. This is because the company has not established a sustainable quality control system all parts of the organization. It can be known that the four types of defects stem from the absence of quality control systems in the ware house and logistics (delivery), therefore the company needs a quality management plan in each section in order to reduce the number of product returns each month.

Research objectives

Based on the explanation outlined in the previous section, this study will be carried out efforts to apply the Deming cycle to the part associated with the type of defect in the company so that it is expected to reduce the return of the product that occurs.

METHODOLOGY

Total Quality Management (TQM) is defined as a way to improve continuous performance improvement in all parts of the organization using all available human resources [2]. As for the benefits of TQM's implementation with deming cycle approach for the company, one of which is to avoid quality deviations generated in the company's business process flow, the resulting products will be in accordance with standards, eliminate rework, improve work time, reduce machine work, and save material use. While Quality Loss Function (QLF) is a mathematical approach used to see the large losses experienced by companies due to defective products [3].

To solve the problem in this study will be carried out systematic steps, the description of the methodological steps can be seen in the following description:

1. Identify the company's business process, this step is done to trace or identify defects found to come from which part of the process in the company. Identifying the company's business process is done to find out the production flow that starts from the beginning of the purchase of raw materials to the end until the product is accepted by consumers and can know the problems that occur in the company thoroughly in each part.
2. Identify the cause of disability on the part of the company, after knowing the process in each part with the company's business process, then the next stage is to identify the problems that occur in the part that causes the defect to occur. This stage is carried out to find out the root cause of the types of defects that occur in the company. To find out the root of the problems that occurred in this study using 5W + 1H tools.
3. Proposed application of Deming cycle, Deming cycle consists of stages Plan, Do, Check, Action involving all resources power in improving the quality of a product produced and carried out in a sustainable manner [4]. The application of deming cycle is done on the part that causes the return of product in the company. Plan, carried out the preparation of a quality plan on the part that has been identified the problem has a relationship with the type of defect that occurs. Do at this stage carry out improvement proposal activities in accordance with the results of the quality management plan in the company's business process using the Deming cycle principle, this principle is used as a framework that directs the organization to improve its performance in a sustainable manner (continuous improvement). Check after the implementation of the Deming cycle in the environment for 1 month, the next stage will be recalculated the percentage of the number of product returns that occur at the time after implementation. This examination process is carried out to prove whether the planning and implementation process that has been carried out in accordance with the target or purpose of this research in reducing the number of product returns. Action, adjustment actions are carried out based on the analysis of results at the check stage. The adjustment process can be in the form of setting new standardization in the company environment in accordance with the results of the Dostage. If the implementation phase of the Deming cycle in the company environment can reduce product returns and reduce losses then the establishment of new standardization needs to be applied by the company. These stages are carried out to maintain or avoid the onset of the same problem repeated, and is done as a new target for the next improvement [5].
4. Analysis, at this stage is done to see if with the application of deming cycle in the company environment can reduce the amount of product return. At this stage of analysis will be done a percentage of the amount of product

return and the amount of losses due to return on conditions before and after the Deming cycle is applied. The results of this analysis are expected to provide an over view to the company of the importance of making quality improvements based on the Deming cycle and can help over come the company's hopes in controlling the quality of its products.

RESULTS AND DISCUSSIONS

Research Results

In this section explained about the results of the research conducted, the results of the study consisted of identifying the company's business process, identifying the cause of disability on the part of the company, and proposing the application of siklus Deming. The results of the study can be seen in the following description.

Identify the Company's Business Process

Identifying the company's business process is done to find out the production flow that starts from the beginning of the purchase of raw materials to the end until the product is accepted by consumers and can know the problems that occur in the company thoroughly in each part. For the results of the company's business process identification can be seen in Figure 1.

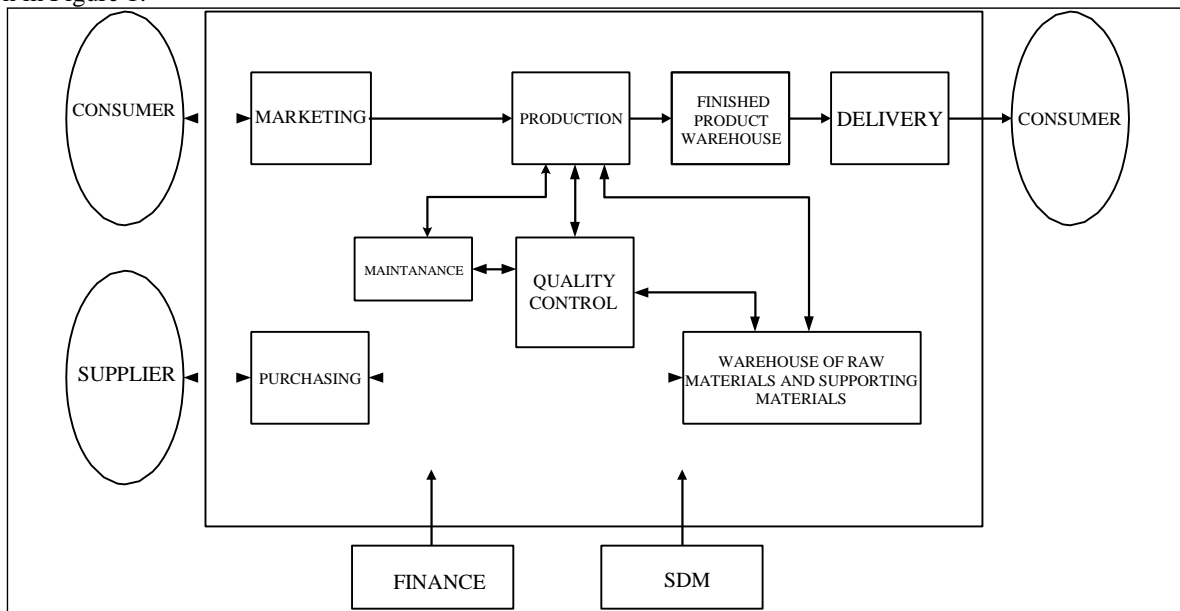


Figure 1. Enterprise Business Process

Based on the results of the company's business process identification, the process flow can be traced to the source of the problem that occurs in the company, the results of the process description associated with problems in the type of defect that occurred can be seen in Table 1.

Identify the Cause of Disability on the Company's Part

Based on data on the type of defect that occurred, namely the defect of the torn packaging seal, contaminated products of foreign objects, clumping products, and the exchange of packaging labels, the 5W + 1H tool was used n n to find out the root of the problems that occurred in the company environment. For the results of identifying the source of the problem associated with the type of defect that occurred can be seen in Table 2 through Table 5.

TABLE 1 Identification of Process Description In Part Associated with Types of Defects

No	Division	Process Description
1	Delivery	Employee delivery in the process of transferring the finished product is carried out in arbitrary or rough and do not do the process of checking the condition of the feasibility of the transport car. The condition of the transport car is not feasible one of them can cause potential product defects such as water seepage when it rains and the tearing of plastic seals.
2	Finished Product warehouse	The finished product warehouse only conducts the packaging process and checks the feasibility of the case and does not check again when the production operator provides a report of the production results that will go into the warehouse for packing.
3	Maintenance	The process of activities carried out only performs repairs when the machine is already said to be damaged and there has been no preventive action to prevent engine damage. When repairing the machine in the middle of the production process, the condition of raw materials is still in the machine, thus allowing the contamination of products with foreign objects during the repair process.

TABLE 2 Results of Identification of Problems Due to Types of Torn Packaging Seal Defects

No	Aspects	Description
1	Why	The process of transferring the finished product to a transport car is done roughly and has not added a check of the feasibility of the transport car.
2	Where	Problems occur in the delivery section.
3	When	A problem occurs in the last year.
4	Who	Employee delivery.
5	How	The problem is solved by providing Standard Operating Procedure and construction of the feasibility work of transport cars (with Add pallets).

TABLE 3 Results of Identification of Problems Due to Types of Defects in Foreign Contaminated Products

No	Aspects	Description
1	What	Products are contaminated with metals/foreign bodies (box).
2	Why	1. The packaging process is done arbitrarily so that it allows the product to be contaminated 2. The process of repairing machinery carried out by maintenance employees is carried out during the production process by not removing products in the machine.
3	Where	1. Problems occur in the packaging. 2. The problem occurs in the maintenance section
4	When	A problem occurred in the last year.
5	Who	1. Employee packaging. 2. Maintenance employees.

TABLE 3 Results of Identification of Problems Due to Types of Defects in Foreign Contaminated Products (continue)

No	Aspects	Description
6	How	1. The problem is solved by providing proposed standard operating procedures and work instructions in the process packaging.
		2. The problem is solved by providing a proposed standard operating procedure and proposed preventive repair schedule of the average engine replacement period.

TABLE 4 Results of Identification of Problems Due to Types of Clumping Product Defects

No	Aspects	Description
1	What	Clumping products (box).
2	Why	The process of delivery is not safe, delivery is done without the use of a cover to protect the product.
3	Where	The problem occurs in the delivery section
4	When	A problem occurs in the last year.
5	Who	Employee delivery.
6	How	The problem is solved by providing Standard Operating Procedure and receipt of the feasibility of the transport car (by adding a tarp as a product cover during the delivery process).

Table 5 Results of Identification of Problems Due to Types of Defects Changed Color Concentration Label

No	Aspects	Description
1	What	The color concentration label (box)
2	Why	Lack of thoroughness when the process of inserting the finished product into box, resulting in the inclusion of packaging labels sent to the consumer
3	Where	The problem occurs in the packaging section
4	When	A problem occurs in the last year
5	Who	Employee packaging
6	How	The problem is solved by providing satandard operating procedure and work instruction in carrying out the process packaging

Based on the analysis of 5W + 1H above can be known the cause of disability experienced by the company.

Proposed Implementation of Deming Cycle

Deming cycle proposal is done to reduce the number of product returns by applying an approach where quality is continuous. The Deming cycle consists of plan, do, check, and action stages. The following proposed application explanation can be seen in the description below.

1. Plan, this stage will be given a quality planning proposal in the delivery, warehouse, and maintenance sections. The proposal plan given one of them in the delivery section in the form of the application of Standard Operating Procedure and work instructions, to support performance on its part is also given a checking form. This is given because the company has not fully carried out the quality management process in an ongoing manner and there has been no record of established standards.
2. Do, the proposal process in all parts of di is done or implemented in the company environment for one month. Due to time constraints in the research process, at this stage, the implementation is only 1 month, namely in June 2021. The proposals given are expected to be implemented continuously by the company in the future.
3. Check, the process of monitoring from the previous stage, seen the conformity of the results with the purpose of this study. This stage calculates the amount of decrease in product return caused by each way and performs the calculation process after the implementation of deming cycle implementation in the company environment.
4. Action, provides new standardization by implementing Standard Operating Procedures (SOP) and work instruction in the company environment. One of the proposals made new standardization by the company is in the employee delivery section. The proposal can be seen in Figure 2 through Figure 4.

DISCUSSION

Based on the results described in the previous section, by applying the Deming cycle to the part related to the type of defect that occurred, there was a decrease in the number of return products. The time before implementation has an average value of product return in one year of 4.19% or equivalent to 15.58 box per month. The smallest product return value was in February 2020 of 1.96% or equivalent to 7 box. After implementing the Deming cycle, the return of products in June 2021 to 1.63% or equivalent to 5 box. The implementation of quality management onan ongoing basis by implementing the Deming (plan-do-check-action) cycle in the company environment can have a very significant impact, especially in reducing the amount of product returns and losses of the company. To measure the extent of the reduction in losses experienced by the company, it can be calculated using the Quality Loss Function formula. Delivery employee instruction can be seen in Figure 2

Work Instructions for Handling and Transfer of Finished Products to Transport Cars	
	<ul style="list-style-type: none">• Prepare a handtruck that will be used to move the finished product into the transport car.• Fill in the form for checking the feasibility of the transport car.• Clean all sides of the tailgate to avoid foreign objects.• Install the pallet on the base of the car.• Move the finished product in the warehouse into a transport car using a handtruck.• Carry out the process of stacking finished products in the car body with a maximum limit of 3 piles.• Cover the pile of finished products in the tailgate using a tarp.• Glue and tie the tarp using a rope to the side of the tailgate.

Figure 2. Delivery Employee Work Instructions

Standar operating procedure employee can be seen in Figure 3

Standard Operating Procedure (SOP) Process of Handling and Transferring Finished Products to Transport Cars		No. Document : - Date of Enactment : June 10, 2021 Revision to : - Revised Date : - Page : 1	
<p>▼ 1. Purpose Ensuring the process of handling and transferring the finished product into the transport car is maintained in quality and</p> <p>▼ 2. Equipment used a. Handtruck . b. Pallet .</p> <p>▼ 3. Parties involved a. Finished Product Warehouse Division(warehouse). b. Employee Delivery.</p> <p>▼ 4. Documents used a. Report the number of finished products. b. Work instructions for handling and transferring the finished product to a transport car c. Form checking the feasibility of the transport car.</p> <p>▼ 5. Implementation procedures a. Receive a report on the number of finished products from the warehouse. b. Check the feasibility of the transport car using the checking form that has been provided. c. Move the finished product from the warehouse to the transport car in accordance with the direction of the work instructions given. d. Send the finished product to the consumer.</p>			
Disposition	Name	Position	Signature
Proposed by			
By			
Approved by			

Figure 3. Standard Operating Procedure Employee Delivery

Form checking for cars feasibility can be seen in Figure 4.

TRANSPORT CAR FEASIBILITY CHECKING FORM		
Driver Name		
Day/Date		
Freight Car Feasibility	Condition of Transport Car	
	Standard	Fit in the field
Car equipment		
Sheeting	Available	
Tarpaulin Condition	Not Leaking	
Pallet	Available	
Pallet Condition	Not broken	
STNK	There and Still Happens	
KIR Book	There and Still Happens	
Driver's License	There and Still Happens	
The condition of the car <i>pickup</i>		
Cleanliness (floor and side of cover)	Clean	
Containers free of nails and loose tonnes of bolts	Not Last	
The vehicle tub is not hollow	Not hollow	
Vehicle Safety Equipment		
Tire Condition	Thick and has contours	
Brake Condition	Bold Canvas	
Tire Pressure	Tidak Kempes (>35 psi)	
RearView Mirror (2 pieces)	Function	
Lights (near and far)	Function	
Penny Lamp	Function	
Horn	Function	
Spare Tire (1buah)	Available	
Safety <i>Hazard Sign</i>	Available	
First aid box	Available	
Proposed by	Checked and Approved by	
Head of Warehouse & Expedition		
Approval Date :/ / 2021 <div style="display: inline-block; vertical-align: middle; margin-left: 20px;"> Sr <div style="display: inline-block; vertical-align: middle; margin-left: 10px;"> <div style="border: 1px solid black; width: 30px; height: 20px; display: flex; align-items: center; justify-content: center;"> <div style="width: 10px; height: 10px; background-color: white; margin-right: 5px;"></div> <div style="width: 10px; height: 10px; background-color: white; margin-right: 5px;"></div> </div> <div style="display: flex; flex-direction: column; margin-left: 5px;"> <div style="font-size: 8px;">Accepted</div> <div style="font-size: 8px;">Rejected</div> </div> </div> </div>		

Figure 4. Form Checking the Feasibility of Transport Cars

Examples of Quality Loss Function calculations before and after applying the Deming cycle are as follows.

$$\begin{aligned} \text{Calculate constant value } K &= \frac{A}{\Delta^2} \quad (1) \\ K &= \text{Rp. } \frac{1.900.000,00}{(15,58^2)} \\ K &= \text{Rp. } 7.827,42 \end{aligned}$$

a) Calculation of Quality Loss function before applying deming cycle from the average number of defects in February 2020 – January 2021:

$$\begin{aligned} \text{Loss} &= K \times (y^2) \quad (2) \\ \text{Loss} &= \text{Rp. } 7.827,42 \times (24^2) \\ \text{Loss} &= \text{Rp. } 4.508.594,51 \\ \text{Average loss} &= \frac{\text{1st month loss} + \dots + \text{12st month loss}}{12} \\ &= \frac{383.543,63 + \dots + 4.508.594,51}{12} \\ &= \text{Rp. } 2.391.929,41 \end{aligned}$$

b) Calculation of Quality Loss function before applying the Deming cycle of the smallest number of defects occurred in February 2020:

$$\begin{aligned} \text{Loss} &= K \times (y^2) \\ \text{Loss} &= \text{Rp. } 7.827,42 \times (7^2) \\ \text{Loss} &= \text{Rp. } 383.543,63 \end{aligned}$$

c) Calculation of Quality Loss function after the implementation of deming cycle in June 2021:

$$\begin{aligned} \text{Loss} &= K \times (y^2) \\ \text{Loss} &= \text{Rp. } 7.827,42 \times (5^2) \\ \text{Loss} &= \text{Rp. } 195.685,50 \end{aligned}$$

CONCLUSION

Based on the results of research proposed the application of deming cycles in the company environment, the conclusions were obtained, namely:

1. Of the four types of defects that occur, proposed Standard Operating Procedure (SOP), work instructions, and checking forms in the packaging, maintenance and delivery sections to reduce the number of product returns.
2. The result of the process of implementing quality management on an ongoing basis with the implementation of deming cycles in the company environment decreased the number of company returns to 1.63%.
3. The results of the loss calculation after implementing the Deming cycle in the company environment with a Quality Loss Function approach of Rp. 195,685.50. There was a decrease in losses of Rp. 187.858.08 or 48.98%.

REFERENCES

1. Widyanto, “Analisis Proses Bisnis Usaha Mikro Kecil Menengah (UMKM) Konveksi Ryan Collection di Kabupaten Kudus”, *Jurnal Administrasi Bisnis*, 6(1), pp. 24-30 (2017).
2. V., Gaspersz, *Total Quality Management Untuk Praktisi Bisnis dan Industri* (Vinchrsto Publication, Bogor, 2011).
3. Zaharuddin, “Analisis Mutu Biodiesel Menggunakan Metode Quality Loss Function dan Rancangan Perbaikan di PT XYZ”, *Jurnal Optimalisasi*, 6(2), pp. 204-212(2020).
4. Nasution, *Manajemen Mutu Terpadu (Total Quality Management)* (Ghalia Indonesia, Bogor, 2005).
5. F., Tjiptono, *Total Quality Management* (Andi Offset, Yogyakarta, 2003).

Design Of Profile Matching Decision Support System Software Against E-Commerce Selection For Sellers

Hadida Dellasaviaputra ^{1, a)} and Fadillah Ramadhan ¹

¹⁾ *Department of Industrial Engineering, Institut Teknologi Nasional Bandung*

^{a)} *E-mail: hadidadellasavia@gmail.com*

Abstract. Lazada, Shopee, and Tokopedia are online e-commerce applications for buying and selling processes that have different facilities and services, in selecting the best e-commerce that sellers hope to increase their sales. The profile matching method is able to identify these problems with e-commerce. This thesis has to design a decision support system software to determine the best e-commerce media used by sellers to increase their sales. The program is designed with Visual Basic for Application (VBA) and the Rapid Application Development (RAD) method in which there is data processing by profile matching and only up to the prototype stage. The results of the questionnaire from the expert seller (resource) act as input. Program testing was done by validating manual and program calculations, blackbox testing, and user acceptance test (UAT). The Conclusion is that the program is fast, dynamic, and suitable for use, 766 kb of storage memory, and the assessment determined by the expert results in a score of 6.00 on Shopee and a score of 5.35 on Tokopedia and Bukalapak.

INTRODUCTION

Electronic Commerce (E-Commerce) is the process of selling or purchasing goods or services through a computer network to receive or place orders on goods or services, but the process of payment and delivery of goods or services does not have to be done online. Such e-commerce transactions can occur between individuals, groups, organizations, businesses, households, individuals, and governments [1]. Lazada, Shopee, Buka Lapak, Tokopedia, and others are an e-commerce online application that facilitates the buying and selling process. Therefore, it is necessary to pay attention to what causes consumers to choose shopping in one e-commerce and what are the reasons and what products are sought after. [2] in other words the selection of e-commerce becomes an important issue for buyers and sellers. Each e-commerce has facilities and services offered differently, so it is necessary to contribute to the quality, service, and facilities owned by each e-commerce to determine the best [3]. As for some people who want to shop online but often have difficulty in shopping, such as the difficulty of finding the desired item and prices that do not match expectations, so it takes the determination of the right marketplace by the seller. Actors or sellers often have difficulty in choosing a suitable application, the factor is the type of goods to be sold, the cost of placing ads, the popularity or absence of the application, the level of difficulty operating the marketplace, and others.

To determine an accurate and fast decision with good solution quality, a decision support system is needed that can facilitate in the process of determining the best e-commerce [4]. The process of selecting alternatives on multiple criteria can take a long time, if the data processing is done manually. In addition, the criteria in a case can vary so that the time needed is long enough. The determination process involves assessing each criterion, so that data processing is required to be done as quickly and dynamically as possible so that the process of updating the displayed data is faster and up-to-date. One of the multi criteria decision making (MCDM) approaches that can be used in decision support systems is a profile matching method that is able to identify various marketplaces with its assessment which will then be decided by prospective sellers in the form of a program to facilitate users in the retrieval process. The decision, so the purpose of this research is to design decision support system software to determine the best e-commerce media used as sellers to increase their sales.

METHODOLOGY

Identify Problems and Research Objectives

Each marketplace has its own advantages and disadvantages. Actors or sellers often have difficulty in choosing a suitable application, the factor is the type of goods to be sold, the cost of placing ads, the popularity or absence of the application, the level of difficulty operating the marketplace, and others. The purpose of this study is to design profile matching decision support system software to determine the best e-commerce media that sellers use to increase their sales. The software design method used is Rapid Application Development (RAD), according to Dennis et al (2012 in [5]) that rapid application development (RAD) is a new class of system development methodologies that emerged in the 1990s. RAD-based methodologies attempt to overcome the weaknesses of both constructed design methodologies by adjusting the SDLC phase so that some parts of the system develop quickly and enter the hands of the user. This way, users can better understand the system and suggest revisions that bring the system closer to what is needed.

System Planning

A system request is a document that explains the business's reasons for building the system and the expected value of the system. Analysis of software development feasibility there are three categories, namely, technical feasibility, economics, and organization. Engineering feasibility is assessed based on risks to similarity of function, technological similarity, the magnitude or smallness of a project, and the suitability to integrate existing systems. Economic feasibility is seen based on cost or expenditure on development, but in this study, an analysis of economic feasibility is not required. The feasibility of an organization is assessed based on the relationship between the project strategy and the level of whether or not the overall system is acceptable to users and related parties.

System Analysis

The first step in this stage is to determine the needs of the software by defining first and then making the need and comparing the existing problem with the need, whether it can help in solving the problem or not, and determine the functional and non-functional needs of the system as limitations and capabilities on the system to be designed. The second step is to identify the business process on the use case diagram by translating from each element. Use case diagrams are created as modeling on the system by describing several actors and the tasks to be performed. The third step of the business process modeler with activity diagram (AD). Activity diagrams describe the various activities combined to support the process. The final step is to realize business processes with sequence diagrams to sort various processes.

System Design

The third stage is the first step is to do user interface design modeling or designing a user interface (UI) based on inputs, processes, and outputs to be created. User interface modeling is made in the form of sketches or images of the program. It will be designed. Data modeling is done to determine the data needed to support business processes and ensure that the data can meet the needs in supporting business processes. Data models are created with entity relationship diagrams (ERDs) that can describe interconnected entities. After the entity relationship diagram (ERD) is made the next step is to display the example of calculation and the result of the calculation of the profile matching method. According to [6] the profile matching method is one of the simple methods in the decision support system by comparing GAP between alternative values and criteria. There are several things that are known about GAP analysis, one of which is the GAP weight value table. In addition, gap analysis must also understand the concept of Priority Scale because in the manufacture of weights with a range of 0-5 based on the priority of each criterion. Profile matching here is tasked with choosing criteria and alternatives to be identified first.

System Implementation

Implementation is the last stage that begins by discussing the activities needed to build the software starting from the construction of the software where the program began to be created. Software testing is done after software construction, the thing that is considered in testing is that the system designed must work. Blackbox testing is done by assessing whether the list of functional and non-functional requirements that have been determined in advance

succeeded or failed obtained from the results of discussions between users and user designers have the right to ask for improvements and if successful then there is no need for improvement. User acceptance test is done if the whole is considered successful, the designer provides a questionnaire about the software as an assessment that the software is feasible or not for use. Documentation creation is done to record on the operation of the application and processing steps to make it easier to evaluate, documentation that is done in the form of image recording when the program is run.

Overall Analysis, Conclusions, and Suggestions

The analysis process carried out is to analyze the program created as a whole starting from the events that occurred or the results obtained during the design of the system to the implementation. The important things that have been obtained from the analysis further become the final conclusions and suggestions that can be done in the next research process.

RESULTS

Coding View

Alternative Add Button Coding

The following is an example image of coding alternative add buttons that can be seen in Figure 1 below.

The image shows a screenshot of a VBA code editor window titled 'CommandButton2' with a 'Click' event selected. The code is written in VBA and includes several conditional statements to check if specific cells are empty and then perform actions like clearing text boxes or enabling/disabling the button. It also includes comments in Indonesian and a sorting routine. The code is as follows:

```
CommandButton2
Click

.Cells(6, 2).Value = TextBox1.Value
TextBox1.Value = Empty
ElseIf .Cells(7, 2).Value = Empty Then
.Cells(7, 2).Value = TextBox1.Value
TextBox1.Value = Empty
ElseIf .Cells(8, 2).Value = Empty Then
.Cells(8, 2).Value = TextBox1.Value
TextBox1.Value = Empty
ElseIf .Cells(9, 2).Value = Empty Then
.Cells(9, 2).Value = TextBox1.Value
TextBox1.Value = Empty
ElseIf .Cells(10, 2).Value = Empty Then
.Cells(10, 2).Value = TextBox1.Value
TextBox1.Value = Empty
ElseIf .Cells(11, 2).Value = Empty Then
.Cells(11, 2).Value = TextBox1.Value
TextBox1.Value = Empty
Else
    TextBox1.Value = Empty
End If
End With
End If

''aktifasi tombol add
If Worksheets("Alternatif").Cells(11, 2).Value = Empty Then
    CommandButton2.Enabled = True
Else
    CommandButton2.Enabled = False
End If

''SORTING BY ID DAN ALI
Dim totaldata As Range
Dim speicific_col As Range

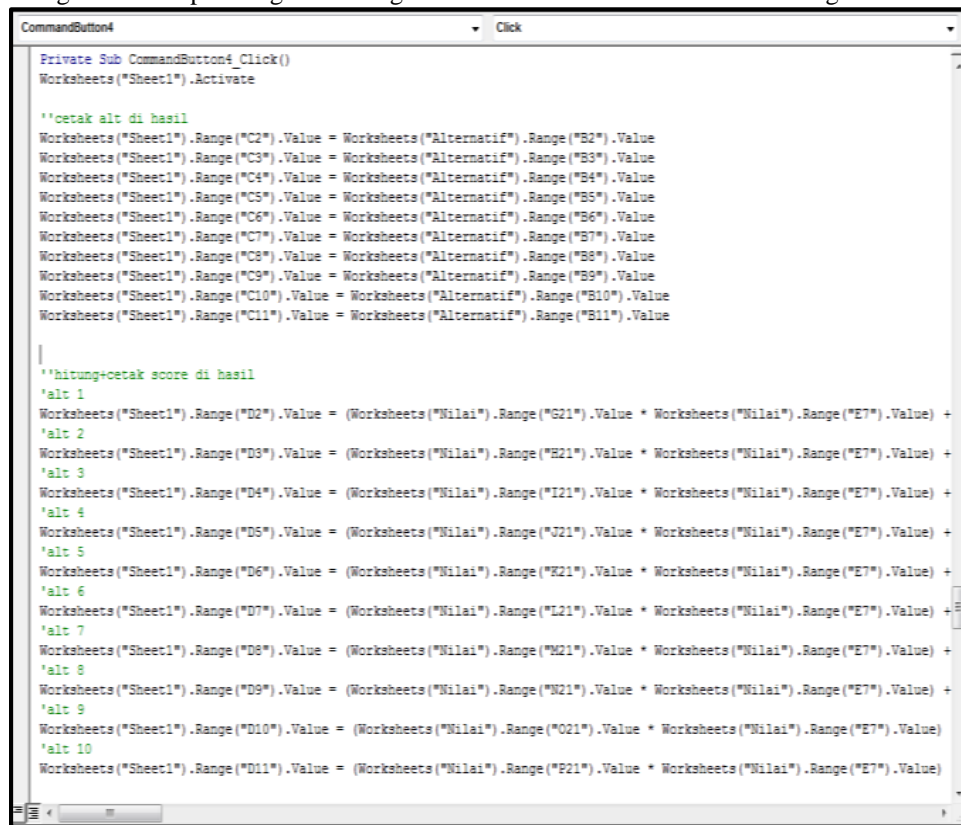
Set totaldata = Worksheets("Alternatif").Range("A:B")
Set specific_col = Worksheets("Alternatif").Range("A:A")
totaldata.sort key1:=specific_col, order1:=xlAscending, Header:=xlYes
```

FIGURE 1. Alternative Add Button Coding

Coding there are conditions that contain if the cells are empty, then the program will print from the textbox (section to enter data) into the empty cell, and the program will automatically look for empty cells to print the inputted data.

Results Button Coding

The following is an example image of coding the results button that can be seen in Figure 2 below.



```
CommandButton4 Click
Private Sub CommandButton4_Click()
Worksheets("Sheet1").Activate

'cetak alt di hasil
Worksheets("Sheet1").Range("C2").Value = Worksheets("Alternatif").Range("B2").Value
Worksheets("Sheet1").Range("C3").Value = Worksheets("Alternatif").Range("B3").Value
Worksheets("Sheet1").Range("C4").Value = Worksheets("Alternatif").Range("B4").Value
Worksheets("Sheet1").Range("C5").Value = Worksheets("Alternatif").Range("B5").Value
Worksheets("Sheet1").Range("C6").Value = Worksheets("Alternatif").Range("B6").Value
Worksheets("Sheet1").Range("C7").Value = Worksheets("Alternatif").Range("B7").Value
Worksheets("Sheet1").Range("C8").Value = Worksheets("Alternatif").Range("B8").Value
Worksheets("Sheet1").Range("C9").Value = Worksheets("Alternatif").Range("B9").Value
Worksheets("Sheet1").Range("C10").Value = Worksheets("Alternatif").Range("B10").Value
Worksheets("Sheet1").Range("C11").Value = Worksheets("Alternatif").Range("B11").Value

'hitung+cetak score di hasil
'alt 1
Worksheets("Sheet1").Range("D2").Value = (Worksheets("Nilai").Range("G21").Value * Worksheets("Nilai").Range("E7").Value) +
'alt 2
Worksheets("Sheet1").Range("D3").Value = (Worksheets("Nilai").Range("H21").Value * Worksheets("Nilai").Range("E7").Value) +
'alt 3
Worksheets("Sheet1").Range("D4").Value = (Worksheets("Nilai").Range("I21").Value * Worksheets("Nilai").Range("E7").Value) +
'alt 4
Worksheets("Sheet1").Range("D5").Value = (Worksheets("Nilai").Range("J21").Value * Worksheets("Nilai").Range("E7").Value) +
'alt 5
Worksheets("Sheet1").Range("D6").Value = (Worksheets("Nilai").Range("K21").Value * Worksheets("Nilai").Range("E7").Value) +
'alt 6
Worksheets("Sheet1").Range("D7").Value = (Worksheets("Nilai").Range("L21").Value * Worksheets("Nilai").Range("E7").Value) +
'alt 7
Worksheets("Sheet1").Range("D8").Value = (Worksheets("Nilai").Range("M21").Value * Worksheets("Nilai").Range("E7").Value) +
'alt 8
Worksheets("Sheet1").Range("D9").Value = (Worksheets("Nilai").Range("N21").Value * Worksheets("Nilai").Range("E7").Value) +
'alt 9
Worksheets("Sheet1").Range("D10").Value = (Worksheets("Nilai").Range("O21").Value * Worksheets("Nilai").Range("E7").Value) +
'alt 10
Worksheets("Sheet1").Range("D11").Value = (Worksheets("Nilai").Range("P21").Value * Worksheets("Nilai").Range("E7").Value)
```

FIGURE 2. Results Button Coding

The coding is reprinted from alternative to "sheet1", it is done to read the data contained in the cells in "sheet1" into the listbox (the display of data based on certain cells), and there is a process of calculating the final result of each alternative inputted, the result will be printed into "sheet1", so that the result of the score calculation can appear into the listbox. It's on the results menu.

Program View

Alternative Add Program View

The following is an example image of an alternative add program display that can be seen in Figure 3 below. The program view image above is a view contained in the alternative menu. Alternate IDs and names will appear in the listbox if the user fills in a blank column and clicks the add button.

ID	NAMA ALTERNATIF
A01	SHOPEE
A02	LAZADA

FIGURE 3. Alternative Add Program View

Results Program View

The following is an example image of the program view results that can be seen in Figure 4 below.

RANK	NAMA ALTERNATIF	SCORE
1	SHOPEE	5.35
2	LAZADA	4.65

FIGURE 4. Results Program View

The appearance of the processing program contains an identity containing the name, age, type of goods, and long use of the application as the identity of someone who performs the assessment. However, this program does not require filling in such data. The listbox contained in the menu contains a rank as a rank of existing alternatives based on the score of the results of automatic calculations performed by the program to display the overall results of the use of this program.

Software Testing Results

The following software testing is a test on profile matching calculations that are calculated manually and programmally.

Manual Calculation

a. GAP value

The following is a table of GAP values that can be seen in Table 1.

TABLE 1. GAP Value

No	Criterion	Alternative			Profile Criterion	GAP A01	GAP A02	GAP A03
		A01	A02	A03				
1	K01	4	4	5	4	0	0	1
2	K02	5	4	4	4	1	0	0
3	K03	5	5	4	5	0	0	-1

Examples of Alternative Calculations A01 in Criterion K01:

$$\begin{aligned}
 \text{GAP A01 on K01} &= \text{Alternative Value(A01)} - \text{Profile Criteria (K01)} \quad (1) \\
 &= 4 - 4 \\
 &= 0
 \end{aligned}$$

b. Mapping GAP

The following is a gap mapping table that can be seen in Table 2.

TABLE 2. Mapping GAP

No	Criterion	Alternative			Profile Criterion	GAP A01	GAP A02	GAP A03
		A01	A02	A03				
1	K01	0	0	1	6	6	5.5	0
2	K02	1	0	0	5.5	6	6	1
3	K03	0	0	-1	6	6	5	0

c. Final Results

The following is a gap mapping table that can be seen in Table 3.

TABLE 3. Manual Calculation Final Result

No	Alternative Name	Final Value	Rank
1	Shopee (A01)	5.90	2
2	Lace (A02)	6.00	1
3	Tokopedia (A03)	5.35	3


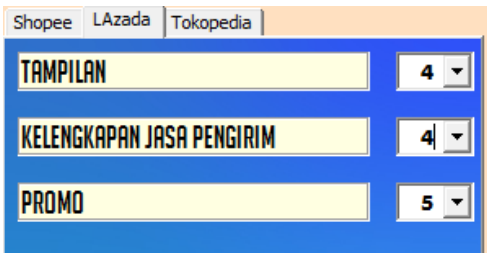

Example of Alternative Final Value Calculation A01:

$$\begin{aligned}
 \text{Final Value A0} &= (\text{Map GAP K01} \times \text{Weight K01}) + (\text{Map GAP K02} \times \text{Weight K02}) + (\text{Map} \\
 &\quad \text{GAP K03} \times \text{Weight K03}) \quad (2) \\
 &= (6 \times 30\%) + (5.5 \times 20\%) + (6 \times 50\%) \\
 &= 5.90
 \end{aligned}$$

Program Calculations

The following is a table on the program that contains a picture as a program calculation can be seen in Table 4 below.

TABLE 4. Program Calculations

No	Program	Picture																
1	Alternative	<table><tr><th>ID</th><th>NAMA ALTERNATIF</th></tr><tr><td>A01</td><td>SHOPEE</td></tr><tr><td>A02</td><td>LAZADA</td></tr><tr><td>A03</td><td>TOKOPEDIA</td></tr></table>	ID	NAMA ALTERNATIF	A01	SHOPEE	A02	LAZADA	A03	TOKOPEDIA								
ID	NAMA ALTERNATIF																	
A01	SHOPEE																	
A02	LAZADA																	
A03	TOKOPEDIA																	
2	Criterion	<table><tr><th>ID</th><th>NAMA KRITERIA</th><th>BOBOT(%)</th><th>PROFILE KRITERIA</th></tr><tr><td>K01</td><td>TAMPILAN</td><td>30%</td><td>4</td></tr><tr><td>K02</td><td>KELENGKAPAN JASA PENGIRIM</td><td>20%</td><td>4</td></tr><tr><td>K03</td><td>PROMO</td><td>50%</td><td>5</td></tr></table>	ID	NAMA KRITERIA	BOBOT(%)	PROFILE KRITERIA	K01	TAMPILAN	30%	4	K02	KELENGKAPAN JASA PENGIRIM	20%	4	K03	PROMO	50%	5
ID	NAMA KRITERIA	BOBOT(%)	PROFILE KRITERIA															
K01	TAMPILAN	30%	4															
K02	KELENGKAPAN JASA PENGIRIM	20%	4															
K03	PROMO	50%	5															
3	Alternative Assessment A01 Shopee																	
4	Alternative Assessment A02 Lazada																	
5	Tokopedia's A03 Alternative Assessment																	
6	Final Results	<table><tr><th>RANK</th><th>NAMA ALTERNATIF</th><th>SCORE</th></tr><tr><td>1</td><td>LAZADA</td><td>6.00</td></tr><tr><td>2</td><td>SHOPEE</td><td>5.90</td></tr><tr><td>3</td><td>TOKOPEDIA</td><td>5.35</td></tr></table>	RANK	NAMA ALTERNATIF	SCORE	1	LAZADA	6.00	2	SHOPEE	5.90	3	TOKOPEDIA	5.35				
RANK	NAMA ALTERNATIF	SCORE																
1	LAZADA	6.00																
2	SHOPEE	5.90																
3	TOKOPEDIA	5.35																

The results of manual calculations obtained in Shopee alternatives are 5.90, Lazada alternatives by 6.00, tokopedia alternatives by 5.35. The results of the manual calculation are declared to be the same as the results of the program calculation, this validation process can be said to be successful. Next can be done to the black box testing process.

Black Box Testing

Black Box Testing is conducted on two categories, namely, a list of functional and non-functional requirements, and included the test results based on the analysis of software needs contained in Table 5 and Table 6 as follows.

TABEL 5. List Requirement Functional

No.	List Requirement (Functional)	Test Results
1	Systems that can input <i>e-commerce</i> selection criteria	Succeed
2	A system that can input the results of respondents' assessments	Succeed
3	Systems that can dynamically change data	Succeed
4	Systems that can input <i>alternatives to e-commerce</i> selection	Succeed
5	Systems that can sort <i>e-commerce</i>	Succeed
6	A system that can reveal the identity of the respondent	Succeed
7	A system that can move display menus easily	Succeed
8	A system that can display identity	Succeed
9	Systems that can display <i>e-commerce</i> assessment results	Succeed

TABEL 6. List Requirement Non Functional

No.	List Requirement (Non Functional)	Test Results
1	100% system service availability	Succeed
2	The system is only used in MS. Excel software.	Succeed
3	The system can be used by anyone.	Succeed
4	The system can only be accessed by one user at the same time.	Succeed
5	Unlimited data charging time	Succeed
6	The system can be used at any time.	Succeed
7	Data can only be changed by <i>the user</i> or user.	Succeed
8	Data can be saved <i>when</i> it has filled in all the data	Succeed

User Acceptance Test (Uat)

The following is a table of user acceptance test calculations that have been filled by 3 users or respondents and can be seen in Tables 7 and 8 as classifications.

TABEL 7. User Acceptance Test (UAT)

Question	Value		
	Sum	Number / Respondent	%
1	11	3.67	91.67
2	9	3.00	75.00
3	10	3.33	83.33
4	10	3.33	83.33

TABLE 7. User Acceptance Test (UAT) (Continue)

Question	Value		
	Sum	Number / Respondent	%
5	11	3.67	91.67
6	12	4.00	100.00
7	11	3.67	91.67
8	12	4.00	100.00
9	10	3.33	83.33
10	12	4.00	100.00
11	10	3.33	83.33
12	9	3.00	75.00
Total Average %			88.19

Examples of Total Percentage Average Calculations:

$$\begin{aligned}
 \text{a. Number / Respondent of Question 1} &= \frac{\text{Sum of Number}}{\text{Number of Respondent}} & (3) \\
 &= \frac{11}{3} \\
 &= 3.67
 \end{aligned}$$

$$\begin{aligned}
 \text{b. Percentage Value of Question 1} &= \frac{\text{Number / Respondent of Question 1}}{\text{Highest Weight Figures}} & (4) \\
 &= \frac{3.67}{4.00} \\
 &= 91.67\%
 \end{aligned}$$

$$\begin{aligned}
 \text{c. Average of Total Percentage} &= \frac{\sum \text{Percentage of Question Value}}{\text{Number of Question}} & (5) \\
 &= \frac{91.67 + 75.00 + 83.33 + \dots + 75.00}{12} \\
 &= 88.19\%
 \end{aligned}$$

TABLE 8. Classification of User Acceptance Test (UAT) Results

Percentage	Information
0%-20%	Sangat Lemah
21%-40%	Lemah
41%-60%	Cukup
61%-80%	Kuat
81%-100%	Sangat Kuat

Source: Riduwan, 2008 in [7]

Based on the average result of the total percentage worth 88.19%, the user acceptance test was declared very strong. Judging from Table 8, the value is included in the percentage classification between 81% to 100% with very strong information. The results obtained are said to be received by the user and not done further iteration.

Documentation (Manual User)

The documentation shown in the images on the program that runs in Figure 5, Figure 6, and Figure 7.

a. Alternatives and Criteria

The image shows two side-by-side windows from a software application. The left window is titled 'Alternatif' and contains a yellow 'ALTERNATIF' button, a red 'BACK' button, and three buttons: 'ADD', 'EDIT', and 'DELETE'. Below these are input fields for 'ID' (containing 'A03') and 'ALTERNATIF'. At the bottom is a table with two columns: 'ID' and 'NAMA ALTERNATIF'. The table contains three rows: 'A01 TOKOPEDIA', 'A02 BUKALAPAK', and 'A03 SHOPEE'. The right window is titled 'Kriteria' and contains a yellow 'KRITERIA' button, a red 'BACK' button, and three buttons: 'ADD', 'EDIT', and 'DELETE'. Below these are input fields for 'ID' (containing 'K06'), 'KRITERIA' (containing 'KELENGKAPAN JASA PENGIRIM'), 'BOBOT' (containing '0.15'), and 'PROFILE KRITEIA' (containing '5'). There is a green 'CEK TOTAL BOBOT' button. At the bottom is a table with four columns: 'ID', 'NAMA KRITERIA', 'BOBOT(%)', and 'PROFILE KRITEIA'. The table contains six rows: 'K01 FITUR APLIKASI' (20%, 5), 'K02 KELENGKAPAN BARANG' (15%, 5), 'K03 PELAYANAN' (20%, 5), 'K04 DESAIN INTERFACE TAMPILAN' (10%, 5), 'K05 KEMUDAHAN PENGGUNAAN APLIKASI' (20%, 5), and 'K06 KELENGKAPAN JASA PENGIRIM' (15%, 5).

ID	NAMA ALTERNATIF
A01	TOKOPEDIA
A02	BUKALAPAK
A03	SHOPEE

ID	NAMA KRITERIA	BOBOT(%)	PROFILE KRITEIA
K01	FITUR APLIKASI	20%	5
K02	KELENGKAPAN BARANG	15%	5
K03	PELAYANAN	20%	5
K04	DESAIN INTERFACE TAMPILAN	10%	5
K05	KEMUDAHAN PENGGUNAAN APLIKASI	20%	5
K06	KELENGKAPAN JASA PENGIRIM	15%	5

FIGURE 5. Alternatives and Criteria

b. Tokopedia, Bukalapak, and Shopee Alternative Assessments

The image shows three side-by-side windows from a software application, all titled 'Penilaian'. Each window has a yellow 'NILAI' button and a red 'BACK' button. Below these are tabs for 'Tokopedia', 'Bukalapak', and 'Shopee'. The first two windows show a list of criteria with dropdown menus for rating. The third window shows the same list of criteria with dropdown menus for rating, and a 'Keterangan Nilai:' box on the right. The 'Keterangan Nilai:' box contains the following text: '1 = Sangat Tidak Baik', '2 = Tidak Baik', '3 = Cukup Baik', '4 = Baik', and '5 = Sangat Baik'.

Kriteria	Rating
FITUR APLIKASI	4
KELENGKAPAN BARANG	4
PELAYANAN	4
DESAIN INTERFACE TAMPILAN	4
KEMUDAHAN PENGGUNAAN APLIKASI	5
KELENGKAPAN JASA PENGIRIM	5

Keterangan Nilai:
 1 = Sangat Tidak Baik
 2 = Tidak Baik
 3 = Cukup Baik
 4 = Baik
 5 = Sangat Baik

FIGURE 6. Alternative Assessment

c. Final Results

RANK	NAMA ALTERNATIF	SCORE
1	SHOPEE	6.00
2	TOKOPEDIA	5.35
2	BUKALAPAK	5.35

FIGURE 7. Final Results

DISCUSSION

This program is not a program that is just made, but this program is able to process the data needed by calculating profile matching methods. This program is made with results that are quite easy to use, the use of the program does not take long enough, the user simply inputs the required data according to what will be decided. The storage memory of this program only requires 766 kb.

This data processing program is dynamic, where data can be changed ranging from identity, alternatives, criteria, and assessments. This can make it easier for users if there is data that needs to be changed based on their needs and users do not need to input data again if there are changes to some data. Dynamic nature is able to develop the results of previous decisions to the latest.

The results of the processing can be obtained quickly, this is due to the easy use of the program. The time and process required to obtain the results of the decision is only the input of data needed. The data processing process is already automatically calculated by the program, so that results or outputs can be obtained quickly. The comparison between programs that are fast and dynamic and those that are not can be seen from the process carried out by each program, for example, in the process of input values, programs that are fast and dynamic only simply enter numbers without having to change formulas or recreate formulas and do not need to look for table cells, while for those that are not fast and not dynamic it is inversely proportional, the user needs to find the cell they want to change and recreate the formula.

CONCLUSION

The program is dynamic, the data can be changed (updated), the results of program processing can be obtained quickly, based on expert seller data named Sukirman it produces a score for Shopee of 6.00, and for Bukalapak and Tokopedia it is 5.35. The storage capacity of this program is 766 kb. Based on the problems that occur especially to users that with this program, the decision can be decided and obtained quickly, even users can change data easily without the need to calculate or create formulas.

REFERENCES

1. Central Bureau of Statistics (BPS). (2019, December 18). *E-Commerce Statistics 2019*, [Online]. Available: <https://www.bps.go.id/publication/2019/12/18/fd1e96b05342e479a83917c6/statistik-e-commerce-2019.html> [December 5, 2020].
2. D., Suleman. "Faktor Penentu Keputusan Konsumen Indonesia Memilih Tempat Belanja di Sebuah E-Commerce (Theory of Planned Behaviour)", *Jurnal Doktor Manajemen*, 1 (2), pp.1-9 (2018).
3. I., Prastitha, I.P.A., Mahadewa, and P., Sugiartawan, "Sistem Pendukung Keputusan Kelompok Pemilihan E-Commerce/Marketplace Menggunakan Metode Profile Matching dan BORDA", *Jurnal Sistem Informasi dan Komputer Terapan Indonesia (JKSIKTI)*, 1(1), pp.13-24 (2018).
4. J.V.B., Ginting, "Penerapan Sistem Pendukung Keputusan dalam Menentukan E-Commerce Terbaik dengan Menggunakan Metode SAW", *Jurnal Media Informatika Budidarma*, 4(1), pp.225-228 (2020).
5. A., Ramadhan. (2019), "Rancang Bandung Sistem Monitoring Anggaran Keuangan Berbasis Web Pada Biro Hukum dan Kerja Sama Luar Negeri", *Applied Information System and Management (AISM)*, 2 (1), pp. 5-10 (2019).
6. D., Nofriansyah and S., Defit, *Multi Criteria Decision Making (MCDM) on Decision Support System* (CV.Budi Utama (Deepublish), Yogyakarta, 2017).
7. R., Supriatna. (2019). *Implementasi dan User Acceptance Test (UAT) Terhadap Aplikasi E-Learning Pada Madrasah Aliyah Negeri (MAN) 3 Kota Banda Aceh*, Tugas Akhir Tidak Terpublikasi, Universitas Islam Negeri Ar-Raniry, (2020).

Production Scheduling Software Design Using First In First Out and Earliest Due Date Methods At PT. Synergy Gem Creations

Ghifari Hamzah^{1, a)}, Fadillah Ramadhan¹

¹⁾Department of Industrial Engineering, Institut Teknologi Nasional Bandung, Indonesia

^{a)}Email: ghifari99hamzah@gmail.com

Abstract. PT. Kreasi Permata Sinergi is engaged in digital printing textile. This company processes fabrics for printing. The problem with this company is that the machine scheduling is still manual. This company also has special customers. This particular customer has to be produced before other normal customers so that the production division has difficulty scheduling machines. This study discusses the design of software for scheduling machines. The program used uses the First In First Out (FIFO) method and Earliest Due Date (EDD) which is adjusted to the conditions of the company. This program helps workers to streamline time in the machine scheduling process. In this program there are features to add, edit, or delete to make the scheduling process easier. The output of this program is a machine schedule that is ready to be printed to be given to machine operators.

INTRODUCTION

Production scheduling is the process of selecting, grouping, and timing in order to produce effective and efficient output. Each production activity requires scheduling to allocate the time, operators, machinery, and equipment used. It can be concluded that production scheduling plays an important role in the production process. At this time the scheduling of production in the company has not been done automatically through the program. The production division needs to manually schedule to schedule the production schedule. One of the scheduling errors is when the production division schedules the production schedule. Examples of errors in scheduling are production divisions less thorough in filling in or entering data, incorrect calculation processes, errors in making visuals such as charts or gantt-charts, and errors in sorting time. In addition, the production division has difficulty in resetting the scheduling in case of changes in scheduling. Even the production division can change the entire scheduling that has been scheduled. It's different if the production division uses a program. An error in using a program is when entering data.

The program the company needs is to minimize scheduling errors. The program can edit, enter orders, delete orders, and schedule orders. Manual scheduling becomes automated. The calculation process until visualization is automatic. If there is an error in entering the data then the production division can change the data. The process of calculation until visualization turns into the latest. Therefore, the importance of the role of technology in the scheduling process.

PT Kreasi Permata Sinergi is engaged in the field of digital printing textile. Customers who want to order products to this company can provide their own designs and own fabrics. If there is no design and fabric this company offers several designs and fabrics provided. This company has several customers who have often ordered to this company so that these customers have more priority than other customers. In the production process, the company must schedule production on several machines. This scheduling is based on the order of customers who order or can be said first in first out (FIFO). The process of scheduling this machine is still done with a handwritten manual on the board. Then switch the shower using Excel but it is still filled manually. This scheduling process sometimes occurs errors, starting from the calculation and the completion time of production. Customers who have ordered will be scheduled for production. But unlike customers who have often ordered or special customers, special customers get special services that the production takes precedence over ordinary customers. The scheduling of this machine

affects the deadline period that has been given by the customer. If it exceeds the deadline that has been set with the customer, the company will negotiate with the customer.

METHODOLOGY

Research stage diagram can be seen in Figure 3

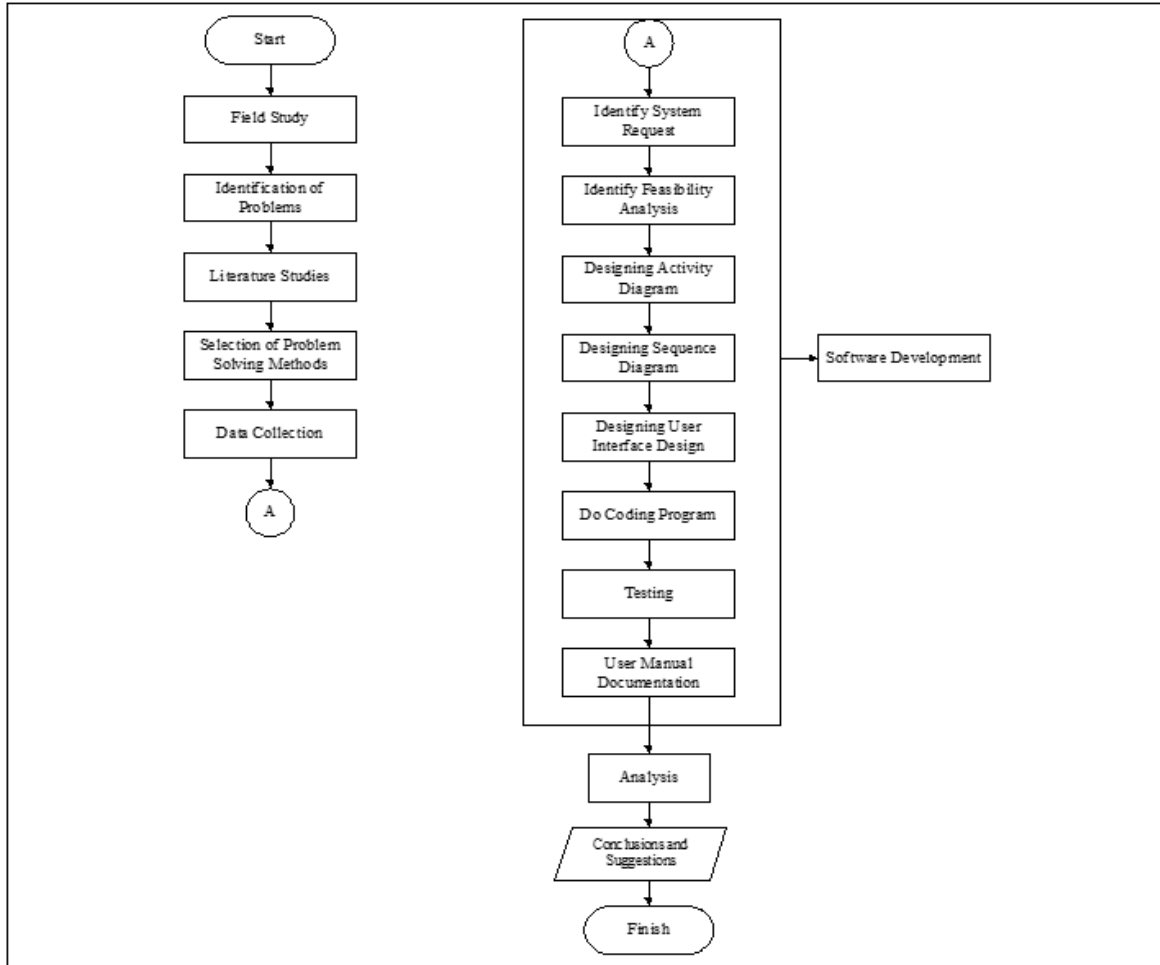


FIGURE 1. Research Stage Diagram

According[1], prototyping is a method of software development, which is a physical model of system work and serves as an early version of the system. The study was conducted using the System Development Life Cycle (SDLC) method. This research was conducted to design production scheduling software using the First In First Out (FIFO) and Earliest Due Date (EDD) methods at PT. Synergy Gem Creation can optimize scheduling process time. This methodology consists of System request, feasibility analysis, use case diagram, activity diagram, sequence diagram, user interface design, program coding, testing, and manual user documentation.

Scheduling

According to [2] scheduling is the work of a set of tasks to be allocated resources in a certain time with two important meanings as follows. Scheduling is a decision-making function for creating or determining schedules. Scheduling is a theory that contains a set of basic principles, models, techniques, and logical conclusions in the decision-making process that provide understanding in the function of scheduling.

System Request

System requests are useful for knowing the needs when designing a system. System request consists of project sponsorship, business needs, business requirements, and business value.

Feasibility Analysis

Feasibility analysis is used to analyze the feasibility of a system created. There are two feasibility analysis, functional requirements and non-functional requirements. Functional requirements need program features to be designed. While non-functional requirements are needed when operational, program security, and performance of the program.

Use Case Diagram

After making a system request and feasibility analysis of non-functional requirements, the next step is to create a use case diagram. Use case diagrams are useful to help in visualizing needs between users with the system or users with other users.

General Flowchart And Activity Diagram

Next create an activity diagram. This diagram is created after the use case diagram with the aim to show the activity of each process in the use case. Activity diagrams are created every single use case.

Sequence Diagram

Sequence diagrams are created after the use case diagram is complete. This diagram is used to describe the interactions, relationships, and methods of the system in the use case diagram. The use of this sequence diagram is almost the same as the activity diagram. One sequence diagram is created every use case.

User Interface Design

The next step is to create a user interface design. User interface design is made to make it easier for users to interact with the system and provide a lot of information that will be displayed by the system to the user. The creation of user interface design is done in excel using the features that have been provided by Excel. In addition to using features in excel, user interface design can be created using userform.

Coding Program

The next step is coding programs. At this stage, I start programming. The programming language used is the VBA Language excel. The place to code programs is in excel. Excel already provides a place to put coding in excel. In addition, excel has also provided several functions so that the function can be directly used without having to create its own function.

Testing

Once the program has been finished, testing is carried out. This test aims to test the entire needs of the user to function properly. If something goes wrong then go back to the coding stage of the program. This process is done until all user needs are functioning properly. In addition, this test aims to match the user's convenience with the program. If the user is not comfortable in using the program then return at the user interface design or coding program stage. This test is done until all the needs on the program function properly and the user feels comfortable using the program.

RESULT

System Request

System request consists of project sponsorship, business needs, business requirements, and business value can be seen in Table 1

TABLE 1. System Request

System Request: Production Scheduling	
Project Sponsor :	CEO of PT. Kreasi Permata Sinergi
Business Needs :	This project was built to
	1. Improve the efficiency of the production scheduling process
Business Requirements:	
The system that supports the production scheduling process is	
	1. Product search features to be scheduled
	2. Admin login feature that manages
	3. Edit production schedule feature
	4. Update feature on scheduling
Business Value:	
	1. Reduce production delays so that they are in accordance with the customer's deadline.
	2. Increase customer trust in the company
	3. Improve scheduling accuracy
	4. Streamline the scheduling process

Feasibility Analysis

This feasibility analysis consists of technical feasibility, economical feasibility, and organizational feasibility can be seen in Table 2

TABLE 2. Feasibility Analysis

Feasibility Analysis
Technical Feasibility
Risks to familiarity with the application:
1. The production process division has experience in the field of production scheduling.
2. There is no division that develops the application of the scheduling process.
Risks to familiarity with technology:
1. The production process division mastered ms.excel
2. Admins managing customer orders simply master ms.excel
Risk to familiarity with project size: Moderate risk
1. The company does not yet have an IT division developer.
Compatibility with existing systems and infrastructure:
The scheduling system is done now by writing on excel and there is no automation or software. So, it is highly compatible production scheduling system using VBA Excel.
Organizational Feasibility
Organizationally, the entire division uses ms.excel so the use of VBA excel will be quite easy. to apply and if there are new people it will be quite easy to provide training in using the software to be created.

Use Case Diagram

Use case diagram is used to describe all business requirements in system request. The use case diagram can be seen in the following image can be seen in Figure 1.

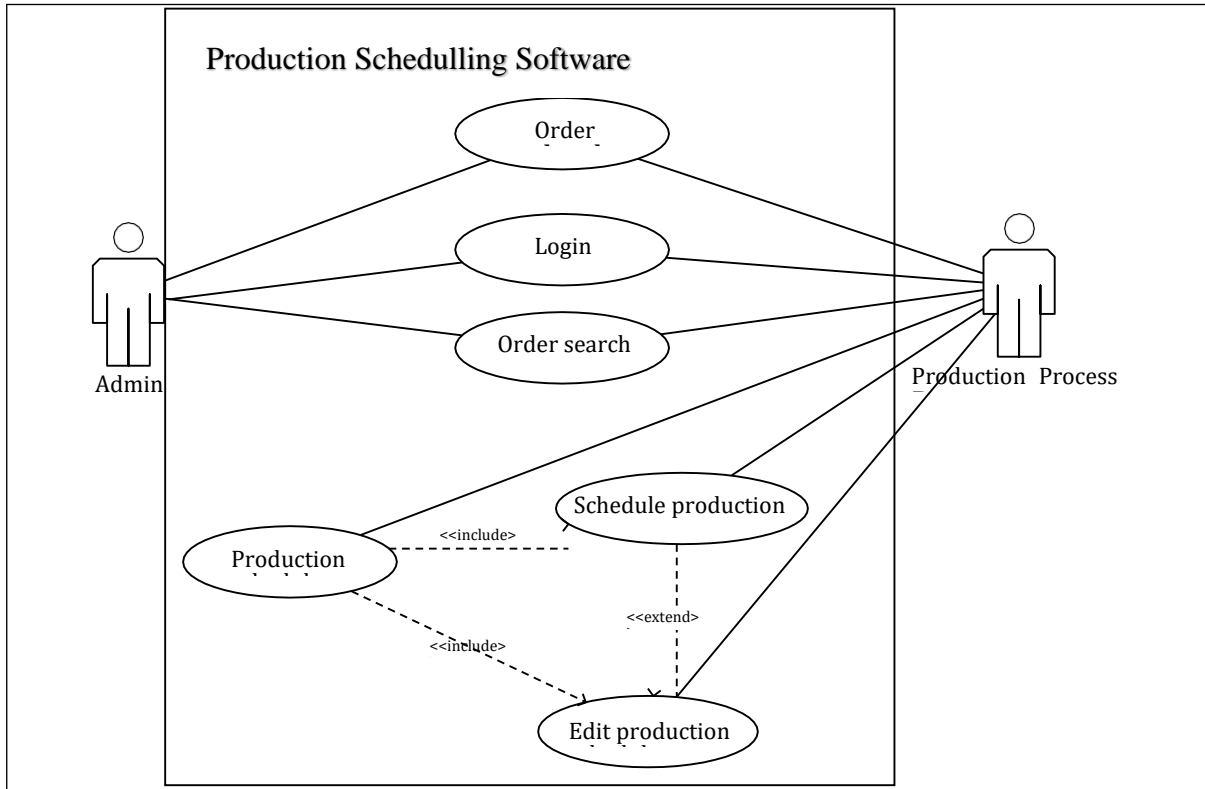


FIGURE 1. Use Case Diagram

Admins and production process divisions have accounts to log into the system. Admins can view databases and add database orders, while the production process division can only see the database and cannot add to the order database. The production process division can schedule according to the orders available in the order database. After scheduling if there is an error in determining the schedule, the production process division can change the order schedule. Admins can't schedule orders. The data search feature can be used by admins and production process divisions.

General Flowchart And Activity Diagram

The general flowchart is divided into two. The first flowchart describes the overall flow of the program. While the second flowchart describes the scheduling process on the program designed. The two flowcharts are related. The first flowchart is the main program flow can be seen in Figure 2.

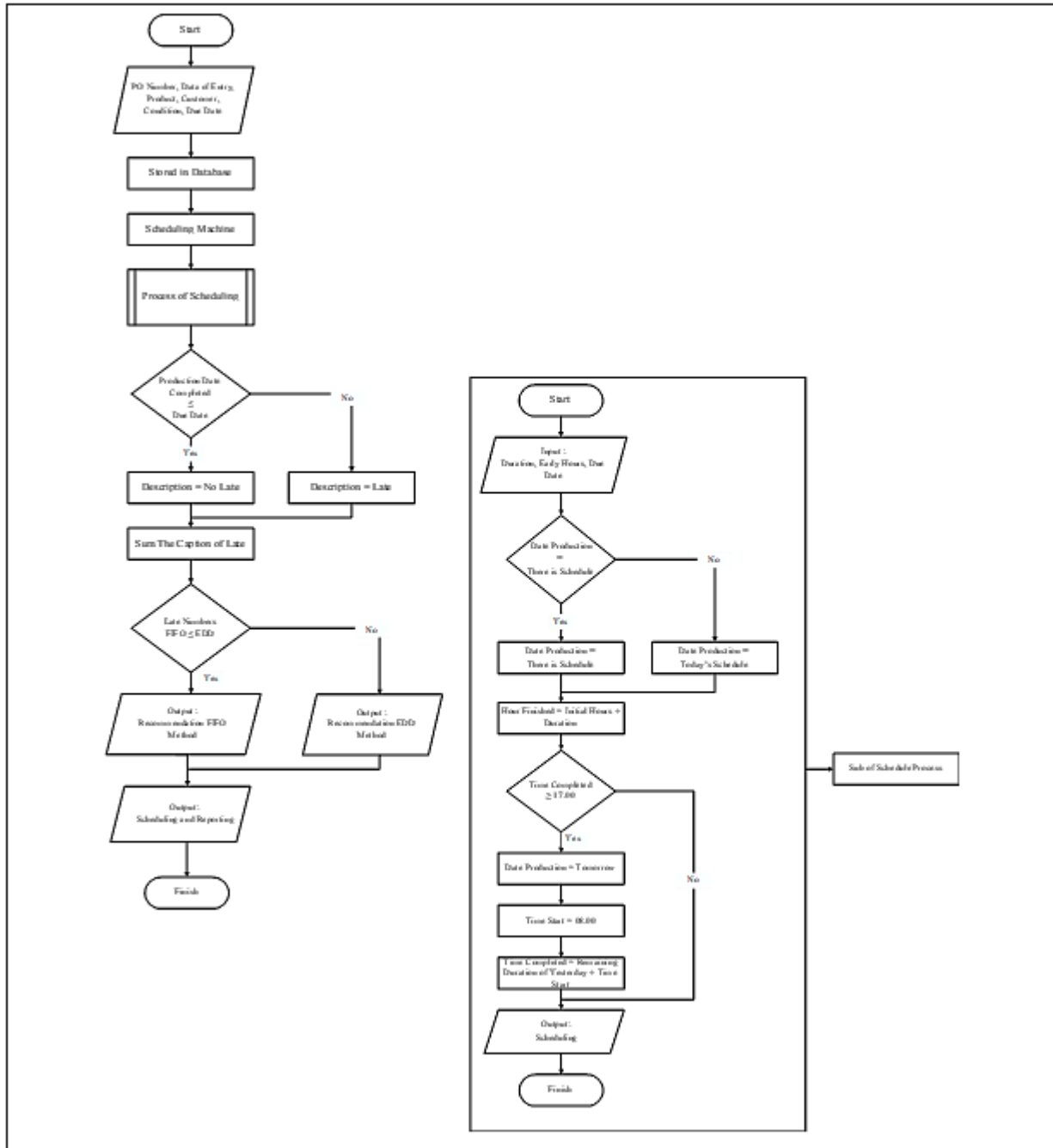


FIGURE 2. Flowchart General Program

The program is run after which it is logged in using a username and password. After that enter po number data, date of entry, product, customer, customer condition, and due date. Next the program will store the data in the order database. Then the production division chooses the engine to be scheduled. There are two engines, the TS300 and TS55. Next is the schedule process. After the scheduling process is complete there is an output in the form of scheduling and reports.

In this scheduling process the program will request input duration, initial hours produced, and due dates. The program will check the scheduling. If there is already a previous scheduling then the production date continues from the previous date. If there is no previous production date then the production date becomes the current date. Next determine the finished production clock by adding the initial hour with the duration. If the finished production

hours exceed 17.00 WIB then continue with tomorrow. The clock starts at 08.00 WIB adjusted to the company's operating hours. Then the finished production clock is the clock 08.00 WIB plus the rest of the duration on the previous day. The scheduling process is complete.

Activity diagrams are created after the use case diagram. This diagram describes every use case in the use case diagram. This diagram contains six use cases in the use case diagram. The activity diagram consists of an order database, login, order search, schedule production, edit production schedule, and production schedule. An overview of each activity diagram can be seen in the Figure 3.

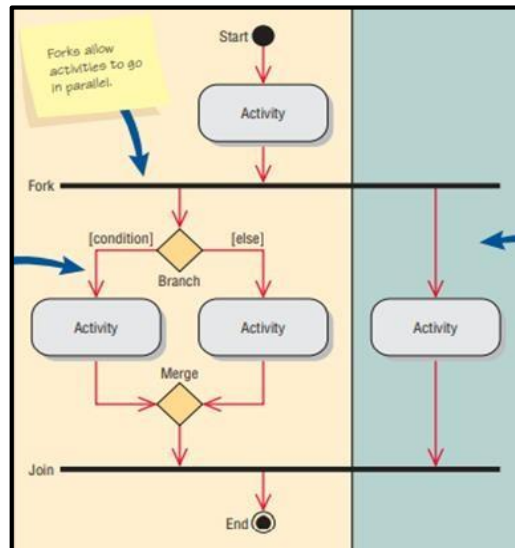


FIGURE 3. Activity Diagram

This sequence diagram is created after the use case diagram is completed. This diagram is to describe the scenario in the use case diagram. The description of each use case is described in this diagram. In the use case diagram consists of six use cases so that in the sequence diagram there are six sequence diagrams. The sequence diagram consists of an order database, login, order search, schedule production, edit production schedule, and production schedule. Each use case will be described and described. An overview of each sequence diagram can be seen in Figure 4.

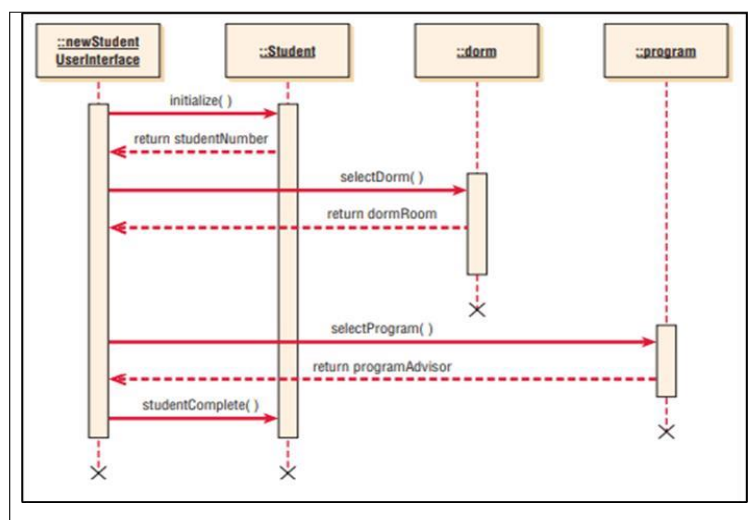


FIGURE 4. Sequence Diagram

User Interface Design

According to [3], user interface design is the way programs and users interact. User interface design is the visual part of software, website, and applications that interact directly with the user and how it displays the information displayed. The user interface design at the design stage can be seen in Figure 5 through Figure 8.



FIGURE 5. UI: Login

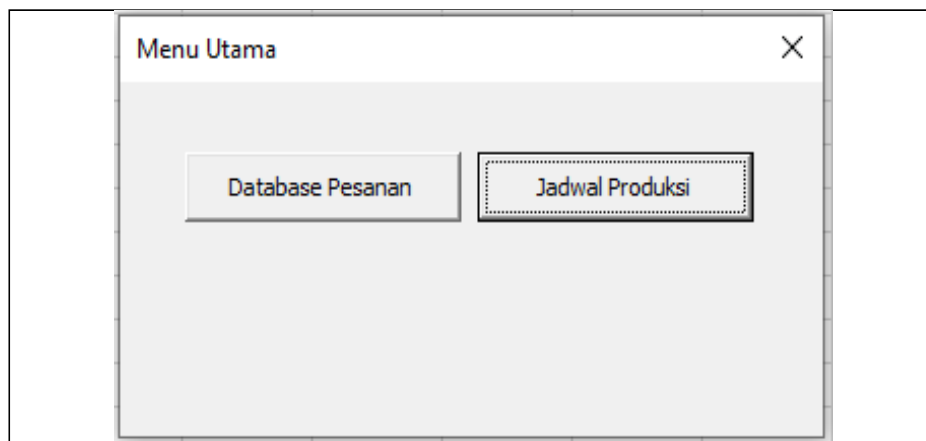


FIGURE 6. UI: Main Menu

Database

Pesanan

Cari

1
2
3
4
5
11
88
12345678999
1052

Keterangan

Nomor PO : Nomor PO :
Produk : Produk :
Tanggal : Tanggal :
Customer : Customer :

Tambah Edit Hapus Daftar Database Kembali

FIGURE 7. UI: Database Menu

Penjadwalan

Pesanan

Jadwal Mesin : TS300

Cari

PO/1
PO/2
PO/3
PO/4
PO/5
PO/6
PO/7
PO/8
PO/9

Keterangan

Nomor PO : Nomor PO :
Produk : Produk :
Tanggal : Tanggal :
Customer : Customer :
Durasi : -

Keterangan Produksi

Tanggal	Mulai	Selesai
-	-	-

Durasi
Menit
Update Edit Jadwal Kembali

FIGURE 8. UI: Scheduling Menu

Data Modeling

The data model used is to use relational databases because excel is a set of cells consisting of rows and columns. Therefore, relational databases are used because they are effective to apply to excel. The data will be stored in the database. The order database can be seen in Table 3.

TABLE 3. Database View

PO number	Date	product	Custo mer	Conditio n	Due Date
PO/1/7	07-Jul-2021	mask	dadang	Normal	7/10/2021
PO/2/7	07-Jul-2021	shirt	didin	Normal	7/10/2021
PO/3/7	07-Jul-2021	mask	dudun	Normal	7/10/2021
PO/4/7	07-Jul-2021	mask	two	Normal	7/10/2021
PO/5/9	09-Jul-2021	trousers	Did	Priority	7/9/2021
PO/6/9	7/9/2021	trousers	sukijem	Normal	7/12/2021
PO/9/9	7/9/2021	Futsal shirt	sutisna	Normal	7/12/2021
PO/7/9	7/9/2021	trousers	sukijang	Priority	7/9/2021

The data will be normalized 1-NF, 2-NF, and 3-NF. Normalize a 1-NF data table if each data attribute has a single value in a single row. Normalization of 2-NF data each attribute is broken down based on **primary key**. The purpose of breaking down attributes based on **primary keys** is to facilitate data renewal. Normalization of 3-NF of each **primary key** does not depend on other attributes. The results of data normalization can be seen in Figure 9.

Customer	PO	Schedulling
Customer's name	* PO's Number	* PO's Number
Product	* Customer_name	* Schedulle
Condition	Due date	Start Timing
Date		Duration
		Production Date
		Notes

FIGURE 9. Normalization Data

Coding Program

According to [4] Visual Basic is a program to create Microsoft Windows-based applications quickly and easily. Visual basic provides tools for creating simple applications to complex or complex applications for both companies / agencies with larger systems" The language used is a VB language that is integrated into excel applications.

Testing

According to [5] software testing is a critical element of software assurance and presents a basic review of specifications, design and coding. Testing can also be interpreted by the process of executing a program with the intent and purpose of finding errors. Testing is done using the black box method. This method tests all functional

requirements, non-functional and all features. This test is done with the production process division and admin. This method uses a user acceptance test to determine the test results. The test results can be seen in Table 4

TABLE 4. User Acceptance Test

No	Question	Valuation			
		A	B	C	D
1	Is this program easy to use?	3			
2	Is the menu easy to understand?	3			
3	Is data filling easy?	3			
4	Is the login feature optimal?	3			
5	Is the database editing feature optimal?	3			
6	Is the feature removing the database optimal?	3			
7	Does the feature add an optimal database?	3			
8	Is the feature of scheduling orders optimal?	3			
9	Is the edit order schedule optimal?	3			
10	Is the schedule report feature optimal?	3			
11	What is the optimal method recompendaing feature?	3			
12	Is this program good enough?	3			

Testing is done at the company. The user acceptance manual is filled in by three related people. All three give value to the user acceptance manual. After processing data the result is 100% so no repair or subsequent iteration is needed.

CONCLUSION

Test results on the design of production scheduling software at PT. Creation of Synergy Gems. This program produces production schedule reports and this program can facilitate the scheduling process that was originally done manual calculations become more automated with this program. The methods used in this scheduling are First In First Out (FIFO) and also earliest due date (EDD) calculations used can run well.

REFERENCES

1. P.M., Ogedebe, and B.P., Jacob, B.P., "Software Prototyping: A Strategy to Use When User Lacks Data Processing Experience", *ARPN Journal of Systems and Software*, 2 (6), (2012).
2. L.M., Pinedo, *Scheduling : Theory, Algorithms, and Systems 4 th Edition* (Springer, New Jersey, 2012).
3. S., Lastiansah, *User Interface* (PT. Elex Media Komputindo, Jakarta, 2012).
4. A., Sunyoto, *Database Programming with Visual basic and Microsoft SQL 2000* (Andi Offset , Yogyakarta, 2007).
5. S. P., Roger, *Software Engineering*, (Andi, Yogyakarta, 2012).

PROPOSED IMPROVEMENT OF THE SCREEN T-SHIRT QUALITY PRODUCTS AT PT. INDO ANUGERAH SEMESTA

Doddy Mudhoffar^{1,a)}, Lauditta Irianti^{1,b)}

¹Department of Industrial Engineering, Institut Teknologi Nasional Bandung, Indonesia

^{a)}Corresponding author: doddymudhoffar18@gmail.com

^{b)}lauditta.irianti@itenas.ac.id

Abstract. PT. Indo Anugerah Semesta is a company that produces t-shirts. This company has a problem, namely defective products as much as 15% of the total production so that it exceeds the standard limits that have been set by the company. It is necessary to improve this matter by using the Failure Mode and Effect Analysis (FMEA) and Fault Tree analysis (FTA) methods. Based on the results of FMEA there are 35 values of Risk Priority Number (RPN) and the results of Pareto there are 6 failure modes with 16 causes of failure which will be searched for the root of the problem. The result of the FTA is that there are 15 root causes. The recommendations given are maintenance of machines and production equipment, making SOPs, evaluating the physical work environment, clarifying the responsibilities of each division.

INTRODUCTION

During the current COVID-19 pandemic, many companies have to maintain or improve the quality of their products so that companies can compete with other companies so that they can dominate the existing market. PT. Indo Anugerah Semesta is an industry that focuses on producing clothing products with various types of products, one of which is screen printing T-shirts. The company has a problem with the defective products of screen printing T-shirts. PT. Indo Anugerah semesta experienced an increase in order on screen printing T-shirt products by 57% of the overall product. Screen printing shirts always experience defects exceeding the standard limits set by the company. The tolerance limit allowed by the company is 2% per work station. The company has never identified the problem so research is needed to make improvements to reduce the number of defects in the screen printing T-shirt manufacturing process.

RESEARCH METHODOLOGY

Data Collection

The required datas for this research are :

1. Production Process
2. Production Process Flow
3. Product Production Data
4. Defective Product Data

Data Processing

Failure Mode and Effects Analysis (FMEA)

The value calculation and analysis for each production is carried out by looking at several stages according to [1]:

- a. Identify the type of production process failure (*Failure Mode*)
- b. Identify potential effects of production failure (*Failure Effect*)
- c. Identify potential causes of failure (*Cause of Failure*)
- d. Identify process control (*Current control*)
- e. Determine the severity value (S)
- f. Determine the value of occurrence (O)
- g. Determine the detection value (D)
- h. Determine the value of the Risk Priority Number (RPN)
- i. Ordering of Risk Priority Number value (RPN)

Pareto Diagrams

Pareto diagrams will be searched to determine the priority of the Risk Priority Number (RPN) value in order to focus on finding the root cause of each failure mode and cause of failure by creating a Pareto diagram with the principle of 80/20 and as an input for analysis using the Fault Tree Analysis (FTA) method.

Analysis and Proposed Improvements

Fault Tree Analysis (FTA) is used to analyze the root cause of each failure mode and cause of failure by performing several stages according to [2]:

- a. Define the problem and boundary conditions of a system under review
- b. Fault tree graphic model depiction
- c. Finding the minimum cut set from fault tree analysis
- d. Conduct qualitative analysis of fault tree

Determination of minimum cut set using qualitative analysis with Boolean Algebra theory according to [3]:

- a. Putting together each fault tree chart for each defect that has been made
- b. Make a description table on the overall fault tree chart
- c. Numbering the entire fault tree chart
- d. Perform calculations to get a cut set that will be given a proposed improvement

Furthermore, it provides a proposed improvement based on the root of the problem obtained from the cut set results to minimize or eliminate known defects by making an improvement to the production of screen printing T-shirt products so that defects do not occur again.

Conclusions and recommendations

This research will result some recommendations for quality improvements to reduce the occurrence of defects during the production process. The recommendations submitted are the result of data processing that has been done and formulated in the analysis section.

RESULTS AND DISCUSSIONS

Data Collection

Production Process

The production process is a way to produce existing products. Production process at PT. Indo Anugerah Semesta conducts production by passing several machine processes, namely cutting machines, screen printing, curing, obras, chains, overdecks, checking.

Production Process Flow

Product process flow as information for production process instructions for screen printing T-shirt products. The process of working on 1 screen printing shirt product there is a processing time of 83 minutes and a product time of 64 minutes.

Product Production Data

Production data is obtained to see the amount of production each month in order to know the percentage of defects in screen printing T-shirt products. Production data obtained from PT. Indo Anugerah Semesta in marketing manager as many as 17600 screen printing T-shirt products in January 2020 to July 2021.

Defective Product Data

Flawed product data obtained from interviews with operational managers is viewed from each work station. Defective product data is used to look for the percentage of defects that occur in screen printing T-shirt production data. Defective product data shows the type of defect at each work station with the number of defective screen printing T-shirt products held by different operators when conducting the production process. Data and presentation of defective products can be seen in Table 1.

TABLE 1. Data and Percentage of Defective Products

No	Work Process	Work Station	Type of Defect	Defect Percentage
1	Making the front and back of screen printing shirts (O-1 , O-2)	Cutting Machine	The size of the front / back is too big	1,51%
			The size of the front / back is too small	
2	Making the hand part of screen printing t-shirts (O-4)	Cutting Machine	The size of the front / back is too big	1,54%
			The size of the front / back is too small	
3	Printing (O-8)	screen printing	wrong color	2,85%
			Wrong precision	
	Wrong position	...
8	Checking and packing (O-11 & I-1)	Checking Desk	T-shirt Screen Printing	
			Bolong Burned	2,55%

Data Processing

Failure Mode and Effect Analysis (FMEA)

The following is the processing of data based on the data that has been obtained for the improvement of problems that occur in PT. Indo Anugerah Semesta is:

a. Identify the type of production process failure (Failure Mode)

The first stage is the identification of the type of defect of the production process to find out the source where the damage occurs. Failure mode is the most important step in the use of the Failure Mode and Effect Analysis (FMEA) method. The results of identification of the type of defect are obtained through interviews and identification of the production process. Failure mode can be seen in Table 2.

TABLE 2. Failure Mode

NO	Work Station	Type of Production Process Defect (Failure Mode)
1	Cutting Machine	The size of the front / back of the screen printing shirt is too big
2		The size of the front / back of the screen printing shirt is too small
3		The size of the sleeve of the screen printing shirt is too big
4		The size of the sleeve of the screen printing shirt is too small
...

12	Checking Desk	Burning perforated screen printing t-shirt
----	---------------	--

b. Identify potential effects of production failure (Failure Effect)

The second stage identifies the potential effects of failure on the production process. The results of identification of the type of defect are obtained through interviews and identification of the production process. Failure Effect can be seen in Table 3.

TABLE 3. Failure Effect

NO	Work Station	Type of Production Process Defect (Failure Mode)	Potential Effects of Production Failure (Failure Effect)
1	Cutting Machine	The size of the front / back of the screen printing shirt is too big	Materials must be reworked
2		The size of the front / back of the screen printing shirt is too small	The material must be reworked (become part of the arm)
3		The size of the sleeve of the screen printing shirt is too big	Materials must be reworked
4		The size of the sleeve of the screen printing shirt is too small	Goods are rejected, and cannot be reworked
...
12	Checking Desk	Burning perforated screen printing t-shirt	Reject items, and cannot be reworked

c. Identify potential causes of failure

The third stage is the identification of potential causes of failure in the production process. The results of identification of the type of defect are obtained through interviews and identification of the production process. Cause of failure can be seen in Table 4.

TABLE 4. Cause of Failure

NO	Work Station	Type of Production Process Defect (Failure Mode)	Potential Effects of Production Failure (Failure Effect)	Potential Causes of Failure (Cause of Failure)
1	Cutting Machine	The size of the front / back of the screen printing shirt is too big	Materials must be reworked	Job specialization does not exist so that it affects operator performance
2				Wrong pattern creation
3				an unfavorable work environment that affects operator performance
...
35	Checking Desk	Burning perforated screen printing t-shirt	Reject items, and cannot be reworked	Smoking Operator

d. Identify process control (Current Control)

The fourth stage is the identification of the control process in the production process. The results of identification of the type of defect are obtained through interviews and identification of the production process. Current control can be seen in Table 5.

TABLE 5. Current Control

NO	Work Station	Type of Production Process Defect (Failure Mode)	Potential Effects of Production Failure (Failure Effect)	Potential Causes of Failure (Cause of Failure)	Process Control (Current Control)
1	Cutting Machine	The size of the front / back of the screen printing shirt is too big	Materials must be reworked	Job specialization does not exist so that it affects operator performance	Perform a visual inspection by the operator by measuring using a meter
2				Wrong pattern creation	
4				an unfavorable work environment that affects operator performance	
...
6	Checking Desk	Burning perforated screen printing t-shirt	Reject items, and cannot be reworked	Smoking Operator	Perform a visual inspection by the operator by measuring using a meter

e. Determining the Severity Value

Severity value is a value in the form of a rating or assessment obtained from an impact that can affect the final product. Determination of severity value obtained is the result of discussions with the company by looking at the company's criteria. Severity values can be seen in Table 6.

f. Determining the Occurrence Value

Occurrence value is an assessment that refers to the frequency of product defects and will be compared to the number of products produced. The results of determining the occurrence rating by looking at the company's criteria are obtained from the results of discussions with the company. Occurrence values can be seen in Table 6.

g. Determining the Detection Value

Detection values are used to prevent or determine failures that may occur and will affect subsequent processes in the production and assembly process. The results of the determination of rating detection by determining the company's criteria are obtained from the results of discussions with the company. Detection values can be seen in Table 6.

h. Determining the Value of the Risk Priority Number (RPN)

Determines the Risk Priority Number (RPN) value using the main variables in FMEA namely severity, occurrence, and detection. Risk Priority Number (RPN) serves to determine the value / weight rating of each failure. After looking at the type of defect (Failure mode) obtained. Determining the Risk Priority Number (RPN) can be seen in Table 6.

i. Ordering of Risk Priority Number (RPN) Values

After getting the Risk Priority Number (RPN) value from each screen printing T-shirt manufacturing process, it will be sorted the highest to lowest values so that further research can be done using the Fault Tree Analysis (FTA) method. The sorting of Risk Priority Number (RPN) values can be seen in Table 6.

TABLE 6. Ordering of Risk Priority Number (RPN) Values

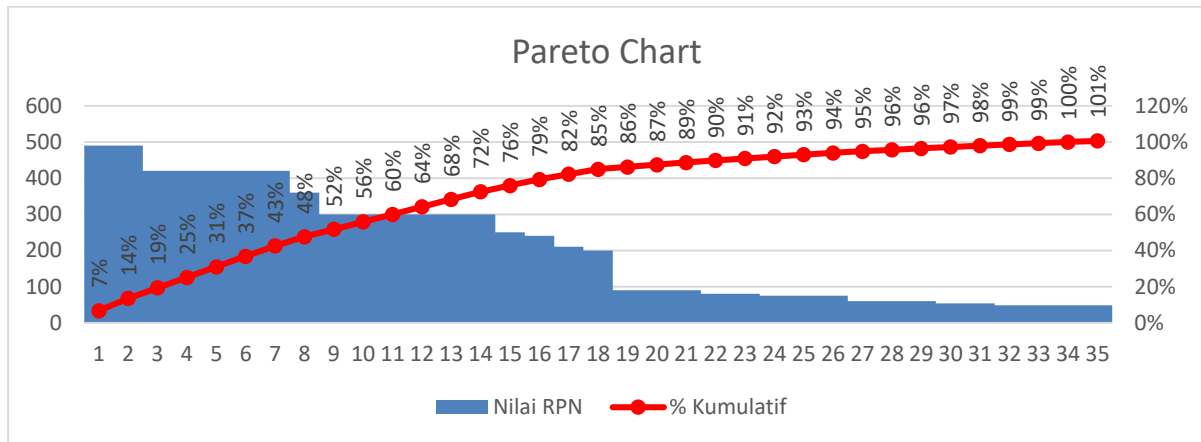
NO	Work Station	Type of Production Process Defect (Failure Mode)	Potential Causes of Failure (Cause of Failure)	S	O	D	RPN (Risk Priority Number)
1	Curing Machine	Fade	Machines that have never been repaired	10	7	7	490
2			Unstable engine heat	10	7	7	490
3			The drying process is not optimal	10	6	7	420
4			Old dry screen printing material	10	6	7	420
...
35	Overdeck Machine	Free Stitch	Inappropriate sewing process	4	3	4	48

Table description:

S = Severity, O = Occurrence, D = Detection

Pareto chart

After the sorting of the highest risk priority number (RPN) value to the next lowest is to determine the priority of improvement using the Pareto diagram. The function of the Pareto diagram here is to determine which priorities will be searched for the root of the problem using the Pareto 80/20 principle. The Pareto diagram can be seen in Figure 1.

**FIGURE 1.** Pareto Chart

The description of the picture can be seen in Table 8.

TABLE 8. Description Of Image

No	Type of Production Process Defect (Failure Mode)	Potential Causes of Failure (Cause of Failure)
1	Fade	Machines that have never been repaired
2		Unstable engine heat
3		The drying process is not optimal
4		Old dry screen printing material
5	Wrong color	Inappropriate color mixing process
6	Wrong precision	Job specialization does not exist so that it affects operator performance
7	Wrong position	Job specialization does not exist so that it affects operator performance
8	Wrong color	Job specialization does not exist so that it affects operator performance
9	Wrong precision	Screen printing process is not appropriate
10		an unfavorable work environment that affects operator performance
11	Wrong position	Screen printing process is not appropriate
12		an unfavorable work environment that affects operator performance
13	The size of the sleeve of the screen printing shirt is too small	Wrong pattern creation
14		Disturbed operator due to unfavorable work environment
15	Wrong color	The color liquid has not been replaced for a long time
16	Burning perforated screen printing t-shirt	Smoking operator
...
35	loose stitch	Inappropriate sewing process

The result of the Pareto diagram and obtained priority to find the root of the problem is at numbers 1-16. 6 failure mode, and 16 cause of failure:

- The type of defects in curing work stations resulted from machines that never repaired, unstable engine heat, non-optimal drying process, old dry screen printing material dry.
- Types of defects in mis-color, wrong precision, and wrong position at screen printing work stations resulted from the process of mixing colors that do not fit, the specialization of the work does not exist so as to correct the performance of the operator, the cloning process is not appropriate, the work environment is less conducive so that it affects the performance of the operator, color fluids have not been replaced for a long time..
- Type of screen printing T-shirt defects burned at the check desk work station caused by the operator smoking.
- Type of defect in the size of the sleeves of the small screen printing t-shirt resulted from the creation of the wrong pattern, the operator who was disturbed due to a less conducive work environment.

Analysis and Proposed Improvements

After getting any priority that will be sought the root of the problem using the principle of Pareto 80/20, then the root analysis of the problem by using the Fault Tree Analysis (FTA) method.

- fade in the curing process
The analysis of fastness defects in the drying process can be seen in Figure 2.

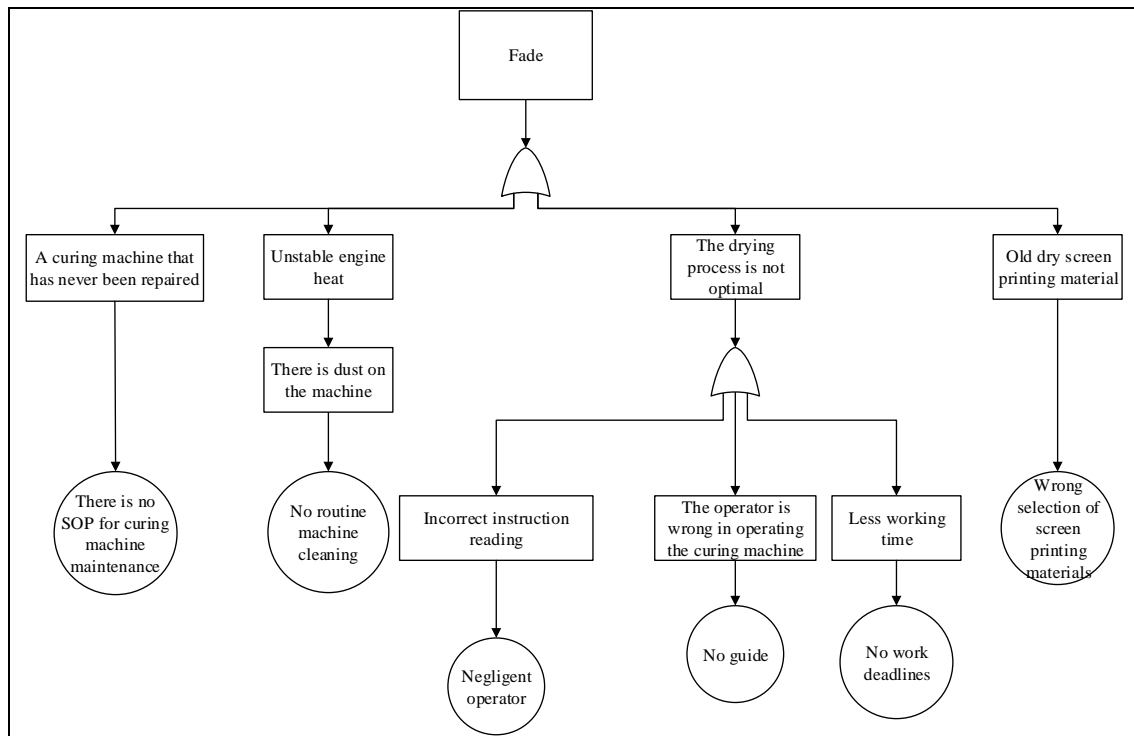


FIGURE 2. Analysis of Fastness Defects in the Drying Process

b. Wrong color in the screen printing process

The analysis of wrong color defects in the screen printing process can be seen in Figure 3.

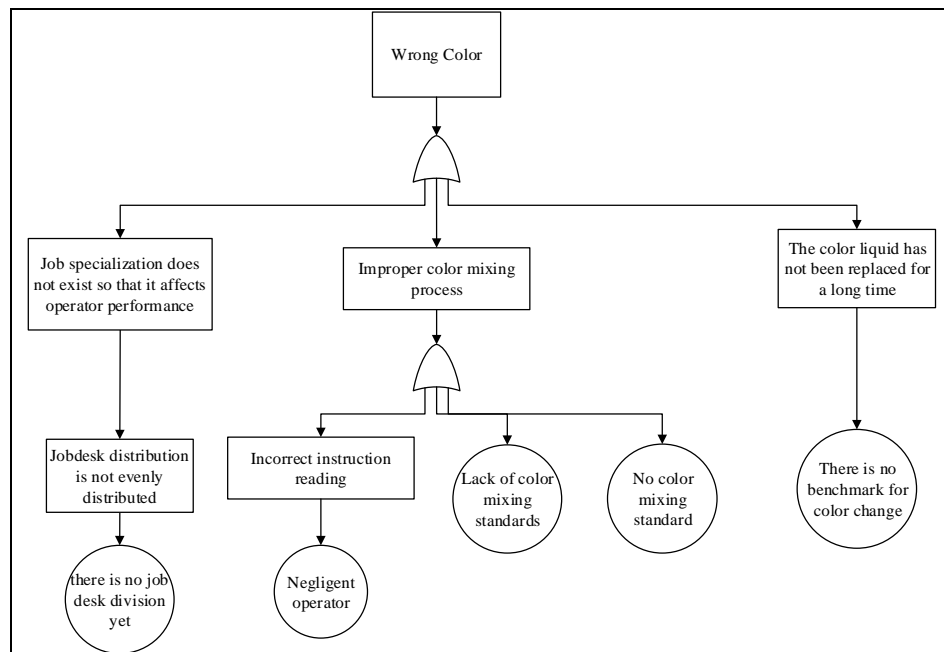


FIGURE 3. Analysis of Wrong Color Defects in the Screen Printing Process

c. Wrong precision in the screen printing process

Analysis of faulty precision defects in the screen printing process can be seen in Figure 4.

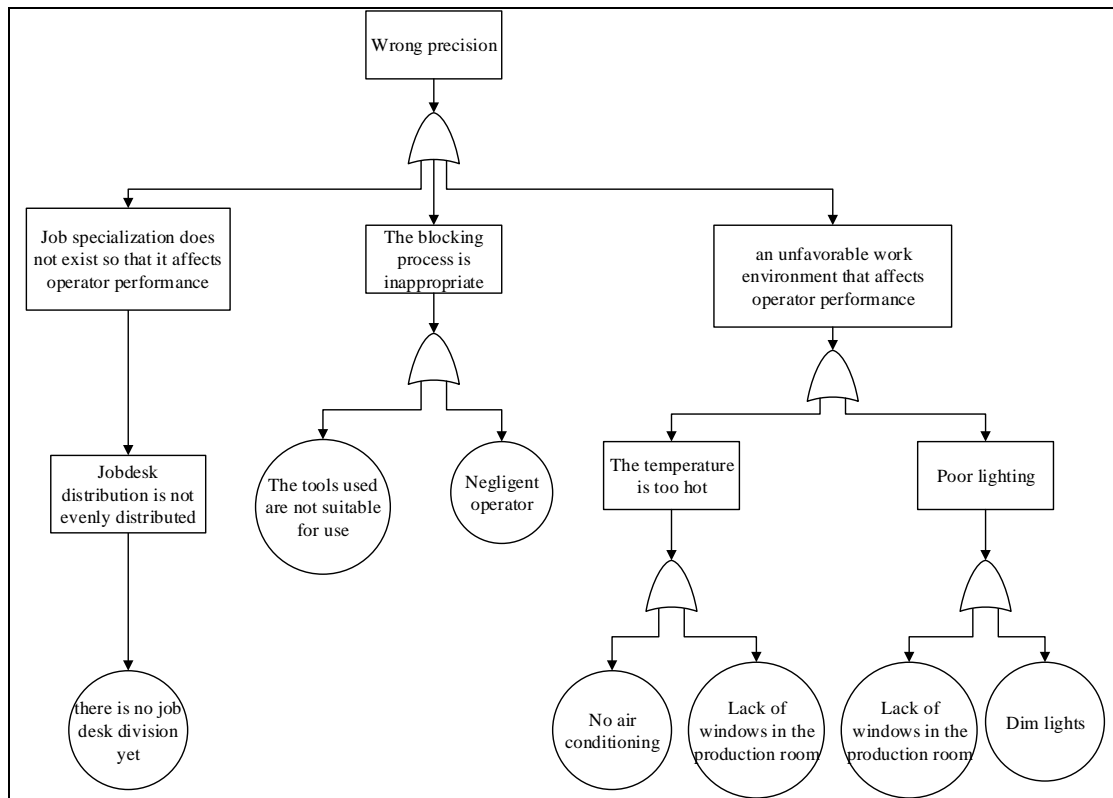


Figure 4. Analysis of faulty precision defects in the screen printing process

d. Wrong position in the screen printing process

The analysis of wrong position defects in the screen printing process can be seen in Figure 5.

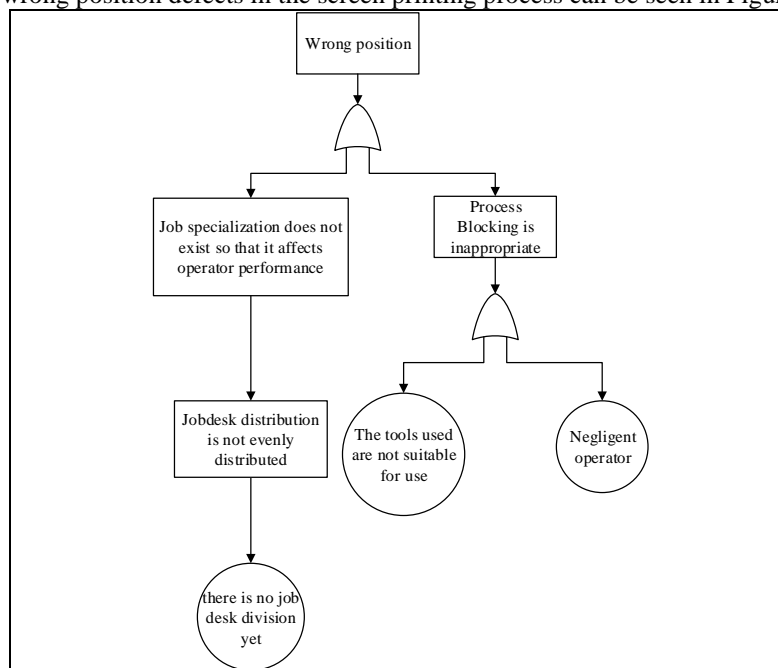


FIGURE 5. Analysis of Wrong Position Defects in the Screen Printing Process

- e. Printing shirt is burned in the checking process

The analysis of defects in the screen printing t-shirt in the checking process can be seen in Figure 6.

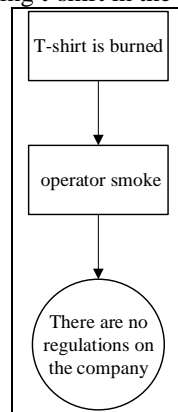


FIGURE 6. Analysis of the Defects of the Screen Printing T-shirt in the Checking Process

- f. The size of the sleeves of the screen printing shirt is too small in the cutting process.

Analysis of the size defect of the sleeve size of the screen printing shirt smallness in the cutting process can be seen in figure 7

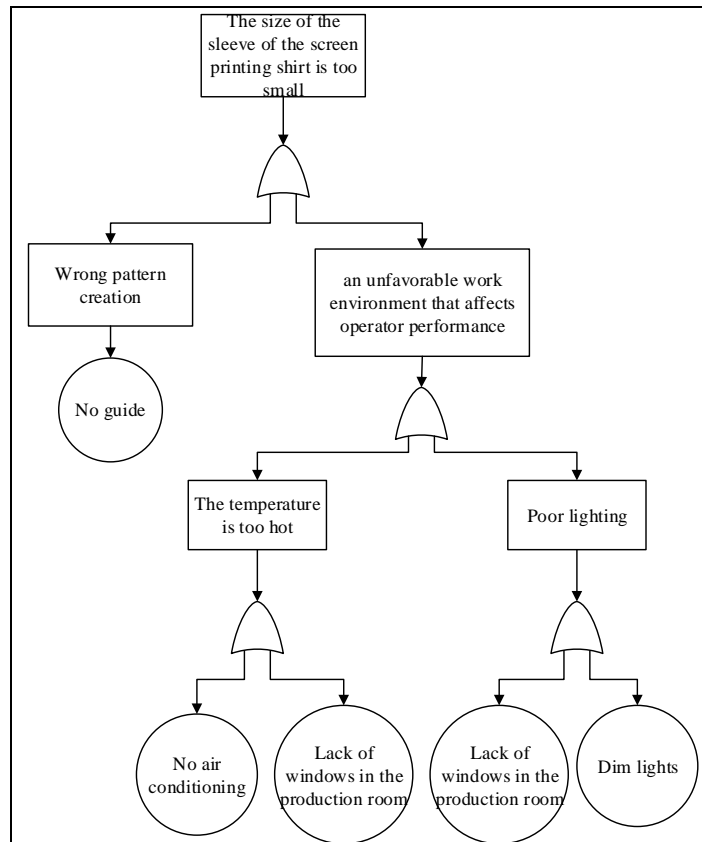


FIGURE 7. Analysis of Defects in Arm Size of T-shirt Screen printing Smallness In The Cutting Process

Furthermore, the determination of the minimum cut set using the Boolean Algebra method so that it gets 15 root problems overall failure mode and cause of failure and will be sought proposals to the root of the problem can be seen in Table 9.

Table 9. Improvement Proposal

Number	Root cause of Disability	Company Condition	Improvement Proposal
1	No SOP curing machine maintenance	Curing machines often have problems	Perform regular maintenance and make spare part changes
2	Wrong selection of screen printing material	Long-used screen printing material dry	The company must re-research the screen printing material used
...
12	There is no air conditioning	The production room is hot and has a few fans	Conduct further evaluation of the physical work environment
13	Lack of windows in the production room	Many rooms don't have windows	
14	Less bright lights	Inadequate room lighting	
15	There is no jobdesk division yet.	the operator works on all work stations	Create special divisions that are each responsible for one work station or one job

CONCLUSION

Based on the results of data processing and analysis, several conclusions were obtained, namely:

- The type of defects in curing work stations resulted from machines that never repaired, unstable engine heat, non-optimal drying process, old dry screen printing material dry.
- Types of defects in mis-color, wrong precision, and wrong position at screen printing work stations resulted from the process of mixing colors that do not fit, the specialization of the work does not exist so as to correct the performance of the operator, the cloning process is not appropriate, the work environment is less conducive so that it affects the performance of the operator, color fluids have not been replaced for a long time.
- Type of screen printing T-shirt defects burned at the check desk work station caused by the operator smoking.
- Type of defect in the size of the sleeves of the screen printing shirt smallness caused by the creation of the wrong pattern, a less conducive work environment that affects the performance of the operator.

Recommendations for improving the quality of PT. Indo Anugerah Semesta as follows :

- The company must perform periodic maintenance of the machines and tools used so that the production process can be carried out optimally.
- The company must follow clear regulations or Standard Operating Procedures (SOPs) in every production process to be clear in doing something.
- Companies should conduct further evaluation of the physical work environment in order to increase productivity in operators.
- Companies are supposed to create special divisions that are each responsible for one work station or one job.
- The company should re-research the color mixing and liquid use policy as well as the selection of good quality screen printing materials.
- The company provides rewards or punishments to operators in order to increase the morale of the operator.
- The company must conduct supervision of the operator while the production process takes place.

REFERENCES

- L., Nuriawati, Evaluasi Penerapan Keselamatan dan Kesehatan Kerja (K3) Berdasarkan Fault Tree Analysis (FTA), Failure Modes & Effect Analysis (FMEA) dan Preliminary Hazard Analysis (PHA) (studi kasus : Jurusan TIPTL SMK Negeri 1 Magelang), *Unpublished Final Project*, Universitas Negeri Yogyakarta, (2017).
- Y., Prawira, Pengendalian Kualitas Batu Pancing Dengan Metode Failure Mode And Effect Analysis (Fmea) Dan Metode Fault Tree Analysis (Fta) Di Pt. Cahaya Castindo Hasanah Cemerlang, *Industrial Engineering Repository Universitas Medan Area* (2019).
- T., Ferdiana and P., Ilham, *Analisis Defect Menggunakan Metode Fault Tree Analysis (FTA) Berdasarkan Data Ground Finding Sheet (GFS) PT. GMF AEROASIA*. Surabaya : Jurnal Universitas Sebelas Maret. (2016).

Control Making for Elevator Simulation of Three Floor Building Based on Arduino Uno

Muhammad Farhan Mustaqim^{1, a)}, Eka Taufiq Firmansjah P.A¹

¹ Mechanical Engineering Departement, Faculty of Industrial Technology , Institut Teknologi Nasional Bandung
Jl. PH.H Mustofa No. 23 Cikutra, Cibeunying Kidul, Neglasari, Cibeunying Kaler, Bandung, Jawa Barat, 40124,
Indonesia

^{a)} Corresponding author: 28farhanmustaqim@gmail.com

Abstract. Lift (elevator) is a tool used to raise and lower loads (good/people) between floors of a multi-storey building using a set of mechanical tools, either with automatic or manual tools. The research proposes to design a control system using the Arduino Uno IDE and create an elevator simulation using the CX-Programmer and CX-Designer. The purpose of the research on the manufacture is to determine the aspect to be achieved by adjusting the speed of the rotating motor, changing the motor rotation up and down, and programming the control system to make it work, and moving the lift using a 12 voltage motor power and the Dual H-Bridge L298N Motor driver. With a capacity of 5 voltages to power the Arduino Uno pin, and inside the Arduino Uno pin, several inputs are six pushbuttons for the first floor to the third floor, which on each floor there are two pushbuttons and a limit switch. A chain of elevator control systems can move according to the designed program

INTRODUCTION

Lift (elevator) is a tool used specifically to transport loads, lifts are also often used in high-rise buildings that require load mobility between floors, this elevator uses an Arduino Uno microcontroller and a driving device using a 12 volt DC motor to be connected to the L298N motor driver. and to Arduino Uno to be programmed so that the control system design can rotate up and down, to find out up and down in the program, the condition of the lift when going up in3 (forward) is high and in4 (reverse) is low clockwise (CW), for the elevator when going down, in3 (forward) is low and in4 (reverse) is high it is counterclockwise (CCW) and makes a lift simulation using CX-programmer and cx-Designer so that it is easy to understand the working principle of the elevator.

METHOD

Process Schema

Figure 1 shows the schematic of the process carried out in the manufacture of a control system for a simulation of a three-story building elevator based on Arduino Uno. Starting from studying theories related to Arduino Uno and simulation software (CX-programmer and CX-designer), then determining what components are needed to design an elevator control system, then designing system tools that have been purchased such as Arduino, pushbuttons, dc motors, motor drivers, etc., the next process is programming the desired Arduino application, then making elevator simulations using CX-programmers and CX-designers to easily understand the working principle, then testing whether the program and system design are correct, if they function properly What is expected is that the documentation of the results of the design made is then concluded and becomes a parameter for further manufacture.

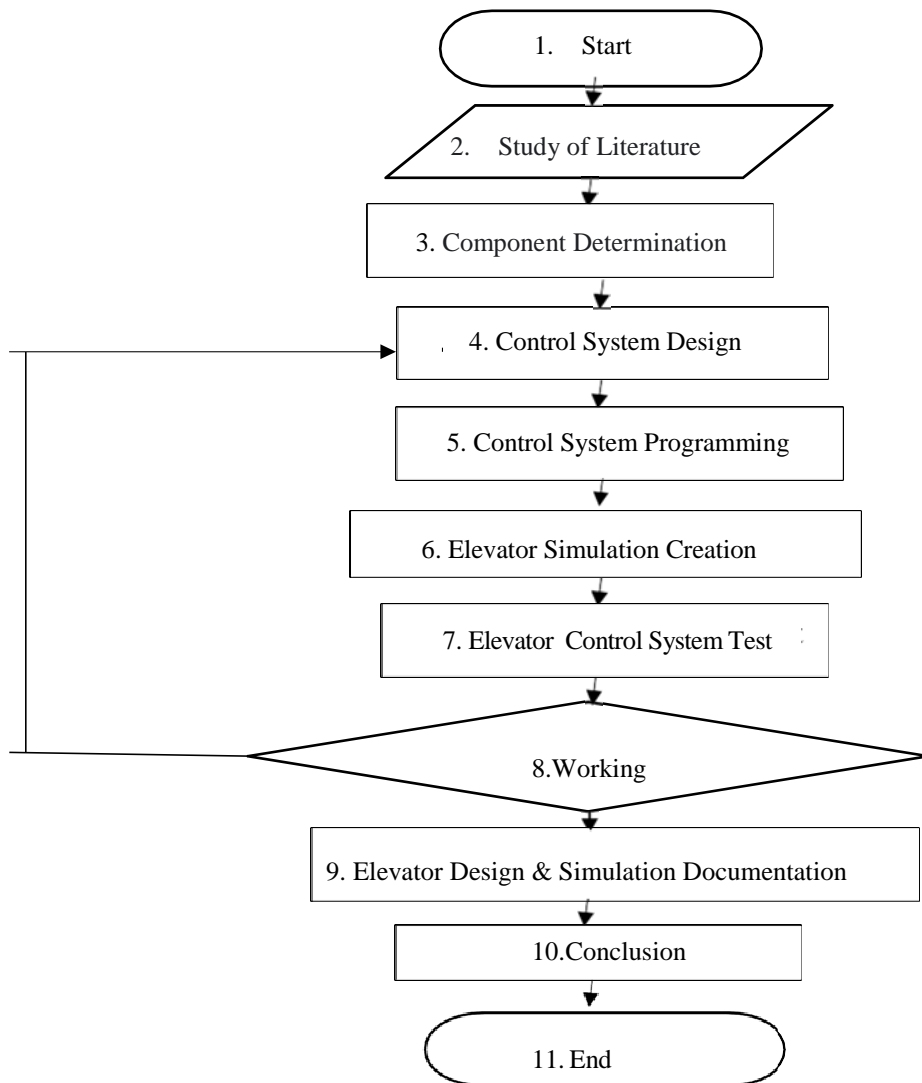


FIGURE 1. Process Schema

Control System Design

The design of the elevator control system of this three-story building functions as an elevator in general, only the difference is that the weight capacity is smaller, by making this elevator control system requires components to move the elevator up and down, and in this elevator design, the author uses the Arduino Uno microcontroller as the system. The control is where Arduino uses 6 volts to 20 volts and the input pins used in the three-story elevator control system are 9 pins (PB1, PB2, PB3, PB4, PB5, PB6, LS1, LS2, LS3) and the output pins use several three. pins (enb, in3, in4). Pushbuttons as elevator buttons to make it easy to go up and down and on each floor install two pushbuttons, on the first floor there are push buttons to go to the second and third floors, and on the second floor there are push buttons to go to the first and third floors, and on the second floor there are push buttons to go to the first and third floors. On the third floor, there is a push button to go to the second floor and the first floor. And there is a motor to drive the lift so that it can go up and down for up and down rotation. The author distinguishes the direction of rotation if the lift goes up the motor rotates in a clockwise direction (CW) if the lift goes down the motor rotates counterclockwise (CCW) The components in this design use The motor driver power supply uses an adapter cable according to the specifications of the motor used (12VDC) the pins used in the motor driver are enb, in3, and in4 which function to regulate the speed

of the PWM motor (Pulse Width Modulation) and in3, in4 to regulate the Forwatt Rivers Motor. To make it easier to understand the elevator control system of this three-story building, it can be seen in the system diagram that shows in Figure 2.

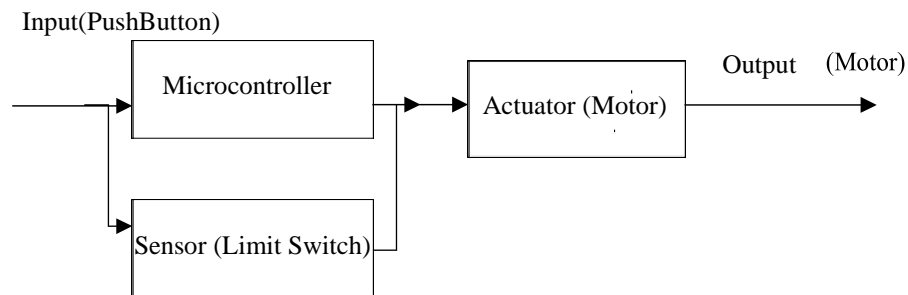


FIGURE 2. System Flowchart

ANALYSIS AND DISCUSSION

Documentation Results of Elevator Control System Design



FIGURE 3. Three-Story Elevator Control System Design Installation

The pin flow for each component of Figure 3 are :

1. Motor Driver
 - a. Enb: pin 11
 - b. In3: pin 8
 - c. In4: pin 6
 - d. GND: Kabel adaptor 12VDC
 - e. 12V: Kabel adaptor
 - f. Out 1: Motor
 - g. Out 2: Motor
2. Arduino Uno
 - a. Push Button 1: pin 2
 - b. Push Button 2: Pin 5
 - c. Push Button 3: Pin 9
 - d. Push Button 4: Pin10

- e. Push Button 5: Pin A1
- f. Push Button 6: Pin A2
- g. Limit Switch 1: Pin 3
- h. Limit Switch 2: Pin 4
- i. Limit Switch 3: Pin A0

Based on the schematic above, the three-story elevator control system shows that Arduino is a very dominant component used for other components and the program is also very influential.

Elevator Simulation Making Documentation Results

Program for the elevator control system of a three-story building that has been created using Arduino Uno software and a program used to create an elevator simulation design (CX-designer) and a program to run a simulation design (CX-Programmer). CX-Programmer shows in Figure 4.

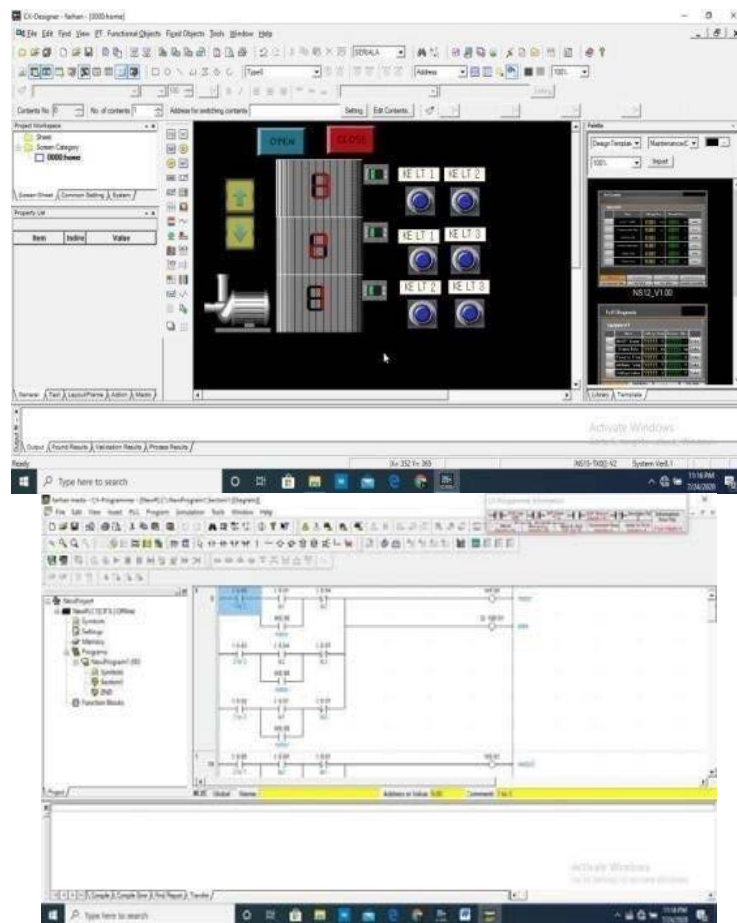


FIGURE 4. CX-Programmer

Analysis

Based on the results of the manufacture of a three-story building elevator control system, there are several analyzes obtained, namely as follows. First, in the elevator control system program to distinguish the direction of rotation of the motor when the lift goes up and down because the rotation of the motor when it goes up and down automatically is different, then in the Arduino Uno program for the lift the condition goes up in3 (forward) for clockwise rotation (CW) high and in4 (reverse) for anticlockwise rotation (CCW) is low, and when the lift condition is down, in3

(forward) is low and in4 (reverse) is high. Second, the enb pin on the motor driver is often detached which will result in excessive voltage, then the effect that occurs on the motor driver is easy to heat and can cause the motor driver to be easily damaged, so the solution is to solder the enb pin.

CONCLUSION

Based on the research that has been done, it can be concluded that the program has been made according to the design and when tested, the control system works well. Adapter cable according to the specifications used 12 volt DC after being tested the motor can move according to the used 12 volt DC.

For better results in further research for the elevator control system of this three-story building, there are several suggestions. First, the project board is used only temporarily and you should use a PCB (PrinterCircuit Board) so that it is not easy to remove the jumper cable. Second, it's best to solder the motor driver's enb pin so that it doesn't come off easily. Third, the cable connection on the DC motor should be soldered so as not to cause the motor driver to heat up and the cable to burn due to overvoltage⁴. Fourth, the elevator control system of this three-story building uses a 12V high torque DC motor (GW4058-31ZY) with the same specifications, where the current required is not more than 2A.

REFERENCES

1. Agus M. (2006). Study on Design of PAU ITB Freight Elevator Controller Using MICRO Control Unit M68HC16Z1-ECBID.
2. Andrianto, Heri. (2016). Arduino Fast Learning And Programming Bandung: Informatics Bandung.
3. Anonim. DC Motor Driver Using Transistor Relay. <http://yosmedia.blogspot.com> (accessed on 10 November 2010).
4. Anonim. The elevator is. <http://id.wikipedia.org/wiki/lift> (accessed on 10 November 2010) <http://aristriwiyatno.blog.undip.ac.id/files/2011/10/Bab-1-Konsep-Umum-Sistem-Kontrol>.
5. Ardiwinoto, (2008). ATmega8/32/8535 AVR Microcontroller & Programming With C Language WINAVR. Bandung: Informatics.
6. Heri, Andrianto. (2008). ATmega16 AVR Microcontroller Programming Using C Language (CodeVisionAVR).Bandung: Informatics.
7. Kadir, Abdul. (2012). Practical Guide to Learning Microcontroller Applications and Programming Using Arduino. Yogyakarta.
8. Kadir, Abdul. (2015). Arduino Programming Smart Book. Yogyakarta: Mediacom.
9. Maarif, Eka Samsul. (2017). OMRON PLC Basic Manual “Good Automation”. Yogyakarta
10. Subarta, Budi. (2013). Module “Logic Gate Circuit Concept”. Jakarta.
11. Wicaksono, Handy. (2009). Book Of Programming Theory And Its Application In System Automation.Yogyakarta.

Manufacturing and Testing Static of Rear Suspension System KMLI Car

Hendriksen Samuel K.^{1, a)} and Marsono¹

¹Mechanical Engineering Department, Faculty of Industrial Technology, Iteas Bandung

^{a)} Corresponding author: hendriksensamuel99@gmail.com

Abstract. The manufacture of the electric car rear suspension KMLI (Indonesian electric car competition) aims to make the suspension fit the regulations and suitable for use. The manufacture of suspension components from the suspension design uses solidwork software based on frame shapes and other components, then the engineering drawing process, the process plan, the preparation process, the manufacturing process, the component manufacturing process and the testing process. The test results for ground clearance without load are 230 mm and ground clearance testing for 125 kg load is 134 mm with a standard ground clearance of 100-170 mm. suspension. From the test results, the electric car rear suspension system can be said to be good and feasible to use.

INTRODUCTION

Kompetisi Mobil Listrik Indonesia (KMLI) is an activity held to test students' competence in designing and manufacturing safe, economical, and environmentally friendly vehicles. At KMLI, the vehicle design refers to the current four-wheeled vehicle design. The dimensions of the vehicle must comply with the established regulations which have a width of 120140 cm and a minimum weight of a vehicle without a driver of 125 kg. For the vehicle to be safe and comfortable, there are several aspects that the designer must pay attention to. Vehicles experience vibrations and shocks both due to the engine and due to bumpy and uneven road surface contours. To reduce vibration or shock, every vehicle must have a suspension system. The suspension system is a mechanism that is between the vehicle body and the wheels that serves to dampen vibrations, the suspension system must be strong enough to withstand static and dynamic loads from the passenger, chassis, and engine. Suspension system design is an important part of the overall vehicle design, it's determines the car's performance [1]. The suspension system on a vehicle is one of the important components of an active suspension system which is divided into 2 types, namely series and parallel types. The ideal suspension system can minimize deflection and vertical acceleration of the vehicle body which ensures safety and comfort in driving for a variety of road surface conditions [2]. In this research, the manufacture and testing of components of the rear suspension system of the KMLI car will be carried out. This study aims to obtain the physical form of the rear suspension system components and apply these components to the KMLI vehicle and to determine the feasibility of the rear suspension system of the KMLI namely the large suspension deflection and ground clearance distance. With the scope of the study, make the existing suspension mechanism with an independent double wishbone model and test the performance of the suspension system, namely the large ground clearance and large spring deflection.

METHODOLOGY

Doing the literature study to find out about the double wishbone coil spring suspension and KMLI car. Also studying the design and manufacture of the KMLI car frame that has been made in previous research and KMLI regulations as a reference and reference for designing an electric car suspension, After determining the suspension then do the manufacture of a double wishbone suspension, after all components are made then all components are assembled and the ground clearance and large deflection spring testing process is carried out with various loadings to determine the feasibility of the suspension mechanism that has been made.

Suspension Design

KMLI rear suspension is made with reference to the design of the densest suspension model in a racing car [3]. The design of the suspension system mechanism that will be made in this study is shown in Figure 1. The process of designing the rear suspension system of the KMLI car was carried out using Solidwork 2017 software.

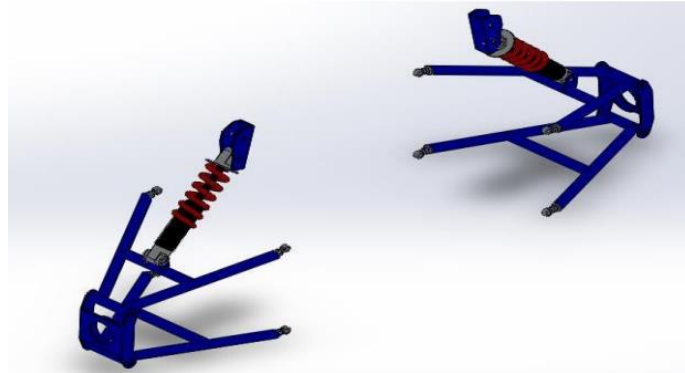


Figure 1. Racing Car Rear Suspension design

Modeling

The modeling is done with software to see if the designed mechanism can function properly. In addition, with the help of software, the size of each component also can be determined with an accurate modeling as shown in Figure 2.

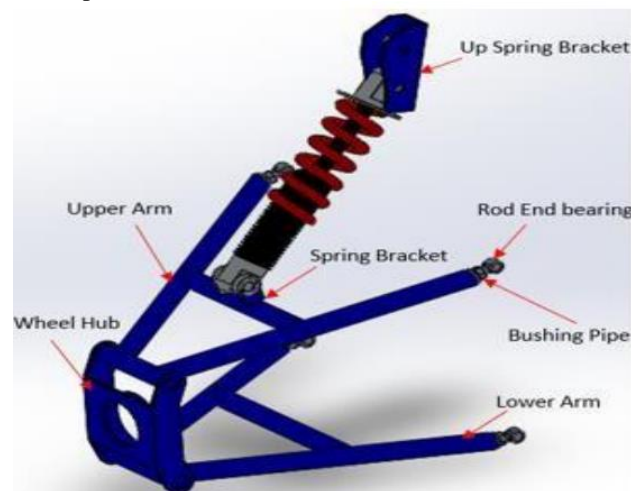


Figure 2. Components of The Rear Suspension

The modeling of the rear suspension system with this software is carried out by considering the use of standard components that available in the market so do not need to be made. Furthermore, the components that are designed and manufactured will follow and adjust to the dimensions of the standard components. This modeling is done with format of 3-dimensional images. The components of the rear suspension system of the KMLI and their assembly structure are shown in Figure 2. The rear suspension system of the KMLI car is composed of components; arm (lower and upper arm), bushing pipe arm, wheel hub, rod end bearing, spring bracket and shock absorber. Some of the components mentioned are already available in the market, while some other components are not available in the market. To get the components that are not yet available on the market, needs to do a manufacturing process.

The components that are already available in the market are rod end bearings (Figure 3) and shock absorbers (Figure 4), while the components that are not available in the market and must be manufactured are; wheel hub (Figure 5), bushing pipe arm (Figure 6), spring bracket (Figure 7), spring bracket (Figure 8), lower arm (Figure 9), and upper arm (Figure 10).



Figure 3. Road and Bearing



Figure 4. Shock Absorber

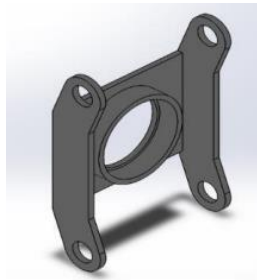


Figure 5. Wheel Hub

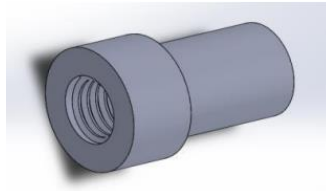


Figure 6. Bushing Pipe

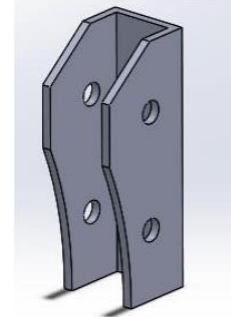


Figure 7. Spring Bracket

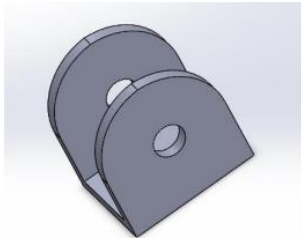


Figure 8. Spring Bracket

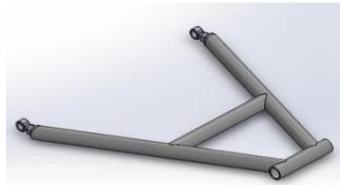


Figure 9. Lower Arm

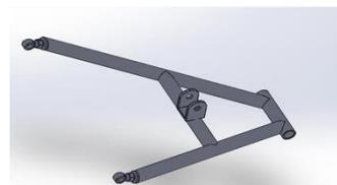


Figure 10. Upper Arm

Component Manufacturing and Assembly

The manufacture of components that can't find on the market, begins with the manufacture of technical drawings. Then process planning for each component. At this stage, detailed preparation of the process stages is carried out, complete with process parameters, tools, and other necessary tools. The manufacture of components of the rear suspension system of KMLI cars, are arm wheel hub, bushing pipe arm, and spring bracket process that carried out between cutting, turning, perforating, threading, welding, and grinding processes. Together with the manufacturing process, a measurement process is also carried out to ensure that the finished components are of the correct size and do not cause problems during assembly. It can be seen in Figure 10 that is making the arm, Figure 11 is making the bushing pipes, Figure 12 is making the wheel hub, Figure 13 is making the spring bracket and Figure 14 is the pictures of the suspension that has been installed. The process of assembling or combining all components is carried out to get a rear suspension system device that can function according to its function as shown in Figure 14.



Figure 10. Making the Arm



Figure 11. Making the Brushing Pipe



Figure 12. Making the Wheel Hub



Figure 13. Making the Spring Bracket



Figure 14. Rear suspension that has been installed on the car frame

Testing Process

The process of making the rear suspension component on this KMLI electric car requires needs considerations and a careful working process so that the suspension can work optimally according to the function. To determine the performance and function of the suspension components, several tests were carried out to determine if the suspension components were feasible or not. Testing by applying a load to the chassis is shown in Figure 15 to obtain the vehicle's ground clearance (Figure 16) and the amount of spring deflection (Figure 17).



Figure 15. Loading Point



Figure 16. Ground Clearance Measurement



Figure 17. Spring Deflection Measurement

RESULTS AND DISCUSSION

Several parameters that need to be known to measure the performance of the rear suspension system of a KMLI car are ground clearance testing and spring deflection testing.

Ground Clearance Testing Results

After the testing, the results obtained ground clearance as shown in Figure 18. The results show the ground clearance at a maximum load of 125 kg is 134 mm, the results can be said to be feasible because the minimum ground clearance distance is 100170mm.

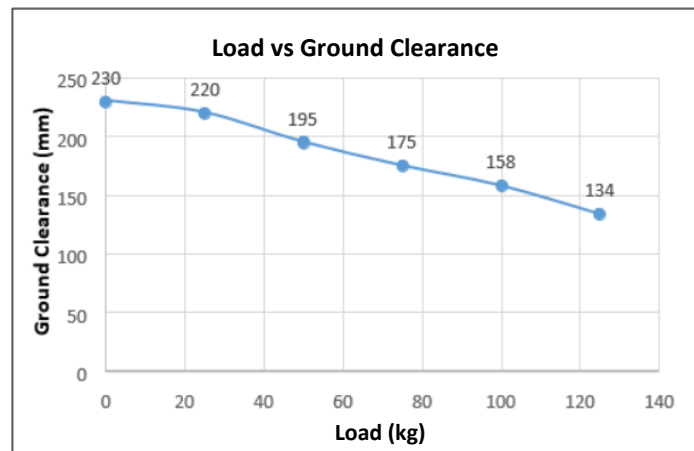


Figure 18. Graph of Ground Clearance Test Results vs Load

Spring Deflection Test and Shock Absorber Length Result

The deflection test on the suspension spring shows the results as shown in Figure 19. The results of testing the spring deflection on the rear suspension system when the load reaches 125 kg is 47 mm. In addition to testing to determine the spring deflection, the shock absorber on the rear suspension system of the KMLI car was also tested to determine the length of the shock absorber when it is under load. From the tests carried out, the results obtained as shown in Figure 20.

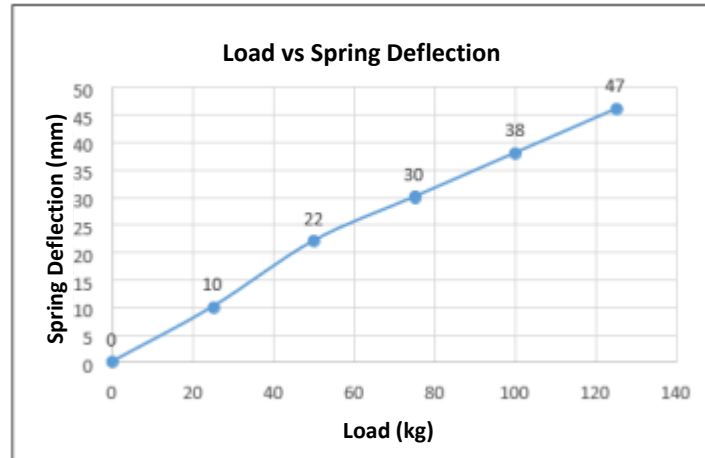


Figure 19. Graph of Spring Deflection Test Results vs Load

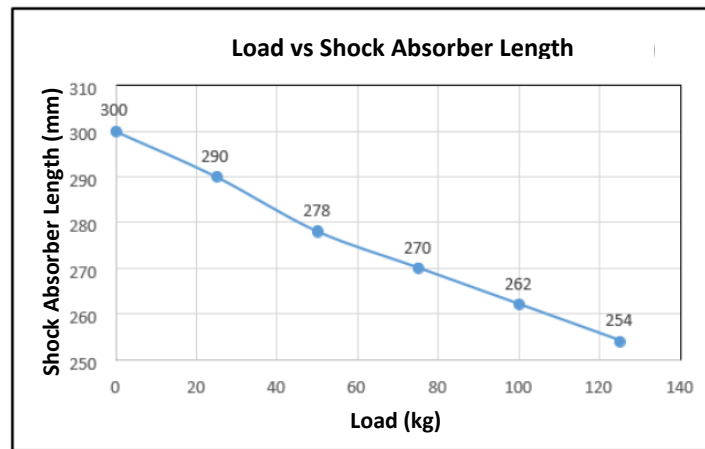


Figure 20. Shock Absorber Length Test Results

These results show that the smallest shock absorber length that occurs at the time of maximum loading is 254 mm. The shock absorber used in this suspension system is a Yamaha mio shock absorber which has a maximum standard length of 310 mm, and a minimum standard length of 207 mm. From the tests that have been carried out on the spring at the beginning, when the condition is installed without a load, and when holding the maximum load, the data is obtained as shown in Table 1.

TABLE 1. Shock Absorber Comparison

No	Long (mm)	0.0	Minimum Length (mm)	Stroke (mm)
1	First	310		103
2	No Load	300	207	93
3	Full Load	254		47

From these data, it is known that the distance of the stroke at no load is 93 mm, while the distance of the stroke at full load is 47 mm. If you look at the standard working conditions of the Yamaha Mio shock absorber, where the minimum standard length is 207 mm, the shock absorber installed on the rear suspension system of the KMLI car can be said to be safe. It can be seen in table 1 that the minimum length of the shock absorber on the rear suspension system of a KMLI car when receiving a maximum load is 254 mm, still far from the standard minimum limit of 207 mm.

CONCLUSION

The conclusion that can be drawn from the results of the research is that the rear suspension system made for KMLI cars can function properly and is within safe limits. This can be seen from the ground clearance at no load and some loads and spring deflection tests at no load and some loads. The test results for ground clearance without a load are 230 mm, while ground clearance with a load of 125 kg is 134 mm. These results can be said to be feasible because of the standard ground clearance of 100-170 mm. The results of the spring deflection test without a load leave a step of 93 mm, while with a load of 125 kg it is 47 mm. These results are said to be feasible based on the Yamaha Mio shock absorber standard that is applied because it can work according to its function. So, it can be said that the suspension system made for this KMLI car is feasible to use.

REFERENCES

1. Benthams, *Design and Strength Analysis of FSAE Suspension*, School of Mechanical Engineering, Southeast University, (2014).
2. O. Bagus., S. Sumardi., and A. Triwiyatno., *Desain Auto Tuning PID Menggunakan Logika Fuzzy Pada Sistem Suspensi Aktif Tipe Pararel Nonlinear Model Kendaraan Seperempat*, Universitas Diponegoro Semarang, (2013).
3. Polban, *Regulasi Kompetisi Mobil Listrik Indonesia XI (KMLI XI)*, Politeknik Negeri Bandung, (2019).

The Role of Nitrogen Gas and Variations of the Magnetic Field on the Characteristics of Flame on Combustion of Premixed Vegetable Oil Blends (B50)

Dony Perdana^{1, a)}

¹ Department of Mechanical Engineering, Universitas Maarif Hasyim Latif (Umaha), Sidoarjo – INDONESIA

^{a)} Corresponding author: dony_perdana@dosen.umaha.ac.id

Abstract. This research examines the role of nitrogen gas, attractive and repulsive magnetic field for vegetable oil fuel, a mixture of coconut oil and jatropha (B50) on the characteristic and stability of the flame in the premix combustion process. The experiment was carried out in a cylindrical burner, mixed vegetable oil vapor was reacted with a mixture of air and nitrogen gas at various air fuel ratios. The results showed that the magnetic field increased the combustion speed because the electron spin became more energetic and the hydrogen proton spin changed from para to orto. The increase in combustion speed was greater in the magnetic field than without. Magnetic field attract exerted the strongest influence on increasing the burning speed and making the flame more stable. This happens, paramagnetic O₂ is pumped into the flame, while H₂O and N₂ as diamagnetic push heat out of the flame, causing faster combustion with an air-fuel ratio of 4.52 - 12.76. While the magnetic fields repel, H₂O and N₂ are attracted into the flame, however, O₂ is pumped out of the flame in the air-fuel ratio range of 4.52-15.1. Meanwhile, without a magnetic field, the air fuel ratios was 4.52-17.51 the highest compared to the magnetic field, produces poor combustion and is not ideal.

Keywords:-air-fuel-ratio; flame-evolution; magnetics-field; vegetable-oil; premix-combustion

INTRODUCTION

Rapid population growth and industrialization have led to a crisis of fossil fuel depletion and environmental degradation. Pollutants such as CO, CO₂, NO_x, and organic matter emitted from burning fossil fuels reduces clean air quality. Therefore, alternative energy sources are the most attractive option to replace fossil fuels. Vegetable oils are a prospective alternative fuel because of its diesel-like properties and is produced from plants with minimal effort [1]. Jatropha, coconut, rapeseed, are some of the vegetable oils used in combustion engines [2]. Researchers have revealed that vegetable oils can reduce HC, CO, and CO₂. However, The main disadvantages of vegetable oils are: highly viscous, and lower volatility, affecting fuel atomization, evaporation and fuel-air mixing [3] including dirty filters and deposits in the engine [4]. There are various solutions proposed: blending, preheat and engine modifications. compression ignition engines use you right vegetable oil or mixed with diesel for operation. some researchers in various countries have succeeded in using a mixture of vegetable oil and diesel [5]. Various biodiesels have been tried as an alternative fuel [6]. It has been shown in all cases that better engine performance reduces smoke, hydrocarbons and carbon monoxide emissions, despite increased nitrogen oxides. Studied the performance characteristics of a multi-cylinder diesel engine using a mixture of 95% diesel fuel with 5% used cooking oil, palm, and coconut respectively, showed over there was a reduction in BP of 1.2%, and 0.7%, this was also a decrease in exhaust emissions including UHC, CO, and NO_x [7]. From all of these studies, combustion stability largely establish engine fruition has not been investigated.

Furthermore, a study is required specifically regarding of nitrogen gas and direction of the magnetic fields in stabilizing combustion. This study provides a discussion of the role of nitrogen gas and the direction of the magnetic field in stability of flame behavior, and combustion characteristics. The application of flame stability is useful for the systematic and steady combustion furnaces and industrial burners during the long term.

MATERIALS AND METHOD

Vegetable Oil Fuel

The vegetable oils tested was a mixture of coconut oil and jatropha (B50). The compositions, physical, and chemical properties of the vegetable oils have been demonstrated in our previous study [8].

Experimental Apparatus

The experimental apparatus is shown schematically in Figure 1. The fuel mixture of coconut oil and jatropha (B50) as much as 600 ml filled to boiler, after that it is heated by the stove to be evaporated at a temperature of 300 oC, and the pressure is kept constants at four bar. The fuel evaporating and nitrogen inlet valve is opened while the air inlet is closed. The next process is to slightly open the air inlet valve and the height difference is recorded in flow control. Differences in fuel and nitrogen flow control are recorded and kept constant Coconut and jatropha oils vapor is mixed with air and nitrogen in the combustion chamber. The reactant mix is passed to a nozzle for 18 mm of diameter, after that, the flame is lighted.

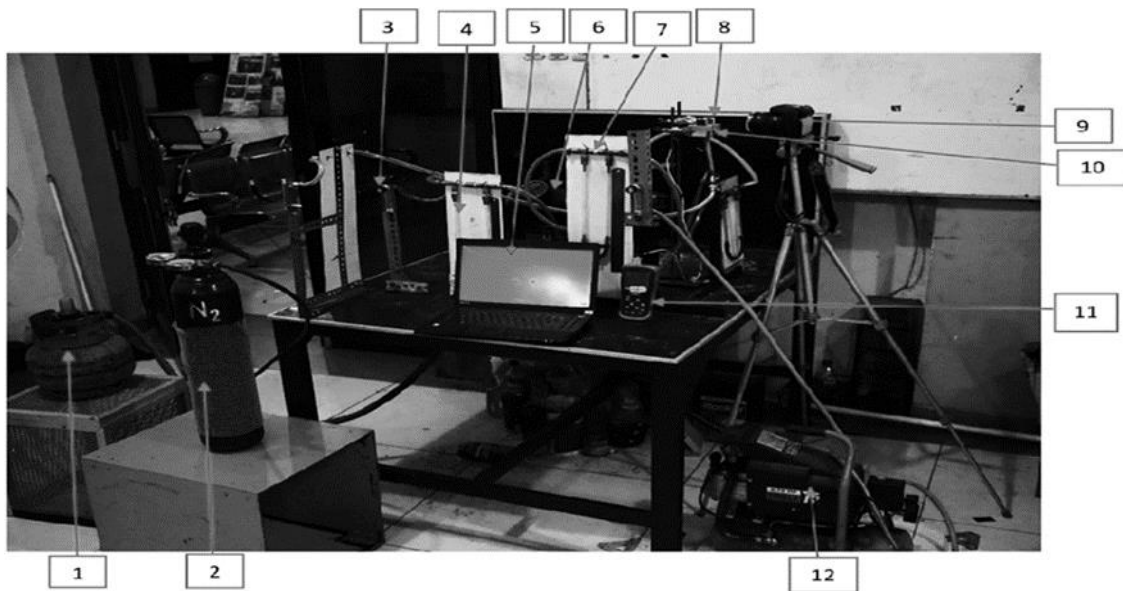


FIGURE 1. Experimental equipment; 1. stoves; 2. nitrogen gas; 3. flowmeter; 4. flowcontrol; 5. laptop; 6. boiler; 7. valve; 8. permanent magnet; 9. high speed camera; 10. burner; 11. thermocouple; 12. compressor

Thermocouple Position Schematic

Two rectangular magnets are placed on a stand made of aluminum plate and fastened for easy removal and re attachment changing the direction of the NN and SN magnetic fields. The image of the premix flame formed at the nozzle mouth taped before the flame was extinguished using a high-speed camera of 120 fps. The data logger is connected to a type K thermocouple placed at a position 2 mm above the burner tip to record the temperature generated in the computer memory as shown in Figure 2.

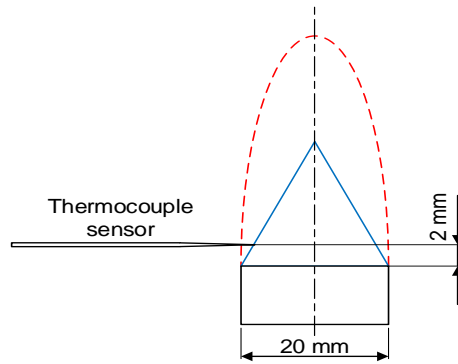


FIGURE 2. Thermocouple Position

RESULT AND DISCUSSION

Stability of the Flame at Various Air Fuel Ratio and the Orientation of Magnetic Field

It is shown in Figure 3 variations in the orientation of the magnetic field and nitrogen affect in stability, shape, and color of the flame at various air-fuel ratios in a mixture of coconut oil and castor oil (B50). Combustion of a mixture of coconut oil and jatropha (B50) without a magnet looks stable.

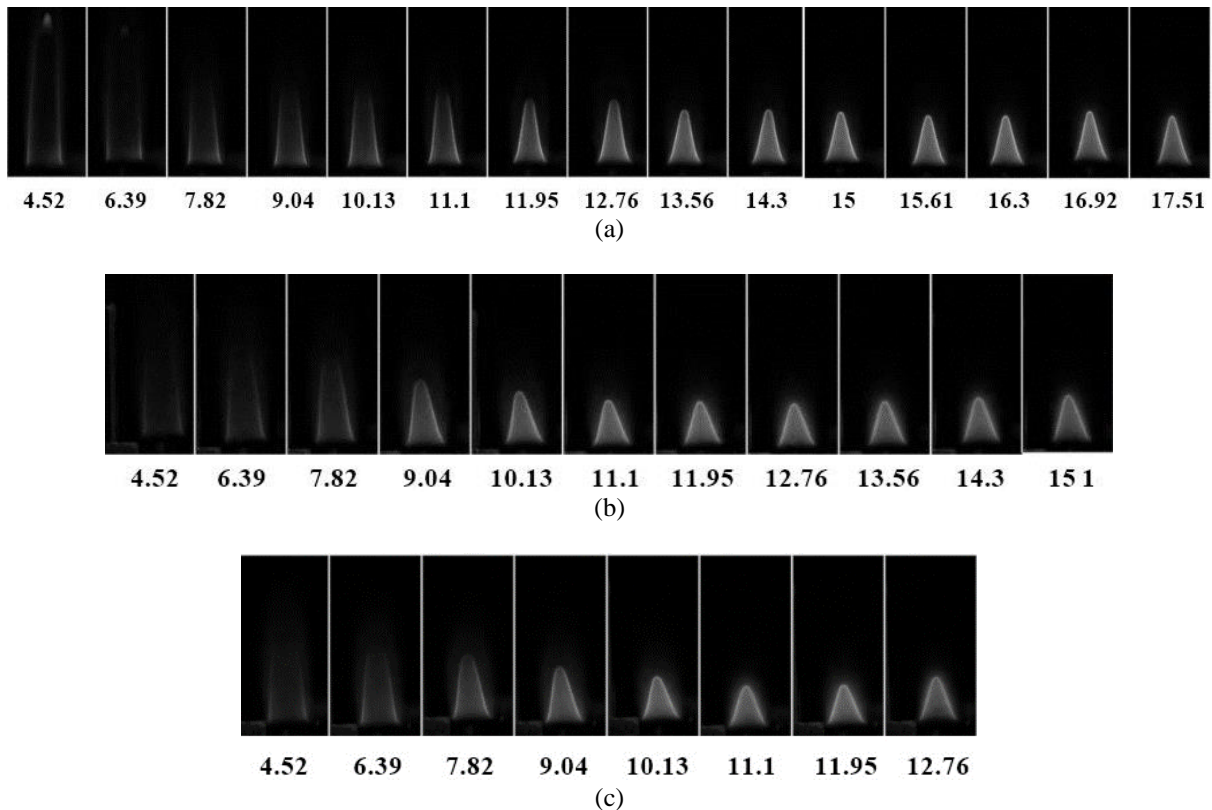


FIGURE 3. Stability and shape of flames various air fuel ratio and orientation of magnetic fields; (a) without; (b) repulsive; (c) attractive

The stability of the flame before the flame lifted off and then blew off occurred at an air fuel ratio of 17.51, while the shape of the flame was rather thin and the color of the resulting flame was ignited starting from an air fuel ratio of

11.95-17.51 shown in Figure 3a. The orientation of the repulsive and attractive magnetic fields affects the stability, this is indicated by the flame slightly wider and lighter at the air-fuel ratio of 15.1 and 12.76 before the flame is lifted and extinguished as shown in Fig.3a and 3b. This happens because O₂ is a paramagnetic and moves in the magnetic field direction while the product H₂O is diamagnetic and carries heat [9]. The second, nitrogen as an inhibitor inhibits the collision of fuel vapors and air reactions. The stability and color of the flame are influenced by the shape of the vortex caused by the presence of a magnetic field, this phenomenon is caused by the north (N) and south (S) magnetic poles forming the Lorentz force. Causes the flame in the middle to be also dragged by the magnetic field so that the flame becomes turbulent. The flame was attracted towards the south magnetic pole because of positive ions (which is much more than the negative ions in the flame), while the negative ions were attracted to the north magnetic pole. The magnetic field pushes the nitrogen from the reactant fuel velocity, therefore the combustion without the nitrogen mixture becomes more perfect.

Temperatures at Various Air-Fuel Ratios and the Orientation of Magnetic Field

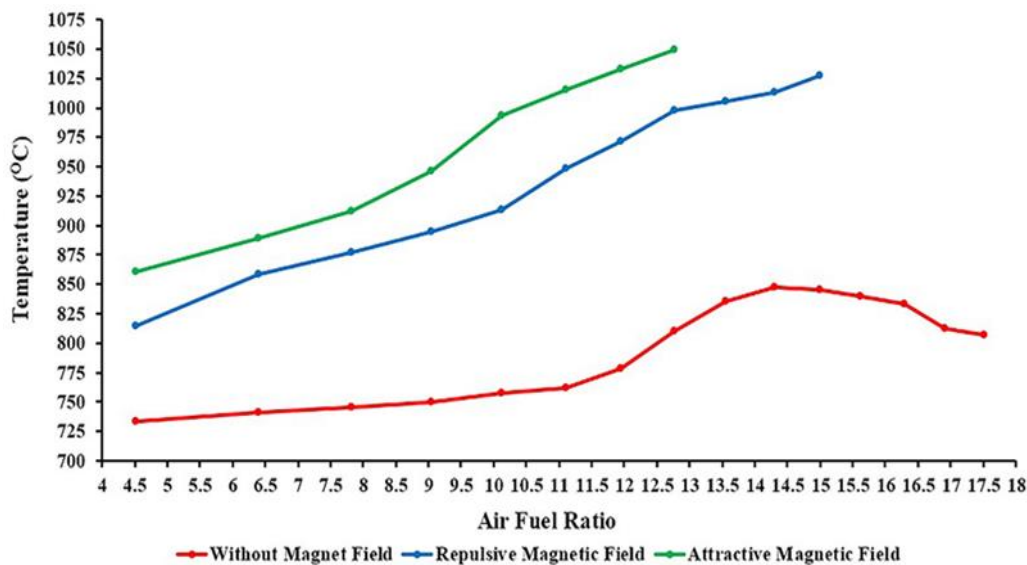


FIGURE 4. Temperature at various air fuel ratio and the orientation of magnetic field

Figure 4 shows the flame temperature of various variations of air-fuel ratio in a mixture of coconut oil and jatropha (B50) against two variations of magnetic and non magnetic fields and influenced by nitrogen gas. The highest burning flame was at an air fuel ratio of 12.76 with an attractive magnetic field of 1050 oC, followed by a repulsive magnetic field of 1028 oC at air-fuel ratio of 15, while the lowest temperature was 807 oC in an unmagnetized manner at an air fuel ratio of 14.3. The higher temperature indicates the premix fire caused by the calorific value of vegetable oil [8] and the increasing speed of combustion produces greater energy or power. The highest flame temperature occurs in an attractive magnetic field compared to a repulsive field or without a magnetic field.

Flame Height at Various Air-Fuel Ratio and the Orientation of Magnetic Field

Figure 5 shows the flame height of various variations of air-fuel ratio in a mixture of coconut oil and jatropha (B50) against two variations of magnetic and non-magnetic fields and influenced by nitrogen gas.

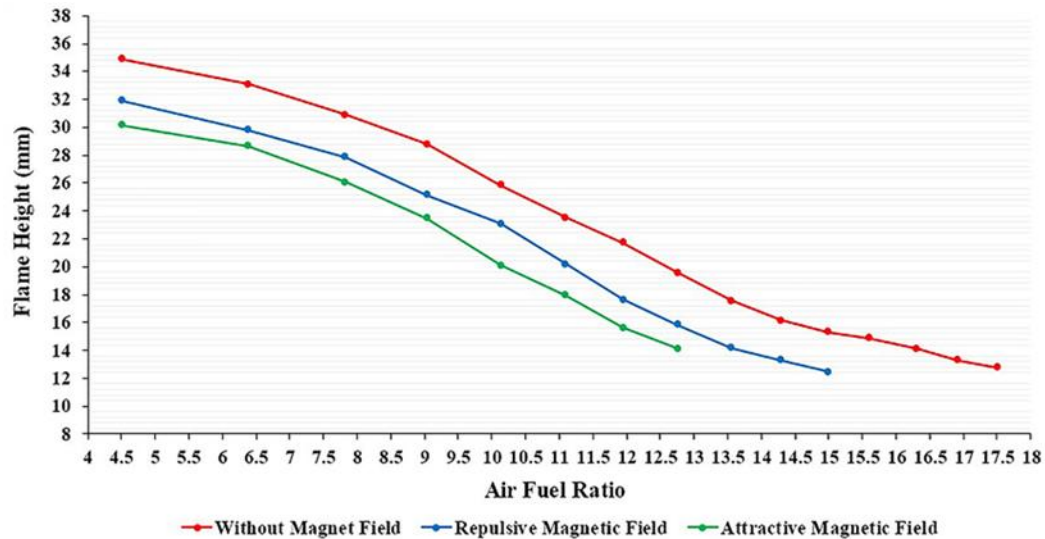


FIGURE 5. Flame height at various air fuel ratio and the orientation of magnetic field

The lower the air fuel ratio, the lower the flame height produced. The highest flame occurred in combustion without a magnetic field of 34.9 mm with an air fuel ratio of 4.52, then the flame height decreased successively at a repulsive magnetic field of 31.91 mm and an attractive magnetic field of 30.16 mm, where premix combustion in both conditions was very fast and short. This indicates that the repulsive and attractive magnetic fields are very reactive compared to those without a magnetic field, but the combustion is incomplete because there is some unburned fuel causing flame stability to be shorter (liftoff then blow off) occurs above the air fuel ratio of 15 in repulsive the magnetic fields and 12.76 attractive. The flame height gradually decreased as the applied magnetic field increases. when combustion has applied a magnetic field and nitrogen causes the flame to become smaller, foggy, and thinner. The possibility of an obstacle in the collision of fuel and air resulting in incomplete combustion. The decrease in flame height produced by premixed combustion follows an increase in the air-fuel ratio.

CONCLUSION

1. Magnetics field around the flame induces the airflow causing a change in flame height. Oxygen flows to the base of the flame on both sides result in increased concentration around the reaction zone. The fuel molecules react with the oxygen molecules causing better combustion with the formation of the inner and outer cones of a very short flame.
2. The use of nitrogen gas causes a decrease in convection heat loss as the strain increases.

However, this research still has shortcomings related to the amount of nitrogen gas concentration, types of vegetable oil and the intensity of the magnetic field which is not large. This is possible, the reduction in plantation areas that affects the amount of vegetable oil production in Indonesia tends to decrease, and the low strength of the magnetic field intensity affects the strength of the combustion characteristics. This study also cannot project the fuel efficiency, volumetric, thermal and polluting emissions of internal combustion engines. So it is necessary to conduct research that is more focused on its application to internal combustion engines for all types of pure vegetable oils and their derivatives, as well as the strength of the magnetic field intensity. So as to produce some data for the progress of the transportation sector.

ACKNOWLEDGEMENTS

Special thanks to Pancrasius Kuda Weruin, ST. and the Department of Mechanical Engineering, Faculty of Engineering, Universitas Maarif Hasyim Latif Sidoarjo, who helped to collect experimental data and funded this research.

REFERENCES

1. A. S. Ramdhas, C. Muraleedharan, and S. Jayaraj, "Performance and emission evaluation of a diesel engine fueled with methyl esters of rubber seed oil", *Renewable Energy*, 30 (12), pp. 1789-1800, DOI: 10.1016/j.renene.2005.01.009 (2005).
2. J. N. Reddy, and A. Ramesh, "Parametric studies for improving the performance of a jatropha oil fuelled compression ignition engine", *Renewable Energy*, 31(12), pp.1994-2016, DOI: 10.1016/j.renene.2005.10.006 (2006).
3. D. H. Qi, K. Yang, D. Zhang, and B. Chen, "Combustion And Emission Characteristics Of Diesel-Tung Oil-Ethanol Blended Fuels Used In A Crdi Diesel Engine With Different Injection Strategies", *Applied Thermal Engineering*, 111, 927-93, DOI: 10.1016/j.applthermaleng.2016.09.157 (2017).
4. S. S. Sidibé, J. Blin, G. Vaitilingom, and Y. Azoumah, "Use Of Crude Filtered Vegetable Oil As A Fuel In Diesel Engines State Of The Art: Literature Review", *Renewable and Sustainable Energy Reviews*, 14 (9), pp. 2748-2759, DOI: 10.1016/j.rser.2010.06.018 (2010).
5. C. D. Rakopoulos, K. A. Antonopoulos, D. C. Rakopoulos, D. T. Hountalas, and E. G. Giakoumis, "Comparative Performance And Emissions Study Of A Direct Injection Diesel Engine Using Blends Of Diesel Fuel With Vegetable Oils Or Biodiesel Of Various Origins", *Energy Conversion and Management*, 47 (18-19), pp. 3272-3287, DOI: 10.1016/j.enconman.2006.01.006 (2006).
6. P. J. Singh, J. Khurma, and A. Singh, "Preparation Characterization Engine Performance And Emission Characteristics Of Coconut Oil Based Hybrid Fuels", *Renewable Energy*, 35 (9), pp. 2065-2070, DOI: 10.1016/j.renene.2010.02.007 (2010).
7. M. A. Kalam, H. H. Masjuki, M. H. Jayed, and A. M. Liaquat, "Emission And Performance Characteristics Of An Indirect Ignition Diesel Engine Fuelled With Waste Cooking Oil", *Energy*, 36(1), pp. 397-402, DOI: 10.1016/j.energy.2010.10.026 (2011).
8. D. Perdana, I. N. G. Wardana, L. Yuliati, and N. Hamidi, "The Role Of Fatty Acid Structure In Various Pure Vegetable Oils On Flame Characteristics And Stability Behavior For Industrial Furnace", *Eastern-European Journal of Enterprise Technologies*, 8 (95), pp. 65-75, DOI: 10.15587/1729-4061.2018.144243 (2018).
9. D. Perdana, L. Yuliati, N. Hamidi, and I. N. G. Wardana, "The Role Of Magnetic Field Orientation In Vegetable Oil Premixed Combustion", *Journal of Combustion*, pp. 1-11, DOI: 10.1155/2020/2145353 (2020).

Performance Enhancement of PTSC by Using Mono and Hybrid Nanofluids

Asaad Yasseen Al-Rabeeah^{1, a)}, Istvan Seres^{2, b)} and Istvan Farkas^{3, c)}

¹Doctoral School of Mechanical Engineering, Hungarian University of Agriculture and Life Sciences, Pater K. u. 1., Gödöllő, H-2100, Hungary

²Institute of Mathematics and Basic Science, Hungarian University of Agriculture and Life Sciences, Pater K. u. 1., Gödöllő, H-2100, Hungary

³Institute of Technology, Hungarian University of Agriculture and Life Sciences, Pater K. u. 1, Gödöllő, H-2100, Hungary

^{a)} Corresponding author: Al-Rabeeah.Asaad.Yasseen.Ali@phd.uni-mate.hu

^{b)} Seres.Istvan@uni-mate.hu

^{c)} Farkas.Istvan@uni-mate.hu

Abstract. The parabolic trough solar collector (PTSC) is one of the most reliable solar thermal technologies. Thermal energy is collected from solar radiation at a certain point. PTSC consists of a reflecting surface, an absorber tube, and working fluid. Solar radiation raises the enthalpy of the fluid inside the tube and increases the temperature of the tube wall. The aim of this study is to improve the thermal efficiency of PTSC by enhancing the working fluid. Furthermore, heat transfer analysis was used to investigate the performance of PTSC. The heat transfer performance is improved by using nanofluids (NFs) rather than convectional heat transfer fluids (oil, water, and ethylene glycol). Mixing nanoparticles into the fluid is an efficient way to improve the thermo-physical properties of NFs, such as thermal conductivity, density, and specific heat capacity. Therefore, the thermal conductivity increases with increasing solid volume fraction, which could raise the heat transfer coefficient. Furthermore, comparing the effects of using mono and hybrid NFs on thermal efficiency for better heat transfer.

INTRODUCTION

Energy efficiency is a major problem within our modern society due to recent environmental issues such as water pollution, air pollution, climate change, and global warming [1, 2]. Alternative energy sources such as solar, geothermal, [3, 4], wind, and biomass have been used recently to reduce pollution and inadequate fossil fuel supply [5]. Thus, developing and using renewable energy sources, such as solar energy, is critical [6]. In the past few years, solar energy research has demonstrated that it can be transformed into thermal energy using trough collector systems and solar concentrators, and subsequently into electrical energy using a steam turbine [7].

The advantages of new heat transfer fluids lead researchers to view them as a feasible choice for heat transfer enrichment in solar energy systems. Many researchers have studied solar energy, focusing on the ability to produce energy from solar radiation intensity and the benefits of solar energy synchronization with other direct and indirect applications such as heating [8]. The parabolic trough collector (ptc) is one of the most extensively used solar power systems to create high and medium temperatures with high efficiency. In 1870, Johan Ericsson invented a 3.25 m² parabolic collector called a "straight steam generator" to produce 373 W of electricity [9].

A solar collector is a device that converts solar energy into heat (fluid or air). It can then be used for hot water or to enhance heating systems. Solar collectors are heat exchangers that convert solar radiation into heat energy [10, 11]. The parabolic trough collector is ideal for generating power at temperatures as high as 400 °C [12]. NFs are a new heat transfer fluid that can be used to improve heat exchanger performance in solar systems. One of the most significant technologies for improving the thermal performance of solar collectors is the use of NFs as working fluids [13]. NFs

are made by mixing working fluids such as water or thermal oil with nanoparticles. Some of the most common nanoparticles are CuO , Al_2O_3 , Al , SiO_2 , Cu and TiO_2 [14].

Using these nanoparticles increases the flow thermal conductivity and thus the heat transfer rate from the hot tube to the working fluid. This article clarifies the use of nfs in ptc. To evaluate the use of nfs in solar systems, heat transfer and performance enhancement in solar thermal collectors must be precisely determined. Many studies have been done on nfs in heat transfer applications, especially solar collectors.

Metallic and nonmetallic nanoparticles were inserted into several base fluids at varying amounts. According to Olia et al., 40% of the research used aluminum oxide (Al_2O_3) nanoparticles to improve ptc thermal performance, while other nanoparticles (CuO , TiO_2 , Fe_2O_3 , etc.) exhibited lower interest for the researchers. Hybrid nfs have many advantages for heat transfer applications. Hybrid nfs have shown good thermophysical characteristics, long-term stability, and heat transmission rate.

According to studies, using nfs in ptc improves their thermal and optical properties. This review study investigates the effects of factors on performance, such as selection of mono and hybrid nanomaterials on base fluids, effect on thermophysical properties, and application of nfs inside ptc technology.

PREPARING OF NANOFLUIDS

NFs Preparation is the first step in doing nanofluid (NF) experiments. There are two primary methods for preparing nanofluids: the 1-step method preparation process and the 2-step method preparation process.

One-Step method

The one-step process involves creating and dispersing the particles in the fluid simultaneously. This approach avoids the dispersion, transportation, storage, and drying of nanoparticles, thereby minimizing nanoparticle agglomeration and increasing the stability of fluids [15]. So, this method can produce uniformly dispersed nanoparticles stable in the base fluid [16]. The various morphologies are affected and determined by the dielectric liquids' thermal conductivity properties.

Due to the inability of the one-step physical technique to synthesize NFs on a large scale and its expensive cost, the one-step chemical method is rapidly developing. The pulse wire evaporation technology is used to create NF. The apparatus includes capacitors, a high voltage DC power source, a gap switch, and a condensation chamber. By delivering a high voltage pulse (300 V) over a tiny wire, the wire evaporates and transforms into plasma in microseconds. The plasma is subsequently condensed into nanopowder by the inert gases Ar and N_2 . The NF is then cascaded into the pulse wire evaporator's exploding container and combined with the nanosized powder to form a hybrid NF. This approach is ideal for making low-cost NFs [17].

Two-Step method

The first step in this process is to produce a dry nanoparticle powder. The two-step preparation approach involves combining base fluids with commercially available nanopowders generated by mechanical, physical, and chemical procedures such as grinding, milling, vapor phase methods, and sol-gel [18].

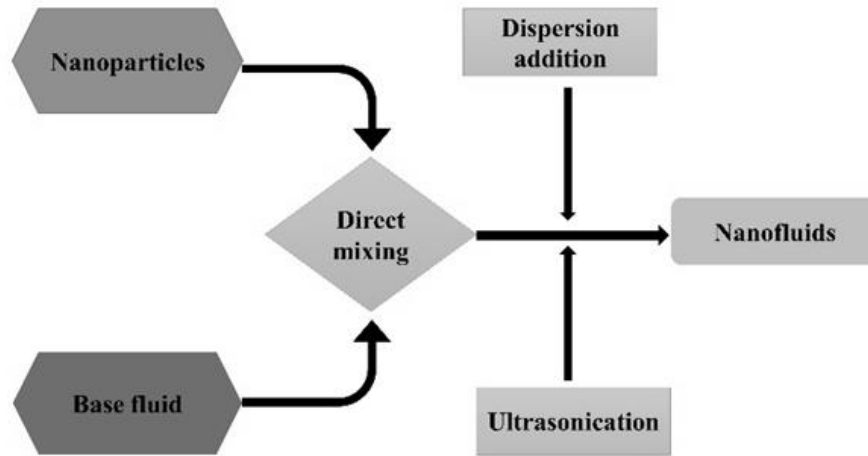


FIGURE 1. Two-step preparation process of NFs.

It is commonly done by compressing the solid sample, evaporating it with noble gases, and mixing it with the base fluid. Generally, nanopowders are stirred with host fluids using an ultrasonic vibrator or a higher shear mixing device. Ultrasonication or stirring on a frequent basis is essential to prevent particle agglomeration [19].

As strong Vander Wall forces limit particle attraction before complete diffusion in the fluid, this approach results in agglomeration and sedimentation. So, to resolve this issue, ultrasonic waves, NF exposure, pH adjustments, and surfactants were utilized. Figure 1 shows the two-step procedure that is most commonly used.

Thermophysical Properties

To analyze the thermal framework of mono and hybrid NFs, detailed thermophysical data is required. The amount of nanoparticles added to the base liquids affects their thermophysical properties. Considering the thermophysical properties of NFs, it is predicted that nanoparticles are continuously dispersed in the base fluids [20]. Their properties include thermal conductivity, viscosity, specific heat, and density [21]. However, the heat transfer coefficient and pressure drop are also important parameters to consider.

These properties depend on nanoparticle shape and size, volume concentration, surfactant, and so forth. The thermal conductivity of a liquid is directly connected to its heat transfer capacity without affecting the flow, pressure drop, or pumping power of nanoparticles in a fluid medium [22]. Fig. 2 shows several factors affecting NF thermophysical properties.

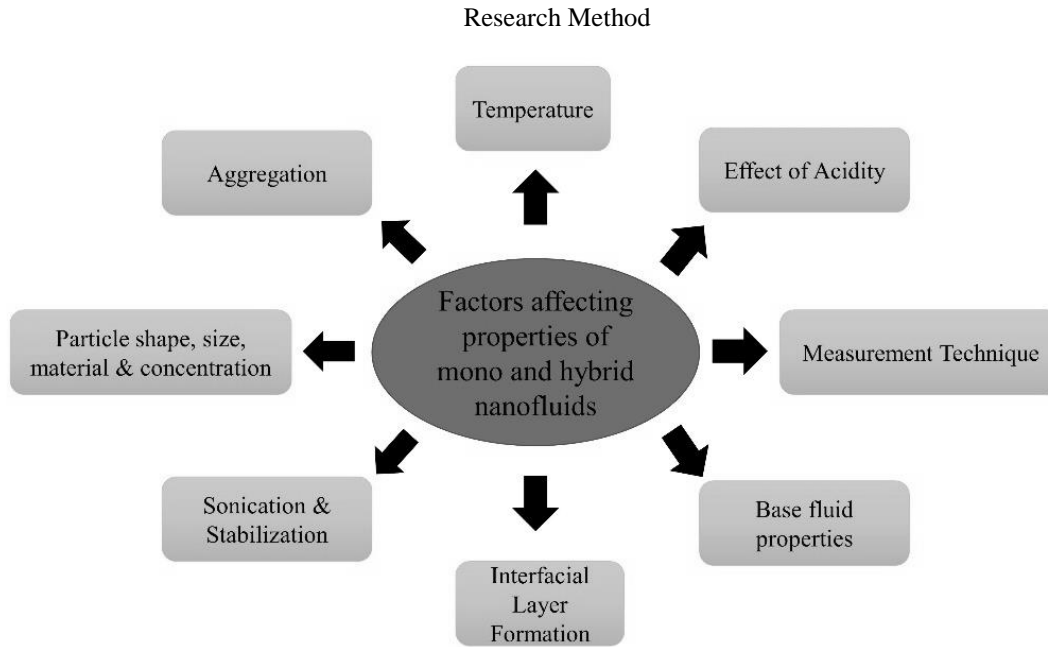


FIGURE 2. Factors affecting of the thermophysical properties of mono and hybrid NFs.

Thermal conductivity

NFs are produced by combining two or more types of nanoparticles into a base fluid to improve thermal conductivity [23]. The size of nanoparticles affects the thermal conductivity of NFs. The researchers studied the effect of particle size on NF thermal conductivity.

The results show that smaller particle size increases the thermal conductivity of NFs. The thermal conductivity of NF improves with increasing temperatures. However, to improve thermal conductivity, the NF must be enriched with chemicals like surfactants [24].

Viscosity

Viscosity is a fluid's resistance to shear or longitudinal deformation. Fluids are classified as Newtonian or non-Newtonian. A Newtonian fluid has a shear stress proportional to the deformation rate under constant pressure and temperature, but non-Newtonian fluids have a viscosity proportional to the shear rate [25]. Because of the NF suspension structure, viscosity plays an essential role in the NF framework's design, with major effects on the pressure drop of flow. In order to use NFs in various applications, their viscosity increase relative to their base fluid must be investigated and evaluated. NFs usually have a higher viscosity than their base fluids [26].

Furthermore, for NFs' use in various applications, the augmentation of the NFs' viscosity compared with their base fluid must be entirely explored and analyzed. NFs usually have enhanced viscosity compared with their basic fluids [27].

Specific heat capacity and Density

The size of nano particles affects the mono and hybrid NFs' specific heat and reduces their specific heat. In addition, smaller particles have more surface atoms than larger particles, implying greater specific heat [28]. Thus, the higher heat capacity of smaller particles can be explained by the bigger number of the surface atoms.

The density of NF improved with the volume concentration of nanoparticles in the base fluid and decreased with temperature. Agglomeration arises when the density of nanoparticles in the base fluid is not sufficient [29].

PERFORMANCE ANALYSIS OF PTSC

The PTSC is formed of several constituent parts and the fluid that flows through it, all of which influence the collector's performance. The PTSC consists of an absorber tube covered by a glass tube fitting at the trough's focal line [30]. Absorber tubes are made of copper or stainless steel and have high absorbance and low emittance. It is covered with a highly absorbent coating to improve performance [31].

The overall efficiency of the PTSC system is based upon two major factors, i.e., the thermal and optical efficiency of PTC, as shown in figures 3 and 4.

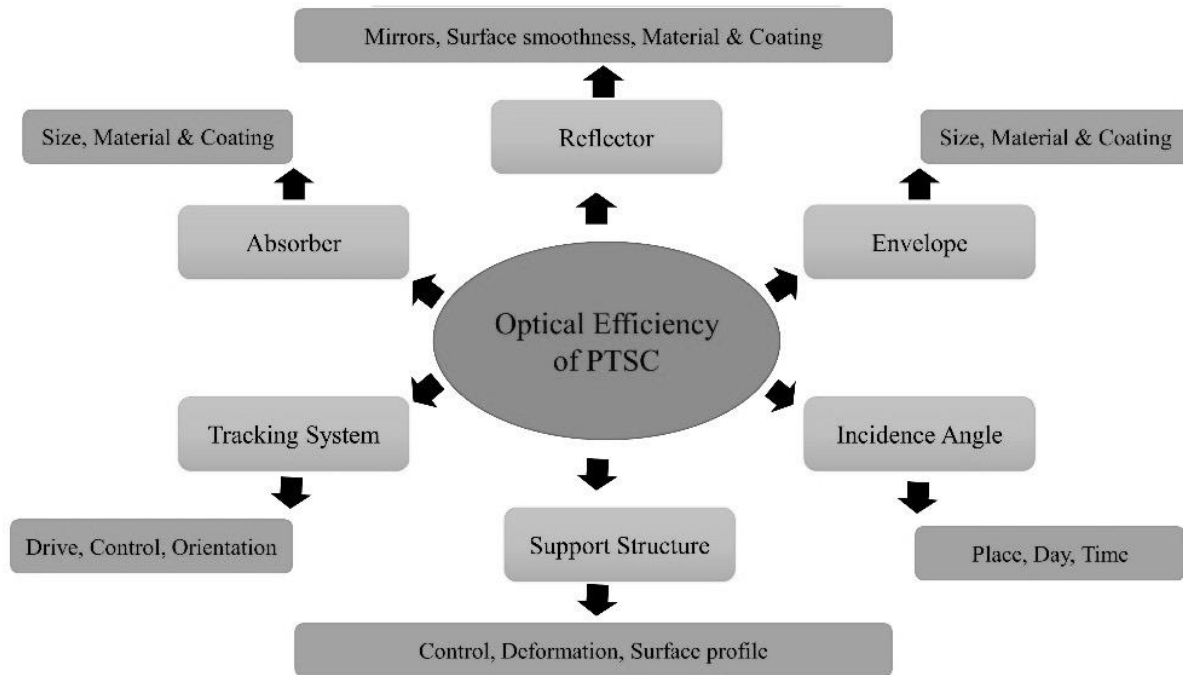


FIGURE 3. Factors affecting the optical efficiency of PTSC.

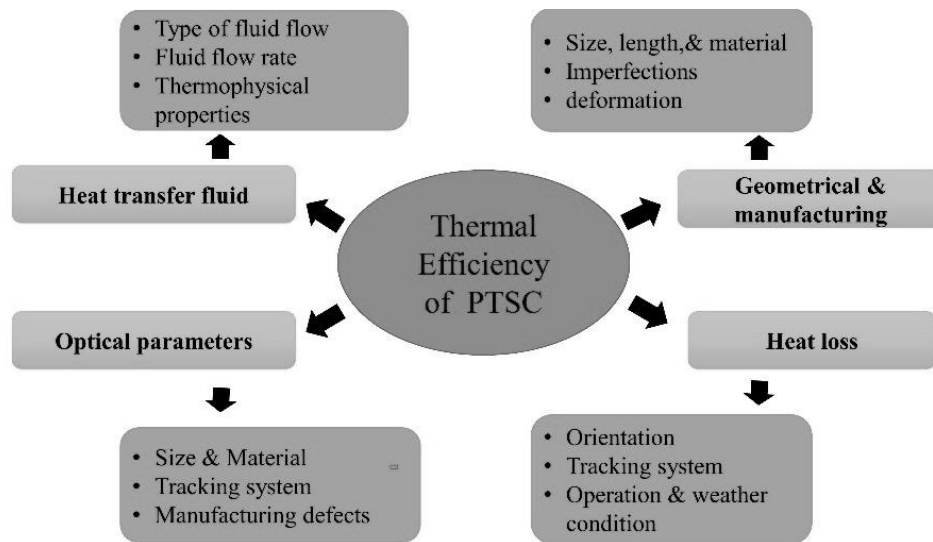


FIGURE 4. Factors affecting the thermal efficiency of PTSC.

CONCLUSIONS

The research reviewed the behavior of mono and hybrid nanofluids in PTSC. This review's findings are as follows:

- The arrangement of two ways, one-step strategy, is useful for creating advanced and stable NFs. A two-step technique is appropriate for mono and hybrid NFs.
- Agglomeration reduces nanofluid heat transfer. This affects the Brownian motion of nanoparticles, reducing their thermal performance.
- Hybrid nanofluid has better thermal conductivity than monofluid. The thermal conductivity of nanoparticles is affected by their morphology (size and shape). The concentration of nanoparticles in NFs with smaller particle sizes is greater than in those with larger ones at constant concentration.
- The viscosity of nanofluid increases with nanoparticle volume concentration and decreases with temperature. As the viscosity of the base fluid decreases, the thermal conductivity and heat transfer rate increase.

ACKNOWLEDGMENTS

This work was supported by the Stipendium Hungaricum Programme and by Doctoral School of Mechanical Engineering, Hungarian University of Agriculture and Life Sciences.

REFERENCES

1. O. Kizilkan, A. Kabul, and I. Dincer, *Energy* 100, pp. 167–176 (2016).
2. K. Nithyanandam and R. Pitchumani, *Solar Energy* 107, pp. 770–788 (2014).
3. Y. Qiu, Y.-L. He, M. Wu, and Z.-J. Zheng, *Renewable Energy* 97, pp. 129–144 (2016).
4. A. Y. Al-Rabeeh, I. Seres, and I. Farkas, *Journal of Engineering Thermophysics* 30, pp. 420–432 (2021).
5. F. G. Üçtuğ and A. Azapagic, *Science of the Total Environment* 643, pp. 1579–1589 (2018).
6. K. Y. Leong, H.C. Ong, N.H. Amer, M. J. Norazrina, M. S. Risby, and K. Z. K. Ahmad, *Renewable and Sustainable Energy Reviews* 53, pp. 1092–1105 (2016).
7. S. K. Verma and A. K. Tiwari, *Energy Conversion and Management* 100, pp. 324–346 (2015).
8. A. Kassem, K. Al-Haddad, D. Komljenovic, and A. Schiffauerova, *Sustainable Energy Technologies and Assessments* 16, pp. 18–32 (2016).

9. J. T. Pytilinski, *Solar Energy* 21, pp. 255–262 (1978).
10. K. Zabara, *Solar & Wind Technology* 3, pp. 267–272 (1986).
11. T. Bouhal, Y. Agrouaz, A. Allouhi, T. Kousksou, A. Jamil, T. El Rhafiki, and Y. Zeraouli, *International Journal of Hydrogen Energy* 42, pp. 13245–13258 (2017).
12. S. E. Ghasemi and A. A. Ranjbar, *International Journal of Hydrogen Energy* 42, pp. 21626–21634 (2017).
13. A. Mwesigye, T. Bello-Ochende, and J. P. Meyer, *Applied Thermal Engineering* 77, pp. 42–56 (2015).
14. J. Ham, J. Kim, and H. Cho, *Applied Thermal Engineering* 108, pp. 1020–1032 (2016).
15. Y. Li, S. Tung, E. Schneider, and S. Xi, *Powder Technology* 196, pp. 89–101 (2009).
16. C.-H. Lo, T.-T. Tsung, and L.-C. Chen, *Journal of Crystal Growth* 277, pp. 636–642 (2005).
17. G.H. Lee, J.H. Park, C.K. Rhee, and W.W. Kim, *Journal of Industrial and Engineering Chemistry* 9, pp. 71–75 (2003).
18. S. Lee, S.-S. Choi, S. Li and, and J. A. Eastman, (1999).
19. X. Wang, X. Xu, and S. U. S. Choi, *Journal of Thermophysics and Heat Transfer* 13, pp. 474–480 (1999).
20. L. Yang, W. Ji, M. Mao, and J. Huang, *Journal of Cleaner Production* 257, 120408 (2020).
21. A. Y. Al-Rabeeah, I. Seres, and I. Farkas, *Facta Universitatis, Series: Mechanical Engineering* (2021).
22. S. Suresh, K. P. Venkitaraj, P. Selvakumar, and M. Chandrasekar, *Experimental Thermal and Fluid Science* 38, pp. 54–60 (2012).
23. L. Qiu, N. Zhu, Y. Feng, E.E. Michaelides, G. Żyła, D. Jing, X. Zhang, P. M. Norris, C. N. Markides, and O. Mahian, *Physics Reports* 843, 1–81 (2020).
24. M. Gupta, V. Singh, S. Kumar, S. Kumar, N. Dilbaghi, and Z. Said, *Journal of Cleaner Production* 190, pp. 169–192 (2018).
25. S. Hussain, H. F. Öztö, K. Mehmood, and M. E. Ali, *Journal of Thermal Analysis and Calorimetry* 137, pp. 1735–1755 (2019).
26. M. Corcione, *Energy Conversion and Management* 52, pp. 789–793 (2011).
27. R. Prasher, D. Song, J. Wang, and P. Phelan, *Applied Physics Letters* 89, 133108 (2006).
28. V. Novotny, P. P. M. Meincke, and J. H. P. Watson, *Physical Review Letters* 28, 901 (1972).
29. M. Abbasi, M.M. Heyhat, and A. Rajabpour, *Journal of Molecular Liquids* 305, 112831 (2020).
30. M. S. Shahin, M.F. Orhan, and F. Uygul, *Solar Energy* 136, pp. 183–196 (2016).
31. R.V. Padilla, G. Demirkaya, D.Y. Goswami, E. Stefanakos, and M.M. Rahman, *Applied Energy* 88, pp. 5097–5110 (2011).

Effect of Hydrolysis Temperature and Acid Solution Concentration on Hydrolysis Of Hyacinth

Moch Rizal Priatna^{1, a)}, Wima Haikal Palit¹⁾, Roni Kurniawan¹

¹ Chemical Engineering Departement, Faculty of Industrial Technology , Institut Teknologi Nasional Bandung
Jl. P.H.H. Mustofa No. 23 Cikutra, Cibeunying Kidul, Neglasari, Cibeunying Kaler, Bandung, Jawa Barat, 40124,
Indonesia

^{a)} Corresponding author: rk.itenas@gmail.com

Abstract. The purpose of this study was to convert cellulose into glucose from water hyacinth plants or *Eichornia crassipes* through acid hydrolysis with variations in temperature, acid concentration, and materials (parts of water hyacinth: stems, leaves, and mixtures stems-leaves) to obtain the best acid hydrolysis conditions based on glucose values obtained. The hydrolysis temperatures used were 90°C, 100°C, and 110°C. The required hydrolysis time is 90 minutes. The type of acid used is H₂SO₄ with concentrations of 2%, 4%, 6%, 8%, 10%, and 12%. The materials used are water hyacinth stems, leaves, and mixtures. Based on the results of the study obtained glucose with the highest concentration of 0.1788 g/mL as much as 9 mL from hydrolysis with an acid concentration of 12% at a temperature of 100°C and the material used was stems with the acquisition of % yield of glucose to dry water hyacinth mass of 44, 51% and % yield of glucose to the mass of water hyacinth by 5.34%.

INTRODUCTION

One of the waters in Indonesia that is filled with water hyacinth plants is the Cirata Reservoir. Cirata Reservoir is located in West Bandung Regency, West Java. Nearly 70% of the Cirata Reservoir is filled with water hyacinth plants. Floating net cage farmers in the waters of the Cirata Reservoir complained about the widespread presence of water hyacinth weeds. Covering the water surface with water hyacinth plants results in reduced oxygen and exposure to sunlight. Thus, the fish in the waters of the Cirata Reservoir are deprived of oxygen. However, in addition to causing negative impacts, water hyacinth plants have benefits in preventing the accumulation of heavy metals, organic fertilizers, fungal growth media and have great potential in the manufacture of biomass such as bioethanol. Water hyacinth contains cellulose 64.51% hemicellulose 15.61% lignin 7.69%. The cellulose contained is broken down into glucose through a hydrolysis process [1]. The glucose will be fermented into bioethanol.

Before hydrolysis of water hyacinth was carried out, pretreatment was carried out by adding 0.5 M NaOH to water hyacinth which had been equalized in size to 1 cm. The process is a delignification that aims to remove the lignin content. This lignin content needs to be removed because it can hinder the hydrolysis process in converting cellulose into glucose [2]. After the delignification stage, the hydrolysis process was carried out using a catalyst. The type of catalyst used is an acid catalyst (H₂SO₄).

Hydrolysis is a chemical reaction between water and another substance that produces new substances and causes a solution to decompose using water. Hydrolysis reactions are generally endothermic reactions (requires heat). The process of hydrolysis of cellulose follows the following equation: $(C_6H_{10}O_5)_n + n H_2O \rightarrow n C_6H_{12}O_6$.

Hydrolysis using an acid catalyst is influenced by temperature, acid concentration, and the material to be hydrolyzed. The effect of temperature on the rate of reaction follows the Arrhenius equation: the higher the temperature, the faster the reaction [3]. The effect of acid concentration in the hydrolysis process, the higher the acid concentration, the higher the sugar content after going through the hydrolysis stage [4]. The material to be hydrolyzed depends on the amount of cellulose contained in the material, the more cellulose contained in the material, the greater the conversion of cellulose to glucose.

This research is intended to produce glucose through acid hydrolysis of water hyacinth plants with variations in temperature, acid concentration, and ingredients (parts of water hyacinth: stems, leaves, and mixture) to obtain the

best acid hydrolysis conditions. Determination of the best acid hydrolysis conditions is reviewed. from the value of the highest glucose concentration which was analyzed by the refractometer method.

METHODOLOGY

Approach

Glucose production from water hyacinth is taken from Cirata Reservoir located in West Bandung Regency, West Java Province. The conversion of cellulose to glucose is carried out through an acid hydrolysis process. Acid hydrolysis was carried out at temperatures of 90°C, 100°C, and 110°C. The required hydrolysis time is 90 minutes. The type of acid used is H_2SO_4 with concentrations of 2%, 4%, 6%, 8%, 10%, and 12%. The materials used are water hyacinth stems, leaves, and a mixture. The result of the hydrolysis is determined by the concentration of glucose through refractometer analysis.

Tools and Materials

The main equipment used is an acid hydrolysis device. The materials used were water hyacinth, 0.5 M NaOH, aqua dest, and H_2SO_4 as shown in Figure 1.

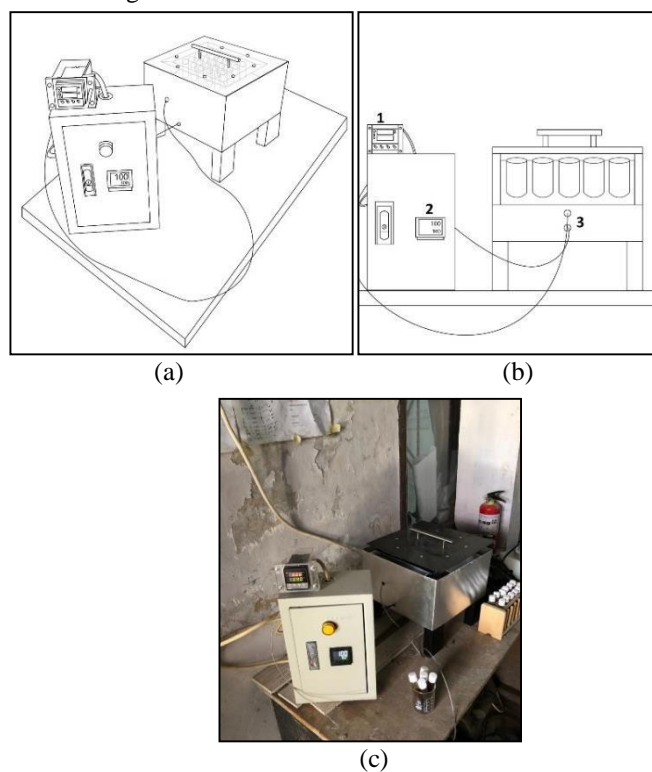


FIGURE 1. Acid Hydrolysis Equipment (a) Equipment Schematic Top View (b) Equipment Schematic Side View (c) Tool Photo

Research Procedure

Raw Material Preparation Stage

The raw material preparation stage in this study aims to prepare raw materials that will be used during the research process, including water hyacinth which is used as a substrate, and water as a supporting component in the study. The initial stage is the process of cutting the water hyacinth substrate into smaller sizes. After the size becomes smaller, the next process is delignification by adding 0.5 M NaOH into the water hyacinth then let stand for 90 minutes. The solution was filtered, then the residue of the solution which was lignin-free water hyacinth was washed with distilled water until the pH of the residue was neutral. Water hyacinth is dried which aims to reduce the water content in water hyacinth to obtain the same ratio. After drying, the dried water hyacinth is blended until it becomes a powder. Then the cellulose content was analyzed at the Center for Pulp and Paper.

Acid Hydrolysis Stage

First, make a solution of H₂SO₄ with concentrations of 2%, 4%, 6%, 8%, 10%, and 12%. 4 grams of dry water hyacinth was put into a test tube with a screw cap and then 9 mL of H₂SO₄ solution was added. The solution was hydrolyzed at various temperatures of 90°C, 100°C, and 110°C for 90 minutes. The hydrolysis process results were analyzed for glucose content by the refractometer method.

RESULTS AND DISCUSSION

Raw Material Preparation

The delignification process will remove the lignin content in water hyacinth so that the conversion of cellulose to glucose during the hydrolysis process is getting better. Lignin dissolved in NaOH solution is marked with black color in the solution which is called black liquor. The results of the remaining delignification process can be seen in Figure 2.



FIGURE 2. Results of the Delignification Process Immersion Remaining

Water hyacinth was also obtained from each part of the water hyacinth. The water content contained in the water hyacinth stem was 88%, the leaf was 69%, and the mixture (stem and leaf) was 78.5%. The dried stems and leaves were analyzed for their cellulose content at the Center for Pulp and Paper located in Dayeuhkolot, Bandung, West Java. The material used for cellulose analysis requires as much as 1 kg of dry matter, where the composition is 650 g of dry stems and 350 g of dry leaves. The method for analyzing the cellulose content used the ASTM D 1103-60 method. The cellulose content of dried water hyacinth stems and leaves according to the test results report was 50.15% (w/w).

Acid Hydrolysis

Acid hydrolysis was carried out by adding sulfuric acid (H₂SO₄) with concentrations of 2%, 4%, 6%, 8%, 10%, and 12%. Acid hydrolysis was carried out on a variety of stem, leaf, and mixed materials. Each material with a mesh size of 40/60 was put into a 4 gram test tube and 9 mL of sulfuric acid was added. Acid hydrolysis is carried out in a

closed heater using a halogen lamp as a heat source. Acid hydrolysis was carried out for 90 minutes at 90°C, 100°C, and 110°C. The use of a small acid concentration aims to avoid corrosive properties and save costs because there is no need to use expensive metal equipment.

Effect of Temperature on Glucose Concentration Result of Acid Hydrolysis

In this study, an analysis of the glucose content of the suspension resulting from the acid hydrolysis process was carried out using a refractometer. The results of the analysis of the effect of temperature on water hyacinth glucose levels are shown in the following Figure 3 - 5.

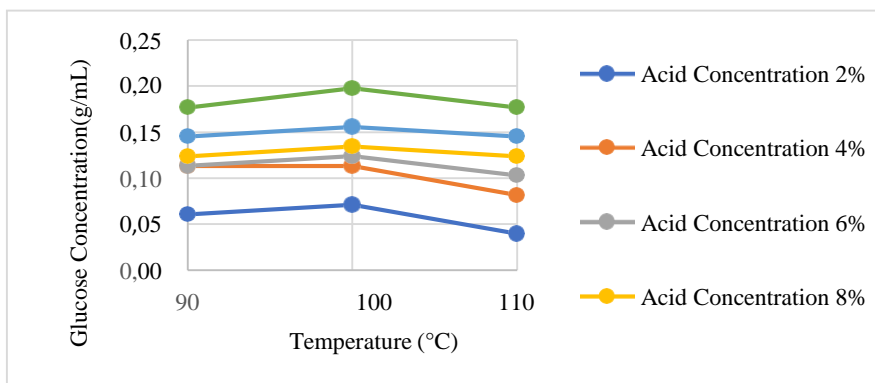


FIGURE 3. The Curve of the Effect of Temperature on the Concentration of Glucose from Acid Hydrolysis in Stem Material

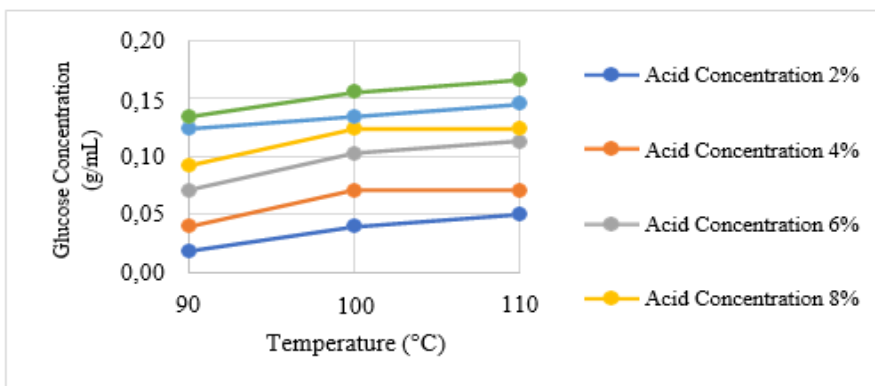


FIGURE 4. The Curve of the Effect of Temperature on the Concentration of Glucose from Acid Hydrolysis in Leaf Material

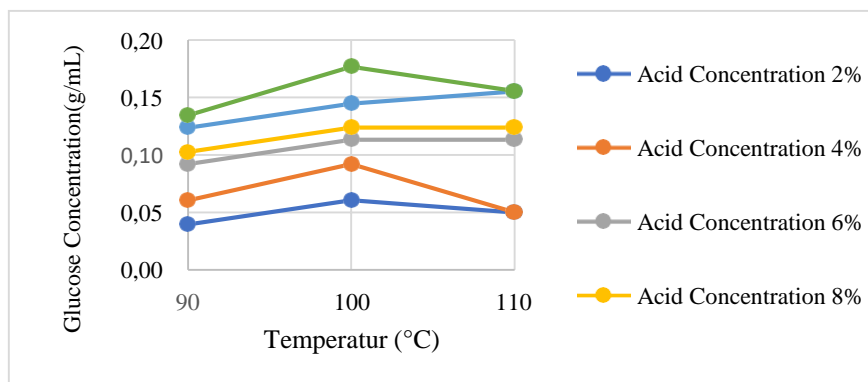


FIGURE 5. The Curve of the Effect of Temperature on the Concentration of Glucose from Acid Hydrolysis in Stem-Leaf Material

Water hyacinth glucose levels were analyzed after going through the acid hydrolysis process using H_2SO_4 . The effect of temperature on the rate of a reaction follows the Arrhenius equation: the higher the temperature, the faster the reaction proceeds. It can be seen in the curves of Figure 3 and Figure 4 that there is a difference between stem and leaf material. The stem material has a higher cellulose content than the leaf material. Therefore, the cellulose converted to glucose will be greater than the leaf material, the maximum limit for acid hydrolysis with stem material at a temperature of $100^{\circ}C$, because if the temperature is more than $100^{\circ}C$, the glucose formed will undergo a caramelization reaction. The caramelization reaction occurs in glucose generally at a temperature of $160^{\circ}C$, but the caramelization reaction can be accelerated if the glucose is in an acidic state. By controlling the level of acidity (pH), the rate of the caramelization reaction can be changed. The rate of caramelization can be accelerated under acidic conditions (especially pH below 3) [5]. In contrast to leaves, leaves have less cellulose content than stems, so the cellulose converted to glucose is also small, which in leaf material the glucose concentration produced is constant and some increases with increasing hydrolysis temperature. The leaf material tends not to experience a caramelization reaction. Likewise, the mixed stem and leaf material obtained various results as shown in Figure 5.

Effect of Acid Concentration on Glucose Concentration Result of Acid Hydrolysis

The results of the analysis of the effect of acid concentration on water hyacinth glucose levels are shown in the following Figure 6 – 8.

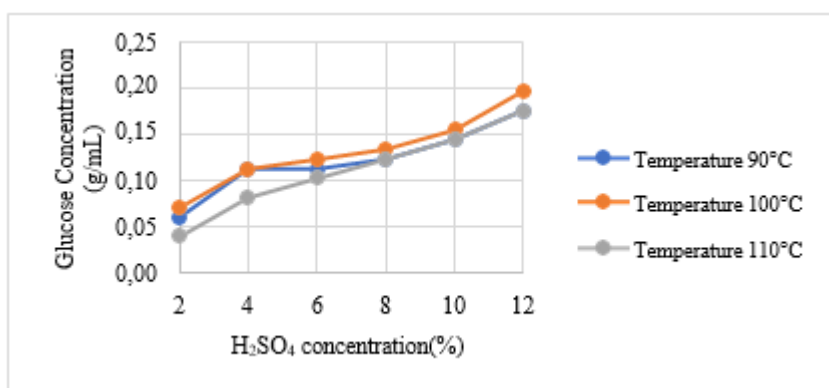


FIGURE 6. The Curve of the Effect of Acid Concentration on Glucose Concentration of Acid Hydrolysis Results in Stem Material

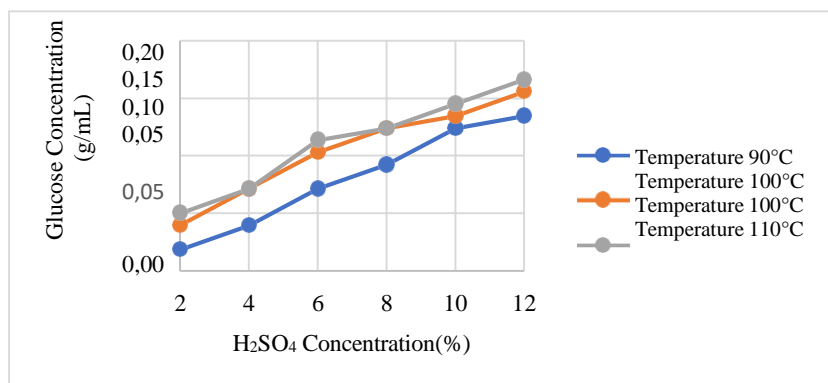


FIGURE 7. The Curve of Effect of Acid Concentration on Glucose Concentration of Acid Hydrolysis Results on Leaf Material

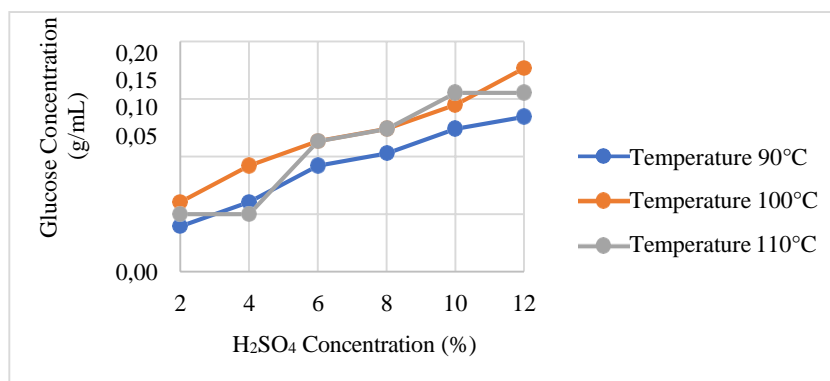


FIGURE 8. The Curve of Effect of Acid Concentration on Glucose Concentration of Acid Hydrolysis Results on Stem-Leaf Material

Figure 6, Figure 7, and Figure 8 show the effect of acid concentration on the glucose concentration resulting from hydrolysis. According to the theory, the use of high concentrations of acid will provide high sugar content after going through the hydrolysis stage [4]. From Figure 6, Figure 7, and Figure 8 it is known that the hydrolysis process of water hyacinth using H₂SO₄ solution accompanied by closed heating at temperatures of 90°C, 100°C and 110°C produces different glucose levels for the six concentrations used. In the hydrolysis stage, the sample is heated by heating using hot steam. The resulting hot steam will increase the ability of H₂SO₄ to break down cellulose into glucose. In addition, the water content contained in the raw materials also affects the glucose levels produced, the less water content contained in water hyacinth, the higher the glucose levels obtained. It can be seen that the higher the concentration of acid used in the hydrolysis process, the higher the concentration of glucose produced. This is by the existing theory. Judging from the curves in Figure 6, Figure 7, and Figure 8, the concentration of glucose resulting from hydrolysis increases with the amount of acid concentration. This is because, at higher acid concentrations, more cellulose breaks down into glucose. In this study, the sulfuric acid concentration of 12% is the maximum concentration that can be used for the acid hydrolysis process. The lower the pH in the acid hydrolysis process, the faster the caramelization reaction.

The caramelization reaction will inhibit the conversion of cellulose to glucose. If caramelization occurs, the concentration of glucose formed will decrease. Figure 6, Figure 7, and Figure 8 show the effect of acid concentration on the concentration of glucose resulting from hydrolysis. According to the theory, the use of high concentrations of acid will provide high sugar content after going through the hydrolysis stage [4]. From Figure 6, Figure 7, and Figure 8 it is known that the hydrolysis process of water hyacinth using H₂SO₄ solution accompanied by closed heating at temperatures of 90°C, 100°C and 110°C produces different glucose levels for the six concentrations used. In the hydrolysis stage, the sample is heated by heating using hot steam. The resulting hot steam will increase the ability of H₂SO₄ to break down cellulose into glucose. In addition, the water content contained in the raw materials also affects the glucose levels produced, the less water content contained in water hyacinth, the higher the glucose levels obtained. It can be seen that the higher the concentration of acid used in the hydrolysis process, the higher the concentration of glucose produced. This is by the existing theory. Judging from the curves in Figure 6, Figure 7, and Figure 8, the concentration of glucose resulting from hydrolysis increases with the amount of acid concentration. This is because, at higher acid concentrations, more cellulose breaks down into glucose. In this study, the sulfuric acid concentration of 12% is the maximum concentration that can be used for the acid hydrolysis process. The lower the pH in the acid hydrolysis process, the faster the caramelization reaction. The caramelization reaction will inhibit the conversion of cellulose to glucose. When caramelization occurs, the concentration of glucose formed will decrease.

Effect of Material on Glucose Concentration Result of Acid Hydrolysis

The results of the analysis of the effect of acid concentration on water hyacinth glucose levels are shown in the following Figure 9 – 11.

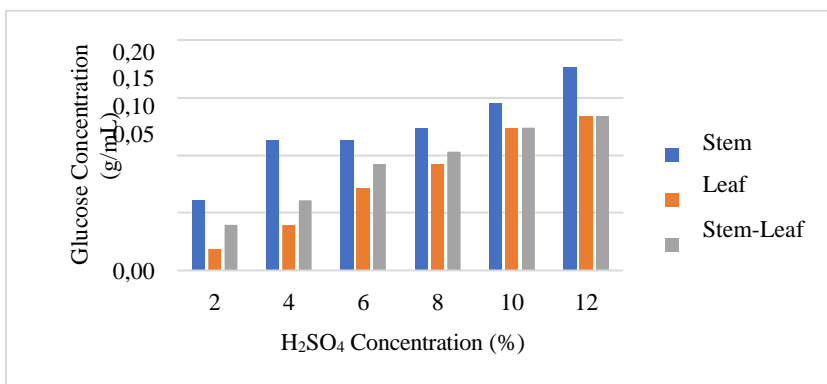


Figure 9. Diagram of the Effect of Materials on Glucose Concentration of Acid Hydrolysis at 90°C Temperature

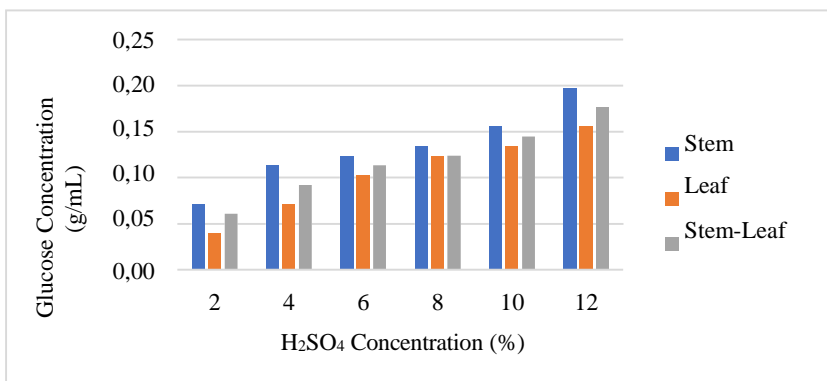


Figure 10. Diagram of the Effect of Materials on Glucose Concentration of Acid Hydrolysis at 100°C Temperature

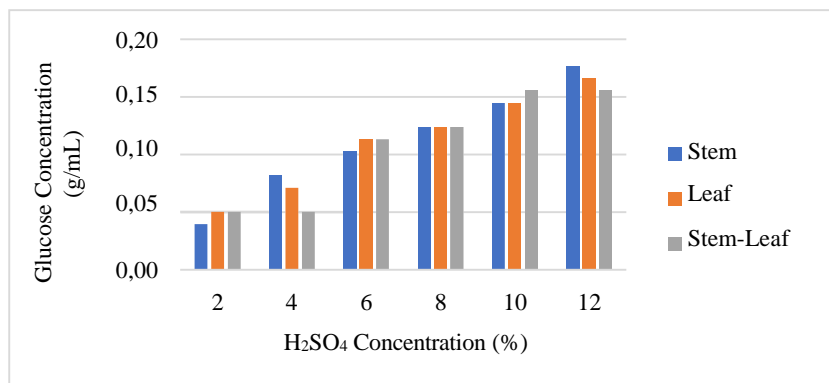


Figure 11. Diagram of the Effect of Materials on Glucose Concentration of Acid Hydrolysis at 110°C Temperature

In Figures 9 and 10, it can be seen that the stem material at the same temperature and acid concentration of glucose produced from acid hydrolysis has a higher glucose concentration than the leaf and mixed material (stem and leaf). This can happen because the stems contain more cellulose than the leaves. The cavity of the water hyacinth stem is the same as that of a banana midrib, so it can be assumed that

The cellulose content in water hyacinth stems is greater than in the leaves. The cellulose content in the banana midrib is 83.3% while the banana leaf has a cellulose content of 10.85% [6]. However, there are exceptions or differences at a temperature of 110°C where the curve in Figure 11 can be seen that the results of the acid hydrolysis glucose concentration from the stem material are not always higher, this is due to the caramelization process. The caramelization reaction will inhibit the conversion of cellulose to glucose. When caramelization occurs, the concentration of glucose formed will decrease.

The cellulose contained in dry water hyacinth which will be used as raw material for the acid hydrolysis process has a composition of 50.15% according to the analysis using the ASTM D 1103-60 method. From the experiments that have been carried out, it was obtained that the glucose with the highest concentration of 0.178 g/mL was 9 mL from acid hydrolysis with an acid concentration of 12% at 100°C and the material used was the stem. The results of the mass conversion of water hyacinth, dry water hyacinth mass, and cellulose mass to the results of the best acid hydrolysis process of each material can be seen in Table 1, Table 2, and Table 3.

TABLE 1. Results of Mass Conversion of Wet Water Hyacinth, Dry Water Hyacinth Mass and Cellulose Mass to the Result of Acid Hydrolysis Process on Stem Material (Hydrolysis Temperature 100°C and Acid Concentration of 12%)

Stem Moisture Content	Wet Stem Mass (g)	Dry Stem Mass (g)	Glucose Concentration (g/mL)	Glucose Mass (g)	% Glucose Yield /Ingredient Wet Stem	% Glucose Yield /Ingredient Dried Stem
88%	33,33	4	0,1978	1,78	5,34%	44,51%

TABLE 2. Mass Conversion Result of Wet Water Hyacinth, Dry Water Hyacinth Mass and Cellulose Mass to Result of Acid Hydrolysis Process on Leaf Material (Hydrolysis Temperature 110°C and Acid Concentration of 12%)

Stem Moisture Content	Wet Stem Mass (g)	Dry Stem Mass (g)	Glucose Concentration (g/mL)	Glucose Mass (g)	% Glucose Yield /Ingredient Wet Stem	% Glucose Yield /Ingredient Dried Stem
69%	12,90	4	0,1662	1,50	11,59%	37,40%

TABLE 3. Mass Conversion Results of Wet Water Hyacinth, Dry Water Hyacinth Mass and Cellulose Mass to the Result of Acid Hydrolysis Process on Stem-Leaf Material (Hydrolysis Temperature 100°C and Acid Concentration of 12%)

Stem-Leaf Water Content	Wet Stem-Leaf Mass (g)	Dry Stem-Leaf Mass (g)	Cellulose Mass (g)	Glucose Concentration (g/mL)	Glucose Mass (g)	% Glucose Yield /Ingredient Dried Stem	% Glucose Yield /Ingredient Dried Stem	% Yield Glucose/ Cellulose
78,50%	18,60	4	2,01	0,1767	1,59	8,55%	39,77%	79,30%

CONCLUSION

From the research that has been done, the best acid concentration value in the acid hydrolysis process is 12% acid concentration at a temperature of 100°C and the material used is stem glucose concentration is 0.1788 g/mL. The %yield value of glucose weight/weight of water hyacinth was 5.34% and the %yield by weight of glucose/weight of dry water hyacinth was 44.51%.

ACKNOWLEDGMENTS

The author would like to thank profusely: Mrs. Dyah Setyo Pertiwi, S.T., M.T., Ph.D. and Mr. Yuno, S.T., M.T., as the Head and Research Coordinator of the Chemical Engineering Department of the Bandung National Institute of Technology, Mr. Ronny Kurniawan, S.T., M.T. as a supervisor who has provided broad insight, direction during research, and support to the author. To both parents and friends who have provided support and assistance to the author.

REFERENCES

1. Nuryana, R., *Eceng Gondok (Eichornia crassipes)*, eprints.polsri.ac.id., (2016). (Accessed on December 8, 2020)
2. Permatasari, H. R., et.al., “Effect of Concentration of H₂SO₄ and NaOH on Delignification of Bamboo Powder (*Gigantochloa Apus*)”, *Jurnal Penelitian Pendidikan Kimia – Kajian Hasil Penelitian Pendidikan Kimia*, Vol. 1 (2): 131 – 140, (2014).
3. Groggins, P. H., *Unit Processes in Organic Synthesis*, 5th ed., p. 775-777. New York: McGraw-Hill Book Company, (1958).
4. Hamelinck, C.N., van Hooijdonk, G., & Faaij, A.P.C., “Ethanol from Lignocellulosic Biomass: Techno-Economic Performance in Short-, Middle- And Long-Term”, *Biomass Bioenergy*, p. 384–410, (2005).
5. Dennis D., *Food Chemistry*, (1993).
6. Bahri, S., “Making Pulp from Banana Stems”, *Journal of Chemical Technology Unimal*, Vol. 4 (2): 36-50, (2015).

Isolation of Linalool From Coriander Seeds by Soxhlet Extraction Method

Apriliana Dwijayanti^{1, a)} and Safril Kartika^{1, b)}

¹ Chemical Engineering Department, Universitas Serang Raya, Taman Drangon Taktakan Serang- Banten- Indonesia.

^{a)} Corresponding author: apriliana.d@gmail.com

^{b)} safril919@gmail.com

Abstract. Isolation of linalool from coriander seeds by sohxlet extraction method – steam distillation has been carried out. This study used solvent variables, namely ethanol, hexane, a mixture of ethanol-hexane ratio of 1:1, and the variable mass of coriander seeds was 30, 35, 40, and 45 grams. This study aims to determine the right solvent to isolate linalool and determine the best yield that can be produced. Coriander seed powder was put into the Soxhlet extractor by adding 400 ml of solvent to isolate the linalool, then the solvent was separated using steam distillation. The extracts obtained were analyzed for the amount of yield, density, linalool functional groups using FTIR. From the research, it was found that ethanol solvent could isolate the most linalool with a yield of 31.52% and a density of 0.8667 gr/ml. In the mass variable, the largest yield was found in the mass of 30 grams of coriander powder by 39.3% and the density of 0.8670 gr/ml. The FTIR analysis showed the average wave number of –OH at 3316 - 3328 cm⁻¹ and group C=C at 1641 cm⁻¹.

INTRODUCTION

Coriander (*Coriandrum sativum*) is a popular spice plant. Coriander is an annual herbaceous plant, and is generally cultivated on a limited basis in the highlands such as in Boyolali, Salatiga, Temanggung, West Sumatra, and others. Based on the shape of the fruit, it can be divided into three types, small round fruit, large round, and oval [1]. The crops are generally sold to traditional markets for household spices. Coriander has a distinctive aroma caused by the chemical components contained in the essential oil. Coriander oil (coriander oil) is an essential oil-producing commodity which is estimated to have high commercial potential and value. Coriander has an essential oil content ranging from 0.4 to 1.1%.

The main component of coriander oil is linalool which amounts to around 60-70% which can be used as raw material for perfumes, pharmaceuticals, food and beverage aromas, bath soaps, candles, laundry soaps, synthesis of vitamin E and pesticides and insecticides. The other supporting components are geraniol (1.6-2.6%), geranyl acetate (2-3%), camphor (2-4%) and contain about 20% hydrocarbon group compounds [2]. Several studies have shown the benefits of coriander solution, including as a preservative in Lombok tofu [3], lowering blood pressure [4] and treating vaginal discharge problems [5].

There are many plant-derived terpenoids with analgesic effects, one of which is linalool. Linalool is a volatile compound found in many plant tissues, namely leaves, fruit, and generally flowers. Linalool is a terpenoid alcohol compound, in liquid form, colorless, fragrant and has an empirical formula of C₁₀H₁₈O, and a structural formula of 3,7 dimethyl-1,6 octadien-3-ol. Linalool is a straight chain alcohol compound. The linalool compound is a

component that determines the intensity of the fragrant aroma, so coriander oil can be used as a raw material for perfume, the aroma is like lavender oil [2].

Linalool is antinociceptive which has the potential to act on the muscarinic, opioid, dopaminergic, adenosinergic, and glutamatergic systems and ATP-sensitive K⁺ channels [6]. Linalool was also found as a sedative and anesthetic in one fish species, *Rhamdia quelen* [7]. Studies from [8] that Administration of linalool @ 120 mg/kg protects cell membranes from oxidative stress. Several studies have also shown that linalool can act as anticancer [9]. While research from shows that the linalool compound extracted from lavender flowers has a sedative effect on reducing the risk of insomnia [10].

Based on [11] review, reflux extraction is the most commonly employed technique for preparative separation. The Soxhlet extraction method integrates the advantages of the reflux extraction and percolation, which utilizes the principle of reflux and siphoning to continuously extract the herb with fresh solvent. Research on linalool isolation using soxhlet extraction with various solvents and masses to determine the optimum yield of linalool compounds is still an interesting research to do.

METHODS

This research is divided into several stages according to the parameters studied. In this case, the parameters to be studied are the influence of the solvent and the mass of the sample. Coriander oil extraction was carried out using a variable solvent of ethanol, hexane and a mixture of ethanol-hexane 1:1. After the solvent variable produced the highest yield, followed by the mass variable from coriander with variables 30, 35, 40, and 45 grams. Coriander seeds are powdered, then wrapped in filter paper and put into a Soxhlet extractor. Extraction was carried out by adding 300 mL of solvent into a round bottom flask and extraction was carried out at the boiling point of the solvent. Coriander oil and solvent are separated from the solvent by distillation, until pure coriander oil is obtained. To determine the content of chemical compounds in coriander oil, analysis was carried out using FTIR. Figure 1 is the process of extracting coriander oil.



FIGURE 1. Coriander Seed Oil Extraction Process Soxhlet Extraction

RESULTS AND DISCUSSION

Yield and Density Analysis

Based on the results of the solvent variables tabulated in Table 1, it was found that ethanol solvent produced the highest yield of 31% with the density of the oil produced was 0.8867. The presence of –OH groups in ethanol and linalool (figure 2) is estimated to have close polarity of ethanol and linalool so that ethanol is able to produce higher yields than hexane or ethanol-hexane mixtures. All stages of extractions, from the pre-extraction and extraction are equally important in the study of medicinal plants. The sample preparation such as grinding and drying affected the

efficiency and phytochemical constituents of the final extractions; that eventually have an effect on the final extracts [12].

TABLE 1. Experimental Results of Solvent Variables

Solvent	Coriander mass (gram)	Oil mass (gram)	Oil volume (ml)	Yield (%)	Oil density (gr/ml)
Heksana	45	4.5404	5.3	10.0898	0.8567
Etanol	45	14.1864	16	31.5253	0.8867
Et : Hx = 1:1	45	9.8013	12	21.7807	0.8168

Furthermore, experiments were carried out with the coriander mass variable using ethanol as a solvent. Based on the results from Table 2, the largest yield was produced by 30 grams of coriander with a yield of 39.3% and a density of 0.867 gr/ml. The average density produced is 0.8682 gr/ml.

TABLE 2. Experimental Results of The Mass Variable

No	Coriander mass (gram)	Oil mass (gram)	Oil volume (ml)	Yield (%)	Oil density (gr/ml)
1	30	11.7913	13.6	39.3043	0.8670
2	35	12.3035	14.2	35.1529	0.8664
3	40	12.3871	14.5	30.9678	0.8543
4	45	13.5404	15.3	30.0898	0.8850

FTIR Analysis

The linalool compound has an alcohol functional group (-OH), an alkene chain and an alkane chain as shown in the Figure 2.

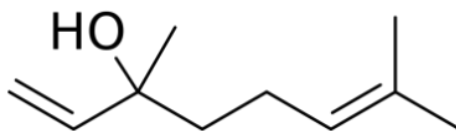


FIGURE 2. Chemical Structure of Linalool

The functional groups found in Linalool have been identified by comparing the vibrational frequencies in wavenumber of the spectrograph patterns obtained from the FTIR spectrophotometer with those on the IR correlation graph. Linalool's FTIR spectrum was carried out in the 4000 – 500 cm⁻¹ spectral region. Figure 3 shows the results of the FTIR analysis for the linalool compound in the hexane solvent experiment. FTIR analysis showed that Linalool contained an (OH) group at 3316 cm⁻¹. The wave number at 1641.12 cm⁻¹ is associated with the C=C group, while at the wavelength 1409 cm⁻¹ it indicates the presence of a (C-H) group. C–O band stretching is also seen at 1015 cm⁻¹

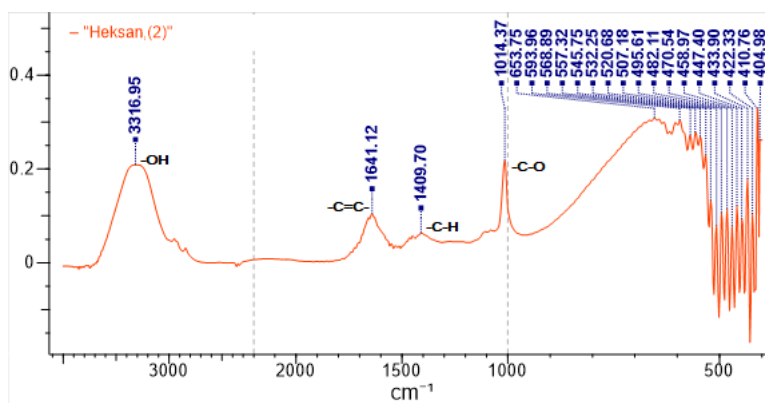


FIGURE 3. FTIR Analysis of Linalool Compound in Hexane Solvent

Figure 4 shows the results of the FTIR analysis for the linalool compound in the ethanol solvent experiment. FTIR analysis showed that Linalool contained an (OH) group at 3328.52 cm^{-1} . The wave number at 1641.12 cm^{-1} is associated with the C=C group, while at the wavelength of 1407.77 cm^{-1} it indicates the presence of a (C-H) group. The stretching of the C–O band is also seen at 1014.37 cm^{-1}

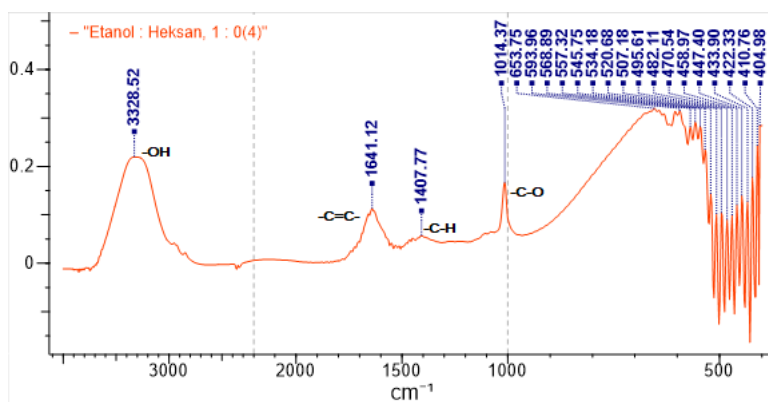


FIGURE 4. FTIR Analysis of Linalool Compound in Ethanol Solvent

Figure 5 shows the results of the FTIR analysis for the linalool compound in the ethanol-hexane solvent mixture experiment. FTIR analysis showed that Linalool contained an (OH) group at 3328.52 cm^{-1} . The wave number at 1641.12 cm^{-1} is associated with the C=C group, while at the wavelength of 1409.7 cm^{-1} it indicates the presence of a (C-H) group. The stretching of the C–O band is also seen at 1016.30 cm^{-1}

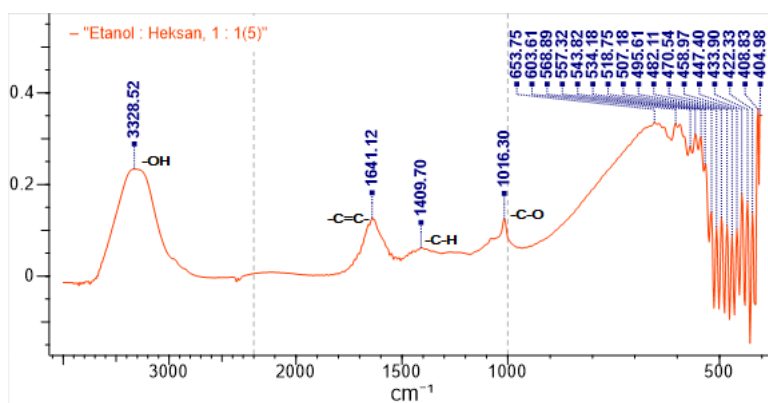


FIGURE 5. FTIR Analysis of Linalool Compounds in A Mixture of Ethanol-Hexane Solvents

CONCLUSION

Of the several solvent variables used, ethanol yielded the largest yield of 31.5253% with a density of 0.8867 gr/ml. While the mass variable that produces the largest yield is 30 grams of sample mass with a yield of 39.3% and a density of 0.8670 gr/ml.

ACKNOWLEDGEMENT

The authors thank the Indonesian Ministry of Education and Technology for funding all of this research. This research has been awarded a 2021 research funding grant from the Indonesian Ministry of Education and Technology.

REFERENCES

1. N.N., Azwanid, "A Review on the Extraction Methods Use in Medicinal Plants, Principle, Strength and Limitation". *Med Aromat Plants*, 4:3.DOI: 10.4172/2167-0412.1000196 (2015).
2. A.G., Guimarães, J.S.S., Quintans, L.J., Quintans-Júnior, "Monoterpenes With Analgesic Activity—A Systematic Review", *Phytother. Res.* 27, pp. 1–15 (2013).
3. E., Hadipoentyanti and S., Wahyuni, "Grouping of Coriander Cultivars Based on Morphological Properties", *Nutfah Plasma Bulletin*, 10 (1) (2004).
4. P.A., Handayani and E.R., Juniarti, "Extraction of Coriander Oil with Ethanol and n-Hexane Solvents", *Journal of Renewable Natural Materials*, ISSN 2303-0623, 1 (1) (2012).
5. C.G., Heldwein, L.d.L., Silva, E.Z., Gai., C., Roman, T.V., Parodi, M.E., Burger, B.Baldisserotto, E.M. de M., Flores, and B.M., Heinzmaan, "S-(+)-Linalool From Lippia Alba: Sedative and Anesthetic For Silver Catfish (*Rhamdia quelen*)", *Vet. Anaesth. Analg*, 41, pp. 621–629 (2014).
6. V.S., Hendrawati, I.N.G., Suyasa, and I. N., Sujaya, "Effectiveness of Garlic Solution (*Alium sativum* L) and Coriander (*Coriandrum sativum*) Against the Durability of Lombok Tofu", *Journal of Environmental Health*, 4 (1) (2014).
7. M.H., Mughal, "Linalool: A Mechanistic Treatise", *J Nutr Food Technol*, 2(1), 1-5, DOI: 10.30881/jnfrt.00014 (2019).
8. D.A., Prastika and S. Sugita, "Effectiveness of Coriander Seed Bathing (*Coriandrum Sativum* L) for The Therapy of Vaginal Problems in Women of Childbearing Age", *Integrated Journal of Health Sciences*, 7(1) (2018).
9. Q.W., Zhang, L.G., Lin, and W.C., Ye, "Techniques for extraction and isolation of natural products: a comprehensive review", *Chinese Medicine*, 13 (20), Pp. 1-26. <https://doi.org/10.1186/s13020-018-0177-x> (2018).
10. M.R., Ramadhan and O.Z., Zettira, "Lavender Flower Aromatherapy (*Lavandula angustifolia*) in Lowering The Risk of Insomnia", *Majority*, 6 (2) (2017).
11. B.R., Rodenak-Kladniew, A., Castro, P., Starkel, C.de Saeger, M.G., de Bravo, and R., Crespo, "Linalool Induces Cell Cycle Arrest and Apoptosis in HepG2 Cells Through Oxidative Stress Generation and Modulation of Ras/MAPK and Akt/mTOR pathways", *Life Sci*, 199, pp. 48–59 (2018).
12. U.V.Nurul, H., Soeharyo, and S., Rahayu, "Effect of Coriander Extract (*Coriandrum sativum*) On Changes in Blood Pressure of Postnatal Mice", *The Soedirman Journal of Nursing*, 11 (3), (2016).

Illumination and Power Monitoring on Internet of Things-Based Solar Panels

Ichsan Nurmansyah^{1,a)}, Waluyo¹, Dini Fauziah¹

¹Departement of Electrical Engineering, Institut Teknologi Nasional (Itenas), Bandung

^{a)}Corresponding author: Ichsannurmansyah1@gmail.com

Abstract. In the research designed a monitoring system tool that is integrated online or often called IoT with the help of thingspeak as web monitoring for measurement, and resources using solar panels, which aims solar panels can be used with offgrid systems and t and light on the power generated with the ease of monitoring data used online., where with Polycrystallin panels derived from silicon materials with a temperature coefficient of -0.075 oC.with the load used is incandescent lamps with a power of 5W,where 54612 lux can generate 4.72A.so that environmental factors can affect solar panel power, and the benefits of IoT systems can facilitate monitoring anywhere and anytime.

INTRODUCTION

In the era of modernization, technological advances can help human needs in everyday life, especially in the energy sector [1]. Electrical energy in this era is something that is very vital and important for everyone. all modern equipment requires electrical energy to operate on the other hand developments such as settlements and industries that run in each area make the supply of electrical energy needed increase, so that the demand for electrical energy is increasing day by day. Meanwhile, the amount of electrical energy derived from fossil fuels is very limited, so new and renewable energy is needed [2]. In the last decade in Indonesia, the use of photovoltaic for power generation is growing rapidly, especially in government efforts. to achieve an electricity ratio of >70% in 2012. This technology was chosen because the location to be electrified is in a remote or isolated location such as the outer islands and separated by mountains/hills, which technically draws the electricity network from the existing one. and economically is not the right decision [3].

On the other hand, the use of alternative energy needs to be controlled and monitored so that the use of this alternative energy can be exactly as needed. Where the existence of the Internet of Things can make it easier for us to control and monitor existing alternative and non-alternative electrical energy systems with the help of the internet and can be from remote places in real time. So that users who are far away from the control panel of their electrical energy system, can control and directly monitor the electrical system at home [4]. In its operation, solar power generation systems have several configurations that are commonly used. These configurations include on-grid, off-grid, and on-grid with battery backup. These configurations can be used to be able to operate a solar power generation system like a conventional generating system that can connect and supply energy to the grid [5].

By implementing a solar power generation system, it can reduce dependence on the use of non-renewable energy sources, as well as reduce carbon emissions generated from conventional plants. In addition, the energy produced by solar power plants can be sold to state power companies.

A Smart Grid is an electricity network that uses digital and other based technology to monitor and manage [6]. Meanwhile, the European Smart Grid Platform Technology (ETP) has a vision that the power system network in Europe must be flexible in meeting consumer needs, easy access, reliable and economical [7]. Meanwhile, according to the US Department of Energy, a smart grid is a power system based on technology sensing, communication, digital control, information technology (IT) and other field equipment that functions to coordinate the existing processes in making the electricity grid more effective and dynamic in its management [8].

The smart grid implementation needs a parameter that can connect values with transmit data online, that is ESP32, where ESP32 is a single 2.4 GHz Wi-Fi and Bluetooth combo chip designed with TSMC ultra-low power 40 nm. This

technology is designed to achieve the best power and RF performance, demonstrating robustness, flexibility, and reliability in a wide range of power applications and scenarios [9]. IoT is an internet network system that can provide, process, and transfer digital information obtained from sensor equipment such as radio frequency identification (RFID), infrared sensors, GPS, scanners, and smart meters [2].

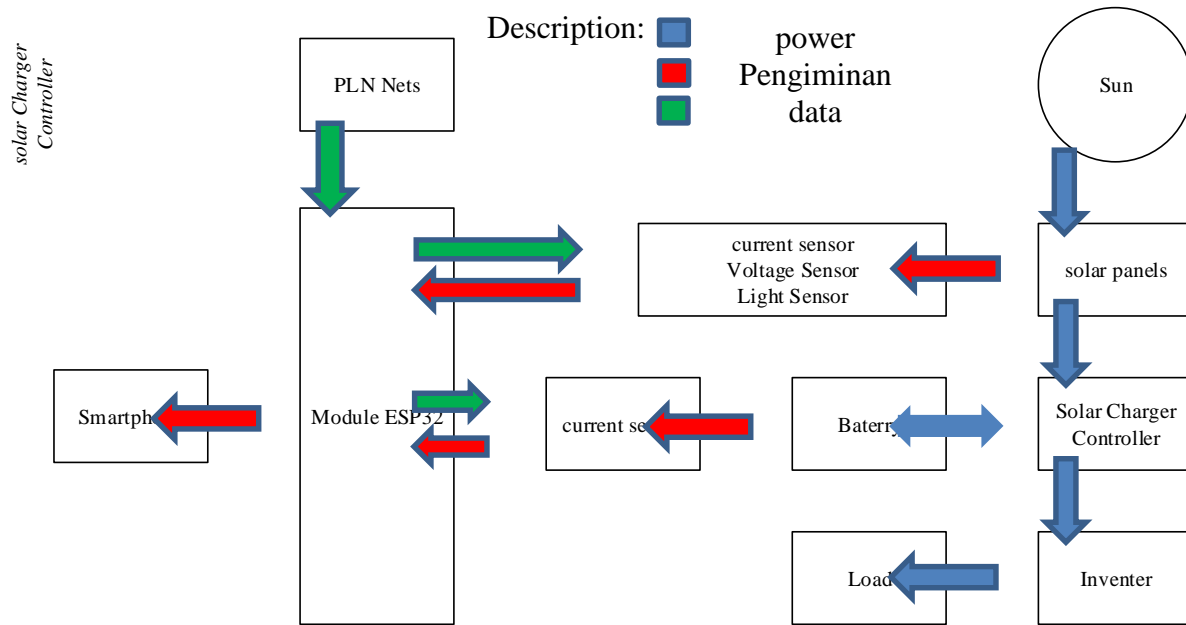


Figure 1 shows that the solar panel will absorb light and be converted into a dc source, after conversion the sensor will work to retrieve data, the output of the solar panel to the solar charger controller will then go to the battery to charge the battery, the battery output will be sent to the solar charger controller which will be used by the inverter to convert the DC source into an AC source which will then be used by the load. while each sensor used to turn it on uses PLN grids with the intention of not losing power. The data value taken by the sensor will go to the ESP32 module, where the ESP 32 module has a Wi-Fi chip installed that is connected to the network so that the data can be sent online to the Thingspeak server which can be accessed via smartphones or laptops.

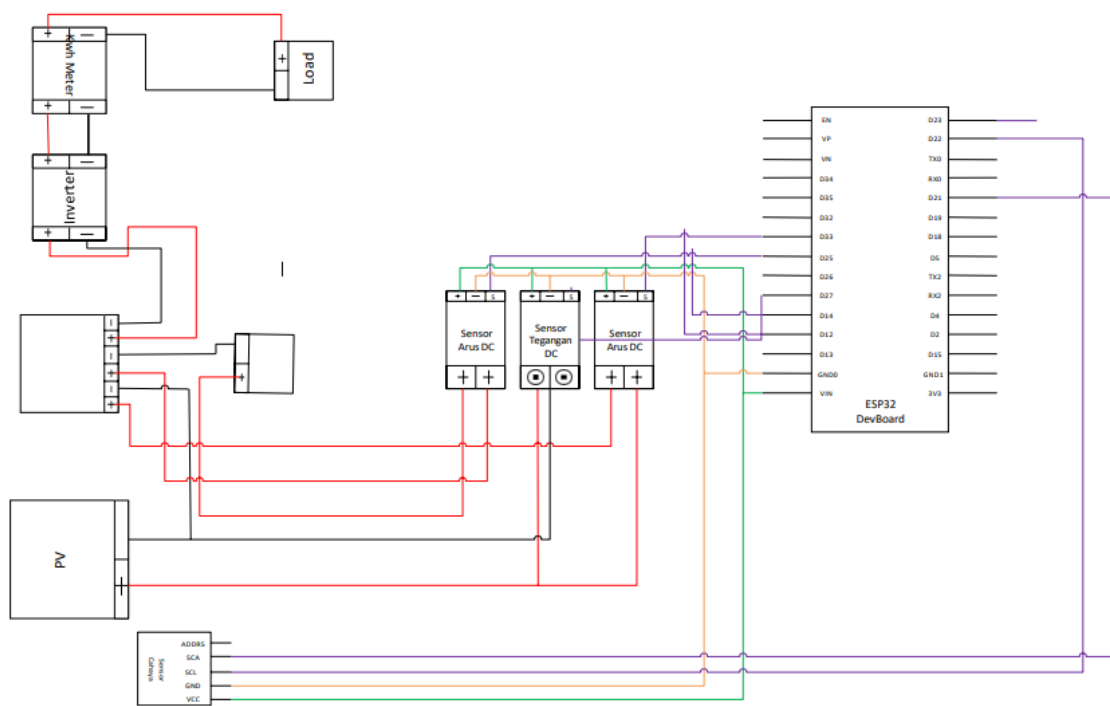


Figure 3. Single Line Diagram

To realize the internet of things system, it requires a sensor which will be connected to the ESP32 microcontroller. With sensors used as follows:

A. Current Sensor ACS712

ACS712 is a current sensor that works based on field effects. This sensor can be used to measure AC or DC current. This sensor module is also embedded with an operational amplifier circuit, so that the sensitivity of current measurement increases and can measure small current changes, with a physical shape and circuit as shown in Figure 3. ACS712 Current Sensor Specifications:

1. Time of increase in output change = 5 s.
2. Wide frequency up to 80 kHz.
3. Total output error of 1.5% at working temperature $T_A = 25^\circ\text{C}$.
4. Internal conductor resistance 1.2 m Ω .
5. Minimum isolation voltage of 2.1 kVRMS between pins 1-4 and pins 5-8.
6. Output sensitivity 185 mV/A.
7. Capable of measuring AC or DC current up to 5 A.
8. The output voltage is proportional to the input AC or DC current

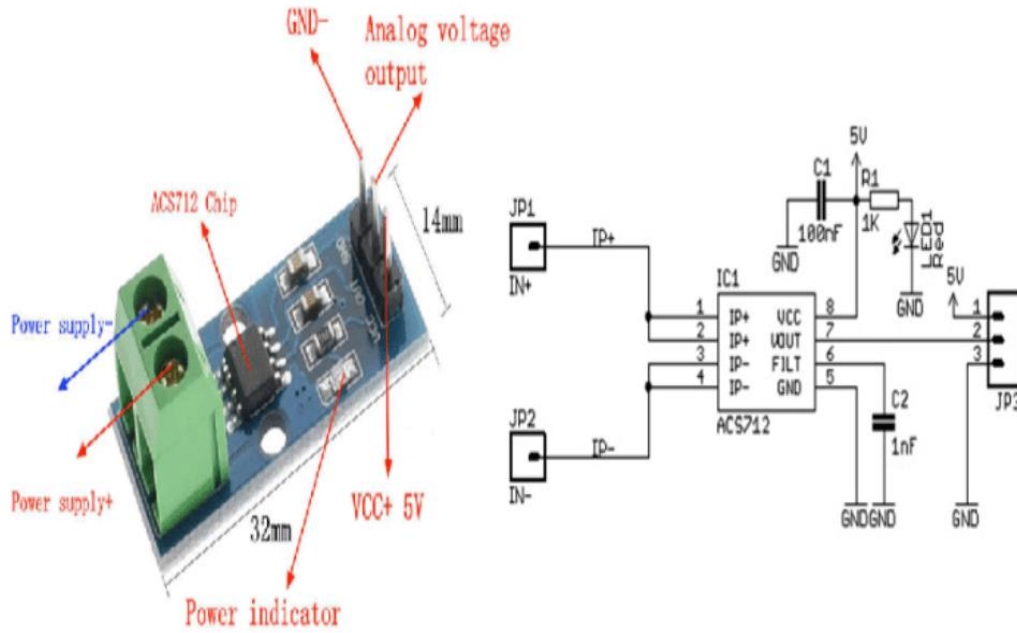


Figure 3. System Block Diagram [10]

B. DC Voltage Sensor 25V

Voltage sensors are used to measure AC and DC voltages. The working principle of this voltage sensor module is based on the principle of suppression of resistance and can change the input voltage reduced to 5 times of the original voltage. The form of the voltage sensor module is as shown in Figure 4 below:



Figure 4. DC Voltage Sensor [11]

The features and advantages:

1. Variation of input voltage: DC 0 - 25 V
2. Voltage detection with range: DC 0.02445 V - 25 V
3. Analog resolution voltage: 0.00489 V
4. DC voltage input interface: positive terminal with VCC, negative with GND
5. Output Interface: "+" 5 / 3.3V connection, "-" connected GND, "s" connected Arduinopin A0
6. DC input interface: red terminal positive with VCC, negative with GND

C. Light Sensor BH1750

BH1750 is a light sensor IC with IC interface. This module provides digital output through the IC bus, so there is no need to add an ADC converter [1]. With a sensor shape like Figure 5.

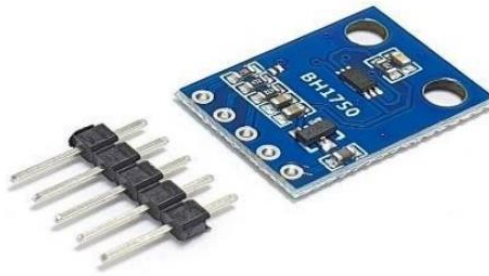


Figure 5. Light Sensor BH1750 [1]

Specification:

1. Power Supply: 4.5 V
2. Resolution: 0 - 65535 lux
3. Interface: IC
4. Output Type: Digital
5. Sensor Chip: BH1750FVI
6. Dimensions: 13.9 x 18.5 mm

D. ESP32

ESP32 functions as a module that connects sensors to the network with the Thingspeak application as a data monitoring center so that the Internet of Things system occurs.

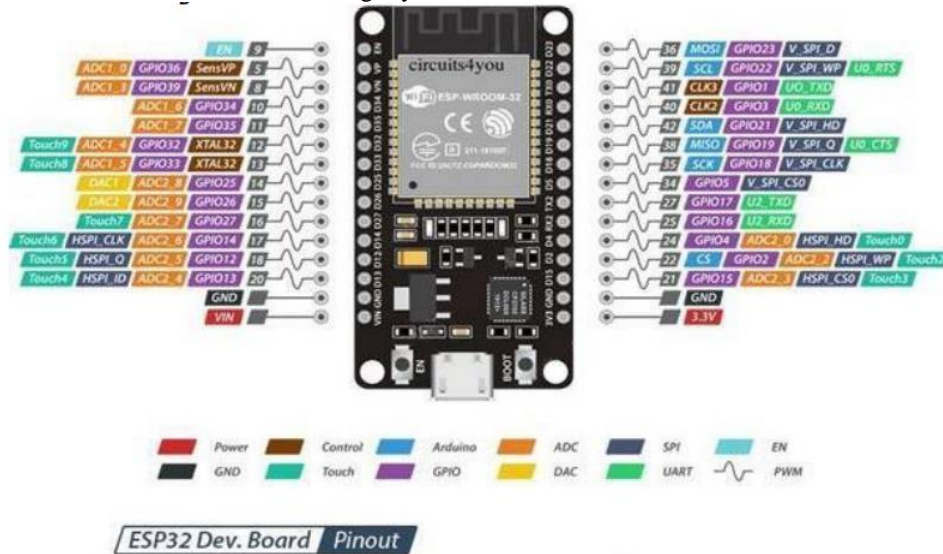


Figure 6. Specification ESP32 [9]

The ESP32 module has the following specifications:

- | | |
|---|-----------------------------|
| 1. Microprocessor | Xtensa Dual-Core 32 Bit LX6 |
| 2. Freq Clock | up to 240 MHz |
| 3. SRAM | 520 kB |
| 4. Wi-Fi transceiver | 11b/g/n |
| 5. Flash memory | 4 MB |
| 6. Bluetooth | 4.2/BLE |
| 7. GPIO | 48 pin |
| 8. Channel ADC (Analog to Digital Converter) | 15 pin |
| 9. PWM (Pulse Width Modulation) | 25 pin |
| 10. Channel DAC (Digital to Analog Converter) | 2 pin |

By looking at these specifications, usage becomes easier and simpler because in 1 ESP32 module the performance is better than other modules and has several ADC, PWM and DAC pins to connect to sensors. In addition, the

ESP32 module has connectivity in the form of Bluetooth and Wi-fi which can be seen from the module block diagram in Figure 7.

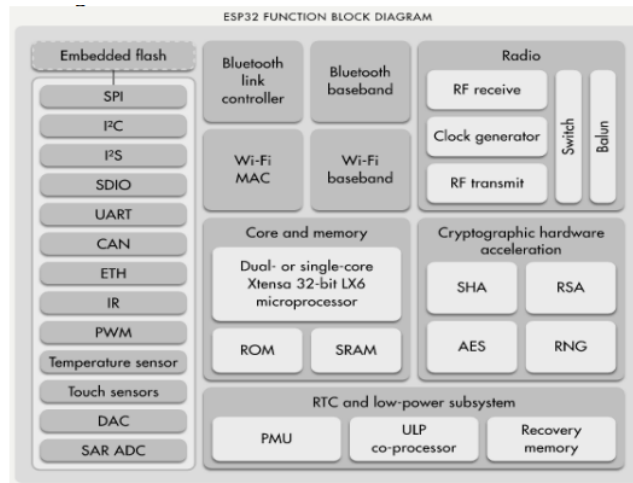


Figure 8. ESP32 Module Block Diagram [12]

Based on Figure 8, the ESP32 has an analog to digital converter (ADC) system. ADC is a converter of analog inputs into digital codes. Generally, ADC is used as an intermediary between sensors which are mostly analog with computer systems such as temperature sensors, light, pressure / weight, flow and so on and then measured using a digital system (computer). The ADC system itself has a waveform with a timing diagram of a trace sequence with a sequence to convert analog to digital as shown in Figure 9.

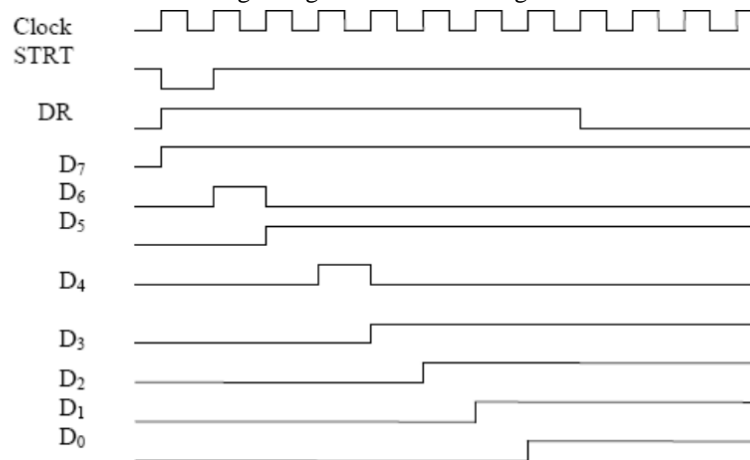


Figure 9. Timing Diagram of a Trace [13]

Tool Calibration

In the calibration used to see the current and voltage using a multimeter to see the comparison results obtained by the multimeter and sensor, this measurement was carried out to see the feasibility of the sensors used in the study. The values obtained are as shown in Table 1 comparison of the sensor with a multimeter.

Table 1. Monitoring and Measurement Results

Measurement To	Panel Flow Monitoring Results	Measurement Results	Error	Battery Current Monitoring Results	Measurement Result	Error
1.	0.03379	0.07	2.07%	0.02319	0.023	1%
2.	0.05801	0.046	0.79%	0.09582	0.014	0.14%
3.	0.2937	0.12	0.40%	0.08474	0.03	0.35%
4.	0.32444	0.2	0.61%	0.02699	0.07	2.59%
5.	0.0992	0.67	6.75%	0.03823	0.11	2.87%
6.	0.08485	0.01	0.11%	0.05913	0.06	1.01%

Table 1. Monitoring and Measurement Results (continue)

Measurement To	DC Voltage Monitoring Result	Measurement Result	Error
1	12	12,1	0,98%
2	12	12,2	0,99%
3	11	12,6	1,16%
4	11	12,9	1,20%
5	12	12,3	1,06%
6	12	12	1%

From the comparison table, we get the error value generated from the mutmeter against the sensor, an error value that exceeds 10% can be categorized that the sensor must be replaced. While in the table the value that exceeds 10% error is only 1 and the other error values are below 10%, so it can be interpreted that the sensor is feasible to use.

Thingspeak Monitoring Data

In monitoring via thingspeak, the sensor will read the results to be later distributed to esp32 as a program and on esp32 it will be sent to the network which will eventually enter thingspeak, with data like Figure 10–Figure 12. Where data retrieval takes 10 minutes apart, in addition, monitoring can be viewed directly through the Thingspeak website.



(a)



(b)

Figure 10. Current and Voltage Graph Thingspeak App

Figure 10(a) shows the current data generated by the solar panel, from a solar panel with a capacity of 100wp. The value obtained is due to the influence of light absorbed by the panel, the effect of the panel not only on light but also on the voltage Figure 10(b). The higher the light absorbed and converted by the panel, the higher the current and voltage values produced.

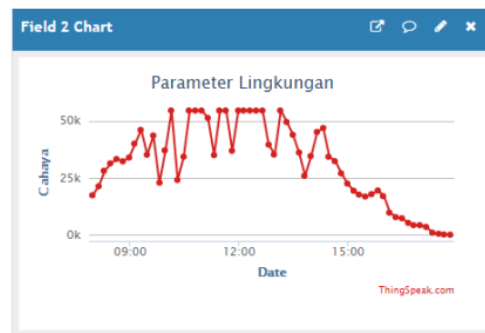


Figure 11. Light Graph Thingspeak

Figure 11 is a graph of the light intensity that obtained. Where research for light intensity is carried out with the same position and angle as the solar panel to the sun, so that the light data obtained will be in accordance with what is obtained on the solar panel. The light data obtained are influenced by the light shining on the solar panel, while the increase or decrease in the value of the data is influenced by the weather around the research site, when the clouds cover the light absorbed by the panel, the data value obtained will be small, but if the cloud conditions do not cover the absorption of light, the value of the data obtained will be high.

The effect of the highest light is during the day from 10.00 am to 14.00 pm because at that time the sun is right above the earth, so that more light is produced which will be absorbed by solar panels and converted into energy needed to turn on the load.

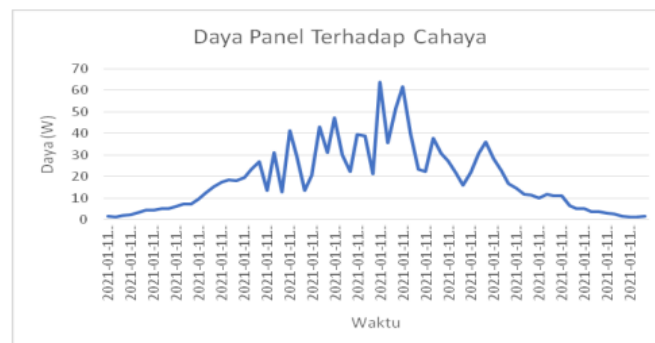


Figure 12. Power vs Time Graph

Figure 12 shows the value of the power that obtained, the power obtained by the solar panel for 12 hours with an interval of 10 minutes. The power results are obtained using the $P = I \times V$ formula, which is done manually, the data results shown in the graph tend to be larger starting from 10.00 WIB to 14.00 WIB because at that time the sun is in the best condition producing light so the value obtained is will be greater than at 6.00 WIB to 10.00 WIB and 15.00 WIB to 18.00 WIB.

CONCLUSION

1. Monitoring data by IoT is more effective than measuring manually, because when using IoT we can monitor data anywhere without having to look directly at the tool.
2. Data results for current, voltage and light intensity can be monitored using the Thinkspeak application, because the system has been integrated online through the ESP32 module hardware.
3. The use of ESP32 which already has an ADC system makes it easier for the system to work, because it can directly convert analog to digital in 1 microcontroller, compared if using a microcontroller module that doesn't have an ADC chip inside.

REFERENCES

1. Limbong, E., "Pengontrol Tirai Jendela Menggunakan Sensor BH1750 Berbasis Arduino Uno", *The University Institutional Repository Universitas Sumatera Utara*, (2018).
2. Hidayatullah, N. A., "Desain dan Aplikasi Internet of Thing (IoT) Untuk Smart Grid Power Sistem", *Jurnal Ilmiah Pendidikan Teknik Elektro* Vol. 2 No. 1, (2017).
3. Simatupang, R., *Dasar Rancangan Pembangkit Listrik Tenaga Surya*, (2014).
4. Kurniawan, B., "Rancang Bangun Sistem Smart Power Untuk Mengontrol dan Memonitoring Energi Listrik Berbasis Internet of Thing (IoT)", *Repository Teknik Elektro Institut Teknologi Nasional Malang*, (2020).
5. Nugraha, S., *Indonesia Energy Outlook*, Ministry of Energy and Mineral Resources, 2017.
6. Muhaemin, C., "Multy Utility Service Infrastructure (MUSI) Berbasis OPLC untuk Implementasi Grid Communication Network", *Electrical Engineering Journal Universitas Mercu Buana* Vol. 8 No. 1, (2017).
7. Pramudita, A., *Internet of Things Integration in Smart Grid*, (2017).
8. Gallagher, P. D., *NIST Framework and Roadmap for Smart Grid Interoperability Standard*, 2010.
9. ESP32.net, *The Internet of Thing with ESP32*, n.d, Available from: www.ESP32.net.
10. Sanni, S.O., Olusuyi, K., and Mahmud, I., "Design and Implementation of Home Appliance Energy Monitoring Device", *International Journal of Electry, Energy and Power System Engineering*, (2019).
11. Pambudi, G. W., *Cara Mengakses Sensor Tegangan DC*, Available from: icronyos.com, (2020).
12. Espressif, *Datasheet ESP32 Series*, Available from: Espressif Inc, (2019).
13. Haryanto, D., *ADC (Analog To Digital Converter), Teknik Natar Muka Analog To Digital Converter*, (2016).

The Power Comparison of Photovoltaic Modules Different Types

Matúš Bilčík¹, Monika Božíková^{1 a)}, Ľubomír Kubík¹, Ján Csillag¹, Patrik Kósa¹,
Tímea Szabóová¹, Ján Čimo², Ľuboš Moravčík², Stanislav Paulovič¹

¹Faculty of engineering, Slovak University of Agriculture, Trieda Andreja Hlinku 2, 949 76 Nitra, Slovak Republic

² Faculty of Horticulture and Landscape Engineering, Slovak University of Agriculture, Trieda Andreja Hlinku 2, 949 76 Nitra, Slovak Republic

a) Corresponding author: Monika.Bozikova@uniag.sk

Abstract. The article presents research results obtained from bifacial and monofacial monocrystalline photovoltaic modules. Identification of power changes was performed for different tilt angles 25° (installed on the building roof). The aim of experimental research was also monitoring of external factors (temperature of photovoltaic module, wind velocity and intensity of solar radiation) which have influence on power balance of photovoltaic system. Finally, computational simulation for identification of photovoltaic system power balance changes for bifacial photovoltaic modules installed on roof with different black and white surface was applied. The measured data were collected from solar invertors FRONIUS IG. The external factors were measured by pyranometer CMP 11 and anemometer A100R. From obtained power graphical relations is clear that the bifacial modules had better power balance than the monofacial and its energy production strongly depend on roof surface material reflection coefficient. For the data comparison was applied correlation analysis on the 2 dimensional graphical relations.

INTRODUCTION

Monitoring of PV systems parameters is important for the PV energy balance detection. The operation parameters were investigated by authors [1, 2]. Solar power generation has proven to be one of the most attractive option for electrical energy production in grid-connected and distributed modes [3, 4]. The possibilities of photovoltaic system application were described in Slovak literature [5–7] and by foreign authors [8, 9]. Monitoring of PV systems parameters is important for the PV energy balance detection. It is known from the sources [8–14] that the power, efficiency and quantity of electricity generated by photovoltaic system depend on many external factors such as: intensity of solar radiation, ambient temperature, wind speed, temperature of PV modules, reflectivity of PV modules surfaces and reflectivity of the roof or the building wall surfaces where are PV modules installed and it also depends on internal factors which are determined by materials and construction of PV modules, angle of construction orientation to the cardinal directions, tilt angle of the PV module etc. The aim of the presented research was power comparison of bifacial and monofacial monocrystalline PV modules with tilt angle 25°.

MATERIAL AND METHODS

The measurements were done on solar power stations in the Czech Republic, which are installed on the roof of the Faculty of Education, Masaryk University. The whole area of the photovoltaic system is 337.2 m². Orientation of this photovoltaic power plant is SW. The PV modules have to be installed with the tilt angle of 25°, which is not optimal from the theoretical point of view (in theory [15] ideal tilt angle for this location is 35°) because the building is important architectonical monument. The photovoltaic system is divided into two sections. The first section of PV system consisting of 288 monofacial monocrystalline panels SI 72-110 (Solartec, Czech Republic). The total power

output of this section is 30 kWp. The second section of the PV system has total power 5 kWp and is equipped by new type of bifacial monocrystalline PV modules SBI2G 72-90BR (Solartec, Czech Republic) (Figure 1). The bifacial modules produce solar power from both sides of the module.

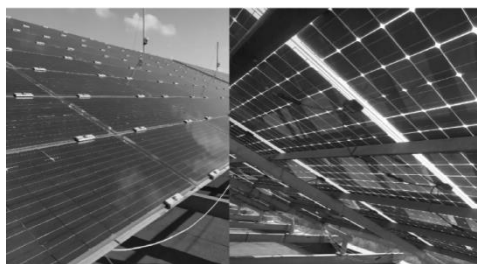


FIGURE 1. Bifacial PV modules SBI2G 72-90BR-MC

For converting DC voltage that is supplied by photovoltaic cells, for AC voltage 230 V with frequency 50 Hz serve 5 voltage converters type FRONIUS IG40 (Fronius, Austria) and 3 voltage converters type FRONIUS IG60HV (Fronius, Austria), efficiency of these converters is 94.3%. The whole photovoltaic system is connected to the main switchboard to the internal power network of the faculty. This makes it possible to supply The generated electricity is supplied to the grid. The solar radiation is measured with pyranometer CMP11 (Kipp&Zonen, Netherlands) and wind velocity is measured by anemometer A100R (Campbell Scientific, United Kingdom).

RESULTS AND DISCUSSION

The power of different types PV modules was compared during the one-year period. Because of huge data sets which were obtained from the experiments, the data selecting procedure was applied on the data files. For presentation of results were chosen model days for every month. Every evaluated day parameters as ambient temperature, relative air humidity, wind speed, intensity of solar radiation were compared with the monthly average for each point of graphical dependencies. The model day was extracted from the data obtained for every season (e.g., autumn) by comparison of experimental day data and the average values were calculated for every time point. Correlation analysis was applied on the experimental data. The model day of the season had a high degree of correlation with the average monthly parameters in terms of statistics. These days were without extreme cloudiness changes [6]. For power evaluation of PV system in model day was selected the time range from 9 a.m. to 4 p.m. when the solar radiation culminates. The power of 30 kWp section with monofacial monocrystalline PV module was recorded with 6 voltage converters and each converter had power 5 kWp. For this section was calculated the average value of power from all converters.

The next part of research was focused on the processing and comparison of powers obtained from bifacial and monofacial PV modules with the same tilt angle 25° . The average values of power were detected by data processing in MS Excel and Matlab 2015b. The selected results are presented in the (Figure 2) where are shown the time relations of power for the different types of PV modules in June and December. From complex power balance evaluation is evident that the monocrystalline bifacial PV modules had 7.6% higher average power balance than the classic monocrystalline PV modules during the year. Monocrystalline bifacial glazing PV modules can also use reflected solar radiation from the roof surface where they are installed. The lowest percentage difference of power 1.4% was found in March. Percentage differences higher than 10% were identified in months from August to December.

All dependencies were statistically processed and the results of correlation analysis for all mentioned measured parameters (intensity of solar radiation, power ambient temperature, wind speed, temperature of PV modules) were summarized. Based on the correlation analysis results is clear that the higher correlation degree 0.91 is between the PV module temperature and intensity of solar radiation. The lowest correlation coefficient 0.30 was found for relation between the PV module temperature and the wind velocity. Second part of the correlation analysis was focused on PV module power. PV module power is most affected by global radiation (35.94%) and PV module temperature (32.70%). The effect of wind speed and ambient temperature on PV module power is very similar, approximately 15%. Presented results are in good agreement with facts in the literature [16].

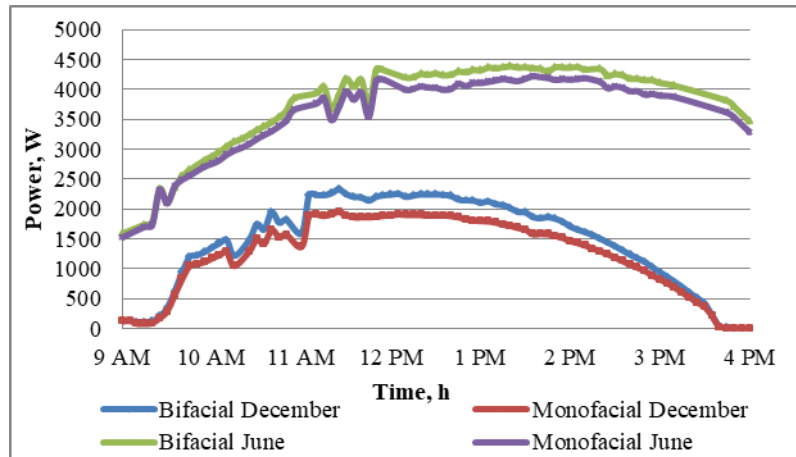


FIGURE 2. Power of PV modules different types in month June and December

In the next part, the influence of material surface under the PV modules was simulated by software Matlab 2015b. PV solar power stations on the roof of the Faculty of Education have on the ground black asphalt board IPA, so the main advantage of bifacial photovoltaic modules was not used in the full range because of low material reflexivity coefficient – albedo. Ideal surface for installation of bifacial PV modules should have maximal value of albedo. For comparison of albedo influence was performed computer simulation for material with higher value of albedo (white facade color – Baunit SilikonTop under the bifacial PV modules). The results of simulation for May are shown on the (Figure 3).

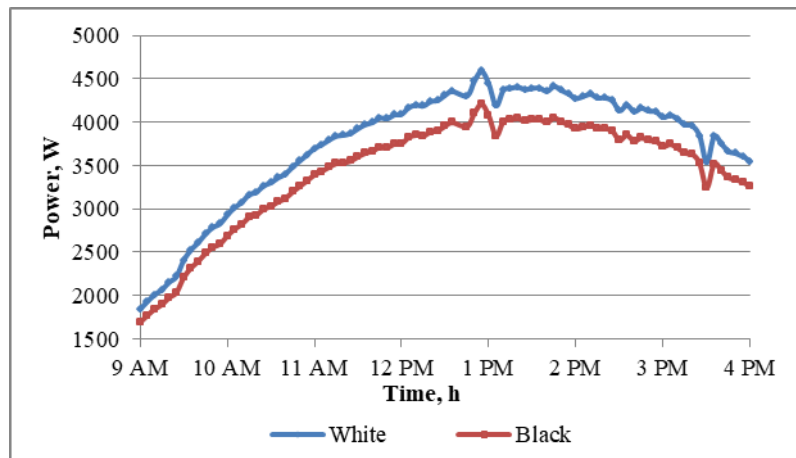


FIGURE 3. Simulation of PV system power with white surface under the bifacial PV modules during model day in May

CONCLUSION

From the presented results is clear that the position of PV module installation represented by tilt angle has significant influence on the PV module and PV system power. By the data analysis was found that bifacial monocrystalline photovoltaic modules have higher positive power balance during the year, but their performance is influenced by many external and internal operational aspects. The most important are external factors mainly weather conditions (maximum influence have intensity of solar radiation) and the reflexivity of material surface under the PV modules. Experimental results point to the fact that the surface albedo can positively affect the performance of the PV system, especially the positive effect on power balance was determined for materials with high reflexivity coefficient.

ACKNOWLEDGMENTS

This publication was funded by the Grant Agency Slovak University of Agriculture (GA SPU), grant number No 03-GASPU-2021.

REFERENCES

4. J. Šafránková, T. Petřík, M. Libra, V. Beránek, V. Poulek, R. Belza and J. Sedláček, *Agronomy Research* **19**, pp. 922–927 (2021).
5. M. Bilčík, M. Božiková, A. Petrović, M. Malínek, V. Cviklovič, M. Olejár and V. Ardonová, *Acta Technologica Agriculturae* **21**, pp. 14–17 (2018).
6. A. Divine, I. Seres and I. Farkas, *Renewable and Sustainable Energy Reviews* **141**, 110808 (2021).
7. S. Reddy, T. K. Mallick and D. Chemisana, *International Journal of Photoenergy* **2013**, pp.20–22 (2013).
8. M. Olejár, V. Cviklovič, D. Hrubý and O. Lukáč, *Research in agricultural engineering* **61**, pp.48–52 (2015).
9. Bilčík, M. Božiková and J. Čimo, *Appl. Sci.* **11**, 2140 (2021).
10. V. Cviklovič and M. Olejár, “Temperature dependence of photovoltaic cells efficiency,” in Trends in agricultural engineering 2013, edited by Czech University of Life Sciences Prague; Faculty of Engineering (Czech University of Life Sciences Prague, Prague, 2013), pp. 128–131.
11. D. Miličević, B. Popadić, B. Dumnić, Z. Čorba and V. Kalić, *Journal on Processing and Energy in Agriculture* **16**, 109–112 (2012).
12. Z. Čorba, V. Kalić and D. Miličević, *Journal on Processing and Energy in Agriculture* **13**, 328–331 (2009).
13. S. Chander, A. Purohit, A. Sharma, S. P. Arvind and M. S. Dhaka, *Energy Reports* **1**, 104–109 (2015).
14. A. D. Kafui, I. Seres and I. Farkas, *Acta Technologica Agriculturae* **22**, 5–11 (2018).
15. Božiková, M. Bilčík, V. Madola, T. Szabóová, L. Kubík, J. Lendelová and V. Cviklovič, *Appl. Sci.* **11**, 8998 (2021).
16. J. Šafránková, M. Havrlík, V. Beránek, M. Libra, V. Poulek, J. Sedláček and R. Belza, “Operation of PV power plants located in different climatic conditions,” Proc. BioPhys Spring 2021, edited by József Horabik (Perfekta info Pawel Markisz, Lublin, 2021), pp. 57.
17. D. Rusirawan and I. Farkas, *Environmental Engineering and Management Journal* **14**, 2747–2757 (2015).
18. M. Libra and V. Poulek, *Photovoltaics theory and practice of solar energy usage* (Czech University of Life Sciences Prague, Prague, 2009), 160 pp.
19. T. Huld and A. M. Gracia Amillo, *Energies* **8**, 5159–5181 (2015).

Data Communication On Motorcycle Rental Based On Internet Of Things

Muhammad Arif Ramdani^{1, a)}

¹⁾Bachelor of Electrical Engineering, Siliwangi University Jl. Siliwangi No. 24 Tasikmalaya West Java Indonesia.

^{a)}Corresponding author: @167002013@student.unsil.ac.id

Abstract. Some things that are certainly considered in motorbike rental are that the service provider must record the identity of the tenant, see the location of the motorbike, and remind the tenant of the rental time. Tenant identity service providers still use manual methods that appear in data reports and service providers have not yet alerted the place of motorbikes and reminders of rental times. Tenant identity data collection, place point notifications, and rental time reminders can be done using the internet of things. This can make it easier for the provision of services to record the identity of the tenant, see the point of a place, and give an alert for the time of the rental, with motorbikes that are rented can be found out and equipped with a reminder of the time of the rental. The results show that the registration system and the system on motorbikes can communicate with each other, the registration system can record the tenant's identity in the form of a NIK well as an E- KTP ID become used as access to motorbike starting and the registration system can store tenant data. The data communication tool consists of two tools, the first registration system consists of keypad integration and the MFRC522 RFID module, the second system on motorbikes from the integration of the voltage sensor, neo m8n GPS, mq7 sensor, gasoline buoy, MFRC522 RFID module, speed sensor, and max6675 sensor and see the condition of the motorbike, the system on the motorbike can remind time of provision in the form of a voice indicator.

INTRODUCTION

Motorcycles are one of the vehicles that can be rented. In motorcycle rental service providers, service providers collect consumer or tenant identity data to handle the tenant's data, service providers generally collect data manually which is still vulnerable to loss of tenant data [1]. Not only is the data collection on the identity of the tenants done manually, but the service providers are also unable to find out the location of the motorbikes and the condition of other motorbikes being rented and there are often delays in returning the motorbikes that are rented [2].

The use of internet of things technology can facilitate communication between devices so that devices can exchange data with other devices [3]. Based on these problems, this study designed data communication on the internet of things-based motorcycle rentals. With this tool, it is possible to make it easier to record the identity of the tenant and find out the condition of the motorbike, including the location of the motorbike being rented and equipped with a sound indicator to remind the rental time.

MATERIALS AND METHODS

Materials

The materials needed in compiling the system so that the system works properly include Arduino mega 2650 mini, nodemcu, MFRC552 RFID module, GPS Neo M8n, monoxide gas sensor (MQ7), temperature sensor (MAX6675), voltage sensor, and hall effect sensor.

System Architecture

The system architecture as shown in Figure 1 has two parts in the architecture of this system, the first part of the registration system which acts as registration of E-KTP, seeing the identity of the tenant, and seeing the condition of the bicycle, the second is the part of the system on the motorcycle which serves to receive data from the registration system and sends sensor data installed on the motorcycle to the registration system.

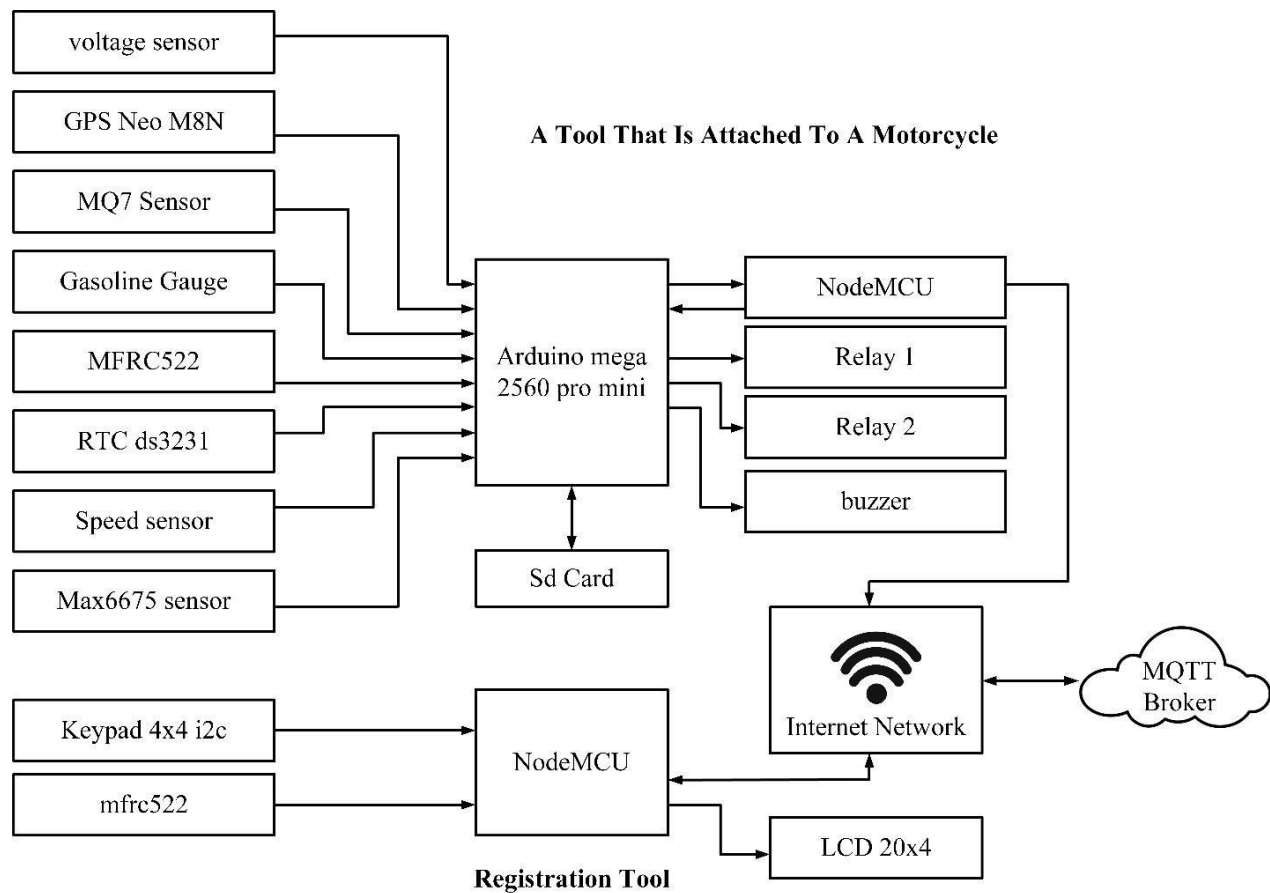


FIGURE 1. Sytem Architeure

System Flow

The system flow is divided into two parts, first the flowchart of the registration system that is made, starting from the system is off, when the system is turned on the system will work and will start connecting connections, if it is connected to the internet network, the system will retrieve data from MQTT and LCDs menu options. After that, the system will check what menu is selected, if menu A data-id E-KTP and rental time is sent to MQTT broker if menu B LCDs the identity of the tenant and if menu C LCDs the condition of the motorbike.

The two flowcharts of the system on the motorcycle are made, starting from the system is off, when the system is turned on, the microcontroller will turn on and the sensors will read and send the readings on the Arduino mega 2560 pro mini and sent by the Arduino mega 2560 pro mini to the Arduino mega 2560 pro mini. node MCU, when node MCU is connected to the internet network, the sensor data is sent to the MQTT broker to be retrieved by the registration system and node MCU also retrieves the tenant id data and rental time at the MQTT broker which has been sent by the registration system, after node MCU has retrieved the id-data the E-KTP and rental time will then be forwarded to the Arduino mega 2560 pro mini to be stored on the sd card, after it is stored on the sd card, when the RFID reads the registered E-KTP then the motorbike can be turned on, and when the rental time has run out the buzzer will sound as a warning rental period has expired.

Wiring System

The design of this tool will be made modeling with the design of the tool. Figure 2 and Figure 3 will show a schematic of the hardware design of the Internet of Things-Based Data Communication Device for Motorcycle Rental, which aims to find out what components are needed in making the system.

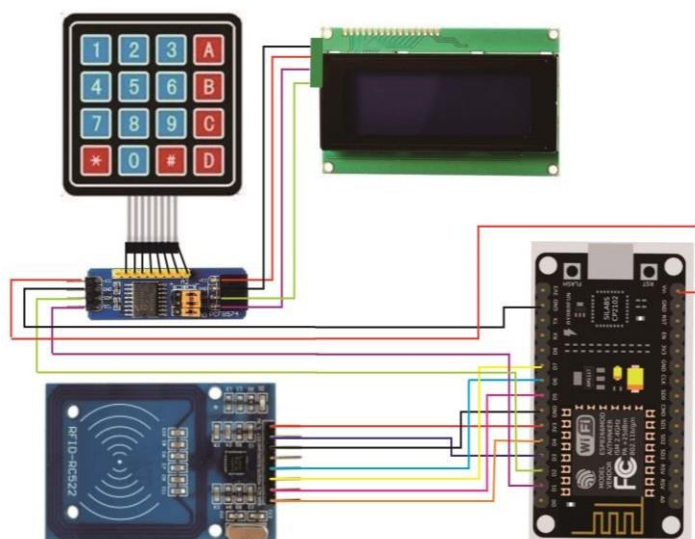


FIGURE 2. Schematic of Registration System Hardware Design

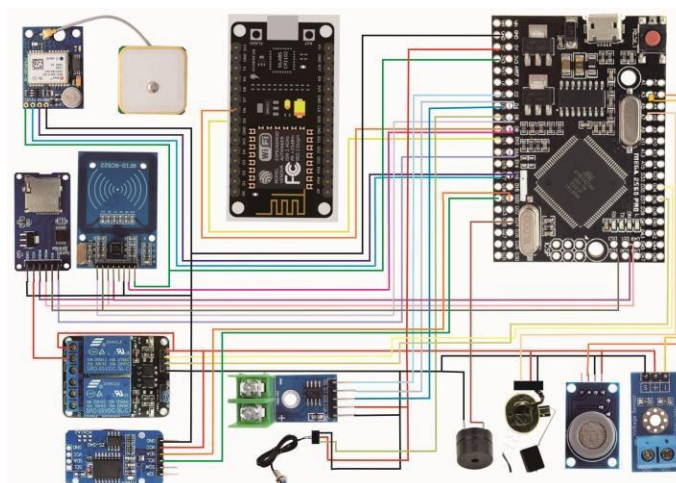


FIGURE 3. Motorcycle System Hardware Design Schematic

RESULTS AND DISCUSSION

Testing Motorcycle Address Input at Registration

Motorcycle address can be seen in Table 1

TABLE 1. Motorcycle Address Input Results on Registration

No	Address What is inputted	Registration System			Motorcycle System			Rental Time Out
		DataID E-KTP	Data date, month, year	Data Time	Data Identity Tenant	Contact Motor cycleA1	Contact Motor cycleA2	
1	A1	sent	sent	sent	Come on stage	Active	Not active	BuzzerSounds
2		sent	sent	sent	Come on stage	Active	Not active	BuzzerSounds
3		sent	sent	sent	Come on stage	Active	Not active	BuzzerSounds
4		sent	sent	sent	Come on stage	Active	Not active	BuzzerSounds
5		sent	sent	sent	Come on stage	Active	Not active	BuzzerSounds
1	A2	sent	sent	sent	Come on stage	Not active	Active	BuzzerSounds
2		sent	sent	sent	Come on stage	Not active	Active	BuzzerSounds
3		sent	sent	sent	Come on stage	Not active	Active	BuzzerSounds
4		sent	sent	sent	Come on stage	Not active	Active	BuzzerSounds
5		sent	sent	sent	Come on stage	Not active	Active	BuzzerSounds
1	Besides A1 and A2	Not sent	Not sent	Not sent	Not showing	Not active	Not active	BuzzerSounds
2		Not sent	Not sent	Not sent	Not showing	Not active	Not active	BuzzerSounds
3		Not sent	Not sent	Not sent	Not showing	Not active	Not active	BuzzerSounds
4		Not sent	Not sent	Not sent	Not showing	Not active	Not active	BuzzerSounds
5		Not sent	Not sent	Not sent	Not showing	Not active	Not active	BuzzerSounds

After testing the motorcycle address input at registration with three motorcycle address inputs as in Table 1, the registration system only sends data on E-KTP, date, month, year, time on the MQTT broker when inputted addresses of available motorcycles and the motorcycle system can be accessed only with the E-KTP that has been registered in the registration system and the buzzer sounds when the rental time is up.

Testing On and Off System Conditions on Motorcycles

Result of testing can be seen in Table 2

TABLE 2. Testing the On and Off Conditions on the Motorcycle System on the Registration System

No	Motorcycle System Condition	Display of Motorcycle Conditions in the Registration System								
		Date, month, year	Time	Location	Temperature	Voltage	Co	Bbm	Speed	Mileage
1	On	New Data	New Data	New Data	New Data	New Data	New Data	New Data	New Data	New Data
2		New Data	New Data	New Data	New Data	New Data	New Data	New Data	New Data	New Data

TABLE 2. Testing the On and Off Conditions on the Motorcycle System on the Registration System (Continue)

No	Motorcycle System Condition	Display of Motorcycle Conditions in the Registration System								
		Date, month, year	Time	Location	Temperature	Voltage	Co	Bbm	Speed	Mileage
3	On	New Data	New Data	New Data	New Data	New Data	New Data	New Data	New Data	New Data
4		New Data	New Data	New Data	New Data	New Data	New Data	New Data	New Data	New Data
5		New Data	New Data	New Data	New Data	New Data	New Data	New Data	New Data	New Data
1	Off	Latest Data	Latest Data	Latest Data	Latest Data	Latest Data	Latest Data	Latest Data	Latest Data	Latest Data
2		Latest Data	Latest Data	Latest Data	Latest Data	Latest Data	Latest Data	Latest Data	Latest Data	Latest Data
3		Latest Data	Latest Data	Latest Data	Latest Data	Latest Data	Latest Data	Latest Data	Latest Data	Latest Data
4		Latest Data	Latest Data	Latest Data	Latest Data	Latest Data	Latest Data	Latest Data	Latest Data	Latest Data
5		Latest Data	Latest Data	Latest Data	Latest Data	Latest Data	Latest Data	Latest Data	Latest Data	Latest Data

After Testing the On and Off Conditions on the Motorcycle System for the Registration System as shown in Table

2. The registration system will display the latest data sent by the motorcycle system on the condition of the motorcyclesystem On and the registration system will display the latest data received from the motorcycle system on the condition of the motorcycle system is Off.

CONCLUSION

Based on the results of research and discussion, it can be concluded that the Data Communication tool on InternetOf Things-Based Motorcycle Rental has succeeded in recording or recording the identity of the tenant in the form of a NIK which can be seen by inputting the address of the motorbike being rented in the registration system, the registration system can also see the condition motorbikes including the location of motorbikes for rent, the system installed on the motorbike can give a warning in the form of a buzzer sound when the rental time has finished.

This data communication tool on motorbike rental needs to be developed again in further research to get more optimal results with one of the developments in the registration system section so that it can record the name and address of the tenant in full and tenant data stored in the registration system can be stored permanently.

REFERENCES

1. R. A. Permana, "Sistem Persewaan Kendaraan Berbasis Web Pada P.O. Karya Aji Makmur," *Emit. J. Tek.Elektro*, 19 (1), pp. 41–45 (2019).
2. I. I. Purnomo, "Sistem Informasi Perancangan Aplikasi Rental Mobil Dengan Metode Visual Basic 6 . 0," *Technologia*, 7 (2), pp. 111–116 (2016).
3. D. Sasmoko, H. Rasminto, and A. Rahmadani, "Rancang Bangun Sistem Monitoring Kekeruhan Air BerbasisIoT pada Tandon Air Warga," *J. Inform. Upgris*, 5 (1), pp. 25–34 (2019).

LoRa Data Communication For Fishing Boat Monitoring

Fadli Padriyana^{1, a)}

¹⁾Bachelor of Electrical Engineering, Siliwangi University Jl. Siliwangi No. 24 Tasikmalaya West Java Indonesia.

^{a)}Corresponding author: padriyana@gmail.com

Abstract. Fishermen really need a monitoring system that can help when an emergency occurs at work so that it is easy to find the location of the incident so that problems can be handled immediately. In this study, a fishing boat monitoring system based on LoRa was developed, this system consists of a node device and a gateway. Node device is a device attached to a fishing boat that will continuously transmit data via LoRa communication so that the boat can be monitored. Setting Air Data Rate (ADR), data length and distance will affect the time on air (TOA) and reception of LoRa communication data. The LoRa module used is LoRa E32 with a working frequency in the 915 MHz band. The test is carried out on the shoreline to the sea in a line of sight (LOS) state. The data sent includes the rotational motion/tilt of the boat (roll and pitch), as well as the coordinates of the location of the boat (longitude and latitude). While the gateway is a device that forwards data to be displayed on the application server dashboard. The application server used in this research is thingsboard. The farthest distance that can be reached in the tests carried out is up to 2.4 km with the Air Data Rate setting at 0.3 Kbps, the data size is up to 55 bytes with an average time on air of 3.017 seconds.

INTRODUCTION

According to statistical data recorded by the National Transportation Safety Committee (KNKT), the trend of water transportation accidents increased from 2013 with 6 accidents to 2018 with 39 water transportation accidents occurred. The causes are varied, from human error to natural factors. Natural factors accounted for 38% of the causes of water transportation accidents, followed by human error with 37%, technical 23% and other factors 2% [1]. Fisherman works using conventional boats made with the skills and knowledge inherited from their ancestors, not using the skills and knowledge from a ship building architect. Therefore the stability and security level of conventional boats is low [2]. Fishermen also need communication devices, so that fishermen can be continuously connected and monitored so that when an emergency occurs it can be handled immediately.

Communication technology in maritime scenarios has been widely discussed, many methods are used to obtain a better system. LoRa is a wireless communication technology with a fairly long range by utilizing the chirp spread spectrum modulation technique so that this technique has a low power consumption [3] and works in the ISM frequency band (433, 868 and 915 MHz). LoRa packet data format consists of three main components, namely preamble, header (optional), and payload. There are two types of LoRa packet data formats (Figure 1), namely Explicit header mode and Implicit header mode. In the explicit header mode format, there is a header in which there is information on payload length, coding rate. And CRC (Cyclic Redundancy Check) serves to check for errors in digital data. Meanwhile, in implicit header mode, the parameters of payload length, coding rate, and CRC are not included in the data packet, and will reduce time on air [4].

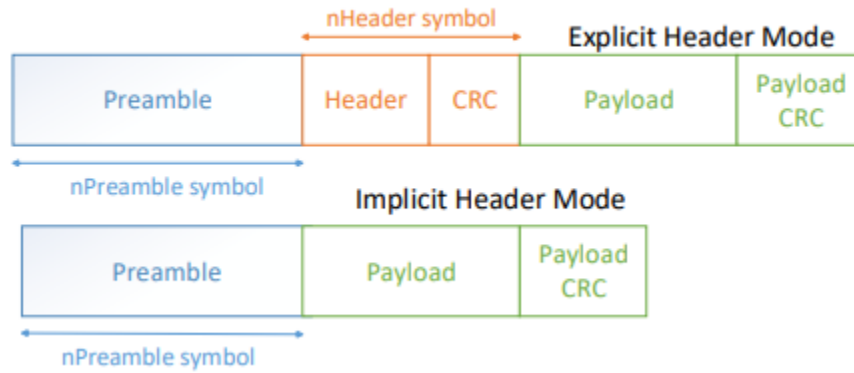


FIGURE 1. LoRa Format Packet Data

Based on the problems that have been described, with sea conditions that are free from obstacles, it will be very advantageous to apply this communication technique [5]. A lora based communication system is designed for fishing boat monitoring. This system consists of node devices and gateways that are connected point to point. The node device will send location data along with the ship's rotational motion that has been detected using the Ublox M8 GPS module and the gy-521 accelerometer sensor to the gateway. the gateway will send data using the mqtt protocol to the broker, thingsboard is set to subscribe to the same data topic as data from the device node so that data can appear on the thingsboard dashboard.

MATERIAL

Material

Building a lora-based communication system for fishing boat monitoring requires components including the LoRa E32 915T20D module as a data sender and receiver, arduino mega mini as a data processor accelerometer sensor gy-521 and ublox neo M8 GPS, and sends it to the lcd display and lora to be forwarded to the gateway, ESP32 to process data from lora, connect gateway with internet so data can be sent to mqtt broker, and also give output to oled display and buzzer.

System Block Diagram

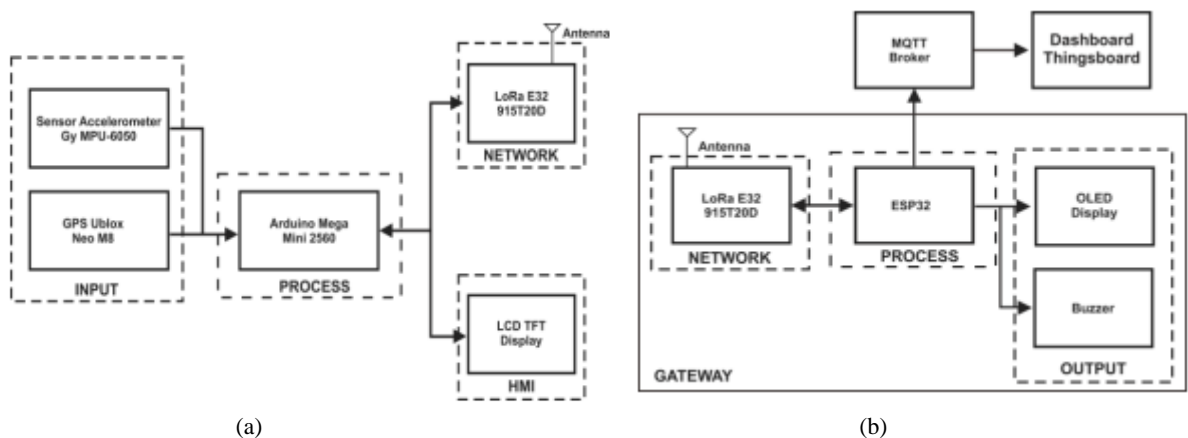


FIGURE 2. (a) System Block Diagram Node Device Figure. (b) System Block Diagram Gateway

Building a lora-based communication system for fishing boat monitoring requires components including the LoRa E32 915T20D module as a data sender and receiver, arduino mega mini as a data processor accelerometer sensor gy-521 and ublox neo M8 GPS, and sends it to the lcd display and lora to be forwarded to the gateway, ESP32 to process data from lora, connect gateway with internet so data can be sent to mqtt broker, and also give output to oled display and buzzer.

System Architecture

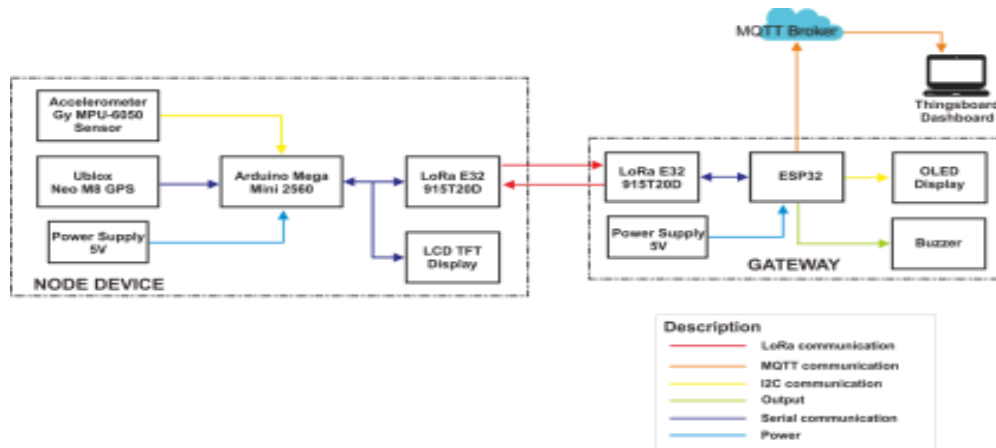


FIGURE 3. The System Architecture

The overall system architecture as shown in Figure 3, explains the interrelationships between components. In this system, both devices require a power supply of 5V. On the device node, the accelerometer sensor is connected to the Arduino Mega Mini with I2C communication using the SCL and SDA Arduino pins, namely pins D21 and D20. The Ublox Neo M8 GPS, LCD TFT display, and LoRa E32 are connected using serial communication to the Arduino Mega Mini. At the gateway, the ESP32 is connected to the LoRa E32 using serial communication. The OLED display is connected to the ESP32 using I2C communication, while the ESP32 is connected to the broker using the MQTT protocol. For the use of pins described in Table 1.a. and 1.b.

TABLE 1.a. Pin Node Device Configuration

No.	Microcontroller pin	Another Component pin	Component name
1	5V	VCC	LCD Touchscreen
2	3.3v	VCC	LoRa, GPS, Accelerometer
3	GND	GND	All component
4	D32	M10	LoRa
5	D34	M1	LoRa
6	D10	RX	LoRa
7	D11	TX	LoRa
8	D36	AUX	LoRa
9	D14	RX	GPS
10	D15	TX	GPS
11	D18	RX	LCD Touchscreen
12	D19	TX	LCD Touchscreen
13	D20	SDA	Accelerometer
14	D21	SCL	Accelerometer

TABLE 1.b. Pin Gateway Configuration

No.	Microcontroller pin	Another Component pin	Component name
1	Vin	VCC	Oled Display
2	3.3v	VCC	LoRa
3	GND	GND	All component
4	D15	M10	LoRa
5	D2	M1	LoRa
6	D4	RX	LoRa
7	D18	TX	LoRa
8	D5	AUX	LoRa
9	D21	SCL	Oled Display
10	D22	SDA	Oled Display
11	D19	Positive	Oled Display

System Flowchart

System flowchart can be seen in Figure 4.a and Figure 4.b

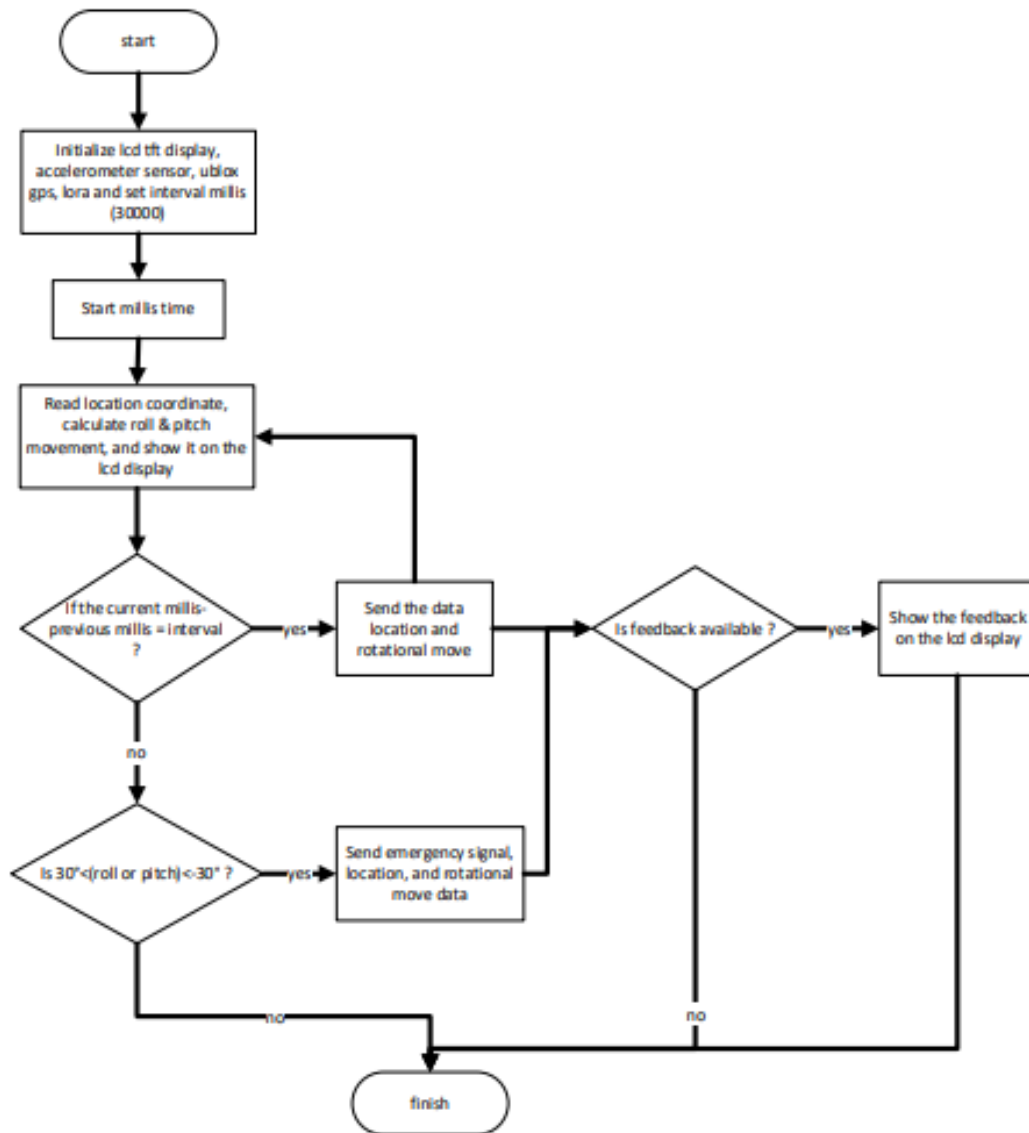


FIGURE 4.a Flowchart System Node Device

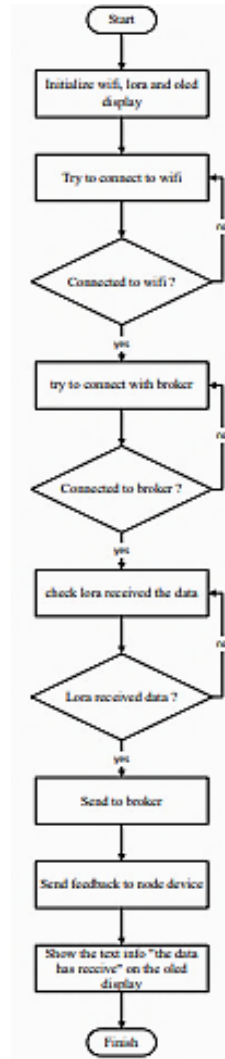


FIGURE 4.b Flowchart System Gateway

RESULTS AND DISCUSSION

LoRa Communication Test

The test focuses on the reliability of lora communication, carried out on the cipatujuh beach with the gate location on the shoreline with a height of about 1 m above ground level, and the node device is carried to the sea by boat. The parameters tested are distance, data size, air data speed and its effect on time in the air. the distances tested are 0.5, 1, 1.5, 2, 2.5 km, and the air data rate is 0.3, 2.4, and 19.2 kbps, while the amount of data tested is based on the lora e32 maximum package capacity specification of 58 bytes, therefore the amount of data in this test is at 10, 25, 55 bytes. The method for calculating time on air is carried out as in equation 1.

$$\text{ToA (second)} = \frac{(\text{Treceivefeedback} - \text{TSend})}{2} \quad (1)$$

Equations are entered into the Arduino program as in figure 5, the feedback received will be in the form of a string containing "|F|1|", and will record the current millis time and enter it into the t-receivefeedback symbolized in the program "time_terima_fb", so that time on air can be calculated by using the millis on arduino.

```

if (dataIn.substring(0, 5) == "|F|1|") { // feedback
  time_terima_fb = millis();
  toa = (time_terima_fb - time_kirim) / 2000;
  Serial.print("waktu terima feedback : ");
  Serial.println(time_terima_fb+String(" milidetik"));
  Serial.println ("toa(time on air)");
  Serial.println("toa = (waktu terima feedback - waktu kirim)/2");
  Serial.print ("toa = ");
  Serial.print(toa);
  Serial.println(" detik");
  fb++;
}

```

FIGURE 5. Equation Time On Air In Arduino Program

Device placement as in Figure 6.(a) node device and (b) gateway



FIGURE 6. (a) Node Device Placement Figure (b) Gateway Placement

The test method is carried out with 10 repetitions, then the values are averaged. The results are grouped by air data rate, it is 0.3, 2.4 and 19.2 kbps. test graph at a data rate of 0.3 kbps in Figure 8 and the detail of test location is showed in Figure 7.

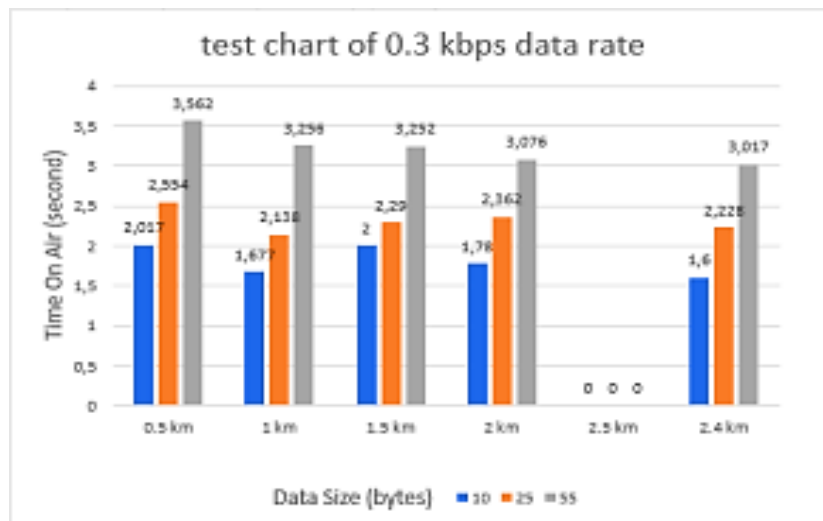


FIGURE 7. Test chart of 0.3 kbps

The graph in Figure 7 shows the results of testing with air data rate of 0.3 kbps, the results show that it is able to reach distances of up to 2.4 km with time on air which increases as the data size gets bigger, and is not affected by distance. With the lowest time on air at a distance of 2.4 km with a data size of 10 bytes and the highest time on air at a distance of 500 meters with a data size of 55 bytes.

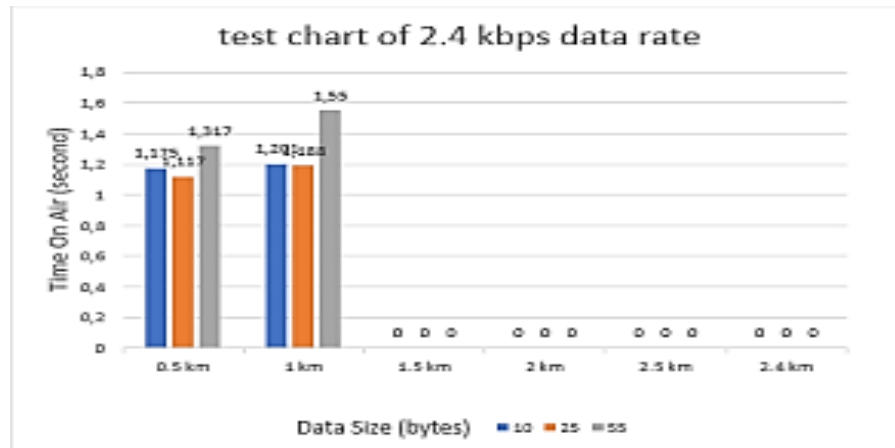


FIGURE 8. Test chart of 2.4 kbps

The graph in Figure 8 shows the results of the test with an air data rate of 2.4 kbps, these results show that it is able to reach a distance of 1 km with greater on air time along with the increase in sending distance, and is not affected by the size of the data. With the lowest on air time at a distance of 0.5 km with a data size of 25 bytes and the highest on air time at a distance of 1 km with a data size of 55 bytes.

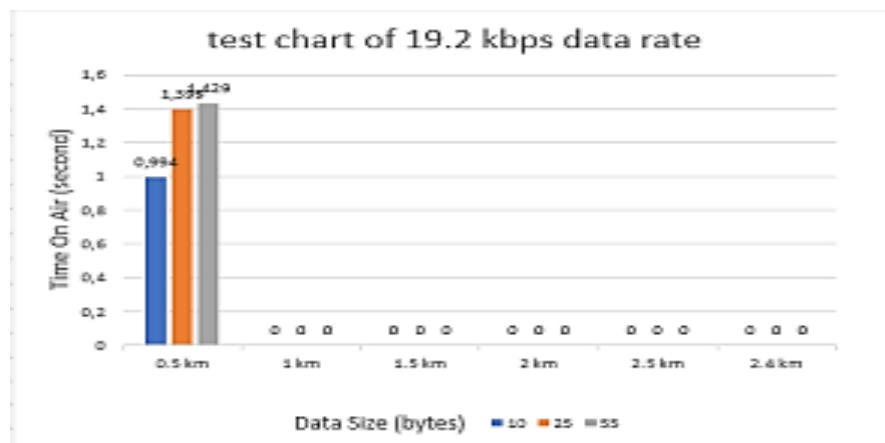


FIGURE 9. Test chart of 19.2 kbps

The graph in Figure 9 shows the test results with an air data rate of 19.2 kbps, these results show that it is able to reach a distance of 0.5 km with greater time on air as the data increases.

MQTT Communication Test

Sending data from the gateway to the broker using the mqtt communication protocol, the broker used is `iot.ee.unsil.ac.id`. with a unique topic, and the Thingsboard application server is set to subscribe to the same data topic. in this case the test is intended to find out the data sent from the gateway can be received and displayed on the thingsboard dashboard. The mqtt communication test is carried out by sending data that is read by the sensor repeatedly 10 times, in Table 2 is the data received from the results of the mqtt communication test which can also be seen in the latest telemetry data on the thingsboard menu of device details as in Figure 10. and shown on thingsboard dashboard as in Figure 11.

TABLE 2. Mqtt Communication Test Results

Pengujian Ke-	Data Diterima				
	Latitude	Longitude	Roll	Pitch	Status
1	- 7.340271	108.22615	13	9	Secure
2	- 7.340271	108.22615	3	4	Secure
3	- 7.340271	108.22615	8	11	Secure
4	- 7.340271	108.22615	11	9	Secure
5	- 7.340271	108.22615	8	5	Secure
6	- 7.340271	108.22615	13	11	Secure
7	- 7.340271	108.22615	9	3	Secure
8	- 7.340271	108.22615	14	10	Secure
9	- 7.340271	108.22615	5	2	Secure
10	- 7.340271	108.22615	6	11	Secure

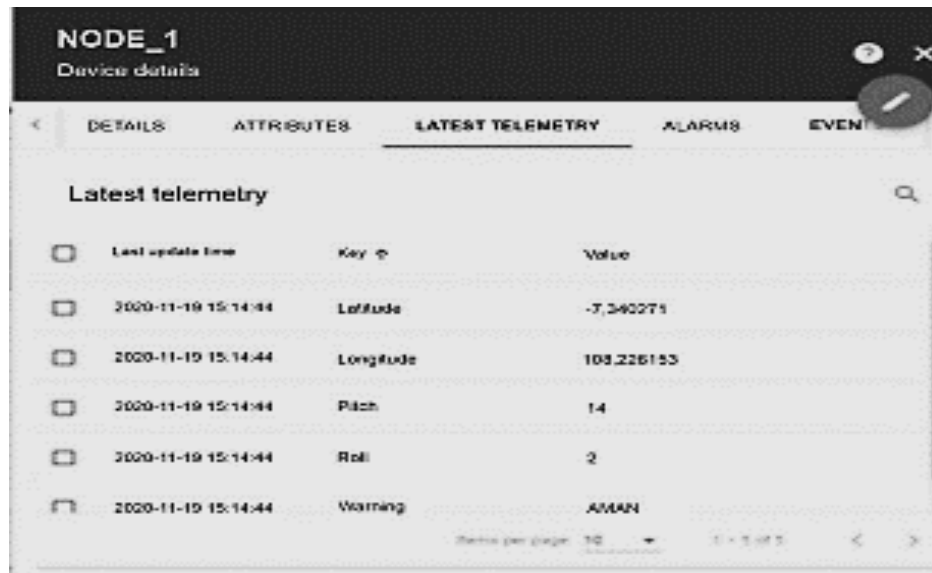


FIGURE 10. Latest Data Telemetry Thingsboard

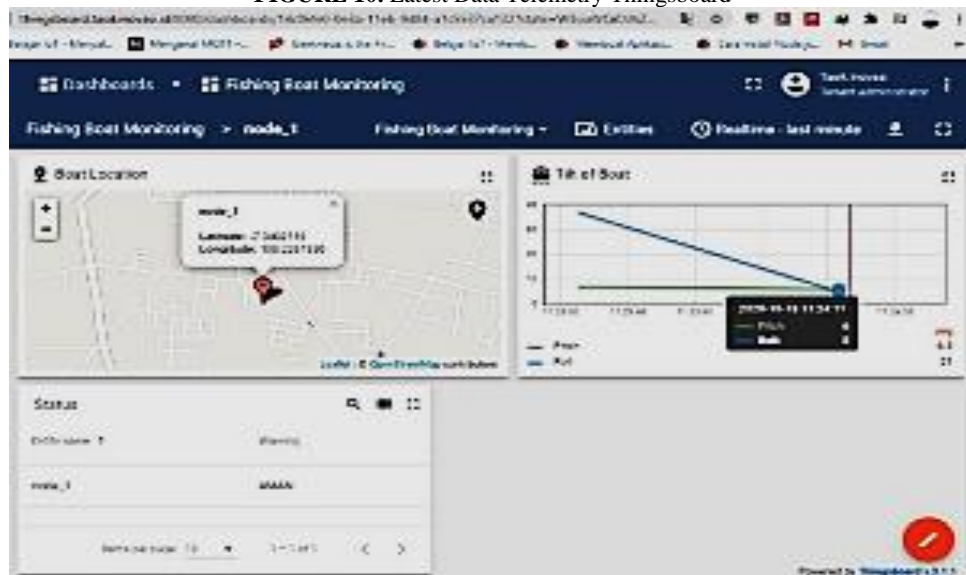


FIGURE 11. Thingsboard Dashboard

CONCLUSION

The test results show that in the 0.3 kbps data rate test, the on-air time is not affected by the distance of delivery, it is still determined by the size of the data, while the 2.4 kbps air data rate test shows the opposite result, namely the on-air time increases as the distance increases. , and is not affected by the size of the data. and in the air test the data rate of 19.2 is only able to reach a distance of 500 meters, the furthest distance that can be achieved by lora communication is 2.4 km with an air data rate setting of 0.3 kbps. and it can be concluded that the higher the air data rate used, the lower the communication distance. And the gateway is capable of forwarding data from the node to the broker.

REFERENCES

1. Komite Nasional Keselamatan Transportasi (2018) 'STATUS LAPORAN Kecelakaan Lalu Lintas dan Angkutan Jalan (LLAJ)', (November).
2. O., Yaakob, F.E., Hashim, M.R., Jalal, and M.A., "Mustapa, Stability, seakeeping and safety assessment of small fishing boats operating in southern coast of Peninsular Malaysia", *Journal of Sustainability Science and Management*, 10(1), pp.50–65 (2015).
3. I.R., Sanchez. and M.D., "Cano, State of the art in LP-WAN solutions for industrial IoT services", *Sensors (Switzerland)*, 16(5). doi: 10.3390/s16050708 (2016).
4. Semtech Corporation (2013) 'SX1272/3/6/7/8 LoRa Modem Design Guide, AN1200.13', (July), p. 9. Available at: <https://www.rs-online.com/> (2013).
5. R., Sanchez-Iborra, I.G., Liano, C. Simoes, E., Counago and A.F., Skarmeta, "Tracking and monitoring system based on LoRa technology for lightweight boats", *Electronics (Switzerland)*, 8(1), pp. 1–18. doi: 10.3390/electronics8010015 (2019).

Implementation of Human Detection on Robot Prototype Using Admp401 Sensor

Ceppy Ari Sugiharto^{1, a)}, Decy Nataliana¹, Niken Syafitri¹

¹ Institut Teknologi Nasional (Itenas), Bandung – INDONESIA

^{a)} Corresponding author: ceppy.ari21@gmail.com

Abstract. The ability of robots to robustly detect and localize what people see and hear is an important task that will be very useful in many robot interactions. In this study, four ADMP401 microphone sensors arranged with a polar directivity pattern to detect the north, south, east, and west directions of the potential presence of disaster victims through sound media using Arduino IDE and Audacity software. The tests carried out are by doing a hand clapping test as well as the noise produced by the victim and the victim's voice without obstruction with obstruction. As a result, the ability of the ADMP401 microphone sensor in detecting the direction of the sound of the potential presence of the victim has an accuracy of up to 81.85%. In this test, the sound of clapping which reduces the sound of the victim's voice is reduced to 57.71% and the victim's voice is reduced to 43.01% due to obstacles that can disperse and dissipate the intensity of the sound power captured by the ADMP401 microphone sensor.

INTRODUCTION

During the 21st century, more than 522 significant earthquakes occurred, with a death toll of more than 430,000 worldwide. The majority of deaths were caused by collapsed buildings trapped underground. If patients are uninjured, healthy, and without fresh air, they can survive for about 72 hours. Eighty percent of survivors can be saved alive within 48 hours of the collapse, but after 72 hours the survival rate decreases exponentially. This time limit can be much shorter due to lack of air supply, ambient temperature, victim's health condition, and so on. Therefore, to reduce deaths after natural disasters, the rapid detection of victims inside the collapsed structure is of utmost importance. The current search method is based on victim testimony to establish possible victims under the rubble [1].

Humans can find sounds. The system formed by the ear and brain can automatically detect the signal, process it, and determine where the sound is coming from. Thanks to the shape of the ear and the delay caused by sound propagation, the brain can find its source within a certain range of failure. From the XIX century to the present, humans have intended to make devices with these human features. To mimic the human ear a different microphone-array system has been applied [2].

The ability of robots to robustly detect and localize what people see and hear is an important task that will be very useful in many robotic interaction scenarios. There are many approaches to identifying active speakers among a group of people. Typical techniques involve audio and vision as input modalities. Several methods take advantage of audio-visual synchronization to identify active speakers. The main problem of this method is to find the correspondence between the acoustic signals from the microphone. Finding correspondence means identifying the temporal location of the signal associated with the same acoustic event [3].

Micro Electro Mechanical Systems (MEMS) can be useful for very low size situations because of their ability to build very small sensors with precise geometries. Microphones and other low-level differential pressure transducers are often used in aeroacoustic measurements for characterization, flow thermal mapping via acoustic pyrometry, and aircraft flight tests [4].

A disaster victim detection robot with an automatic waypoint system for return trips has been implemented by [5]. In this study, the robot uses the RCWL-0516 microwave sensor to detect the potential presence of living disaster victims based on small movements behind the rubble. Disaster victims tend to have a survival instinct by making small movements to be free from the burden of rubble. In addition, the victim also has the potential to produce sounds so that the rescue team can identify the position of the victim who is still alive. Therefore, this research will design and implement a prototype system for detecting disaster victims through the sound produced by victims using four ADMP401 sensors arranged in such a way that they can localize and recognize the potential direction of sound produced by disaster victims.

MATERIAL AND METHOD

The system design consists of hardware and software. The hardware consists of a series of ADMP401 microphone modules, 28BYJ-48 stepper motors, Arduino Uno R3, project boards, and ISD1820 modules. The software used in this design is using Arduino IDE and Audacity. Figure 1. presents a block diagram of the designed system.

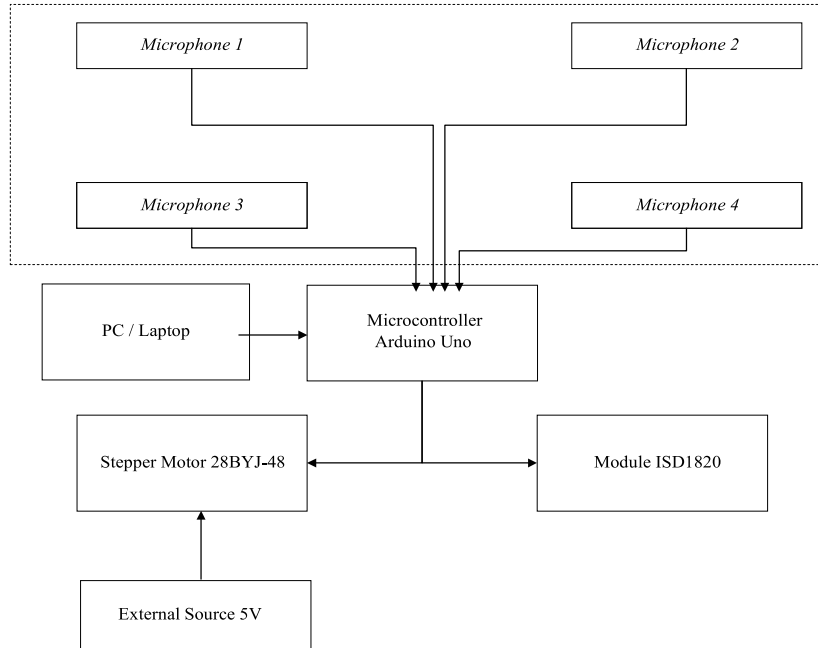


FIGURE 1. System Block Diagram

Based on the system block diagram in Figure 1, the design in this study aims to develop and implement a prototype of a disaster victim detection robot with a detection system using four ADMP401 microphones placed on an acrylic/wooden pattern with a polar directivity pattern. In this study, one personal computer (PC) is used as a source or power supply for Arduino Uno and a power bank as an external source +5V for the 28BYJ-48 stepper motor. An external +5V source is used because when the stepper motor draws a very large current from the Arduino Uno, the Arduino Uno may be damaged. In addition, sourcing the stepper motor via the Arduino Uno gives inconsistent results (step rotation errors such as stuck or won't move). After four ADMP401 microphones detect sound from four possible sound directions with a sound intensity level difference approach, the detection data from the microphone is sent to Arduino Uno to provide a signal to the actuator, namely the 28BYJ-48 stepper motor in the form of moving steps towards the sound source and ISD1820 in the form of a voice line. "victim detected".

System Flowchart

The system flowchart explains how the stages of the system are integrated with each other starting from the detection of victims through sound by the ADMP401 microphone to the actuator, namely the 28BYJ-48 stepper motor by taking steps towards the potential victim's voice and the "victim detected" voiceline from the ISD1820 module. The following Figure 2 show the flow diagram of the designed system.

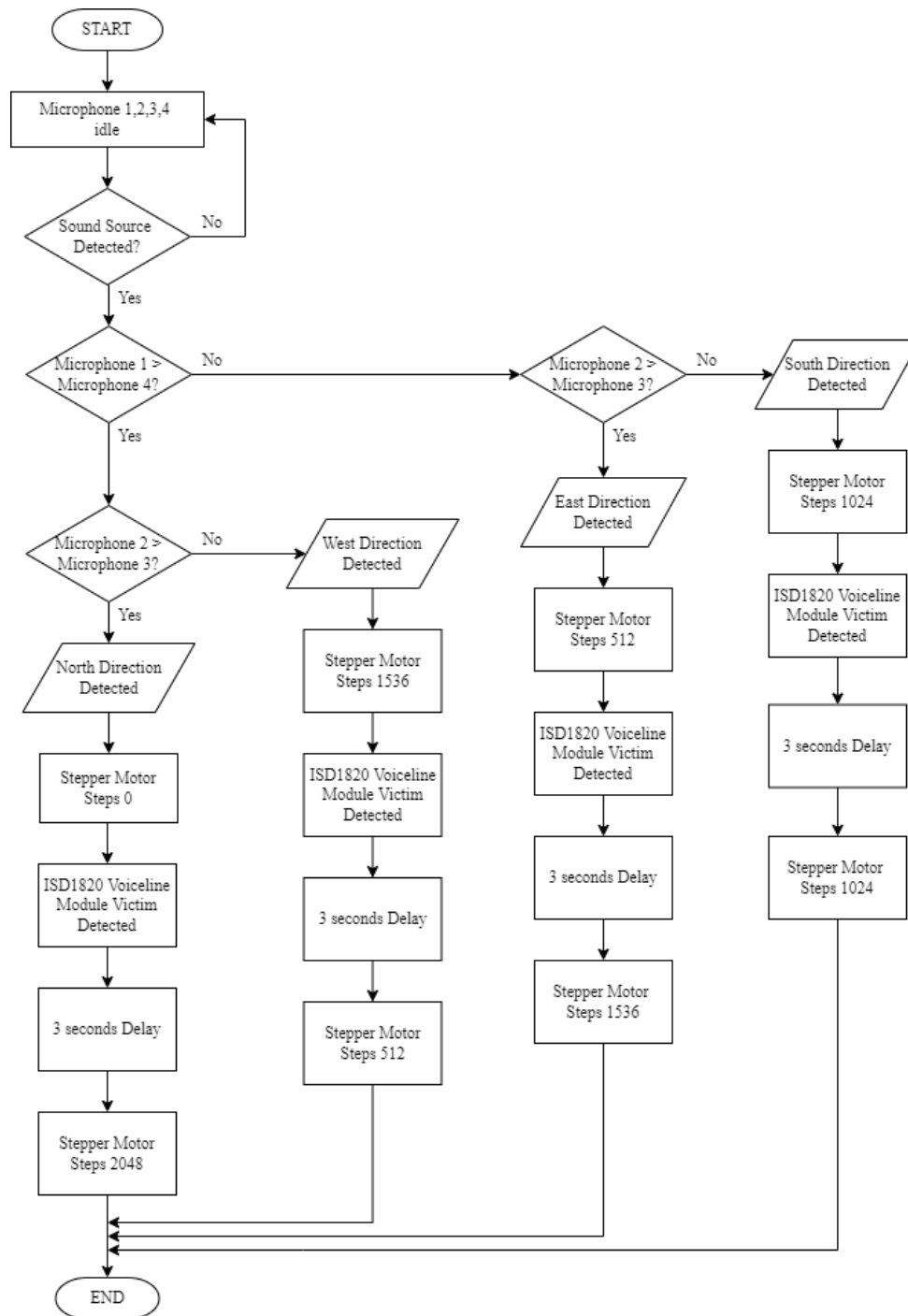


FIGURE 2. System Flowchart

In Figure 2, it can be seen how the flow diagram of the entire system is designed. First, microphones 1, 2, 3, and 4 are in an idle state, which is less than 14. Previously, the system designed for the microphone was to convert the acoustic signal received by the microphone into 10-bits ADC data from 0 to 1023. So, the sound intensity level is characterized by changes in low and high data from 0 to 1023. After microphones 1, 2, 3, and 4 detect a sound signal in the form of an acoustic signal, the idle data that is < 14 will increase according to the intensity of the received sound power. The method used to determine the direction is to compare the intensity of the sound power of the four microphones. The comparison method designed is when microphone 1 $>$ microphone 4 and microphone 2 $>$ microphone 3, then the direction that is read is north. When microphone 1 $>$ microphone 4 and microphone 3 $>$ microphone 2, the direction that is read is west. When microphone 4 $>$ microphone 1 and microphone 2 $>$ microphone 3, the direction that is read is east. When microphone 4 $>$ microphone 1 and

microphone 3 > microphone 2, the direction that is read is south. Furthermore, when the direction of the victim's voice has been detected, the stepper motor will take steps according to the direction of the potential sound. Since the stepper motor cannot recognize the starting point or recognize the angle, unlike the servo motor, it is necessary to manually adjust it by performing manual steps until the direction of the pointer is in the north direction. This stepper motor runs in full-step mode, so the number of steps required for one revolution is 2048. The initial position of the stepper motor is in the north direction. When the north direction is detected, the stepper motor will not perform steps or 0 steps, when the east direction is detected, the stepper motor will perform steps of 512 steps, when the south direction is detected, the stepper motor will perform steps of 1024 steps, and when the west direction is detected, the stepper the motor will perform steps of 1536 steps. This system is also given a delay of 3 seconds so that changes can be observed. Steps that occur after the delay function to return the direction pointer to its initial position, namely the north position. This stepper motor can rotate at a maximum speed of 15 revolutions per minute (RPM). If divided by one minute, the stepper motor will make one revolution in 2 seconds at a rotational speed of 15 revolutions per minute (RPM). After adding 3 and 2 seconds of delay time and stepper motor revolution time, it is obtained that 5 seconds is used to adjust the microphone delay in detecting the direction of the victim's voice. In the process of giving a delay of 3 seconds too, the ISD1820 module will provide a "victim detected" voiceline.

RESULT AND DISCUSSION

Victim's Voice Direction Detection Test

This test was carried out using the comparison method of sound intensity on four ADMP401 microphones by testing hand-clapping which was assumed to be the noise produced by the victim and testing the sound with medium intensity sound produced by the victim. In addition, the test is divided into two, namely with obstacles (door barriers) and without obstacles. The detection distance tested ranges from 0.5 meters to 5 meters in increments of 0.5 meters. Table 1 present south direction applause trial without obstacle.

TABLE 1. South Direction Applause Trial Without Obstacle

No	Distance (m)	South Direction Test				Description
		Microphone 1	Microphone 2	Microphone 3	Microphone 4	
1	0.5	229	281	436	487	Detected, right direction
		326	406	617	481	Detected, right direction
		234	238	437	260	Detected, right direction
2	1	370	236	269	402	Detected, right direction
		275	192	416	312	Detected, right direction
		393	361	449	452	Detected, right direction
3	1.5	234	145	192	281	Detected, right direction
		291	267	372	330	Detected, right direction
		274	222	354	292	Detected, right direction
4	2	143	154	192	232	Detected, right direction
		139	176	194	277	Detected, right direction
		146	232	384	272	Detected, right direction
5	2.5	207	198	296	254	Detected, right direction
		312	371	398	410	Detected, right direction
		184	123	284	204	Detected, right direction
6	3	159	147	247	193	Detected, right direction
		101	139	160	155	Detected, right direction
		226	216	273	290	Detected, right direction
7	3.5	303	265	307	325	Detected, right direction
		151	106	187	192	Detected, right direction
		126	97	141	226	Detected, right direction

TABLE 1. South Direction Applause Trial Without Obstacle (continue)

No	Distance (m)	South Direction Test				Description
		Microphone 1	Microphone 2	Microphone 3	Microphone 4	
8	4	135	164	163	170	Detected, wrong direction
		113	98	155	140	Detected, right direction
		100	158	219	166	Detected, right direction
9	4.5	96	101	120	134	Detected, right direction
		120	133	132	142	Detected, wrong direction
		90	92	97	103	Detected, right direction
10	5	88	90	107	111	Detected, right direction
		75	81	89	94	Detected, right direction
		73	79	77	83	Detected, wrong direction

Table 2 present south direction applause trial with obstacle.

TABLE 2. South Direction Applause Trial with Obstacle

No	Distance (m)	South Direction Test				Description
		Microphone 1	Microphone 2	Microphone 3	Microphone 4	
1	0.5	129	120	213	234	Detected, right direction
		154	144	243	228	Detected, right direction
		136	155	176	180	Detected, right direction
2	1	151	164	181	172	Detected, right direction
		138	143	191	184	Detected, right direction
		131	125	167	166	Detected, right direction
3	1.5	98	114	132	140	Detected, right direction
		93	101	125	112	Detected, right direction
		70	67	88	101	Detected, right direction
4	2	51	61	54	53	Detected, wrong direction
		47	48	57	76	Detected, right direction
		61	62	78	82	Detected, right direction
5	2.5	21	22	25	26	Detected, right direction
		40	41	39	40	Detected, wrong direction
		31	32	39	37	Detected, right direction
6	3	31	30	36	29	Detected, wrong direction
		23	24	28	33	Detected, right direction
		24	28	42	44	Detected, right direction
7	3.5	25	25	28	35	Detected, right direction
		18	18	22	24	Detected, right direction
		27	31	38	37	Detected, right direction
8	4	21	21	26	28	Detected, right direction
		24	26	29	32	Detected, right direction
		17	22	24	26	Detected, right direction
9	4.5	22	23	29	28	Detected, right direction
		25	23	27	31	Detected, right direction
		19	21	25	25	Detected, right direction
10	5	19	19	22	24	Detected, right direction
		21	23	31	27	Detected, right direction
		18	23	22	25	Detected, wrong direction

Table 3 present south direction victim's voice trial without obstacle.

TABLE 3. South Direction victim's Voice Trial Without Obstacle						
No	Distance (m)	South Direction Test				Description
		Microphone 1	Microphone 2	Microphone 3	Microphone 4	
1	0.5	111	98	138	135	Detected, right direction
		154	103	196	181	Detected, right direction
		123	129	152	157	Detected, right direction
2	1	88	94	114	175	Detected, right direction
		97	85	100	135	Detected, right direction
		101	88	114	125	Detected, right direction
3	1.5	87	81	108	115	Detected, right direction
		67	63	85	90	Detected, right direction
		78	74	81	110	Detected, right direction
4	2	118	128	147	152	Detected, right direction
		81	114	120	124	Detected, right direction
		107	119	133	149	Detected, right direction
5	2.5	89	74	114	122	Detected, right direction
		87	96	110	104	Detected, right direction
		81	86	85	96	Detected, wrong direction
6	3	79	88	122	103	Detected, right direction
		56	54	68	62	Detected, right direction
		74	66	81	82	Detected, right direction
7	3.5	38	40	45	56	Detected, right direction
		33	31	44	47	Detected, right direction
		39	56	69	70	Detected, right direction
8	4	66	69	79	94	Detected, right direction
		32	33	53	60	Detected, right direction
		81	80	90	86	Detected, right direction
9	4.5	79	79	85	88	Detected, right direction
		66	69	68	74	Detected, wrong direction
		62	57	64	59	Detected, wrong direction
10	5	43	39	45	51	Detected, right direction
		35	32	47	49	Detected, right direction
		48	52	50	59	Detected, wrong direction

Table 4 present south direction victim's voice trial with obstacle.

TABLE 4. South Direction Victim's Voice Trial with Obstacle						
No	Distance (m)	South Direction Test				Description
		Microphone 1	Microphone 2	Microphone 3	Microphone 4	
1	0.5	79	87	100	96	Detected, right direction
		83	82	92	95	Detected, right direction
		73	77	89	87	Detected, right direction
2	1	61	65	76	73	Detected, right direction
		59	60	72	70	Detected, right direction
		62	51	69	65	Detected, right direction
3	1.5	44	41	56	55	Detected, right direction
		46	38	50	51	Detected, right direction
		39	44	42	47	Detected, wrong direction

TABLE 4. South Direction Victim's Voice Trial with Obstacle (continue)

No	Distance (m)	South Direction Test				Description
		Microphone 1	Microphone 2	Microphone 3	Microphone 4	
4	2	37	38	46	54	Detected, right direction
		22	22	24	29	Detected, right direction
		60	60	77	63	Detected, right direction
5	2.5	22	23	27	28	Detected, right direction
		34	37	35	42	Detected, wrong direction
		35	35	39	39	Detected, right direction
6	3	37	39	41	43	Detected, right direction
		34	35	43	43	Detected, right direction
		47	50	49	53	Detected, wrong direction
7	3.5	18	18	26	22	Detected, right direction
		30	36	45	40	Detected, right direction
		20	23	27	27	Detected, right direction
8	4	17	18	23	26	Detected, right direction
		10	10	14	13	Detected, right direction
		14	18	24	20	Detected, right direction
9	4.5	16	19	18	20	Detected, wrong direction
		19	19	22	21	Detected, right direction
		22	19	24	20	Detected, right direction
10	5	15	15	19	18	Detected, right direction
		14	18	17	22	Detected, wrong direction
		9	9	9	9	Not detected

As seen in Table 1, Table 2, Table 3, and Table 4, the test was carried out three times every 0.5 meters. By the algorithm that has been designed, when microphone 3 > microphone 2 and microphone 4 > 1, the direction shown is south. An example can be taken in Table 1. at 0.5 meters in the first experiment, microphone 3 which is worth 436 is greater than microphone 2 which is worth 281, and microphone 4 which is worth 487 is greater than microphone 1 which is worth 229. If microphone 1 > microphone 4 or microphone 2 > microphone 3 then in the south direction test, the result is that the detected direction is not correct. For detection, if the value of microphone 1, microphone 2, microphone 3, and microphone 4 is more than the idle value of 14, it can be indicated that the sound source is detected. In Table 4. there are test data that are not detected, namely at 5 meters. This indicates that at 5 meters if the intensity of the sound power is not large enough, the ADMP401 microphone sensor cannot detect the sound source of the potential victim. Therefore, this study was only carried out from 0.5 meters to 5 meters because with medium sound intensity, the microphone had difficulty detecting at 5 meters. Medium sound intensity is used to take the midpoint of low sound intensity and high sound intensity.

In the obstacle and unobstructed test, take the example in Table 1. at 0.5 meters the first test of microphone 3 produces 436 data, and Table 2. at 0.5 meters the first test of microphone 3 produces 213 data, without obstruction tends to have a strong intensity the greater sound is due to the obstacle test (door barrier) the intensity of the sound power produced by the potential victim is dispersed or dissipated so that the intensity of the sound power from the victim's sound source decreases in quality due to collision with the obstacle being tested. The total average score obtained in the unhindered clapping test was 234.40. The total average value obtained in the clapping test with obstacles was 75.97. The total average score obtained in the test of the victim's voice without obstruction is 99.13. The total average value obtained in the test of the victim's voice with obstruction is 43.30. If it is seen from the average value data, in the presence of obstacles, the sound of clapping produced by the victim is reduced to 57.71% and the voice of the victim is reduced to 43.01%. Table 5 present microphone testing average.

TABLE 5. Microphone Testing Average

No	Distance (m)	Average Value							
		Hand clapping				Victim's voice			
		Without obstruction		With obstruction		Without obstruction		With obstruction	
		Closer mic	Further mic	Closer mic	Further mic	Closer mic	Further mic	Closer mic	Further mic
1	0.5	522.87	373.45	213.87	167.45	206.70	164.04	103.16	89.125
2	1	378.53	278.5	180.70	154.41	169.08	133.25	72.75	63.75
3	0.6	315.41	252.33	134.70	113.79	130.75	113.41	61.33	52.08
4	2	267.20	205.41	85.125	72.20	117.95	99.41	50.87	44.20
5	0.7	286.16	215.70	51.95	42.16	97.83	78.83	42.20	34.33
6	3	233.75	191	44.79	36.95	76.79	65.91	42.625	36.375
7	0.8	234.5	189.58	37.66	30.66	62.70	51.25	32.41	26.29
8	4	175.29	143.5	32.33	26.875	62.33	49.29	23.66	18.41
9	0.9	132	111.41	28	22.833	58.04	50.04	21.33	17.45
10	5	97.37	84.25	23.79	19.25	44.20	35.58	18.37	15.41

As seen in Table 5., the average value generated by the ADMP401 microphone sensor in detecting the potential presence of victims from 0.5 meters to 5 meters. The closer mic defines the two microphones that are closer to the sound source and the farther mic defines the two microphones that are further away. This average value is calculated to determine whether the intensity of the sound power is higher or lower than the average result. An example can be taken in Table 1. testing at 0.5 meters for the second test, with an average value of a closer mic of 522.87, microphone 3 which produces a value of 617 proves that the intensity of the sound power at the time of testing is slightly greater than the average. average. However, in the third test of microphone 3 which produces a value of 437, it proves that the intensity of the sound power at the time of testing is slightly lower than the average. The total accuracy of the four-way unobstructed clapping test has a value of 85.825%. The total accuracy of the clapping test with a four-way obstacle has a value of 79.125%. The total accuracy of the victim's voice test without four-way obstruction has a value of 84.975%. The total accuracy of the victim's voice test with four-way obstruction has a value of 77.475%. Therefore, testing the ADMP401 microphone sensor in detecting the potential presence of the victim's voice direction has an accuracy of up to 81.85%.

Recording Testing and Signal Analysis

Two ADMP401 microphones to detect the direction and recording media, two micro SD as storage media, a micro SD card adapter module as a liaison between micro SD and Arduino Uno, two Arduino Uno as a microcontroller, project board as a coupling medium, and push buttons which are used for the record and stop button. Microphone A and microphone B are placed at 13.5 cm. The sound source test is closer to microphone A than to microphone B. The recording settings used in this test are recording frequency at 16000 Hz and buffer size 254. Figure 3 shows testing recording on Audacity software

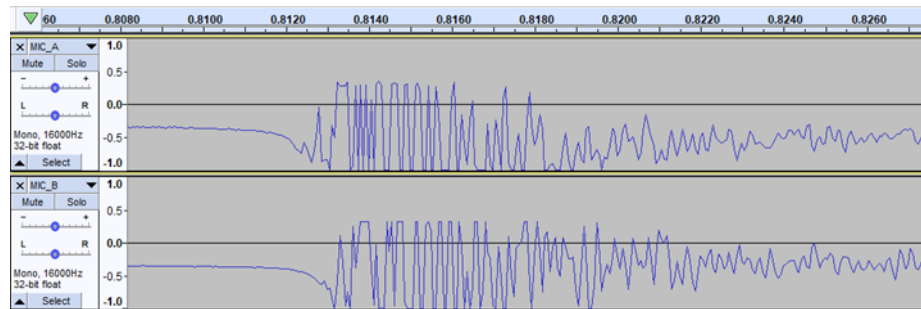


FIGURE 3. Testing Recording on Audacity Software

As seen in Figure 3, microphone A first receives the resulting sound signal, while microphone B gets a delay and then receives the resulting signal. This proves that the closer the sound source is to the microphone, the faster the microphone will receive an acoustic signal from the sound source. Figure 4 present RMS testing on Audacity software.

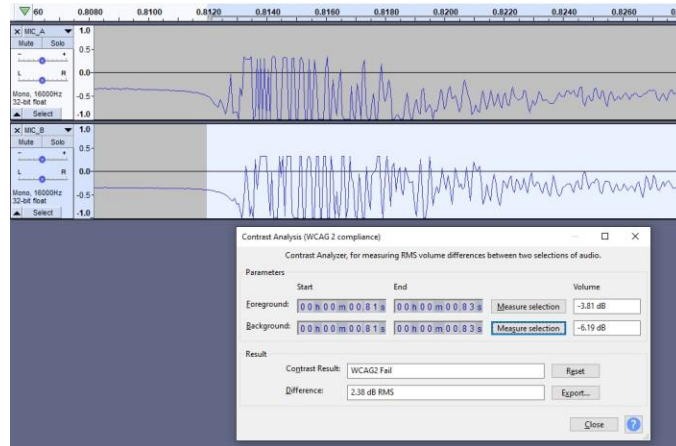


FIGURE 4. RMS Testing on Audacity Software

As seen in Figure 4., microphone A produces a Root Mean Square (RMS) of -3.81 dB while microphone B produces a Root Mean Square (RMS) of -6.19 dB. This proves that the distance from the sound source to the microphone can create different sound strengths. In addition to non-real-time data, this test also carried out real-time experiments on two microphones connected to the Arduino Uno and the signal could be seen on the serial plotter. Figure 5 shows signal form on serial plotter.

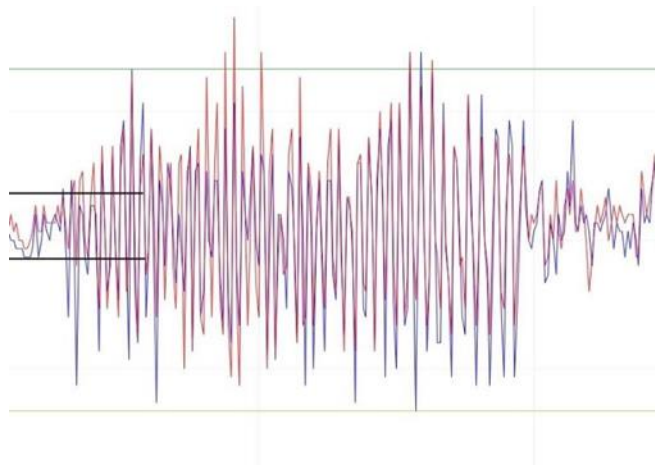


FIGURE 5. Signal Form on Serial Plotter

As seen in Figure 5., the blue microphone A signal responds to the acoustic signal from the sound source first then the red microphone B, this proves that microphone A, which is closer to the sound source, receives an acoustic signal first than the microphone B.

CONCLUSION

Based on the results of research and analysis, several things can be said, namely the ADMP401 microphone sensor can detect the presence of the victim's voice up to a distance of ± 8 meters. Obstacles can reduce the sound of clapping up to 57.71% and the voice of the victim up to 43.01%. The ADMP401 microphone sensor can detect the presence of the victim's voice with a total accuracy of up to 81.85%, with an accuracy of clapping hands without the obstruction of 85.825%, the accuracy of the victim's voice without obstruction 84.975%, the accuracy of clapping with obstruction of 79.125%, and accuracy of the victim's voice with the obstruction by 77.475%. The high and low intensity of the sound received by the microphone depends on the intensity of the sound from the victim and the distance between the victim and the microphone.

ACKNOWLEDGEMENTS

The author would like to thank parents, lecturers, and colleagues who have helped and encouraged the author since the start of this research.

REFERENCES

1. D. Zhang, S. Sessa, R. Kasai, S. and Cosentino, "Evaluation of a Sensor System for Detecting Humans Trapped Under Rubble: A Pilot Study", *MDPI*, 18, (2018).
2. C.F. Scola and M.D. Orteg, "Direction of Arrival Estimation - A Two Microphones Approach", *BTH*, 96, (2010).
3. J. Cech, R. Mittal, A. Deleforge, and J.S. Riera, "Active-Speaker Detection and Localization with Microphones and Cameras Embedded Into a Robotic Head", *HAL*, (2013).
4. L. Swathy and L. Abraham, "Wireless Acoustic Signal Monitoring Using MEMS Sensor and ATmega on LabVIEW Platform", *IJCSMC*, 3 (8), 257 – 266, (2014).
5. I.F. Ammarprawira, M.S. Fauzi, A.A. Jabbaar, and N. Syafitri N, "Implementation of Automatic Waypoint for Return Trip on Autonomous Robot with Reference Point for Potential Disaster Victims". *ELKOMIKA*, 8,1. doi: <http://dx.doi.org/10.26760/elkomika.v8i1.203>, (2020).

Web Camera-Based Spectrometer System Precision Testing in Wavelength Measurement

Silviana Dwi Cahyani^{1, a)}, Hendi Handian Rachmat¹

¹ *Institut Teknologi Nasional (Itenas), Bandung – INDONESIA*

^{a)} Corresponding author: 0437silviana@mhs.itenas.ac.id

Abstract. A spectrometer is a device to produce the wavelength spectrum of an object. By applying existing technology, we designed a simple web camera-based spectrometer with a DVD piece as dispersion. This study aims to develop a laboratory-scale spectrometer for learning and research facility. To validate the spectrometer, we examined the precision. The input of the system is a light source derived from LED lights of various colors. The method used is to compare the measurement results with the existing wavelength literature. The spectrum wavelength was calculated accurately by an installed Theremino spectrometer software on the PC after the light passing through the web camera and the DVD piece. The wavelength value of the measurement results is processed to obtain the system's precision value. The precisions obtained are red 0.489 %, green 1.287 %, and blue 1.855%, which are relatively optimizing result for the simple laboratory's scale spectrometer.

INTRODUCTION

Each color has a different wavelength. When light is bent on a diffraction grating or prism side, different wavelengths of light will be bent to different degrees, this causes the wavelength value for each color will be different. To measure the wavelength required a measuring instrument, namely a spectrometer. A spectrometer is a tool that is applied to measure and produce a spectrum of wavelengths from an object [1].

Along with the development of technology as it is today, it is easier to design a system with the same function but with a simpler method, one of which is designing a spectrometer system using a web camera and DVDs as dispersing agents. In general, spectrometers use a prism to separate a mixture of wavelengths into their component lengths. But in this design uses DVD chips as a dispersion in the spectrometer system.

This web camera-based spectrometer is designed to determine the wavelength value of each color with near-zero precision. Because a good precision value is close to zero. The system precision value is obtained from the system test on the resulting wavelength value. The resulting wavelength will be compared with the literature for visible light and ultraviolet light, namely 400-800 nm for visible light wavelengths and 200-400 nm for ultraviolet light wavelengths [2].

This web camera-based spectrometer system is designed to evaluate the measurement of visible and ultraviolet light wavelengths with a system precision value that is close to zero so that the spectrometer can be used on a laboratory scale and can be used for learning media or other related research.

MATERIAL AND METHOD

The description of the system designed in this study consists of the functions and specifications of the designed system. The function of the designed system is to measure the wavelength value using a web camera-based spectrometer, so that the precision of the designed system can be known. The input of the system is a light source from an LED lamp, and the output of the system is a light spectrum and wavelength value. The specifications of the designed system are as follows:

1. Web camera as a medium to capture light which will be forwarded to the recorder.
2. Personal Computer (PC) as a display.
3. DVD chip as a diffraction grating.
4. Cardboard as a slit case.
5. Red, green, and blue lights are used as light sources.
6. Software using the Theremino Spectrometer.

System Design and Implementation Method

The working principle of the system is explained in a block diagram to make it easier to determine the software, hardware, and mechanical construction that helps the system work. The block diagram of the system is shown in Figure 1.

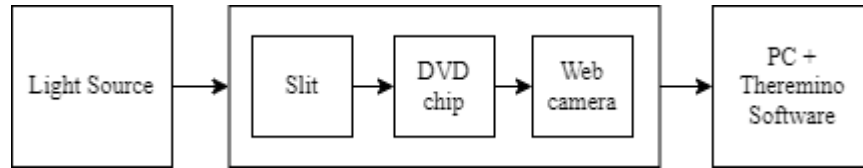


FIGURE 1. Web Camera-based Spectrometer System Block Diagram

Based on Figure 1., the way the system works begins by directing the light source from the LED lamp to the system. Light from the source will then go to the system by passing through the slit. Slit serves to focus light from the source to the system. The light that has passed through the slit will then pass through the DVD as dispersion and will then go to the web camera as a detector to display the measurement results on a PC that has the Theremino Spectrometer software installed to measure its wavelength. The input to the system is in the form of light from LED lamps and the system output is a color spectrum and wavelength value. The measurement results on the system are stored on a PC in the form of image data.

Mechanical and Hardware Construction Sub System

In system design, mechanical construction and hardware are used to support the work of the system. To simplify the design, mechanical construction in the form of a case is used to place the web camera. The case is made of paper that has a thickness of 0.2 cm. The case is in the form of a block with dimensions of 30 cm \times 7 cm \times 7 cm. The case is slit with a width of 5 mm in the vertical direction. The mechanical construction of the system is shown in Figure 2(a).

In the system, there is also hardware that is used to support the work of the system. The hardware in the form of a web camera that functions as a detector, with the specifications of the web camera used is video resolution: 640 \times 480 pixels and Video format: 24-bit RGB. The web camera used is given a DVD chip as a diffraction grating. The light from the source will be captured by the web camera and will be forwarded to the PC as a recorder that will display the results of the wavelength measurement. In Figure 2(b). shown a web camera and a DVD chip on the system.

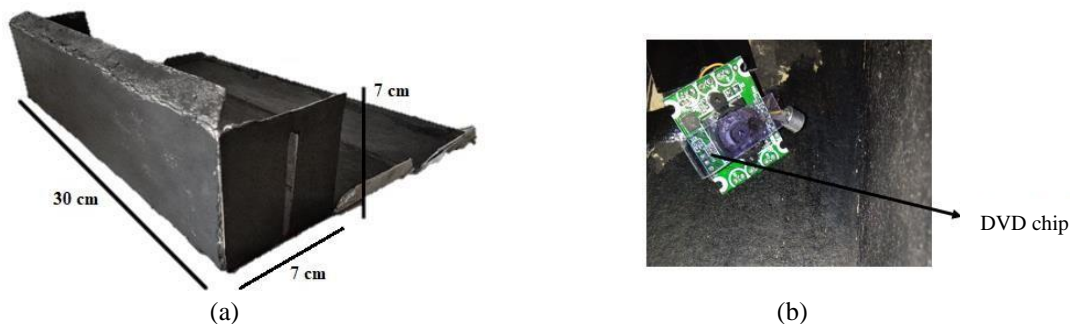


FIGURE 2. (a) System Mechanical Construction; (b) Web Camera and DVD

Sub System Software

Web camera-based spectrometer system works by using software to determine the wavelength value. The software used is the Theremino Spectrometer. Theremino Spectrometer is software used to determine the color spectrum in visible light and UV light. This software calculates the intensity of light that comes at each pixel from the camera. The camera does not need to distinguish the colors of the photons collected, what matters is the intensity [3]. In Figure 3. The measurement results from the Theremino software are shown.

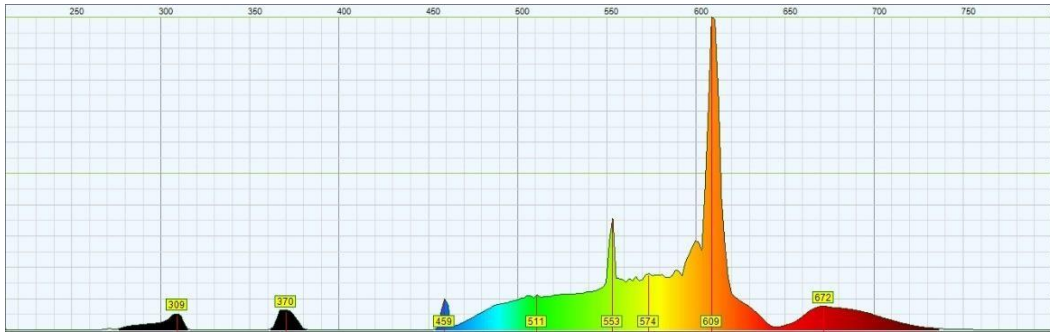


FIGURE 3. Measurement results by Theremino software

According to Figure 3, the Theremino software will measure the wavelength of light transmitted by the webcam. The measurement results in the form of a color spectrum and wavelength values will be stored on the PC.

System Testing Method

System testing begins by calibrating the system. Calibration is done on the Theremino software by directing the light source with a white light on the slit so that the light will be received by the web camera and will be measured by the Theremino. The Theremino software will display the color spectrum and wavelength values. The Theremino has a Trim Point to adjust the spectrum when calibrating. The Trim Point value on the Theremino is 436 nm for the blue spectrum, and 546 nm for the green color [3]. If the resulting spectrum is by the Theremino software specifications, then the calibration is successful and can be tested with different colors.

After the system is calibrated, the test is continued by determining the color spectrum for red, green, and blue, using LED lights of the same color. The test is done by directing the light source at the system, and the system will measure the wavelength. The test was carried out 10 times for each color. And the measurement results, color spectrum, and wavelength values are stored on a PC that has the Theremino Spectrometer software installed for further analysis of the precision values.

RESULT AND DISCUSSION

Tests were carried out on red, green, and blue lights with 10 times testing for each color. The measurement results produce a color spectrum and wavelength value. In Figure 4, the color produced by the testing system is red in the first test.



FIGURE 4. Color spectrum and wavelength value of red color test

In Figure 4., the color spectrum and wavelength values of the system test results are shown in red during the 1st test. The wavelength value generated by the system is 683 nm. This value is derived from literature values for the wavelength of red visible light, 610-750 nm [4]. The average wavelength measurements of red, green, and blue in the system are shown in Table 1.

TABLE 1. Average Wavelength		
No	Color	Average Wavelength (nm)
1	Red	683,1
2	Green	543,4
3	Blue	463,6

Table 1. shows the average value of the measured wavelength on the web camera-based spectrometer system. The resulting wavelength for the system for red is 683.1 nm; green 543.4 nm; and blue is 463.6 nm. The results obtained by the system are by the literature on the wavelength of the visible light region with red color 610-750 nm, green 500-560 nm, and blue 435-480 nm [4].

The results of the system test with the output in the form of a color spectrum and a wavelength value are then processed to obtain a system precision value for the resulting wavelength. The test results on the sample were carried out 10 times to determine the system precision value. The system precision is calculated for each color tested by using the precision formula in Equation (1).

$$precision (\%) = \frac{|(mean\ value)-(i-th\ measurement\ value)|}{mean\ value} \times 100\% \quad (1)$$

By performing calculations on the results of measuring the wavelength of each color, system precision values for each color are obtained, as shown in Table 2.

TABLE 2. System Precision Value		
No	Color	Precision (%)
1	Red	0,489
2	Green	1,287
3	Blue	1,855

In Table 2., the system precision value for wavelength measurement produces a value close to zero. The precision results of the red, green, and blue colors are 0.489%, 1.287%, and 1.855%, respectively. The results of the calculation of the precision of the system on the measurement of the wavelength obtained are relatively small and close to zero. Therefore, the system has good accuracy.

With the precision value obtained in the system, the system can be used to analyze the concentration of glucose solutions or other solutions. Because in general a spectrometer can be used to measure the concentration of a solution by measuring the absorbance at a wavelength using the Lambert-Berr law [2]. With the obtained wavelength, it can be measured the concentration of a solution.

CONCLUSION

Based on testing and analysis of a webcam-based spectrometer system design, the system produced good precision values for the colours tested (i.e., red, green, and blue). The system precision values for red, green, and blue are 0.489%; 1.287%; and 1.855%, respectively.

ACKNOWLEDGEMENTS

We would like to express our deepest gratitude to all those who have contributed to the smooth running of this research activity.

REFERENCES

1. I. Novianty, *Vis-Nir Reflectance Spectroscopic Analysis to Determine the Maturation Process of Strawberries*, Department of Physics, Faculty of Mathematics and Natural Sciences, IPB University, Bogor, (2008).
2. Dachriyanus, *Spectroscopic Structural Analysis of Organic Compounds*, Institute of Information and Communication Technology Development of Andalas University, Padang, (2004).
3. Theremino. (n.d.), *Theremino Spectrometer*, Retrieved from Theremino: <https://www.theremino.com/en/>
4. E. Triyati, "Ultra-Violet and Visible Light Spectrometers and Applications in Oceanology", *Oseana*, X(1): 40-41, (1985).

Automatic Fish Feeder Design Based on IoT

Tubagus Nur Muhammad Rizqi Zakaria^{1,a)}, Fahmi Arif¹

¹ Department of Industrial Engineering, National Institute of Technology (Itenas), Bandung - INDONESIA

^{a)}Corresponding author e-mail: tbnur001@gmail.com

Abstract. The feeding of fish at irregular times and temperatures are the problems in the fish cultivation business. The research is to design automated fish feeder that can provide fish food at the right time and temperature. Automatic fish feeder is designed by using the Internet of Things method. Automatic fish feeder could feed through a scheduled times that are at 8 am, 1 pm, and 6 pm, and through the optimal growth temperature of tilapia fish which is at 25-30°C. The user will also get the information about the feeding that has been done through email and smartphone. The test result shows that the prototype works well on a big stream pond and has an opposite entry lane. Maximum wifi reach for this tool is 19 meters if there's a wall between and 20 meters if there are no walls in range. The limitation of this tool is it has to be placed near the big stream water source and the feeding spreads about 80% of the whole pond.

INTRODUCTION

In line with the increasing intensity of development of Sukabumi City, the population growth increases, therefore food needs also increase. Tilapia became one of the needs in demand according to data from the central statistics agency of Sukabumi City tilapia production in 2018 was 510.05 tons and in 2019 increased to 652.62 tons. The increasing demand for tilapia is widely used by businesspeople to breed tilapia. One of them is a tourist spot located in Sukabumi City, applying tilapia cultivation in each pond, fish cultivation in this tourist spot is added to increase the income obtained from fish cultivation. The high demand for fish encourages many businesses including tourist attractions to produce many fish that certainly have good quality. Feeding in tourist attractions is usually done at uncertain times that cause 15% of the seedlings of fish cultivated to die, the death of this fish is caused by irregular feeding and the time of the feed given does not consider the temperature of the water. Feeding fish is not in accordance with the time or not fed is a case that often occurs when cultivating fish, and for the tourist attractions themselves, employees sometimes forget about fish feeding because they are busy by work that is far from the pond plus the owner of the tourist attractions who often go out of town so that monitoring of fishponds is rarely noticed. Automatic fish feeder allotment ponds on the market have the disadvantage of not applying temperature settings in feeding and using electricity above 15 watts with a voltage of 220 volts and for the price offered is quite expensive around Rp.400,000 - Rp.1,000,000 while for the needs needed in tourist attractions located in Sukabumi City does not need tools with expensive prices due to the scale of the fishpond itself. 12 are or equivalent to 1200m² sees the temperature around Sukabumi City that tends to be cold automatic fish feeder which is expected to reduce feeding if the temperature decreases to keep the condition of the fish healthy. The necessary fish feed shelter is also expected to come from plastic waste because utilizing plastic waste is expected to reduce existing plastic waste, selected plastic waste that can accommodate ±15 kg of fish feed so that refilling fish feed only every once a week, therefore the use of used gallons becomes an option besides being able to accommodate ±15 kg of fish feed form from sunken gallons at the end can help stored feed to get out easily.

Feed that is not given can cause a decrease in the quality of fish can even cause death in fish if feeding is not done for a long time. Feeding with attention to time and temperature is very necessary so that the results of fish cultivation can be maximized. The quality of fish is influenced by the timeliness of feeding fish because fish will only eat when the stomach is almost empty or when the fish is very hungry [1]. Feeding is also good to adjust to the temperature of the water when feeding is done. The optimal temperature for fish growth is between 25-30°C [2]. The effect of rising water temperature at 34°C for 2 hours can cause stress in fish [3]. Feeding time must be on time so that the growth of optimal fish so that when harvesting is done will be obtained fish with good quality fish feeding time should be done three times in a day at 8:00, 13:00, and 18:00 [4]. Feeding should also pay attention to the temperature because the decrease or increase in water temperature can cause stress in the fish therefore fish tend to eat less if they are not. The temperature of water in the pool decreases or increases below the optimal value it is better to reduce the quantity of feed in accordance with [5]. Temperatures

below 25°C to 18°C are conditions where fish decrease their appetite and if below 18°C will be a dangerous condition to fish [2].

Research focuses on making automatic fish feeder based on IoT at a low price and can feed based on optimal temperature for tilapia growth. Automatic fish feeder is expected to be able to conduct scheduled feeding with a good feeding time and considering the optimal water temperature of the tilapia growth itself. Automatic fish feeder made is also used as a tool to monitor feed that has been or has not been done so that owners of tourist attractions will get notifications either via smartphone or via email so that the owner can feel calm about the feeding has been done or has not been added every day will get a report in the form of excel files containing about water temperature, time, and feed reports that have been done.

RESEARCH METHODOLOGY

The design method used in this study is a method developed by Desai (2015) that starts from determining the purpose of making the tool to the testing of the tool that was made.

Formulation of The Problem

The health of fish is very influential on the benefits obtained when the harvest takes place, therefore feeding with the right time and temperature will help the growth of the fish itself, while for a good time in feeding fish according to [4] namely at 8:00, 13:00, and 18:00. A good temperature in feeding is when the optimal temperature for fish growth is between 25-30°C, a reduction in the amount of feed will also be done when the temperature is below optimal and above optimal because according to Hermanto (2000) fish will consume a little feed if there is a decrease in temperature and will increase again when the next temperature increase to reach the optimal temperature then will decrease again if it rises above optimal. The reduction of feed is done when temperatures below 25°C to 18°C are conditions where the fish decreases its appetite and if below 18°C will be a dangerous condition to the fish and for a dangerous temperature increase for tilapia and can cause stress if it is 2 hours at 34°C [3].

Identification of Needs

The equipment needs used in the design of this IoT-based automatic fish feeder are Arduino Uno, ESP8266 V1, Motor Servo, Sensor DS18B20, Real-Time Clock (RTC), and used gallon feed storage with a capacity of 15 kg.

Tool Planning

System design is done by considering the price of the materials needed so as not to incur unnecessary costs. The material selected in the design of this automatic fish feeder uses the ESP8266 wifi module due to its relatively cheap price and small module size so it does not take up much space. The servo motor was selected SG90, RTC used namely DS1302 and arduino used arduino uno R3 CH340 clone. Automatic fish feeder controller selected using the app Blynk, this application was chosen because of its easy use and can be downloaded by anyone for free. An automatic fish feeder is designed using a 9 volt battery, so it is more energy efficient. The assumption for the reduction of feed that occurs is 50% for the decrease or increase in temperature that occurs with a maximum decrease limit of 18°C and a maximum limit of 34°C increase, if it exceeds the limit then there will be no feeding.

Implementation of Tools

Automatic fish feeder implementation is done by connecting the entire component to the microcontroller so that all components can work accurately. The implementation of the tool is also related to writing code so that the tools made can move in accordance with the given commands. Code writing must also be in accordance with the wire diagram created so that the tool can work according to the design made. Wire diagrams in this design are used to connect temperature sensor modules, ESP8266 V1, RTC, and servo motors to microcontrollers.

Integrating Tools

Integration between the application and the tool is done by entering the unique code of the application blynk into the program in microcontroller. When the internet is connected. The microcontroller will connect to the blynk application with the help of unique code and wifi module ESP8266 this condition is characterized by the appearance of connected writing on the display application.

Tool Testing

Tool testing is first done by testing the suitability between code written with wire diagrams to make sure the designed tool is working in line with expectations. The next test is testing component that is done is the testing of ESP8266 components, temperature sensors, and servo motors. ESP8266 testing is done to determine the effective distance from the use of ESP8266. Sensor testing is done to know that the sensor is working properly, and for servo motor testing is done so that when applying the servo motor as a fish feed lid opener there are no problems.

RESULT

The design of automatic fish feeder made using gallons of unused water and then arranged using wood formed like a chair as a buffer and for microcontroller components are stored in a black plastic box so that it can be protected from rain as shown in Figure 1. How to use this tool is that the user simply connects the device to the power source can use an adapter or battery, then the tool will turn on and connect to the wifi network that has been applied before. This tool will calculate the time in real time and if it meets the conditions at 8.00 WIB or 13.00 WIB or 18.00 WIB then the tool will provide feed. The display of feeding operation control is shown in Figure 2. At the optimal temperature, the tool will release 100% feed, while at non-optimal temperatures, the amount of feed released is reduced by 50%. Next the user will get a notification through the application on the user's smartphone and email, as illustrated in Figure 3. In addition, users can also set the feed output time through a smartphone.

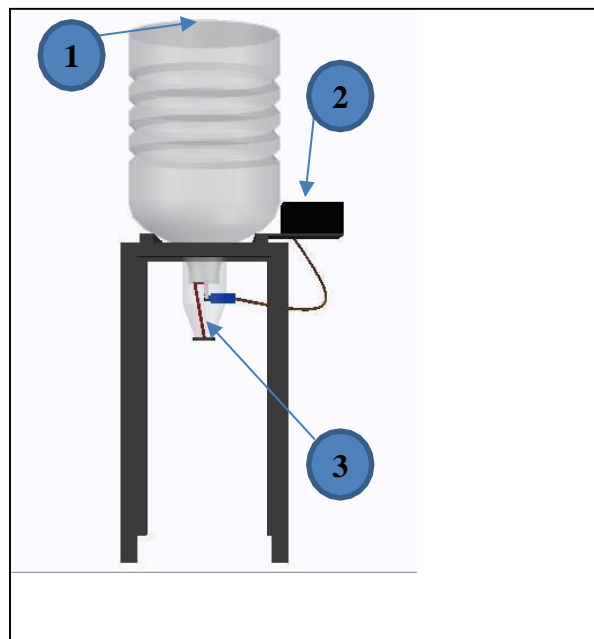


FIGURE 1. Illustration of Automatic Fish Feeder

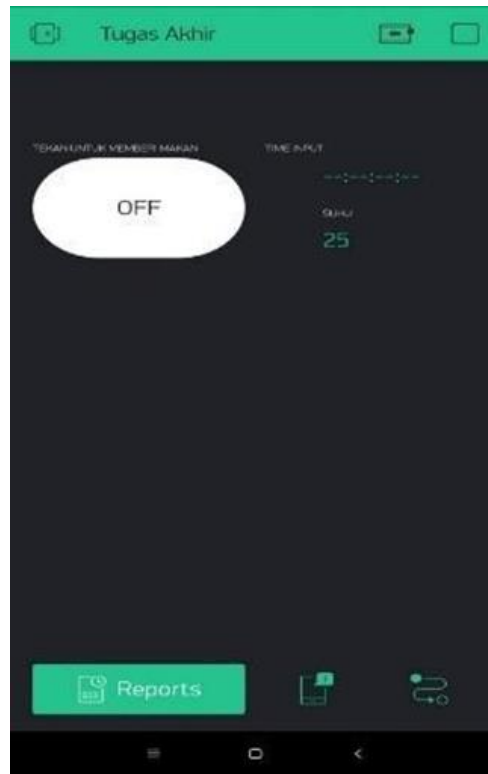


FIGURE 2. Automatic Fish Feeder Controller Page

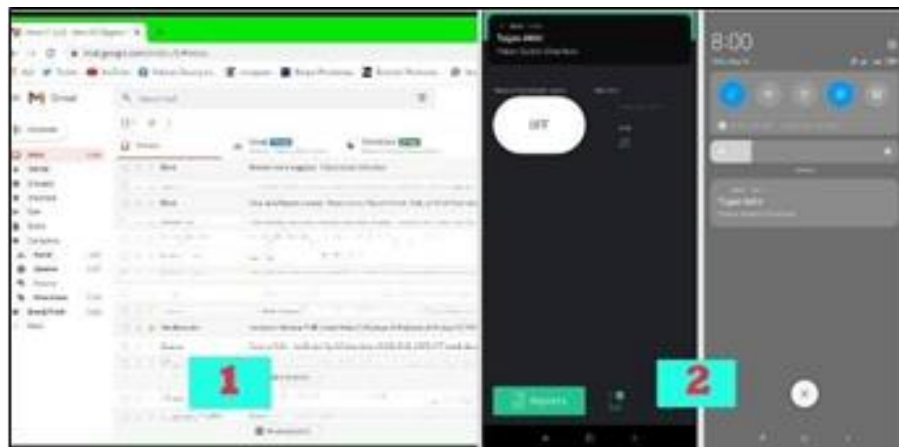


FIGURE 3. Notification View

Automatic fish feeder testing is initially done testing the components first whether it can work as desired or not. The first test is that the DS18B20 water temperature sensor component is tested by placing the sensor with gea S-006 thermometer in a glass containing water and for testing is done using 3 glasses of high temperature water, medium temperature, and low temperature the results of the test can be seen in Table 1.

TABLE 1. DS18B20 Sensor Testing

Testing	DS18B20 Sensor	GEA S-006 Thermometer
High Temperature Water	37 °C	37 °C
Medium Temperature Water	28 °C	28 °C
Low Temperature Water	19 °C	20 °C

The second test is to test the movement of the servo motor whether it can move to any angle $+90^\circ$ and angle -90° , the test is done by storing the servo motor above from the arc image degrees and then in the test whether it moves to the desired angle what not and for the results of the test produced according to Figure 4 the servo motor can move to an angle of $+90^\circ$ and -90° . The third test is to test the range of the ESP8266 V1 when blocked by the wall and when it is not blocked by the wall.



FIGURE 4. Servo Motor Testing

The third test is to test the range of the ESP8266 V1 when blocked by the wall and when it is not blocked by the wall. Test results are shown in Table 2.

TABLE 2. ESP8266 V1 Range Testing

Obstacle	Range	Connected (Y/N)	Obstacle	Range	Connected (Y/N)
None	1 Meter	Y	Wall	1 Meter	Y
	2 Meter	Y		2 Meter	Y
	3 Meter	Y		3 Meter	Y
	4 Meter	Y		4 Meter	Y
	5 Meter	Y		5 Meter	Y
	6 Meter	Y		6 Meter	Y
	7 Meter	Y		7 Meter	Y
	8 Meter	Y		8 Meter	Y
	9 Meter	Y		9 Meter	Y
	10 Meter	Y		10 Meter	Y
	11 Meter	Y		11 Meter	Y
	12 Meter	Y		12 Meter	Y
	13 Meter	Y		13 Meter	Y
	14 Meter	Y		14 Meter	Y
	15 Meter	Y		15 Meter	Y
	16 Meter	Y		16 Meter	Y
	17 Meter	Y		17 Meter	Y
	18 Meter	Y		18 Meter	Y
	19 Meter	Y		19 Meter	Y
	20 Meter	Y		20 Meter	N
	21 Meter	Y		21 Meter	N
	22 Meter	N		22 Meter	N
	23 Meter	N		23 Meter	N
	24 Meter	N		24 Meter	N
	25 Meter	N		25 Meter	N
	26 Meter	N		26 Meter	N

The last test is to test the automatic fish feeder tool that has been made. The test was done using a small glass of water with varying temperatures to test the suitability of the servo opening time. The results of the test can be seen in Table 3.

TABLE 3. ESP8266 V1 Range Testing

No.	Temperature	Time	Servo Movement	Duration of Open Servo (seconds)	Status
1	25	6.00 WIB	Opened	10	Appropriate
2	29	6.30 WIB	Opened	10	Appropriate
3	28	7.00 WIB	Opened	10	Appropriate
4	25	7.30 WIB	Opened	10	Appropriate

TABLE 3. ESP8266 V1 Range Testing (continued)

No.	Temperature	Time	Servo Movement	Duration of Open Servo (seconds)	Status
5	27	8.00 WIB	Opened	10	Appropriate
6	27	8.30 WIB	Opened	10	Appropriate
7	26	9.00 WIB	Opened	10	Appropriate
8	26	9.30 WIB	Opened	10	Appropriate
9	25	10.00 WIB	Opened	10	Appropriate
10	25	10.30 WIB	Opened	10	Appropriate
11	19	13.00 WIB	Opened	5	Appropriate
12	19	13.30 WIB	Opened	5	Appropriate
13	21	14.00 WIB	Opened	5	Appropriate
14	20	14.30 WIB	Opened	5	Appropriate
15	20	15.00 WIB	Opened	5	Appropriate
16	19	15.30 WIB	Opened	5	Appropriate
17	19	16.00 WIB	Opened	5	Appropriate
18	19	16.30 WIB	Opened	5	Appropriate
19	20	17.00 WIB	Opened	5	Appropriate
20	20	17.30 WIB	Opened	5	Appropriate
21	34	19.00 WIB	Opened	5	Appropriate
22	33	19.30 WIB	Opened	5	Appropriate
23	32	20.00 WIB	Opened	5	Appropriate
24	32	20.30 WIB	Opened	5	Appropriate
25	33	21.00 WIB	Opened	5	Appropriate
26	33	21.30 WIB	Opened	5	Appropriate
27	33	22.00 WIB	Opened	5	Appropriate
28	32	22.30 WIB	Opened	5	Appropriate
29	31	23.00 WIB	Opened	5	Appropriate
30	32	23.30 WIB	Opened	5	Appropriate

In addition to testing the feasibility of the automatic fish feeder tool is also carried out trials on the ground. The results of the trial directly on the ground obtained a distribution of feed about 80% of the entire pool. From the test results, it is known that the pool that is suitable for the application of automatic fish feeder is a pool that has a large water current and has an in and out path of opposing water. Another limitation of this tool is that if applied in areas that are difficult internet network then users will not get notifications from feeding that has been done.

CONCLUSION

This research shows that an automatic fish feeder designed is able to work well under expected conditions. Each component selected, also works well on every test scenario, which means each component is fit for use in an automatic fish feeder tool. The automatic fish feeder design produced in this study can detect temperature and time well so that it can make the output of servo movement and servo length with proper opening time. Further development can be done by adding GSM modules so that they can be used to overcome the limitations of wifi and internet networks.

REFERENCES

1. Tahapari, E., & Suhenda, N. 2009. "Determination of Different Feeding Frequency on The Growth of Patin Pasupati Fingerlings." *Berita Biologi*, 9(6), 693–698.
2. Sihombing, P. C. 2018. "Effect of Water Temperature Differences On and Survival of Tilapia Seeds (*Oreochromis niloticus*)." USU Institutional Repository, 1. Sihombing.
3. Joseph, J. B., & Sujatha, S. S. 2010. "Real-time Quantitative (PCR) Applications to Quantify And The Expression Profiles of Heat Shock Protein (HSP70) Genes In Nile Tilapia, *Oreochromis niloticus* (L.) and *Oreochromis mossambicus* (P.)." *International Journal of Fisheries and Aquaculture*, 2(1), 44–48.
4. Rajaguguk, E., Mulyadi, & MT, U. 2013. "Effect of Feeding Time on the Growth and Smoothness of Red Tilapia Fish (*Oreochromis niloticus*) with Resiculation System." *Journal of Chemical Information and Modeling*, 53(9), 1689–1699.

5. Tang, G., Muhammad, U., & Mulyadi. 2019. "Different Temperature Influences on Growth Rate and Smoothness of Jams Fish Seeds (*Kryptopterus lois*).” *Journal of Fisheries and Marine Affairs*, 24(2), 101–105.

Seasonal Performance Evaluation of Hybrid Solar Collectors In a Hot Climate Area

Ahssan Alshibil^{1, a)}, Piroska Vig^{2, b)} and Istvan Farkas^{3, c)}

¹*Doctoral School of Mechanical Engineering, Hungarian University of Agriculture and Life Sciences, Godollo, Hungary*

²*Institute of Mathematics and Basic Science, Hungarian University of Agriculture and Life Sciences, Godollo, Hungary*

³*Institute of Technology, Hungarian University of Agriculture and Life Sciences, Godollo, Hungary*

^{a)}Corresponding author: ihssanm.ali@uokufa.edu.iq

^{b)}vig.piroska@uni-mate.hu

^{c)}farkas.istvan@uni-mate.hu

Abstract. The most significant factor in solar electrical systems is the conversion efficiency, which decreases when the cell temperature increases. The hybrid solar collector (PV/T) is an advanced technology that enhances the performance of these systems by removing the heat via collectors placed behind the photovoltaic modules. In this study, the effect of the four seasons a year on the PV/T system is evaluated. Using functional tools in the simulations of the solar systems, TRNSYS was selected for evaluation of the performance of the PV/T in a hot climate area. Kabul City was used in the software as the weather source of the system, which was modelled on the TRNSYS. The simulation results show that the winter season for the selected area is the most efficient of all seasons in the electrical behavior of the PV/T. Flowed by autumn, spring and summer. Besides, the thermal performance was higher in the autumn flowed by summer, spring, and winter.

INTRODUCTION

Solar energy is the world's cheapest and cleanest energy source. Many studies and commercial operations have been conducted to exploit solar energy. Solar energy harvesting technologies are classified as solar photovoltaic, thermal, and photovoltaic-thermal [1]. This paper touches on the modern technique, which is solar-photovoltaic-thermal units (PVT).

In recent decades, many scientists have focused on photovoltaic thermal systems because of their superior performance versus stand-alone solar panels and collectors. B. J. Huang et al. [2] built PV/T collector, controller, storage tank, and pump. There was a daily average of 38% thermal efficiency and overall daily efficiency of 50%. In their research, He et al. [3] constructed a free-convection PV/T system. According to the researchers, the average thermal performance of the PV/T system is approximately 0.4, with a total efficiency of up to 0.55. Kalogirou and Tripanagnostopoulos [4] compared commercial PV/T solar arrays in terms of geographical location, load source temperatures, photovoltaic cells material, energy demands, and affordability. In their assessment, Charalambous et al.[5] entirely and systematically established the PV/T system in terms of theories, modelling, experimental investigation, performance, and influencing factors. For various configurations, Dubey and Tiwari [6] established an explicit formula for the characteristic equation of a PV/T flat-plate collector system. The water-heating system was also assessed. Amori and Abd-Raheem [7] developed and tested four collectors of various layouts in the Iraqi climate. They decided that model with a double duct is best suited for rural areas and is easy to build. A piece of work deals with the dynamic simulation of a PV solar house with integrated PV. Alshibil et al. [8] presented a thermodynamic model of the flat plat-based PV/T module; they investigated the electrical and thermal performance in the months of February, June, and October. System performance was high in June.

In this article, seasonal evaluation of the hybrid solar collector is examined for the electrical and thermal behaviour of the system. It introduces the behaviour of the PV/T module in the four seasons of a hot climate area.

Using functional tools in the simulations of the solar systems, TRNSYS is selected for evaluation of the performance of the PV/T module. Kabul City was used in the software as the weather source of the system, which was modelled on the TRNSYS.

The most significant role performed by this study is to determine which season is the most efficient in terms of electrical and thermal performance among the four in the study area.

SYSTEMS DESCRIPTION

PV/T module used in this study has 72 monocrystalline photovoltaic cells type and copper plate as an absorber with copper pipe for fluid circulated in the system, and low iron glass cover extra tempered. Figure 1 shows the module used for evaluation.

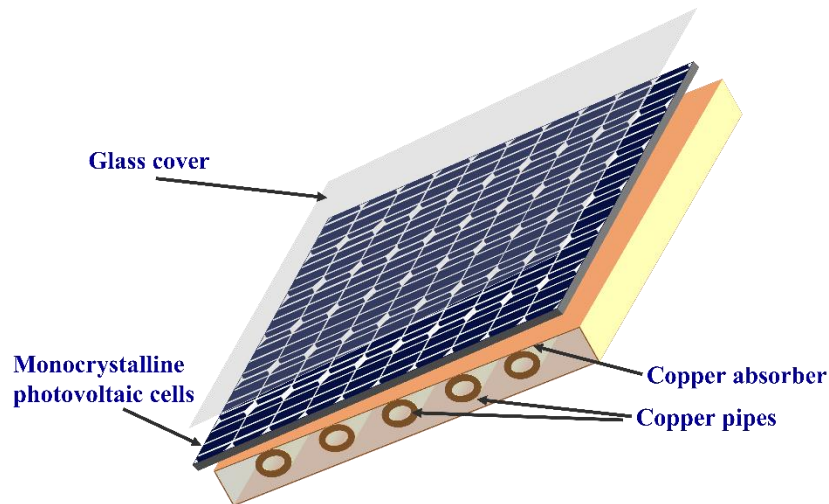


FIGURE 1. Photovoltaic thermal module

This module has 1.427 m^2 as an aperture area and 1.27 m^2 as an absorber area. It is connected to the thermal storage tank with a volume tank is 0.3 m^3 . Module electrical efficiency is 12.9%. 180 W is a nominal power.

SIMULATION MODEL

TRNSYS is chosen for the assessment of the performance of the PV/T solar systems because it is a functional tool in the simulations of solar systems. Kabul City was utilized as the weather source for the system, which is structured in TRNSYS as a hot climate metrological component in the model. Figure 2 demonstrates the study model.

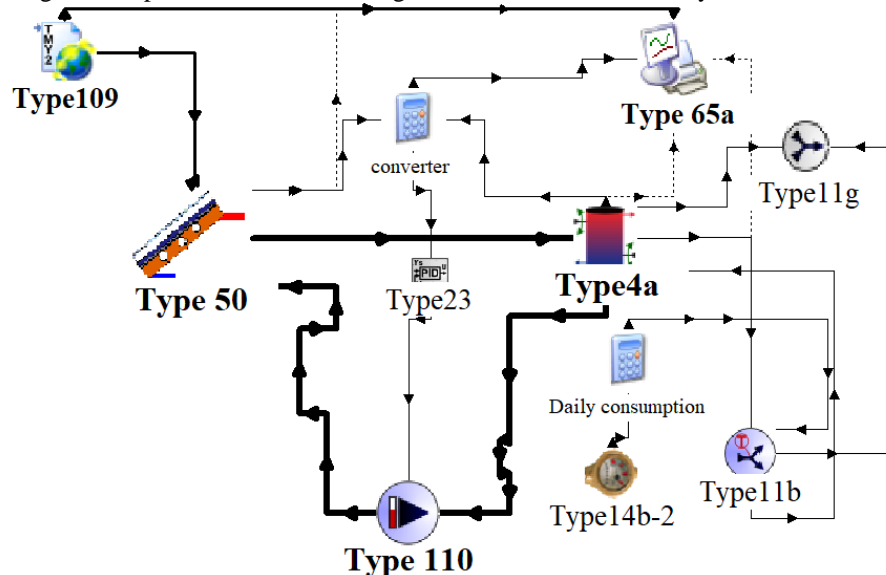







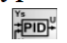



FIGURE 2. Simulation model of the PV/T system

The components utilized in the preceding model are shown in Table 1, with the details of each component linked to its corresponding symbol in the model (see Figure 2).

TABLE 1. Model components of the TRNSYS software

Component symbol	Details
 Type109	The metrological source of whether data of study area
 Type 50	The photovoltaic-thermal module
 Type4a	Thermal storage tank
 Type 110	Variable speed water-pump
 Type14b-2	Profile of water-consumption (water draw)
 Type11g	Tee- joint of liquid
 Type11b	Tempering valve
 Type23	Temperature controller
 Type 65a	Online-printer for outputs results of components

STUDY RESULTS AND DISCUSSION

The outputs results of the system were obtained as a daily result with 3 minutes as an interval for the simulation step. The location selected during the simulation is Kabul city. The simulation time for processing the TRNSYS-model is one year from 0 h to 8760 h during four seasons winter, spring, summer and autumn. Figure 3 shows the radiation of Kabul city for four seasons. Besides, Figure 4 shows the average hour of sun daylight time of the study.

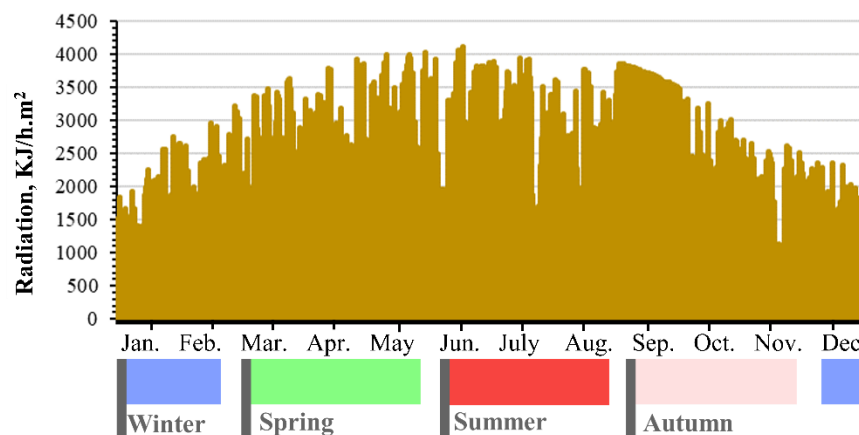


FIGURE 3. Radiation distribution during four seasons

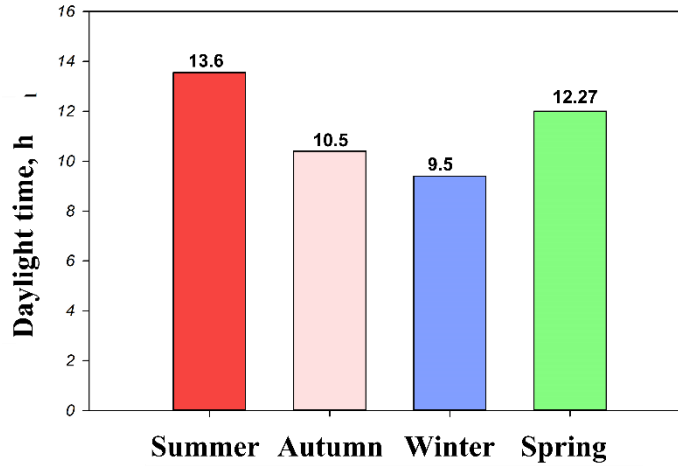


FIGURE 4. Sun daylight time

The first comparison between the four seasons is the evaluation of the electrical performance efficiency. Figure 5 shows the electrical efficiency of the PVT during the seasons in Kabul city. The results were average values for each season during a day from 5 am to 7 pm.

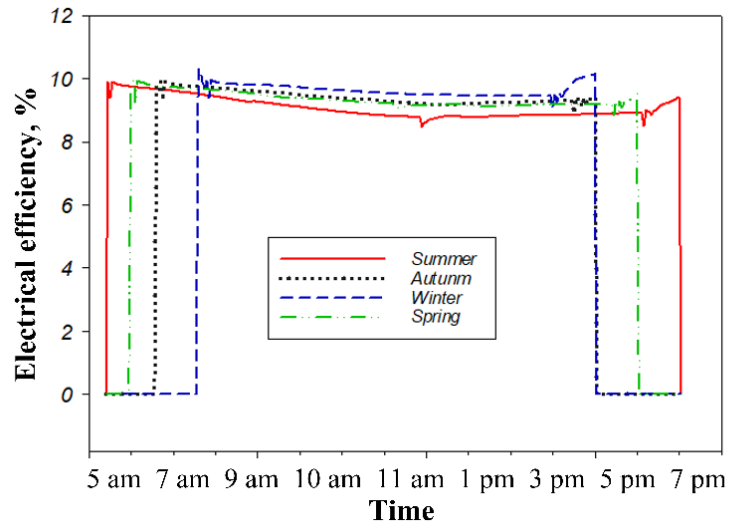


FIGURE 5. Electrical efficiency of the module during the seasons

As shown in Figure 5, the highest efficiency was in the winter season because of the season's low temperature. In contrast, as well known, the electrical efficiency increases when cell temperature is decreased.

Figure 6 represents the comparison results of the thermal performance of the module during Kabul city.

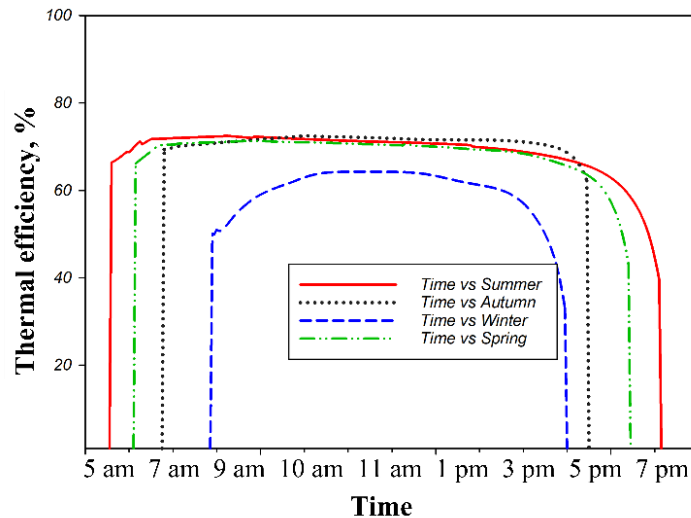


FIGURE 6. Thermal efficiency of the module during the seasons

The highest efficiency as measured by the thermal performance assessment of the module was approximately evenly distributed over the three seasons: autumn, summer, and spring. The thermal efficiency is lower during the winter months.

CONCLUSION

This article presented the behavior of the photovoltaic-thermal system in a hot climate metrological source using TRNSYS software during a four-season of Kabul city.

In conclusion, based on the simulation results in the TRNSYS tool, based on an average value of over a year, thermal efficiency was more efficient in the autumn. Flowed by summer, spring and winter. Autumn season was higher than summer by 2.7%, summer higher than spring by 1.6% and spring higher than winter by 13.5%.

Besides, electrical efficiency was more efficient in the winter. Flowed by autumn, spring and summer. The winter season was higher than autumn by 2.2%, autumn higher than spring by 0.82% and spring and summer 2.8%.

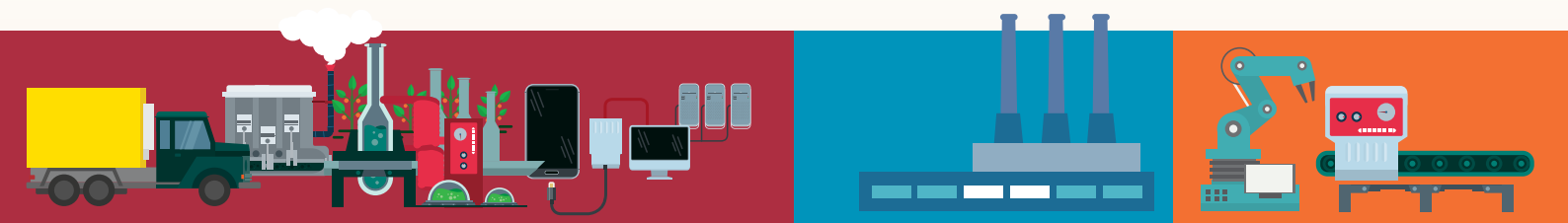
Based on the above results, overall, the most effective season for the PVT module is autumn, flowed by summer, spring and winter.

ACKNOWLEDGMENTS

This work was supported by the Stipendium Hungaricum Programme and by the Doctoral School of Mechanical Engineering, the Hungarian University of Agriculture and Life Sciences.

REFERENCES

1. A. M. A. Alshibil, P. Víg, and I. Farkas, *European Journal of Energy Research* 1, 17–20 (2021).
2. W. C. H. and F. S. S. B. J. Huang, T. H. Lin, *Solar Energy* 70, 443–448 (2001).
3. W. He, Y. Zhang, and J. Ji, *Applied Thermal Engineering* 31, 3369–3376 (2011).
4. S. A. Kalogirou and Y. Tripanagnostopoulos, *Applied Thermal Engineering* 27, 1259–1270 (2007).
5. P. G. Charalambous, G. G. Maidment, S. A. Kalogirou, and K. Yiakoumetti, *Applied Thermal Engineering* 27, 275–286 (2007).
6. S. Dubey and G. N. Tiwari, *Solar Energy* 82, 602–612 (2008).
7. K. E. Amori and M. A. Abd-Raheem, *Renewable Energy* 63, 402–414 (2014).
8. A. M. A. Alshibil, P. Víg, I. Farkas, “Heat Transfer Behaviour of Hybrid Solar Collector Module for Liquid-Based Type,” in *International Workshop IFToMM for Sustainable Development Goals, Proceedings of I4SDG Workshop*, edited by G. Quaglia et al. (Springer Nature, Switzerland, 2021), pp. 20–29.



Organized by:
Faculty of Industrial Technology, Institut Teknologi Nasional (Itenas) Bandung, West Java Indonesia.
Supported by:
Institut Teknologi Nasional (Itenas) Bandung, West Java Indonesia.

